Vol. 9, Part A-1, No. 10, October 1971

Journal of Polymer Science

Part A-1: Polymer Chemistry

Contents

(*continued inside*)

Published by INTERSCIENCE PUBLISHERS a division of John Wiley & Sons, Inc.

Journal of Polymer Science: **Part A-1: Polymer Chemistry**

Contents (continued)

(continued on inside back cover)

The Journal of Polymer Science is published in four sections as follows: Part A-1, Polymer Chemistry, monthly; Part A-2, Polymer Physics, monthly; Part B, Polymer Letters, monthly; Part C, Polymer Symposia, irregular.

Published monthly by Interscience Publishers, a Division of John Wiley & Sons, Inc., covering one volume annually. Publication, Executive, Editorial, and Circulation Offices at 605 Third Avenue, New York, N. Y. 10016. Second-class postage paid at New York, New York and additional mailing offices. Subscription price, $325.00 per volume (including Parts A-2, B, and C). Foreign postage $15.00 per volume (including Parts A-2, B, and C).

JOURNAL OF POLYMER SCIENCE: PART A-1 VOL. 9, 2753–2762 (1971)

Structure of Chlorinated Poly(vinyl Chloride). II. Distribution of Cl Atoms in the Polymer Chain

D. DOSKOČILOVÁ, B. SCHNEIDER, E. DRAHORÁDOVÁ, J. ŠTOKR, and M. KOLÍNSKÝ, *Institute of Macromolecular Chemistry, Czechoslovak Academy of Sciences, Prague 6, Czechoslovakia*

Synopsis

The distribution of chlorine atoms in the chain of solution-chlorinated PVC (CPVC) composed of —CH_2—CHCl— (1), —CHCl—CHCl— (2), and —CCl_2—CHCl— (3) monomeric units is described by first-order Markoffian statistics based on the assumption that the chlorination mechanism is independent of tacticity. In this case, all the statistical parameters can be obtained from experimentally determined concentrations of CH_2, CHCl and CCl_2 units. Populations of the sequences (11) and (111) calculated from the statistical parameters agree with experimental values determined from infrared and 220 MHz NMR spectra. From infrared spectra, suspension-chlorinated CPVC contains blocks of intact PVC.

It is now a well established fact[1–5] that the chain of chlorinated poly(vinyl chloride) (CPVC) is composed of CH_2, CHCl, and CCl_2 units and that the relative amounts of these units can be determined from the chlorine content on analysis and from the ratio of CH_2 and CHCl bands in NMR spectra. Experiments described in our previous paper (Part I)[5] have shown that chlorine does not enter the CHCl group of the original PVC, and this was explained on steric grounds. Consequently, only the following three types of two-carbon sequences (monomeric units) can occur in CPVC: monochloroethylene, —CH_2—CHCl— (MCE, 1); 1,2-dichloroethylene, —CHCl—CHCl— (DCE, 2); and 1,1,2-trichloroethylene, —CCl_2—CHCl— (TCE, 3). The general experience that on the average only one Cl atom per monomer unit can be introduced into PVC, together with the proposed steric rules imply that chlorine cannot enter a CH_2 group neighboring with a TCE unit, so that TCE units must always be flanked by MCE units, forming the sequence (131). No limitations concerning the combination of MCE and DCE units into higher sequences were indicated by previous experiments. In order to obtain information about the distribution of longer sequences in CPVC, we have now attempted to formulate more rigorously the statistics governing the construction of the CPVC chain and to verify this by comparison with the results of an analysis of infrared and 220 MHz NMR spectra.

STATISTICAL ANALYSIS OF HOMOGENEOUSLY CHLORINATED PVC

Under the assumption that chlorination proceeding in a physically homogeneous medium does not depend on the tacticity of the original PVC, a CPVC chain generated according to the rules summarized in the introduction can be described by first-order Markoffian statistics with three possiblities. Such a statistics is generally characterized by three placement probabilities $P(i)$, with $i = 1, 2, 3$, and by nine transition probabilities P_{ij} $(i, j = 1, 2, 3)$, obeying the relation $\sum_{j=1}^{3} P_{ij} = 1$. All these probabilities are related by the general equations[6]

$$\begin{aligned} \frac{P(1)}{P(2)} &= \frac{(1 - P_{33})(P_{21} + P_{23}) - P_{23}P_{32}}{(1 - P_{33})P_{12} + P_{32}(1 - P_{11} - P_{12})} \\ \frac{P(3)}{P(2)} &= \frac{P_{12}P_{23} + (P_{21} + P_{23})(1 - P_{11} - P_{12})}{(1 - P_{33})P_{12} + P_{32}(1 - P_{11} - P_{12})} \end{aligned} \tag{1}$$

For CPVC, let the placement probabilities $P(1)$, $P(2)$, $P(3)$ correspond to the analytical concentrations of MCE, DCE, and TCE units, respectively. If the transition probabilities are known, the placement probability of any higher sequence may be generated from these, e.g., $P(1312) = P(1)P_{13}P_{31}P_{12}$. In our case, the transition probabilities P_{23}, P_{32}, P_{33} are equal to zero, so that

$$\begin{aligned} P(1) &= P_{21}/(P_{12} + P_{21} + P_{13}P_{21}) \\ P(2) &= P_{12}/(P_{12} + P_{21} + P_{13}P_{21}) \\ P(3) &= P_{21}P_{13}/(P_{12} + P_{21} + P_{13}P_{21}) \end{aligned} \tag{2}$$

and

$$\begin{aligned} P_{11} + P_{12} + P_{13} &= 1 \\ P_{21} + P_{22} &= 1 \\ P_{31} &= 1 \end{aligned} \tag{3}$$

From this and from the equality $P(13) = P(31)$ we may immediately derive an expression for the transition probability P_{13}:

$$\begin{aligned} P(3)P_{31} &= P(1)P_{13} = P(3) \\ P_{13} &= P(3)/P(1) \end{aligned} \tag{4}$$

enabling us to calculate, from the experimentally determined values $P(1)$ and $P(3)$, the placement probability of alternating MCE–TCE sequences of any length:

$$\begin{aligned} P(31)^n &= P[1(31)^n] \\ &= P[(31)^n 1] \\ &= [P(3)/P(1)]^{n-1}P(3) \end{aligned} \tag{5}$$

From the values $P(1)$ and $P(3)$ it is also possible to calculate the placement probability of limited sequences of length n (i.e., sequences containing n and not more than n units)

$$\begin{aligned} P_0(31)^n &= P(31)^n\{1 - [P(3)/P(1)]\}^2 \\ &= P(3)[P(3)/P(1)]^{n-1}\{1 - [P(3)/P(1)]\}^2 \end{aligned} \tag{6}$$

the sum of limited placement probabilities

$$\sum_{n=1}^{\infty} P_0(31)^n = P(3)\{1 - [P(3)/P(1)]\} \tag{7}$$

as well as the average limited sequence length

$$\begin{aligned} \overline{n_0(31)^n} &= \sum_{n=1}^{\infty} nP_0(31)^n \Big/ \sum_{n=1}^{\infty} P_0(31)^n \\ &= 1/\{1 - [P(3)/P(1)]\} \end{aligned} \tag{8}$$

As far as the distribution of the remaining MCE units, and of the DCE units is concerned, only the transition probability ratio P_{21}/P_{12} can be determined directly from experimental data:

$$P(1)/P(2) = P_{21}/P_{12} \tag{9}$$

For a complete characterization of the proposed first-order Markoffian statistics, one more parameter (e.g., one of the remaining transition probabilities) is needed. This may be obtained if we assume that in the domains excluding the immediate vicinity of TCE units, the placement of MCE and DCE units obeys simple Bernoulli statistics, and that also the distribution of the limited $(31)^n$ sequences among the remaining units is simply Bernoullian.

Let us designate as $P(1_3)$ the fraction of MCE units next to TCE units ("bound" MCE) and as $P(1^*)$ the remaining "free" MCE units. Then

$$\begin{aligned} P(1_3) &= \sum_{n=1}^{\infty} (n + 1)P_0(31)^n \\ &= P(3)\{2 - [P(3)/P(1)]\} \\ P(1^*) &= P(1) - P(1_3) \\ &= P(1) - P(3)\{2 - [P(3)/P(1)]\} \end{aligned}$$

The system composed of the units (1*), (2), and all the limited sequences $(31)^n$ of different length ($n = 1 - \infty$) can be regarded as a Bernoullian system with an infinite number of possibilities, defined by the relations:

$$P(2) + P(1^*) + \sum_{n=1}^{\infty} P_0(31)^n = A$$
$$P(2)' + P(1^*)' + \left[\sum_{n=1}^{\infty} P_0(31)^n\right]' = 1 \tag{10}$$

In this system

$$P(22)' = P(2)'^2$$
$$= P(2)^2/A^2$$

From here we have:

$$P(22) = P(22)'A$$
$$= P(2)^2/A$$

and the transition probability is

$$P_{22} = P(22)/P(2)$$
$$= P(2) \Big/ \left[P(1^*) + P(2) + \sum_{n=1}^{\infty} P_0(31)^n\right]$$
$$= P(2)/[P(1) + P(2) - P(3)] \tag{11}$$

All the parameters of the first-order Markoffian statistics can now be easily calculated. With them, the content of MCE sequences (unchlorinated PVC) of any length can be calculated from the relation

$$P(1)^n = P(1)P_{11}^n \tag{12}$$

as well as the average length of limited MCE (unchlorinated PVC) and DCE sequences:

$$\overline{n_0(1)^n} = 1/(1 - P_{11}) \tag{13}$$

$$\overline{n_0(2)^n} = 1/(1 - P_{22}) \tag{14}$$

EXPERIMENTAL

The methods of preparation, analysis, and of NMR and infrared spectral measurements of the investigated samples of CPVC were described in our previous communication,[5] and the same notation of samples is used throughout. In addition to the commercial suspension PVC used in our previous communication, PVC polymerized in the laboratories of this Institute was used in some of the suspension chlorinations (series 40/1–8). This was prepared in a manner analogous to that described[5] for α-d-PVC.

Tacticity of all the original PVC samples was determined from infrared spectra,[7] and syndiotacticity s was equal to 55%. Additional experimental data were obtained by the measurement and analysis of 220 MHz NMR spectra [15% (w/v) solutions of CPVC in $SOCl_2$ measured at 65°C].

RESULTS AND DISCUSSION

Solution-Chlorinated CPVC

Experimental data obtained by chlorine analysis and quantitative evaluation of 60 MHz NMR spectra of CPVC samples chlorinated in solution to a various degree are summarized in the first part of Table I; statistical parameters calculated from these data are given in the second part. In order to verify the validity of the proposed statistics, it would be necessary to compare calculated and experimental values for the populations of some of the higher sequences. An attempt was made to obtain such information from a more detailed analysis of infrared spectra and from NMR spectra measured at 220 MHz.

In infrared spectra, use was made first of all of C—Cl stretching vibrations. In unchlorinated PVC, two bands appear in this range (Fig. 1): The band at 600–640 cm^{-1} is assigned[8] to S_{HH} type Cl atoms, the contents of which corresponds to the fraction of syndiotactic plus one half of heterotactic triads ($ss + si$), which in turn is equivalent to the content of syndiotactic diads (s), i.e., overall syndiotacticity of the polymer. The other band at 660–690 cm^{-1} is assigned to S_{CH} type Cl atoms, corresponding to isotactic plus one half of heterotactic triads ($ii + is$), which again is equivalent to the content of isotactic diads (i). (The symbol S_{XY} designates a secondary chlorine atom, with indexes corresponding to atoms lying in a *trans* position with respect to the Cl atom.) By chlorination of one CH_2 group in ii and is triads, the original S_{CH} type Cl atom changes to an S_{ClC} type, or remains of type S_{CH}. The newly formed CHCl groups must have Cl atoms of type S_{CH} or S_{ClH}. All these types of Cl atoms, as well as the CCl_2 groups formed by chlorination, absorb above 660 cm^{-1}. By introduction of one Cl atom into one CH_2 group in ss and si triads, the corresponding S_{HH} type Cl atom either changes to an S_{ClH} type, or remains of S_{HH} type, with equal probability. The newly formed CHCl groups have an S_{ClH} type Cl atom. By introduction of two Cl atoms into one CH_2 group in ss and si triads, the corresponding S_{HH} type Cl atom changes to S_{ClH}. This, as well as the newly formed CCl_2 group, absorb

TABLE I
Statistical Parameters Calculated from Experimetal Data for Solution-Chlorinated CPVC

Sample	Cl, %	R^a	j^b	$P(1)$	$P(2)$	$P(3)$	P_{11}	P_{12}	P_{13}	P_{21}	P_{22}
CPVC-A	64.2	0.54	0.46	0.66	0.24	0.10	0.60	0.25	0.15	0.70	0.30
CPVC-B	66.4	0.33	0.58	0.48	0.46	0.06	0.42	0.46	0.12	0.48	0.52
CPVC-C	67.2	0.37	0.64	0.50	0.36	0.14	0.36	0.36	0.28	0.50	0.50
CPVC-D	68.3	0.29	0.70	0.42	0.46	0.12	0.32	0.42	0.26	0.39	0.61
CPVC-E	69.7	0.25	0.79	0.36	0.48	0.16	0.17	0.39	0.44	0.29	0.71
CPVC-F	69.8	0.25	0.79	0.36	0.48	0.16	0.17	0.39	0.44	0.29	0.71

[a] Number of additional Cl atoms per monomeric unit.

[b] Ratio of CH_2/CHCl groups from band areas in NMR spectra.

TABLE II
Average Sequence Lengths and Some Sequence Populations in Solution Chlorinated CPVC

Sample	$\overline{n_0(1)}$	$\overline{n_0(2)}$	$\overline{n_0(31)}$	$P(11)$	$P(12)$	$P(111)$	$[P(11) + P(12)]$	
							Calcd	IR[a]
CPVC-A	2.5	1.4	1.2	0.40	0.17	0.24 (0.26)[b]	0.57	0.55
CPVC-B	1.7	2.1	1.1	0.20	0.22	0.08	0.42	0.40
CPVC-C	1.6	2.0	1.4	0.18	0.18	0.06	0.36	0.37
CPVC-D	1.5	2.6	1.4	0.13	0.18	0.04	0.31	0.31
CPVC-E	1.2	3.4	1.8	0.06	0.14	0.01	0.20	0.18
CPVC-F	1.2	3.4	1.8	0.06	0.14	0.01 (0.00)[b]	0.20	0.17

[a] Experimental values from infrared spectra.
[b] Experimental value from 220 MHz NMR spectra.

above 660 cm^{-1}. Similarly, if both CH_2 groups in *ss* or *si* triads are chlorinated by one Cl atom each, none of the Cl atoms in the newly formed sequence —CHCl—CHCl—CHCl— can be of type S_{HH}. To summarize, no S_{HH} type Cl atoms can be formed by chlorination. Consequently, the band at 600–640 cm^{-1} assigned to S_{HH} type Cl atoms in

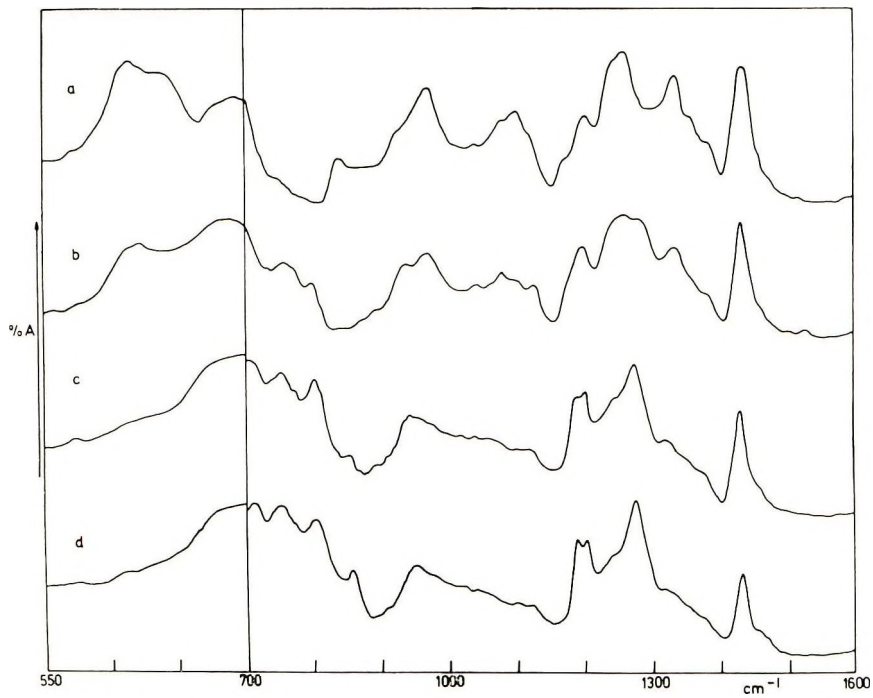

Fig. 1. Infrared spectra of chlorinated PVC: (*a*) unchlorinated VPC; (*b*) suspension-chlorinated CPVC-4, $j = 0.57$; (*c*) solution-chlorinated CPVC, sample B, $j = 0.58$; (*d*) solution-chlorinated CPVC, sample F, $j = 0.79$.

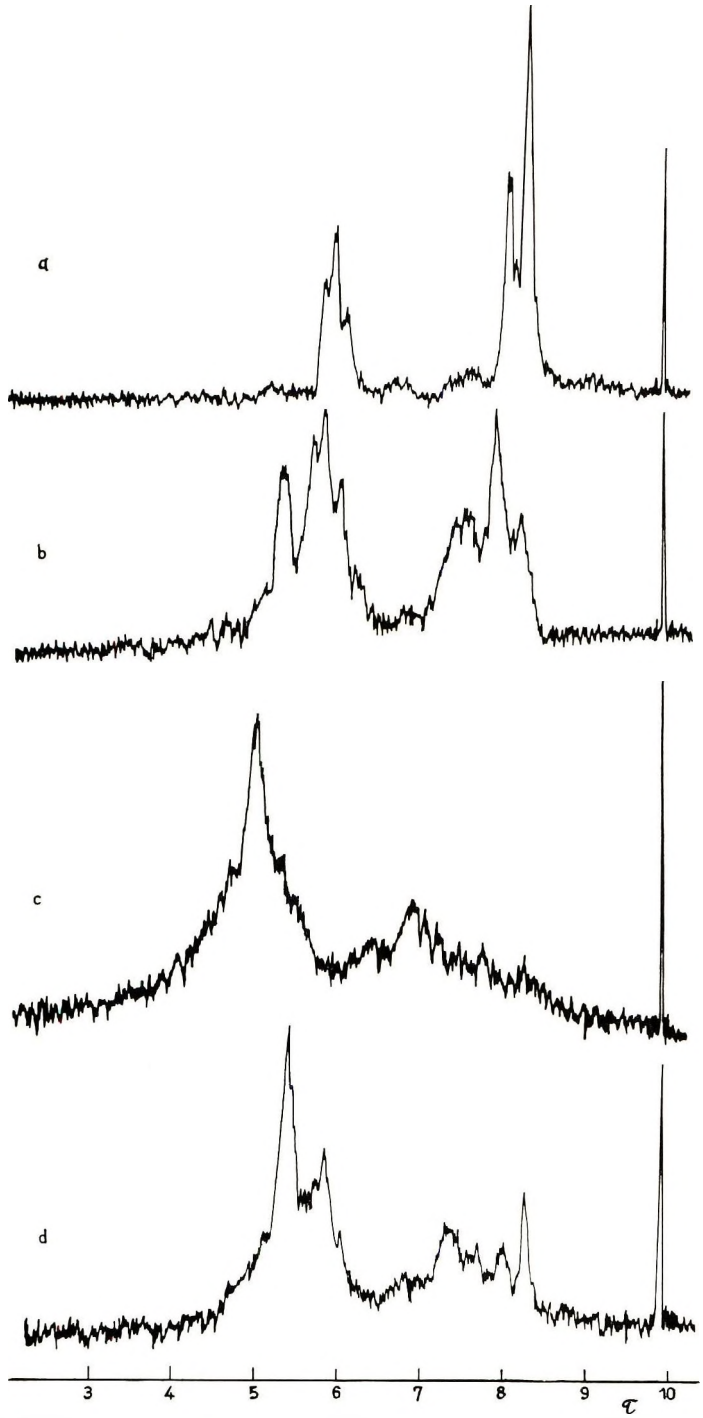

Fig. 2. NMR spectra of chlorinated PVC: (*a*) unchlorinated PVC; (*b*) solution-chlorinated CPVC, sample A, $j = 0.46$; (*c*) solution-chlorinated CPVC, sample F, $j = 0.79$; (*d*) suspension-chlorinated CPVC, sample 40/8, $j = 0.93$.

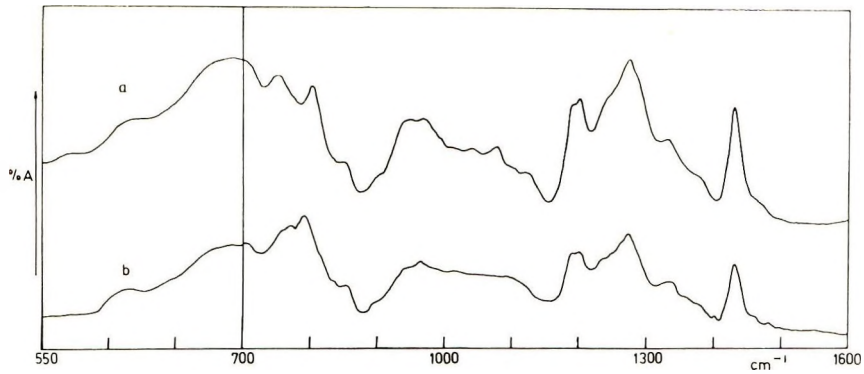

Fig. 3. Infrared spectra of suspension-chlorinated CPVC: (*a*) sample CPVC-8, j = 0.91; (*b*) sample 40/8, j = 0.93.

CPVC is a measure of the content of the group —CH_2—CHCl—CH_2—, i.e., of (11) sequences of type *ss* and *si*. In addition, S_{HH} type Cl atoms appear in one half of the groups —CH_2—CHCl—CHCl—, corresponding to (12) and (21) sequences of the same tacticity. The area of the band at 600–640 cm^{-1} (Fig. 1) should therefore correspond to $P(11) + P(12)$ in the syndiotactic fraction of the polymer. Experimental values of this band area, expressed as a fraction of the original *s* diads in unchlorinated PVC, are shown in Table II. These values are seen to agree well with the values $P(11) + P(12)$ calculated from the statistical parameters for the whole polymer on the assumption that the chlorination mechanism does not significantly differ in the syndiotactic and isotactic units. This indicates that the basic assumption is at least approximately correct.

In NMR spectra of unchlorinated PVC, methylene group protons in *s* diads absorb at highest field (τ = 8.29), and the peaks of the *i* diads are centered at a field lower by about 0.2 ppm. Shifts between centers of bands of various tetrad sequences differing by steric arrangement are of the order 0.01–0.05 ppm, and the bands of all the tetrads are moreover split by spin–spin interaction, so that the methylene proton band area extends over about 0.5 ppm. By chlorination of neighboring methylene groups, all these bands are shifted downfield, extending the methylene proton band range to 2.0 ppm. In 220 MHz spectra (Fig. 2), a few pronounced peaks appear on the methylene proton band in CPVC, but their assignment to various sequences is very difficult because of the enormous variety of steric arrangements and substitution types present. Only the sharp peak at highest field (τ = 8.29) may be assigned to residual unchlorinated syndiotactic PVC units. It is known[4] that substitution by one Cl atom at the β-carbon causes a downfield shift of the corresponding methylene proton band by 0.2 ppm, whereas substitution on the δ-carbon may be expected to be negligible. The band at τ = 8.29 is therefore assumed to correspond to sequences of at least three MCE units (111), the central of which is syndiotactic. Bands of (111) sequences centered

on an isotactic diad are, of course, overlapped by bands of methylene groups in more highly chlorinated sequences. If we assume that the chlorination mechanism does not depend on tacticity, then the overall population of (111) units can be determined from the relative band area of the band at $\tau = 8.29$ and from the known content of syndiotactic placements in the polymer. Experimental values obtained in this way from 220 MHz spectra of the solution chlorinated samples A and F are indicated in parentheses in Table II, and good agreement with the value $P(111)$ calculated from statistical parameters is found. For a true verification of the proposed statistics, of course, an experimental determination of the content of a larger number of various sequences would be required. Such information could be obtained, e.g., by analysis of the methine proton band in NMR spectra of chlorinated β,β-d_2-PVC, which will be the subject of a subsequent communication.

Suspension-Chlorinated CPVC

From infrared spectra, suspension chlorinated CPVC contains more S_{HH} type Cl atoms (band at 600–640 cm^{-1}) than solution chlorinated CPVC of the same molar chlorine content (Fig. 1). Also from NMR spectra, a higher content of unchlorinated (111) sequences (band at $\tau = 8.29$, Fig. 2) is indicated. Besides that, in the whole range of infrared spectra of all suspension chlorinated CPVC samples, typical bands of unchlorinated PVC, corresponding to relatively long sequences of MCE units are clearly evident (Fig. 1); infrared spectra of all these samples, even of those with a low j value, can be constructed by a superposition of the spectra of unchlorinated PVC and of CPVC solution chlorinated to a very high degree in suitable proportion. From this we assume that, at arbitrary values of j, chlorination proceeds to a very high degree in some parts of the polymer, whereas other parts remain intact. The relative content of intact PVC decreases with increasing j, but it also seems to depend on the character of the original PVC used for chlorination (Fig. 3). As long as a reliable method for a quantitative determination of residual PVC in suspension chlorinated samples of CPVC is not available, a statistical analysis of these samples does not seem warranted.

We wish to thank Dr. W. Brügel of BASF, Ludwigshafen, for the kind measurement of 220 MHz NMR spectra, and to Ing. V. Kuška of the Institute of Petrochemistry, Nováky, for the chlorination of PVC samples.

References

1. J. Petersen and B. Ranby, *Makromol. Chem.*, **102,** 83 (1967).
2. S. Sobajima, N. Takagi, and H. Watase, *J. Polym. Sci. A-2,* **6,** 223 (1968).
3. P. Q. Tho and P. Berticat, *Europ. Polym. J.*, **4,** 265 (1968).
4. G. Svegliado and F. Zilio Grandi, *J. Appl. Polym. Sci.*, **13,** 1113 (1969).
5. M. Kolínský, D. Doskočilová, B. Schneider, J. Štokr, E. Drahorádová, and V. Kuška, *J. Polym. Sci. A-1,* **9,** 797–800 (1971).
6. F. P. Price, *J. Chem. Phys.*, **36,** 209 (1962).

7. J. Štokr, B. Schneider, M. Kolínský, M. Ryska, and D. Lím, *J. Polym. Sci. A-1*, **5**, 2013 (1967).

8. B. Schneider, J. Štokr, D. Doskočilová, M. Kolínský, S. Sýkora, and D. Lím, in *Macromolecular Chemistry Prague 1965* (*J. Polym. Sci. C*, **16**), O. Wichterle and B. Sedláček, Eds., Interscience, New York, 1968, p. 3891.

Received March 2, 1971

JOURNAL OF POLYMER SCIENCE: PART A-1 VOL. 9, 2763–2773 (1971)

Emulsion Polymerization. VII. Effects of Instantaneous Chain Termination During the Interval of Particle Nucleation*

J. L. GARDON *M&T Chemicals Inc., Rahway, New Jersey 07065*

Synopsis

In the Smith-Ewart treatment of particle nucleation all particles were assumed to grow as if they contained exactly one radical. Modification of particle growth rate by chain termination in growing particles and reinitiation of nongrowing particles by radicals entering them was neglected in this interval although such effects were taken into account after the particle number became constant. The present theory eliminates this inconsistency for the case where chain termination is instantaneous. This refinement does not change previous predictions for the final number of particles, the steady state rate or the particle radius. Unlike the old theory, the present theory predicts continuous decay of the average number of radicals per particle from the initial value of unity to the steady-state value of one half. It also provides new theoretical predictions for the shape of the conversion-time curve at the initial stages of the reaction. Experimental data are reviewed in the context of the theory. Experimental particle sizes, steady-state conversion rates, and conversions at completion of particle nucleation were often in good quantitative agreement with the theoretical predictions. The predicted maximum in the conversion rate at the time when particle nucleation became completed was observed in a few instances. The theoretically predicted initial shape of the conversion-time curve may not be always observable due to experimental difficulties mainly associated with induction effects.

INTRODUCTION

In emulsion polymerization, a new polymer particle is nucleated by a polymeric radical not captured by an existing particle.[1–4] In the Smith-Ewart model for particle nucleation[1–3] radicals captured by existing particles were accounted for only insofar that they did not nucleate new particles; their effect upon the growth rate of the capturing particles by chain initiation or chain termination was neglected. Each growing particle was assumed to contain a single radical so that the average number of radicals, Q, per particle was postulated to be unity throughout the interval of particle nucleation.

Contrary to this, the value of Q was assumed[1–3] to be responsive to the rates of chain initiation, propagation and termination at the stages of polymerization where the particle number became constant. In a special

* Presented at the Symposium on Polymer Colloids, American Chemical Society Meeting, Chicago, Ill., September 1970.

case, when the termination rate is very fast, Q was shown to assume the value of one half. Slow termination within particles[5-7] or termination by radical desorption[6-8] was shown to cause Q to be become time-dependent, with values higher or lower than one half, respectively.

The interval of particle nucleation was heretofore less rigorously described by the theory than the subsequent interval where the particle number is constant. Below, a theory for the interval of particle nucleation is presented which takes chain termination and particle reinitiation into account. For sake of the convenience, instantaneous termination is assumed, although this assumption has no general validity.[6-9] The theory is presented in the context of a mechanistic picture described in detail elsewhere[1-4] and is a refinement on previous treatments of this problem.[10,11]

GENERAL EXPRESSIONS FOR CONVERSION RATE

An equation for conversion rate can be derived[2,3] by using the sole assumption that the locus of polymerization is within the monomer swollen latex particle.

$$dP/dt = (k_p/N_A)\ (d_m/d_p)\phi_m N_t\ Q \tag{1}$$

Here P is volume of polymer per unit volume (cubic centimeters) of water, k_p is the propagation rate constant, N_A is the Avogadro number, d_m and d_p are densities of monomer and polymer, ϕ_m is the volume fraction of monomer in the particles, N_t is the number of particles per unit volume of water at time t and Q is the average number of radicals per particle.

The value of ϕ_m was shown to an insensitive function of particle size as long as there is enough unconverted monomer present in the reactor to keep the particles saturated.[12]

If termination is instantaneous, two radicals cannot coexist in the same particle. A radical entering a particle already containing a growing radical causes instant termination of both radicals. A radical entering a dead particle initiates the growth of a single chain in it. When steady state is reached, each particle is either growing or is dead half of the time so that Q becomes one half. At this steady state, the particle nucleation is already complete so that the particle number is at its final value, N. The conversion rate corresponding to these assumptions is the Smith-Ewart rate, B.

$$B = 0.5\ (k_p/N_A)\ (d_m/d_p)\phi_m N \tag{2}$$

If the assumptions above do not hold, the rate is not constant even if ϕ_m remains independent of time. The equation below shows the difference between dP/dt and B.

$$dP/dt = B(Q/0.5)\ (N_t/N) \tag{3}$$

During particle nucleation, N_t/N is bound to be less than unity. As to Q, it can deviate from 0.5 not only as a result of termination rate effects[3-9] but also because at early stages of the reaction the number of particles

containing a single radical is higher than predicted by the steady state condition of equal initiation and termination rates. This latter effect is the main subject of the present investigation.

Equation (3) is generally applicable for the so-called intervals I and II[2,3] without regard to the rate and mode of termination. A simplification is possible if termination is instantaneous. The number of live and dead particles at any given time is N_1 and N_0 such that:

$$N_t = N_1 + N_0 \tag{4}$$

and the value of Q is:

$$Q = N_1/N_t \tag{5}$$

Combination of eqs. (3) and (5) gives:

$$dP/dt = B(2N_1/N) \tag{6}$$

MATHEMATICAL MODEL FOR INTERVAL OF PARTICLE NUCLEATION

Integral Equations for the Number of Particles

The number of radicals produced per cubic centimeter of water per second is R and is contant.[13] The effective interface between the water and the organic phase (micelles + particles) is assumed to be saturated with soap molecules and its value is constant during particle nucleation, S square centimeters per cubic centimeter of water[13]. Particles absorb radicals at a rate proportional to their surface.[2] When the surface of all monomer swollen latex particles, $4\pi(\sum n_i r_i^2)_t$, where n_i is the number of particles with radius r_i in per cubic centimeter of water, reaches the value of S, particle nucleation stops. All radicals enter the organic phase, but radicals captured by particles do not nucleate new particles. This model gives the differential equation of particle nucleation:

$$dN_t/dt = R[1 - (4\pi/S)(\sum n_i r_i^2)_t] \tag{7}$$

If the mechanism of particle nucleation is not by radical capture into micelles but by precipitation of oligomeric polymer radicals from water, the mathematical form of eq. (7) does not change,[2,4] although the significance of the parameter S may differ.[2]

In analogy to eq. (4), the surfaces or live and dead particles are to be separately treated:

$$(\sum n_i r_i^2)_t = (\sum n_i r_i^2)_1 + (\sum n_i r_i^2)_0 \tag{8}$$

Live particles are formed when new particles are nucleated at a rate equal to dN_t/dt [eq. (7)] and when dead particles absorb radicals at a rate equal to $4\pi(\sum n_i r_i^2)_0 R/S$. Live particles are destroyed when they capture a radical at a rate equal to $4\pi(\sum n_i r_i^2)_1 R/S$.

Similarly, dead particles are formed when radials enter live particles at a rate of $4\pi(\sum n_i r_i^2)_1 R/S$ and are destroyed when they capture radicals at a

rate $4\pi(\sum n_i r_i^2)_0 R/S$. In the corresponding integral equations below, the time Υ is an auxiliary variable such that $0 < \Upsilon < t$ and the values of the summed surfaces in integrals correspond to those at time Υ.

$$N_1 = R\int_0^t [1 - (8\pi/S)(\sum n_i r_i^2)_1]\, d\Upsilon \tag{9}$$

$$N_0 = (4\pi R/S)\int_0^t [(\sum n_i r_i^2)_1 - (\sum n_i r_i^2)_0]\, d\Upsilon \tag{10}$$

Integral Equations for Particle Surfaces

To solve the equations for particle numbers the time dependence of particle surfaces must be specified. Earlier work[2] showed the time dependence of the cubed radius of a particle containing a single radical:

$$dr^3/dt = K = (3/4\pi)(k_p/N_A)(d_m/d_p)\phi_m(1 - \phi_m) \tag{11}$$

It follows that a live particle created at time Υ will have an increment square radius equal to $K^{2/3}(t - \Upsilon)^{2/3}$ at time t.

The total surface (or summed squares of radii) of live particles contain three components: the positive contributions by the surfaces of newly nucleated particles and of dead particles transformed into live ones by radical capture are coded with single and double asterisks; the negative contribution of live surface loss due to radical capture by live particles is coded a triple asterisk.

At time Υ and during $d\Upsilon$, the number of particles nucleated is $(dN_\Upsilon/d\Upsilon)d\Upsilon$ shown in eqs. (7) and (8). At time t each such particle has a surface, $K^{2/3}(t\text{-}\Upsilon)^{2/3}$, so that the total surface of such particles is:

$$(\sum n_i r_i^2)_1{}^* = \int_0^t R\{1 - (4\pi/S)[(\sum n_i r_i^2)_1 + (\sum n_i r_i^2)_0]\}K^{2/3}(t\text{-}\Upsilon)^{2/3} d\Upsilon \tag{12}$$

At time Υ the number of live particles created by radical entry into dead ones during $d\Upsilon$ is $[4\pi(\sum n_i r_i^2)_0/S]Rd\Upsilon$. Each of these particles has a number-average cubed radius at time Υ equal to $[(\sum n_i r_i^2)_0/N_0]^{3/2}$, and at time t this cubed radius is increased by $K(t - \Upsilon)$. At time t, the average squared radius of each of these particles is $\{K(t - \Upsilon) + [\sum n_i r_i^2)_0/N_0]^{3/2}\}^{2/3}$. It follows that:

$$(\sum n_i r_i^2)_1{}^{**} = \int_0^t \{K(t - \Upsilon) + [(\sum n_i r_i^2)_0/N_0]^{3/2}\}^{2/3}[4\pi(\sum n_i r_i^2)_0/S]Rd\Upsilon \tag{13}$$

At time Υ during $d\Upsilon$, the number of live particles turned into dead ones is $4\pi(\sum n_i r_i^2)_1/S)Rd\Upsilon$ and each has an average squared radius of $(\sum n_i r_i^2)_1/N_1$ to give:

$$(\sum n_i r_i^2)_1{}^{***} = \int_0^t 4\pi[(\sum n_i r_i^2)_1{}^2/N_1](R/S)d\Upsilon \tag{14}$$

The total surface of live particles is calculated from the following summed squared radii:

$$(\sum n_i r_i^2)_1 = (\sum n_i r_i^2)_1{}^* + (\sum n_i r_i^2)_1{}^{**} - (\sum n_i r_i^2)_1{}^{***} \tag{15}$$

The surface of dead particles is derived in analogy to eq. (14) to be:

$$(\sum n_i r_i^2)_0 = (4\pi R/S)\int_0^t \{[(\sum n_i r_i^2)_1^2/N_1] - [(\sum n_i r_i^2)_0^2/N_0]\}d\Upsilon \quad (16)$$

Integral Equations for Conversion and Particle Volume

The volume of all live particles can be calculated from three components derived in analogy to eqs. (13)–(16).

$$(\sum n_i r_i^3)_1^* = \int_0^t R\{1 - (4\pi/S)[(\sum n_i r_i^2)_1 + (\sum n_i r_i^2)_0]\}K(t - \Upsilon)d\Upsilon \quad (17)$$

$$(\sum n_i r_i^3)_1^{**} = \int_0^t \{K(t - \Upsilon) + [(\sum n_i r_i^2)_0/N_0]^{3/2}\}[4\pi(\sum n_i r_i^2)_0/S]Rd\Upsilon \quad (18)$$

$$(\sum n_i r_i^3)_1^{***} = \int_0^t 4\pi[(\sum n_i r_i^2)_1^{5/2}/N_1^{3/2}](R/S)d\Upsilon \quad (19)$$

$$(\sum n_i r_i^3)_1 = (\sum n_i r_i^3)_1^* + (\sum n_i r_i^3)_1^{**} - (\sum n_i r_i^3)_1^{***} \quad (20)$$

Similarly, the volume of dead particles is derived in analogy to eq. (16):

$$(\sum n_i r_i^3)_0 = (4\pi R/S)\int_0^t \{[(\sum n_i r_i^2)_1^{5/2}/N_1^{3/2}] - [(\sum n_i r_i^2)_0^{5/2}/N_0^{3/2}]\}d\Upsilon \quad (21)$$

Numerical Solutions in Dimensionless Variables

As earlier,[2] the dimensionless variables ν, y, x, and ξ are introduced:

$$\nu/N = \nu_1/N_1 = \nu_0/N_0 = 4(5/12\pi)^{2/5}S^{-3/5}(K/R)^{2/5} \quad (22)$$

$$y/(\sum n_i r_i^2) = y_1/(\sum n_i r_i^2)_1 = y_0/(\sum n_i r_i^2)_0 = 4/S \quad (23)$$

$$x/t = \xi/\Upsilon = (12\pi/5)^{3/5}K^{2/5}(R/S)^{3/5} \quad (24)$$

The dimensionless equations for particle numbers corresponding to eqs. (9) and (10) are:

$$\nu_1 = (5/3)\int_0^x [(1/\pi) - 2y_1]d\xi \quad (25)$$

$$\nu_0 = (5/3)\int_0^x (y_1 - y_0)d\xi \quad (26)$$

The dimensionless equations for particle surfaces corresponding to eqs. (15) and (16) are:

$$y_1 = 5/3\int_0^x \{[(1/\pi) - y_1 - y_0](x - \xi)^{2/3} + y_0[x - \xi + (y_0/\nu_0)^{3/2}]^{2/3} - (y_1^2/\nu_1)d\xi \quad (27)$$

$$y_0 = 5/3\int_0^x [(y_1^2/\nu_1) - (y_0^2/\nu_0)]d\xi \quad (28)$$

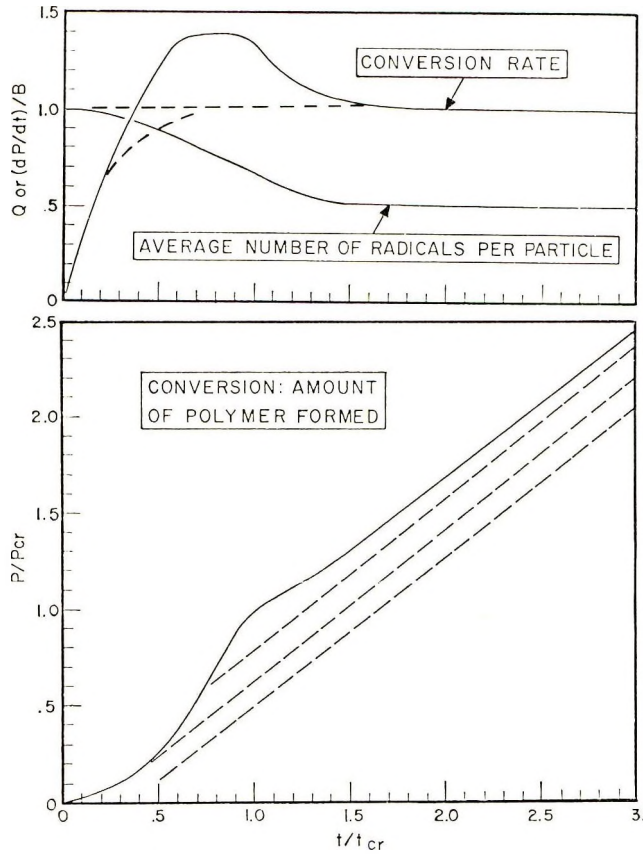

Fig. 1. Variation of conversion rate, average number of radicals per particle, and conversion with time: (——) theory; (- -) experimental results with positive induction times. According to the theory, particle nucleation should stop at time $t = t_{cr}$. The time-dependent theoretical rate is dP/dt and B is the Smith-Ewart rate. The average number of radicals per particle is Q. The volume of polymer per unit volume of water is P, and P_{cr} is the value of P at t_{cr}. The values of t_{cr}, B, and P_{cr} are shown in Table I.

Simultaneous numerical solutions by use of the Simpson rule[2] define the time dependence of particle numbers and particle surfaces. Once this is known, the variation of total particle volume and of conversion with time can be calculated. The dimensionless variable[2] representing these quantities is z:

$$z = 4(12\pi/5)^{1/5}S^{-6/5}(R/K)^{1/5}(\sum n_i r_i^3) \tag{29}$$

$$z = 1.425S^{-6/5}(R/K)^{1/5}P/(1 - \phi) \tag{30}$$

Combination of eqs. (17)–(21) and (29) gives:

$$z = (5/3)\int_0^x [(1/\pi) - y_1](x - \xi)d\xi \tag{31}$$

TABLE I
Summary of Theoretical Predictions

Definition	Results of present theory[a]	Typical expected experimental result[b]	Results of present theory divided by that of Part II[2]
Number of particles per cc of water	$N = 0.208\, S^{0.6}(RK)^{0.4}$	9.6×10^{14}	1.000
Root-mean-cube average radius, cm	$r = 1.05[d_{water}/d_p(m/w)]^{0.333}S^{-0.2}(K/R)^{0.3333}$	5.5×10^{-6}	1.000
Time when particle nucleation stops, sec	$t_{cr} = 0.341(S/R)^{0.6}K^{-0.4}$	252	0.935
Volume polymer, when particle nucleation stops, cc/cc water	$P_{cr} = 0.198(1 - \phi_m)S^{1.2}(K/R)^{0.2}$	0.02[c]	0.950
Steady-state conversion rate, cc polymer/cc of water per sec	$B = 0.435(1 - \phi_m)(KS)^{0.6}R^{0.4}$	5.02×10^{-5} [c]	1.000

[a] The parameter K is given in eq. (11). Other parameters: $S = A_S N_A[S]$ and $R = 2k_d N_A[I]$, where A_S is the area per soap molecule, k_d is decomposition rate constant, [S] and [I] are molar soap and initiator concentrations in water; m/w is the monomer/water ratio.

[b] Styrene/water = 40/60, 50°C, 0.1% $K_2S_2O_8$ and 0.5% Na lauryl sulfate in water; cf. Part II.[13]

[c] If m/w is 40/60, the indicated value of P_{cr} is at 3% conversion and the indicated value of B corresponds to a rate of 0.5%/min.

By definition, particle nucleation stops at the critical time x_{cr} when the sum, $y_1 + y_0$, becomes equal to $1/\pi$. The calculated values of critical variables are $x_{cr} = 0.3737$ and $z_{cr} = 0.286$. Following eqs. (5) and (6), Q and the deviation from the Smith-Ewart rate are defined:

$$Q = \nu_1/\nu \tag{32}$$

$$(dP/dt)/B = 2\nu_1/\nu_{cr} \tag{33}$$

It is noteworthy that the value of Q at x_{cr} is 0.655. The results of numerical integrations are shown in Figure 1 and Table I.

DEVIATION FROM STEADY STATE AFTER PARTICLE NUCLEATION IS COMPLETE

Since at time t_{cr}, corresponding to x_{cr}, when particle nucleation is complete, Q has not yet reached the steady-state value of 0.5, the rate of decay of Q from its critical value 0.655 to 0.5 is of interest.

The calculations outlined above show that the surface of all live particles divided by that of all particles is 0.63 at t_{cr}, close to $(N_0/N)_{cr} = 0.655$. It is thus justifiable to assume that particles in this case absorb radicals at a rate independent from their size, although in reality they absorb radicals at a rate proportional to their surfaces.

Live particles are formed when radicals enter into dead particles at a rate, $[(N - N_1)/N]R$, and are destroyed when they enter live particles at a rate $(N_1/N)R$. The value of Q is N_1/N. It follows that:

$$dN_1/dt = R[1 - 2(N_1/N)] \tag{34}$$

$$dQ/dt = (R/N)\ [1 - 2Q] \tag{35}$$

The equivalents of eqs. (34) and (35) in dimensionless variables are:

$$dQ/dx - 1.425(1 - 2Q) \tag{36}$$

$$dz/dx = 0.372Q \tag{37}$$

The solutions for the boundary conditions $Q = 0.655$, $z = 0.286$ and $x = 1.152$ are trivial. The results are plotted on Figure 1.

DISCUSSION

The mathematical approximations involved in previous work,[1,2] where chain termination was neglected for the interval of particle nucleation is now found to have caused negligible error in calculating the quantities shown in Table I. The errors are smaller than their previous cursory estimates[2,10,11] indicated.

There is a large body of experimental data obtained mainly with styrene, methyl methacrylate, and other monomers, and reviewed earlier[3,9,13] which shows good quantitiative agreement with the theoretical prediction for the particle number N, the particle size r, and the steady-state conversion rate

B. Burnett's[14] heretofore uninterpreted results may serve as an illustration for this body of data. The styrene/water ratio was 0.126, the concentration of $K_2S_2O_8$ and potassium stearate in water were 0.075% and 1.25%, respectively, and the temperature was 40°C. The conversion corresponding to the theoretical value of P_{cr} was 9.1%. The theoretical values shown in Table II were calculated by using the equations of Table I with the parameters of Part II.[13]

On considering the uncertainties in the values of the parameters,[13,15] the agreement is as good as can be expected. Also, very recently Breitenbach[16] found very good agreement between theoretical and experimental steady-state conversion rates in styrene polymerization by using various levels of α,α'-azobismethylbutyronitrile–γ-Na sulfonate initiator and sodium palmitate soap.

The exact values of P_{cr} are difficult to establish experimentally. In most practical recipes, its theoretical value should be in the 0.005 to 0.05 range, corresponding to few per cent conversion if the monomer/water ratio is in the practical range of 30/70 to 50/50. The available data reviewed elsewhere[2,3] are consistent with the theory in that particle nucleation was found to stop at low conversion.

While N, r, and B can be accurately determined, and while the order of magnitude of P_{cr} is also experimentally available, the experimental difficulties are very great for obtaining meaningful values for t_{cr}, and meaningful conversion–time curves for the initial stages of the reaction. Even careful purification of reactants and careful exclusion of oxygen will not completely eliminate an induction time. The theory predicts a negative apparent induction time; since the linear portion of the conversion–time curve at $t > t_{cr}$ extrapolates to a negative value of the time as shown in Figure 1. Most often, positive induction times are experimentally found because inhibiting impurities are not completely eliminated from the reaction mixture. Some of the reported[14,16–18] conversion–time curves falling within the interval of particle nucleation are largely linear, indicating that inhibition effects may have forced the conversion-time relationships to follow one of the dotted lines of Figure 1.

If the monomer/water ratio of the charge is lower than in industrial recipes and just high enough to allow the monomer droplets to keep the particles saturated with monomer until particle nucleation stops but not further, the only portion of the total conversion-time curve expected to be linear is that predicted to exist between $0.5\,t_{cr}$ and t_{cr} which has a slope 30% to 40% higher than that corresponding to B. If the monomer/water ratio is even lower, the monomer concentration in the particles (ϕ_m) cannot

TABLE II

	Experiment	Theory
$N \times 10^{-14}$	7.6	4.7
Conversion rate, %/min	0.97	0.79

remain constant at $t < t_{cr}$, and the effective value of K must decrease with increasing time. At constant K the conversion rate is expected to increase with time at $t < 0.9\ t_{cr}$. This effect can be offset if K decreases and an apparently linear conversion–time relationship with a slope lower than the theoretical B may be obtained as in Breitenbach's[16] experiments involving sodium lauryl sulfate surfactant.

The theory represented by Figure 1 predicts that initially the conversion rate should be lower than the steady-state rate; that a few minutes after the start of the reaction it should pass through maximum exceeding the steady-state rate by about 40%; and that subsequently it should quickly reach the steady-state rate. In radiation-initiated polymerization of ethyl acrylate and methyl acrylate at a high enough monomer/water ratio, Hummel[19,20] was able to eliminate induction effects. For these monomers, the shape of the plots of conversion rate against time was similar to that of Figure 1. Gerrens[21] also reported a maximum in the conversion rate at about 5 min after the start of reaction in the emulsion polymerization of methyl methacrylate with relatively high concentration of persulfate. Van der Hoff[22] experimented with styrene at low surfactant concentration and obtained an inflection point in the conversion time curve similar to that shown in Figure 1. These are the only instances where maxima in the rate–time relationship were reported in the region of t_{cr}. Initially low rates, which increased until a steady state was reached, were found for styrene and methyl methacrylate with x-ray initiation by Hummel[19,20] and with persulfate initiation by Gerrens.[21,23] Manyasek[24] also found similar curves in the persulfate-initiated polymerization of styrene and chloroprene.

Mrs. D. Wood carried out the calculations on the computer.

References

1. W. V. Smith and R. H. Ewart, *J. Chem. Phys.*, **16**, 592 (1948).
2. J. L. Gardon, *J. Polym. Sci. A-1*, **6**, 623 (1968) (Part I).
3. J. L. Gardon, *Brit. Polym. J.*, **2**, 1 (1970); *Rubber Chem. Technol.*, **43**, 74 (1970).
4. C. P. Roe, *Ind. Eng. Chem.*, **60**, 20 (1968).
5. J. L. Gardon, *J. Polym. Sci. A-1*, **6**, 665 (1968) (Part III).
6. W. H. Stockmayer, *J. Appl. Polym. Sci.*, **24**, 314 (1957).
7. J. T. O'Toole, *J. Appl. Polym. Sci.*, **9**, 1291 (1965).
8. J. Ugelstad and P. C. Mork, *Brit. Polym. J.*, **2**, 31 (1970).
9. J. L. Gardon, *J. Polym. Sci. A-1*, **6**, 687 (1968) (Part IV).
10. A. G. Parts, D. E. Moore, and J. G. Watterson, *Makromol. Chem.*, **89**, 156 (1965).
11. J. G. Watterson, A. G. Parts, and D. E. Moore, *Makromol. Chem.*, **116**, 1 (1968).
12. J. L. Gardon, *J. Polym. Sci. A-1*, **6**, 2859 (1968) (Part VI).
13. J. L. Gardon, *J. Polym. Sci. A-1*, **6**, 643 (1968) (Part II).
14. G. M. Burnett and R. S. Lehrle *Proc. Roy. Soc.* (London) **A253**, 331 (1959).
15. T. P. Paxton, paper presented at the 43rd National Colloid Symposium, Division of Colloid and Surface Chemistry, American Chemical Society, June 23–25, 1969; *Reprints*, p. 45; *J. Colloid Interface Sci.*, in press.
16. J. W. Brietenbach, K Kuchner, H. Fritze, and H. Tarnowiecki, *Brit. Polym. J.*, **2**, 13 (1970).
17. I. D. Robb, *J. Polym. Sci. A-1*, **7**, 417 (1969).

18. J. W. Breitenbach and H. Edelhauser, *Makromol. Chem.*, **44**, 196 (1961).
19. D. Hummel, *Angew. Chem.*, **75**, 330 (1963).
20. D. Hummel, G. Ley, and C. Schneider, *Advan. Chem. Ser.*, **34**, 60 (1962).
21. H. Gerrens, *Ber. Bunsenges. Physik Chem.*, **67**, 741 (1963).
22. B. M. E. Van der Hoff, *Adv. Chem. Ser.*, **34**, 6 (1962).
23. E. Bertholome, H. Gerrens, R. Herbeck, and H. M. Weitz, *Z. Elektrochem.*, **60**, 334 (1956).
24. Z. Manyasek and A. Rezabek, *J. Polym. Sci.*, **56**, 47 (1962).

Received March 19, 1971
Revised April 20, 1971

JOURNAL OF POLYMER SCIENCE: PART A-1 VOL. 9, 2775–2787 (1971)

Synthesis and Characterization of Poly-β-Hydroxybutyrate. I. Synthesis of Crystalline DL-Poly-β-Hydroxybutyrate from DL-β-Butyrolactone

D. E. AGOSTINI,* J. B. LANDO, and J. REID SHELTON,
Case Western Reserve University, Cleveland, Ohio 44106

Synopsis

The polymerization of β-butyrolactone was investigated as a possible monomer for a proposed synthesis of the naturally occurring polyester, D-poly-β-hydroxybutyrate (D-PHB). The racemic DL-monomer was used in this initial study to determine the best conditions and catalyst system for use in a subsequent study of the polymerization of optically active β-butyrolactone. In so doing it was found that certain organometallic catalysts (Et_2Zn and Et_3Al) plus a cocatalyst of water produced highly crystalline samples of polyester from the racemic monomer. This paper describes the synthesis and characterization of the racemic polymer obtained using these catalyst systems, and compares the results obtained with certain other catalysts that were also investigated for this purpose. Examination of the DL-PHB by infrared, NMR, x-ray, and electron microscopy shows that it is possible to synthesize a crystalline racemic polymer that is virtually identical (excepting optical activity) to the naturally occurring polymer, D-PHB.

INTRODUCTION

D-Poly-β-hydroxybutyrate (D-PHB) is a naturally occurring polyester, synthesized by various types of bacteria by the condensation of D-(−)-β-hydroxybutryl coenzyme A. As formed in nature, the polymer is highly crystalline and optically active, and physiologically functions as both a source of energy and carbon supply for the bacteria.[1] Early workers[2–4] presented evidence for the structure (I) of D-PHB:

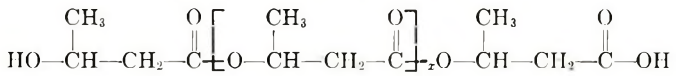

I

Although much work has been done in the synthesis of a similar polymer, poly-β-hydroxypropionate (II) from β-propiolactone,[5–11] optically active PHB has never been synthesized in the laboratory.

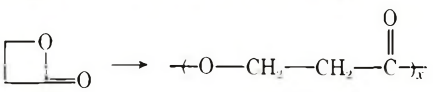

III II

* Present address: Dow Chemical Co., Midland, Michigan

There have been some reports of the polymerization of DL-β-butyrolactone (IV) by using organometallic catalysts;[9-11] however, the properties of the resulting polymers were much different from those of naturally occurring PHB.

This paper describes an investigation of catalyst systems and conditions for the polymerization of β-butyrolactone which was undertaken to determine the feasability of using this monomer for an attempted synthesis of a polyester equivalent to the natural polymer. The DL-PHB obtained in the study proved to be of special interest due to the unexpected degree of crystallinity observed in this synthetic polymer.

EXPERIMENTAL

Materials

β-Butyrolactone (IV). This compound was prepared by a modification of Johansson's experiment.[12] To β-bromobutyric acid (V) (83.5 g, 0.5 mole) was slowly added a solution of 31.8 g (0.3 mole) of Na_2CO_3 in 300 ml of H_2O. The mixture was stirred several minutes to insure complete neutralization of the acid and then added to 1500 ml of $CHCl_3$. The reaction mixture was stirred vigorously for 6 hr at 40°C. After cooling to room temperature, the $CHCl_3$ layer was separated, and the aqueous layer was washed twice with ether (100-ml portions). The ether solution was combined with the $CHCl_3$ layer and dried over Na_2SO_4 for several hours. The solvents were removed by evaporation under vacuum and the crude lactone was first distilled under reduced pressure and then redistilled over CaH_2 under reduced pressure. IV was a clear liquid, by 47.5–49°C/6.5 mm. The overall yield was 50%.

β-Bromobutyric Acid (V). This acid was synthesized by the method of Michael and Shadinger[13] which involved the addition of dry HBr to a benzene solution of crotonic acid.

Triethylaluminum (Et_3Al). This catalyst was obtained from Alfa Inorganics, and no further purification was required. A 30% solution of Et_3Al in benzene (distilled over Na) was used as a catalyst for the polymerizations with water as cocatalyst.

Preparation of PHB

The naturally occurring PHB used as reference in this study was isolated from *Bacillus cereus* according to a patented procedure by Baptist[14] which involved centrifugation of cells, drying from acetone, and finally extraction of PHB with $CHCl_3$. Enough $CHCl_3$ was used so that the extract was approximately a 2% solution. PHB was precipitated from the $CHCl_3$ solution with a mixture of diethyl ether–petroleum ether and washed several times with the precipitating agent before air drying.

The synthetic DL-PHB was prepared from racemic (IV) (2.05 ml, 25 mmole) which was introduced into an ampoule with a known amount of

H_2O (0.25–1.00 mmole). Then a known amount of Et_3Al (0.25–1.00 mmole, as a 30% solution in C_6H_6) was slowly added with agitation at 0°C under a dry N_2 atmosphere. After the ampoule was sealed the reaction mixture was allowed to undergo polymerization at the desired temperature (ranging from 0 to 55°C) for various periods of time.

Polymerization was terminated by addition of ether containing a small amount of H_2O. The addition of ether precipitated the polymer which was collected, washed successively with 0.1 *N* HCl and acetone, dissolved in $CHCl_3$, and filtered. The PHB was then precipitated with ether–petroleum ether (1:1), filtered off, washed several times with ether, air-dried, and finally vacuum-dried. Unreacted monomer was analyzed along with internal standard (anisole) on a Matronic Model 500 dual column gas chromatograph. A $3^1/_2$-ft × $^1/_4$ in. copper column packed with 10% Carbowax 6000 on non-acid-washed Chromosorb P (30–60 mesh) was used. Conversions varied from 35 to 55% depending on temperature, time, and concentration of catalyst and cocatalyst.

Polymer Characterization

Infrared spectra were recorded as either KBr pellets or $CHCl_3$ solutions on a Beckman double-beam IR 8 spectrophotometer. NMR spectra were determined on 0.5–1.0% solutions in $CHCl_3$ using the Varian A60-A instrument with tetramethylsilane as a reference compound.

Melting points were obtained from the DuPont Model 900 differential Thermal Analyzer with the use of glass beads as reference and at a heating rate of 10°C min. The scale was 20°C/in. with a ΔT of 0.2°/in.

A Picker unit operated at 35 kV and 15 mA with a Cu target x-ray tube as the source was used for obtaining flat plate pictures of the polymer as a powder or film. Debye-Scherrer powder patterns were obtained from a Picker unit operated at 25 kV and 30 mA with the use of a Cr target x-ray tube as source.

Electron micrographs of polymer crystals were recorded for samples precipitated from dilute xylene solutions. The suspension was evaporated onto carbon coated slides, shadowed with platinum, transferred onto copper grids, and examined on a Hitachi HU 11 electron microscope at magnifications of 6600–34,600. Pictures were recorded on $3^1/_4$ × 4 in. plates and enlarged photographically.

Intrinsic viscosity was measured to establish the relative molecular weights. Measurements were made at 30°C in an Ubbelohde viscometer in $CHCl_3$ solution.

RESULTS AND DISCUSSION

Polymerization of DL-(IV) with the use of a catalyst system of Et_2Zn–O_2 produced a low molecular weight polymer ($[\eta]$ = 0.09 dl/g). Because the racemic monomer was used, the polymer would not necessarily be expected to be stereoregular, since random introduction of D- and L-monomer units

should give an atactic configuration. Examination of the x-ray diffractogram (flat plate) and comparison to that of a naturally occurring sample of PHB showed that two intense reflections that were present for natural polymer were also present for the DL synthetic polymer. Although x-ray data had shown the natural polymer to be much more crystalline, the synthetic polymer was partially crystalline.

By using DL-IV and a catalyst system consisting of Et_2Zn–H_2O, a polymer of higher molecular weight ($[\eta]$ = 0.11 dl/g) was obtained. A flat plate x-ray diffractogram showed that this polymer was more crystalline than the previous sample; however, it too appeared to be less crystalline than the sample isolated from bacteria.

Cherdron et al.[8] had observed that polymerization of III by a system of Et_3Al–H_2O (molar ratio of 1:0.66) produced a polyester of optimum molecular weight and degree of conversion. The synthesis of DL-PHB in this laboratory by using the same catalyst system in the same molar ratio likewise produced a high molecular weight polyester. The x-ray data showed that this polymer had only a slight degree of crystallinity compared to the naturally occurring PHB.

Table I contains some of the results of the polymerization of DL-IV with Et_3Al–H_2O. Increased catalyst concentration increased the conversion as expected, since more active sites are available on which polymerization can take place. This also accounts for the observed lowering of molecular weights with higher catalyst concentrations. Increasing temperature also has the effect of increasing the conversion while decreasing the molecular weight.

Polymerization of DL-IV with a catalyst system of Et_3Al–H_2O (molar ratio of 1:1) produced DL-PHB that had a lower molecular weight for the soluable fraction but a higher overall degree of conversion than that of the same system in a molar ratio of 1:0.66. This is consistent with prior observations.[11] Attempts to put this polymer into chloroform solvent

TABLE I
Bulk Polymerization of DL-β-Butyrolactone with Et_3Al-H_2O[a]

Et_3Al, mole-%[b]	H_2O, mole-%	Temp, °C	Time, hr	$[\eta]$, dl/g[c]	Conversion, %
4.00	4.00	53	92.5	0.11	52
3.00	3.00	53	93.0	0.18	41
2.00	2.00	53	94.0	0.24	38
3.00	2.00	53	114.0	0.25	38
4.00	4.00	24	125.0	0.26	48
3.00	3.00	24	124.0	0.33	39
2.00	2.00	24	158.0	0.40	36
3.00	2.00	24	114.0	0.40	35
3.00	3.39	0	124.0	0.39	55

[a] Monomer, 2.05 ml (25 mmole).
[b] Approx. 30% solution in benzene.
[c] In $CHCl_3$ at 30°C.

TABLE II
Comparison of Debye-Scherrer Powder Patterns of Naturally Occurring D-PHB and Synthetic DL-PHB

D-PHB		DL-PHB	
d spacing, Å	Intensity[a]	*d* spacing, Å	Intensity[a]
6.55	S	6.54	S
5.60	W	—	—
5.25	S	5.22	S
4.48	W	4.48	W
3.98	M	3.96	M
3.53	M	3.47	M
3.27	W	3.27	M
2.94	W	2.91	W
2.55	W	—	—

[a] S = strong; M = medium; W = weak.

yielded an insoluble and a soluble fraction. The insoluble polymer, when examined by x-ray diffraction, appeared to be practically identical to the naturally occurring PHB. The *d* spacings were calculated from the Debye-Scherrer powder pattern, and Table II shows the comparison of the *d* spacings of bacteriologically produced D-PHB to those of synthetic DL-PHB. The x-ray data showed the chloroform-soluble fraction of the polymer to be highly crystalline also, but slightly less so than the insoluble fraction.

It was previously observed[15,16] that the x-ray pattern was characteristic of PHB isolated from all the bacterial sources; thus, the diffractograms serve as valuable fingerprints and are essentially the same for a wide range of molecular weights. This was also the case noted in the synthetic, crystalline samples of DL-PHB prepared in this laboratory.

From our results and comparisons to the naturally occurring polymer it is apparent that some type of stereospecific catalysis is taking place. Although the synthetic polymer is not optically active, it must consist of mainly isotactic configurations to account for its highly crystalline nature. Since the natural PHB consists of chains that contain repeat units all of D configuration, while both D and L units must be present in DL-PHB, two possibilities must be considered for the synthetic, optically inactive PHB. Since naturally occurring PHB has two chains in its unit cells[17] there exists the possibility that each unit cell of the crystalline DL polymer contains one D chain and one L chain. This would result in a racemic crystal. The second possibility is that the crystalline polymer is composed of separate crystals of polymers containing either pure D or pure L chains. Both of these two possibilities are consistent with either copolymers with long D and L blocks or with separate D or L chains.

Alkyls of zinc and aluminum with a cocatalyst of water have been reported to polymerize propylene oxide (PO) to a highly crystalline polymer.[18,19] These catalyst systems were said to be stereospecific in polymerizing PO to isotactic polymers.

Because the scattering powder of an O atom is very similar to that of a $-CH_2$ group, it was observed that there was no difference between the x-ray diffractogram of optically active poly(propylene oxide), PPO, and that of racemic PPO.[20] However, since the scattering powder of an S atom is measurably different from that of a $-CH_2$ group, it is possible to detect differences in the crystal structures of optically active and racemic poly(propylene sulfide) PPS. A recent paper reported the results of structural investigations carried out on both forms of PPS by x-ray diffraction.[21] These studies showed that the racemic PPS prepared from Et_2Zn–H_2O consisted of crystallites composed of separate chains of D- and L-configuration.

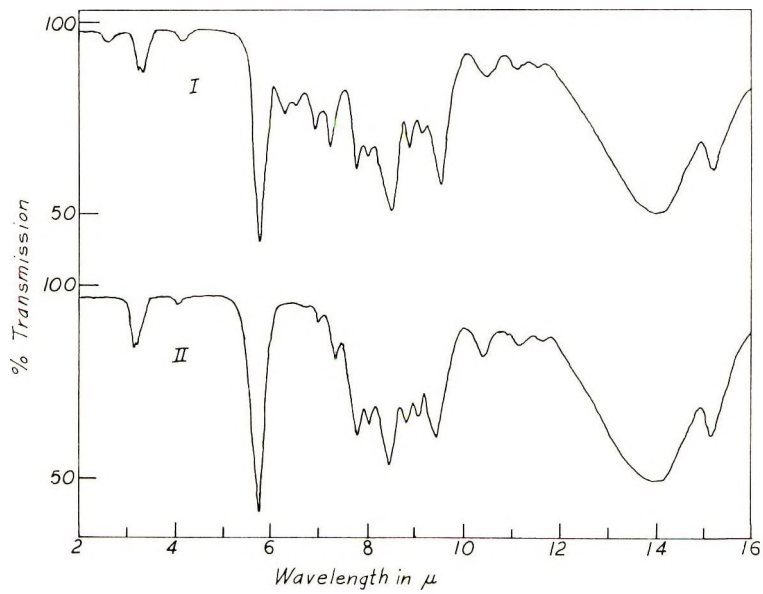

Fig. 1. Infrared spectra of (*I*) synthetic DL-poly-β-hydroxybutyrate and (II) naturally occurring D-β-hydroxybutyrate.

An attempt was made to obtain x-ray intensity data from oriented fibers of synthetic DL-PHB, but the polymer was too brittle and could not be drawn, even at temperatures near its melting point. Thus, the question still remains as to whether racemic or separate D and L crystals exist in the unit cell of this polymer. It seems clear, however, that once a chain is initiated it tends to propagate by addition of monomer of like configuration to give isotactic sequences.

The apparent stereospecific character of this polymerization has been investigated by using optically active monomer as described in a companion paper (Part II).[22] Further discussion of the mechanism is presented in that paper on the synthesis of optically active PHB.

A thorough characterization of the synthetic DL-PHB was undertaken by using infrared, NMR, x-ray, and electron microscopy. The results are

reported below and compared to the corresponding data obtained for the naturally occurring polymer.

Infrared spectra of the polymers prepared in this laboratory were essentially identical to spectra of the natural polymer and also to the spectrum reported by Yamashita et al.[11] The infrared spectrum (*I*) of a sample prepared from Et_3Al-H_2O (1:1) is shown in Figure 1. The major absorption peak was at 5.75 μ and corresponds to the ester C=O stretching mode. Absorbing in the range of 8.4–9.4 μ were several bands corresponding to a C—O—C stretch. The somewhat low molecular weight of this sample (compared to the higher molecular weight samples of bacterial PHB) can be seen by the distinct OH absorption peak at 2.8 μ which is due to OH as an endgroup. Because this endgroup is capable of undergoing dehydration,

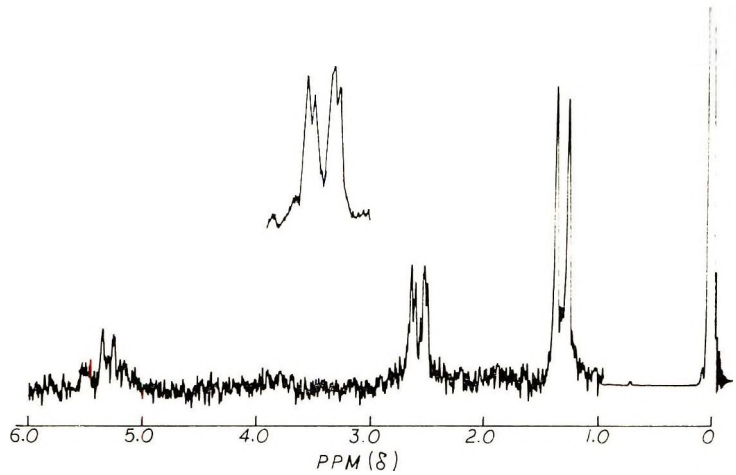

Fig. 2. NMR spectrum of DL-poly-β-hydroxybutyrate.

a band at 6.3 μ was observed and corresponds to a C=C endgroup absorption. The infrared spectrum (*II*) of a high molecular weight sample of *Bacillus cereus* D-PHB is also recorded in Figure 1. It should be noted that two endgroup absorptions observed in spectrum (*I*) are not present in spectrum (*II*); however, lower viscosity samples isolated from other bacterial sources did show these two end groups absorbing in the indicated regions.

The NMR spectrum of DL-PHB is shown in Figure 2. This spectrum was identical to that of the *Bacillus cereus* D-PHB. For both samples the

$$\text{—}\overset{|}{\underset{|}{\text{CH}}}\text{—}$$

—CH_3 resonances appeared as the expected doublet at 1.3 δ and the —CH— proton as the multiplet at 5.3 δ. The —CH_2 protons, however, were nonequivalent in both spectra and appeared as two sets of doublets at 2.6 δ [also shown in enlarged portion of spectrum) separated by chemical shift differences of 2 Hz. Comparison of these nmr spectra with that of a DL-

PHB sample of very low crystallinity showed the same splitting for the —CH_2— protons, all of which shows that each of the two protons in a given repeat unit are in a different chemical environment. Consideration, for example, of the Newman projections of the most stable conformation of either the D- or the L-asymmetric C atoms, VI, shows the *trans* interaction of H_A with H_C should give rise to one doublet, while *gauche* interaction of H_B with H_C should account for the other doublet. Both, of course, should have characteristic chemical shifts which differ and thus produce a set of doublets in the NMR spectrum.

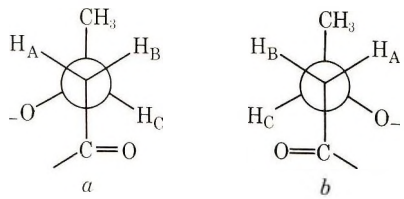

VI

These results differentiate this type of proton stereochemical nonequivalence from that arising from stereochemical differences in the arrangement of a series of monomer units, such as the nonequivalence of —CH_2— protons in isotactic and syndiotactic poly(methyl methacrylate.)[23]

The melting points of the synthetic DL-PHB were in the usual range (165–175°C) reported for the polyesters isolated from the various bacterial sources.[16]

As mentioned previously in this discussion, the DL-PHB was shown to be highly crystalline consistent with isotactic chains of D and L configuration rather than an atactic distribution. A picture of the x-ray diffractogram is shown in Figure 3. Lundgren et al.[16] had shown that the x-ray diffractograms of PHB from six different isolates were identical to the one recorded by Alper, et al.[15] for *Bacillus cereus* D-PHB. It was also shown that the polymer from these six sources were of varying viscosity average molecular weights (2,000–59,000). From their x-ray data it was confirmed that a regular helical conformation of the molecule exists in the crystal.[17] Examination of our identical x-ray diffractograms demonstrates that the crystalline DL-PHB synthesized in this laboratory also possesses the same helical structure in the crystal, although as discussed above this polymer may exist as separate D and L crystals or as racemic crystals.

The extensive work of Lundgren et al. on the characterization of bacterial D-PHB also included the morphological features of the polymer as observed with an electron microscope. Their micrographs of crystals of PHB from different bacteria revealed similar morphologies. The isolates were of varying molecular weights and the samples with low viscosities were slow to recrystallize and yielded few crystals. In most cases, however, they ob-

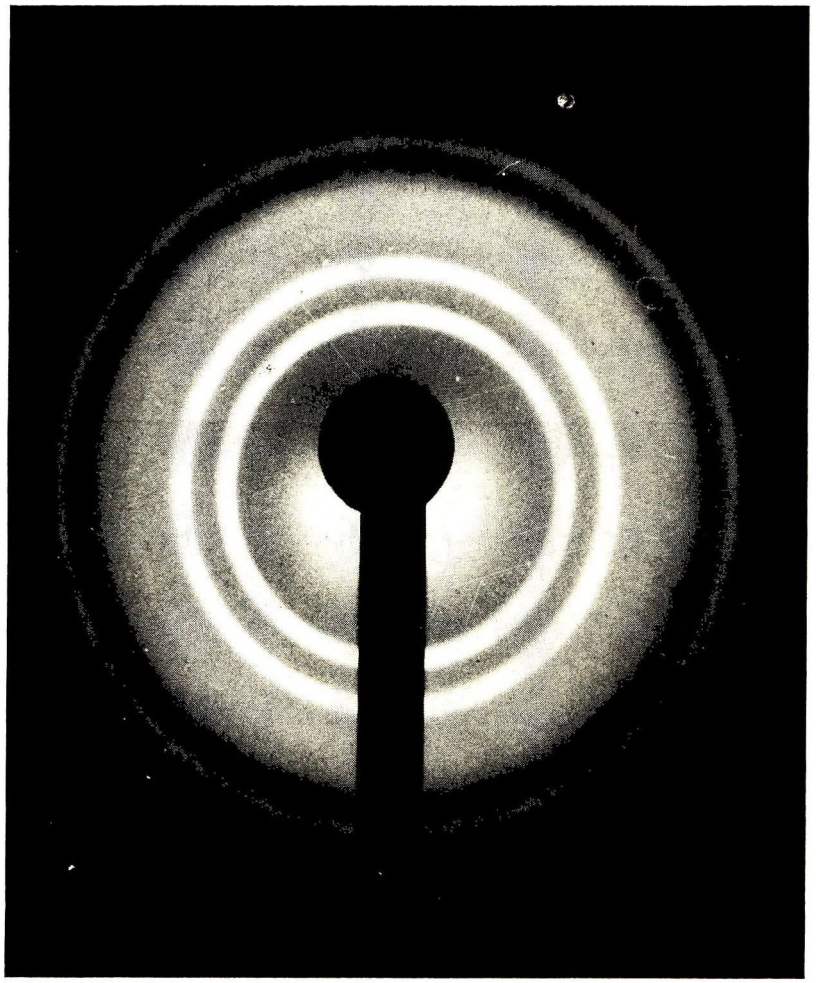

Fig. 3. X-Ray diffractogram of synthetic DL-poly-β-hydroxytyrate.

served that lath-shaped crystals were present with folds seen in the lath. In some instances larger crystals showed some lamellar morphology, but not as extensive as that noted by Alper et al.[15] for *Bacillus cereus* polymer crystals.

As part of the characterization of DL-PHB synthesized in this laboratory, a study was made on the morphological features of this new polymer. Through a comparison of the micrographs of the synthetic polymer (Fig. 4) with those of Lundgren et al.[16] it was evident that the crystals were of similar morphology. Again, the lath-shape of the crystals was observed. Admittedly, the crystals were rather small, because steps were not taken to grow larger ones. Also, the micrographs were indicative of low molecular weight and the lamellar morphology was not as extensive as that which was observed for the *Bacillus cereus* crystal by Alper and co-workers.[15]

It can be inferred from these data that synthesis of PHB from DL-IV with a catalyst of Et_3Al–H_2O produces a polymer with virtually identical crystallographic and morphological properties as those of the polymer produced in bacteria by the condensation of D-(−)-β-hydroxybutyrl coenzyme A. In fact, this syntetic DL polymer is identical to the naturally occurring polymer in all other respects, both chemically and physically, except it is optically inactive.

One of the initial objectives of this study was to obtain a polymer with a molecular weight approaching that of the highest reported for bacterial PHB. Although the Et_3Al–H_2O catalyst system was ultimately selected as adequate in this respect, several other systems were also investigated.

(*a*)

Fig. 4 (*continued*)

(*b*)

Fig. 4. Electron micrographs of synthetic DL-poly-β-hydroxybutyrate.

For example, it was known that III could be polymerized by using a catalyst system of Et_2Zn–ROH,[9] and consequently this system was included in our study of the polymerization of DL-IV. Variation of catalyst to cocatalyst and catalyst to monomer showed that molecular weights were approximately the same as those obtained from Et_2Zn–H_2O and slightly lower than those of Et_3Al–H_2O, but the crystallinity of the resulting PHB was almost nonexistent. The same type of study using Et_3Al–ROH showed similar results. The effect of alcohol in diminishing the stereospecificity of the catalyst is rather surprising. The major difference with alcohol, as compared to water as cocatalyst, is the nature of the "active" catalyst formed by reaction with the metal alkyl. The "active" catalyst in the Et_2Zn–

ROH system is most likely EtZnOR or $Zn(OR)_2$ and for the Et_3Al–ROH, either Et_2AlOR, $EtAl(OR)_2$, or $Al(OR)_3$, depending on the amount of ROH used. In the case of either Et_2Zn–H_2O or Et_3Al–H_2O the "active" catalysts have been shown to involve —Zn—O—Zn—O— and —Al—O—Al—O— structures, respectively.[11,18] The formation of "active" catalyst similar in nature to the alcohol reaction product could also explain why the Et_2Zn–O_2 system produced a polymer of very low crystallinity. It is known that Et_2Zn reacts with O_2 to give peroxides and alkoxides[24–27] as shown in eq (1).

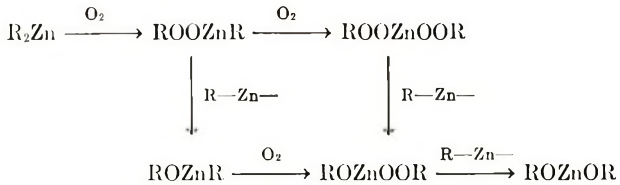

(1)

Since these structures are similar to those produced by the reaction of ROH with Et_2Zn or Et_3Al, it might be expected that polymers produced by both of these systems would be similar as observed in their low crystallinity in each case.

Many of the catalyst systems that have been used to polymerize propylene oxide were found to be ineffective in polymerizing DL-IV to a high molecular weight polymer. For example, the binary catalysts consisting of inorganic compounds (BaO, CaO, ZnO, CaF_2, and HF) with Et_2Zn,[27] which were particularly effective in the polymerization of PO were ineffective with IV.

It was found from this study that the catalyst system of Et_3Al–H_2O (1:1) was highly stereospecific in polymerizing DL-β-butyrolactone to a relatively high molecular weight polyester. The x-ray diffractograms of this racemic polymer showed it to be highly crystalline, and comparison of its Debye-Scherrer powder pattern to that of bacterially synthesized D-PHB showed the same *d* spacings which indicates the same helical conformation. Electron micrographs of DL-PHB revealed the same lamellar morphology as the naturally occurring D-PHB. The results of all other measurements made on the synthetic polymer (e.g. infrared, NMR, melting point, intrinsic viscosity) were comparable to those observed on the naturally occurring polymer. Thus, a racemic polymer has been synthesized that is essentially identical to the naturally occurring polymer, D-PHB in all respects except optical activity.

This work was supported in part by The Goodyear Tire and Rubber Co., Akron, Ohio.

References

1. M. Doudoroff and R. Stainer, *Nature*, **183**, 1440 (1959).
2. M. Lemoigne, *Ann. Inst. Pasteur*, **39**, 144 (1925).
3. M. Lemoigne, *Ann. Inst. Pasteur*, **41**, 148 (1927).
4. D. H. Williamson and J. F. Wilkinson, *J. Gen. Microbiol.*, **19**, 198 (1958).

5. T. L. Gresham, J. E. Jansen, and F. W. Shaver, *J. Amer. Chem. Soc.*, **70**, 998 (1948).
6. T. Shiota, Y. Goto, and K. Hayaski, *J. Appl. Polym. Sci.*, **11**, 753 (1967).
7. V. H. Cherdron, H. Ohse, and F. Korte, *Makromol. Chem.*, **56**, 179 (1962).
8. V. H. Cherdron, H. Ohse, and F. Korte, *Makromol. Chem.*, **56**, 187 (1962).
9. S. Inoue, Y. Tomoi, T. Tsuruta, and J. Furukawa, *Makromol. Chem.*, **48**, 229 (1961).
10. Y. Yamashita, Y. Ishikawa, T. Tsuda, and S. Miura, *Kogyo Kagaku Zasshi*, **66**, 104 (1963).
11. Y. Yamashita, Y. Ishikawa, T. Tsuda, and S. Miura, *Kogyo Kagaku Zasshi*, **66**, 110 (1963).
12. H. Johansson, *Ber.*, **48**, 1256 (1915).
13. A. Michael and G. H. Shadinger, *J. Org. Chem.*, **4**, 128 (1939).
14. J. N. Baptist, U.S. Pats. 3,036,959 and 3,044,942 (1962).
15. R. Alper, D. G. Lundgren, R. H. Marchessault, and W. A. Cote, *Biopolymers*, **1**, 545 (1963).
16. D. G. Lundgren, R. Alper, C. Schnaitman, and R. H. Marchessault, *J. Bacteriol.*, **89**, 245 (1965).
17. K. Okamura and R. H. Marchessault, *Conformation of Biopolymers*, Vol. 2, G. N. Ramachandran, Ed., Academic Press, London, New York, 1967, pp. 709–720.
18. R. Sakata, T. Tsuruta, T. Saegusa, and J. Furukawa, *Makromol. Chem.*, **40**, 64 (1960).
19. E. J. Vandenberg, *J. Polym. Sci.*, **47**, 486 (1960).
20. E. Stanley and M. Litt, *J. Polym. Sci.*, **43**, 453 (1960).
21. H. Sakakihara, Y. Takahashi, H. Tadokoro, P. Sigwalt, and N. Spassky, *Macromolecules*, **2**, 515 (1969).
22. J. R. Shelton, D. E. Agostini, and J. B. Lando, *J. Polym. Sci. A-1*, **9**, 2785, (1971).
23. F. Bovey, *Accts. Chem. Res.*, **1**, 175 (1968).
24. R. Demuth and V. Meyer, *Ber.*, **23**, 394 (1890).
25. C. H. Bamford and D. M. Newitt, *J. Chem. Soc.*, **1946**, 688.
26. M. H. Abraham, *Chem. Ind.* (London), **1959**, 750.
27. K. Okazaki, *Makromol. Chem.*, **43**, 84 (1961).

Received April 19, 1971
Revised May 25, 1971

JOURNAL OF POLYMER SCIENCE: PART A-1 VOL. 9, 2789–2799 (1971)

Synthesis and Characterization of Poly-β-Hydroxybutyrate. II. Synthesis of D-Poly-β-hydroxybutyrate and the Mechanism of Ring-Opening Polymerization of β-Butyrolactone

J. REID SHELTON, D. E. AGOSTINI,* and J. B. LANDO,
Case Western Reserve University, Cleveland, Ohio 44106

Synopsis

Synthesis of the naturally occurring polyester, D-poly-β-hydroxybutyrate (PHB) was accomplished by using an optically active monomer. Polymerization of D-(+)-β-butyrolactone (β-BL) of 73% optical purity with a catalyst system of Et_3Al–H_2O produced a polymer with a similar optical activity and essentially identical to the natural polymer as isolated from bacterial cells. This paper describes the synthesis and characterization of this optically active polyester along with a suggested mechanism to account for the observed stereospecific polymerization of β-BL with this catalyst system.

INTRODUCTION

A description of the naturally occurring polyester, D-poly-β-hydroxybutyrate (D-PHB), is presented in the companion paper.[1] In that paper catalyst systems for possible use in the synthesis from β-butyrolactone of the naturally occurring polyester were evaluated by using the DL monomer. It was found that organometallic catalysts such as triethylaluminum plus water cocatalyst produced highly crystalline samples of polyester from the racemic monomer.[1] This catalyst system was used in the present study.

Synthesis of the natural polymer, D-PHB, had not been reported prior to the present study which was announced in a recent communication.[2] The results reported here shed new light on the mechanism of polymerization of β-lactones with this catalyst system.

EXPERIMENTAL

Materials

The synthesis of β-butyrolactone (β-BL), β-bromobutyric acid (β-BBA), and the triethylaluminum–water catalyst system is described in the previous paper.[1] The DL-β-BBA was resolved to its L-(+)-isomer by reaction

* Present address: Dow Chemical Co., Midland, Michigan.

with D-(+)-α-(1-naphthyl)ethylamine and separation of the resulting diastereoisomers by fractional crystallization from C_6H_6/ethyl acetate solvent. Conversion to D-(+)-β-butyrolactone occurred by internal S_N2 attack of the neighboring carboxylate anion on the saturated carbon.

The procedure for obtaining the naturally occurring polymer as well as the synthesis of PHB using triethylaluminum (Et_3Al) catalyst and water cocatalyst has been described in the companion paper.[1]

Determination of Optical Purity

β-BBA. To 1.45 g (8.7 mmole) of partially resolved β-BBA, $[\alpha]_D^{23} = +9.7 \pm 0.1°$ (c = 0.90, ethanol), was added 4 ml of freshly distilled $SOCl_2$. The mixture was refluxed for 2 hr and the excess $SOCl_2$ was evaporated under vacuum. The crude acid chloride was added to 2.4 g (20 mmole) of D-(+)-α-phenylethylamine (α-PEA) (Norse Chem.), $[\alpha]_D^{24} = +36.8°$ (neat), in 20 ml anhydrous C_6H_6 at 0°C. The reaction mixture was heated 15–20 min on a steam bath, and then washed twice with 10 ml H_2O, once with 10 ml 2N HCl and again with H_2O. The benzene solution was dried ($MgSO_4$) and the solvent removed under vacuum to yield an oil which crystallized at −78°C. The crude amide, I, was used without further purification.

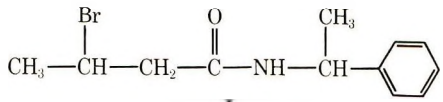

I

NMR spectra for I were taken on the Varian A60-A using 10–20% solutions of I in $CHCl_3$. Optical purity was calculated from the observed distribution of diastereomers of I as explained later.

β-BL. Optically active α-methoxy-α-trifluoromethylphenylacetic acid (MTPA) was synthesized according to the method of Dale et al.[3] and converted to its acid chloride by refluxing with freshly distilled $SOSl_2$ and a trace of NaCl for 50 hr. β-Hydroxybutyranilide (II) was synthesized according to the method of Iwakura, et al.[4] The acid chloride of MTPA was then esterified by reaction with II using the method of Dale et al.[3]

Optical purity was calculated from NMR data as explained in the next section. Proton resonance was done on the Varian A60-A or HA 100 using 10–20% $CHCl_3$ solutions with tetramethylsilane as reference compound. Fluorine resonance was done at −20°C on the Varian A-56/60 using SO_2ClF as solvent and Cl_3CF as internal standard.

RESULTS AND DISCUSSION

Determination of Optical Purity

It was desired to establish the limiting value of optical purity that could be expected in the synthetic polymer based on the optical purity of

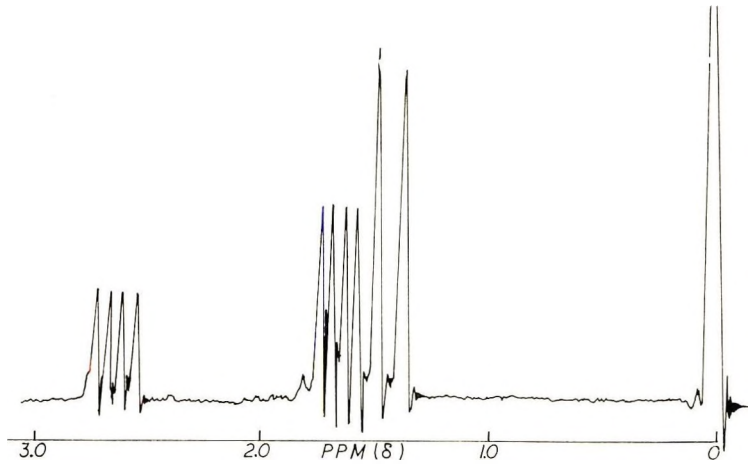

Fig. 1. NMR spectrum of *N*-(α-phenylethyl)-β-bromobutyramide (I) synthesized from DL-acid and D-amine.

the starting materials, L-(+)-β-bromobutyric acid and D-(+)-β-butyrolactone. This assumes that preferential polymerization of one of the antipodes over the other does not occur, and that the specific rotation of the polymer is directly proportional to the optical purity of the monomer units incorporated into the chain.

To determine the optical purity of these two starting materials we chose Mislow's NMR method[5] whereby enantiomers A_D and A_L are converted to diastereomers, A_DB_D and A_LB_D. It is well known that diastereomers differ in their NMR spectra;[6] thus, it is possible to obtain distinguishable values for the two diastereomers, and integrated intensities provide a measure of the relative amounts of each diastereomer. It is then possible to calculate the optical purity of the mixture of enamtiomers, A_D and A_L, by using the formula:

$$\text{optical purity} = (R - 1)/(R + 1) \times 100\ \%$$

where

$$R = A_DB_D/A_LB_D$$

The reliability of this method is illustrated by results obtained with a mixture of diastereomeric amides prepared by reaction of racemic β-BBA with D-(+)-α-PEA. Figure 1 shows a portion of the 60-MHz NMR spectrum of a $CHCl_3$ solution of D,D-I and L,D-I. The $-CH_3$ protons of the amine portion appear at 1.46 δ downfield from TMS and show no apparent chemical shift differences as indicated by the appearance of only one doublet. There are, however, large enough chemical shift differences to be observed in the signals of the $-CH_3$ protons of the acid portion, and also of the $-\overset{|}{C}H_2$ protons. The two sets of $-CH_3$ doublets appear at 1.68

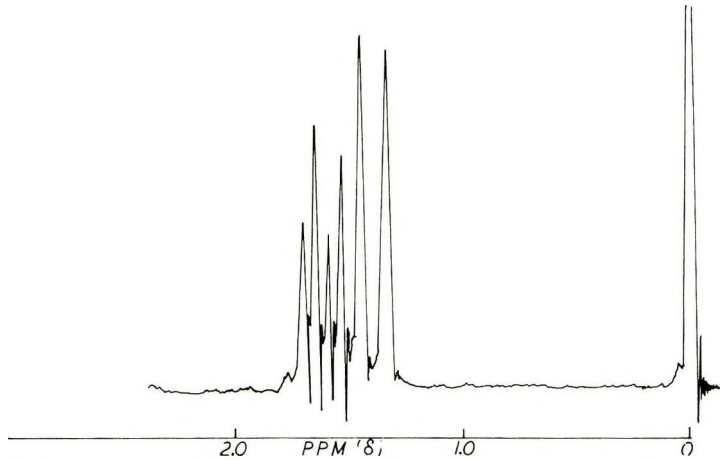

Fig. 2. NMR spectrum of *N*-(α-phenylethyl)-β-bromobutyramide (I) synthesized from L-Acid and D-Amine.

δ and 1.72 δ, and the —CH_2 doublets appear at 2.63 δ and 2.68 δ for D,D-I and L,D-I, respectively. The data thus show an equal mixture of the two diastereoisomers as expected, and the optical purity corresponds to 0%.

To determine the optical purity of optically active β-BBA a partially resolved mixture of the acid, $[\alpha]_D^{24}$ + 9.7° (c = 0.90, ethanol) was reacted (as its acid chloride) with D-(+)-α-PEA, $[\alpha]_D^{24}$ + 36.8° (neat), to form the diastereomeric amide mixture. In Figure 2 is shown the 60-MHz NMR spectrum of the —CH_3 proton resonances of a $CHCl_3$ solution of this mixture of diastereomers. Calculation of R through integration of the —CH_3 doublets shows an optical purity corresponding to 21.9%. Assuming that the maximum specific rotation of L-(+)-β-BBA is proportional to optical purity, then the equation

$$\text{max. } [\alpha]_D = \text{obs. } [\alpha]_D/\text{optical purity}$$

applies. Calculation of the quantity yields a value of +44–45° for the specific rotation expected for a 100% optically pure sample of β-BBA.

Because the per cent of racemization in the reaction of L-(+)-β-BBA going to D-(+)-β-BL was never reported, it was necessary to obtain this information by determination of the optical purity of the lactone formed. Conversion to diastereoisomers suitable for analysis by NMR was first attempted by reaction with an optically active amine, since β-butyrolactone is known to react with various primary amines to give two types of derivatives[7] as indicated in eq. (1).

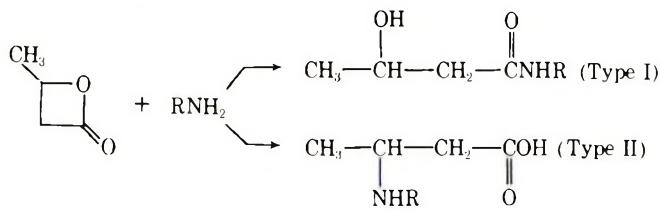

(1)

It was our objective to make the type I amide, but reaction of β-BL with D-(+)-α-PEA, and with a number of other asymmetric amines (e.g., α-NEA and amphetamine), yielded a mixture of the type II amino acid along with low molecular weight PHB and the desired amide. Since formation of the amino acid involves the asymmetric center, such products are unsuitable for the determination of optical purity.

Iwakura, et al.[4] found that reaction of β-BL with aniline produced exclusively the type I amide (II). Reaction of the

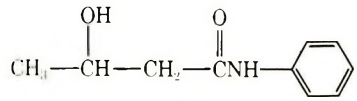

II

OH functional group with an optically active acid chloride should give diastereomeric esters which could be studied by NMR in the manner used to determine the optical purity of β-BBA.

Starting with partially resolved β-BBA, enriched in the L-(+)-isomer (approx. 50% optically pure), β-BL was synthesized. The lactone, which was enriched in the D-(+)-isomer, was reacted with aniline to form II. When II was reacted with the acid chloride of optically active α-methoxy-α-trifluoromethylphenylacetic acid (MTPA ≈99% optically pure) the resulting ester (III) showed very little chemical shift differences

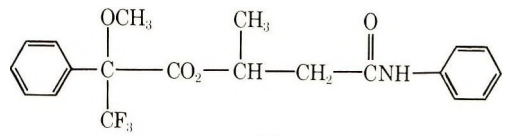

III

for proton resonances. Fluorine reasonance, however, showed large chemical shift differences for the two $-CF_3$ singlets. Calculation of R through integration showed a ratio of diastereomers corresponding to an optical purity of 41% for the β-BL.

These data show that the cyclization of L-(+)-β-BAA to D-(+)-β-lactone is accompanied by some racemization, since the optical purity of the lactone is less than that of the starting acid (50%). The lactone is thought to be formed by attack of the neighboring carboxylate anion on carbon via an intramolecular S_N2 type displacement causing inversion of configuration.[8] Although some formation of lactone through an S_N1 displacement cannot be ruled out, it seems more likely that some of the β-bromobutyrate was racemized (e.g., by S_N2 attack of the Br^- ions produced in the reaction) before the neighboring carboxylate anion attacked.[9-12] Equation (2) shows the possible stereochemical pathways including both alternatives to account for the observed decrease in optical purity.

The limiting value of optical purity possessed by the monomer used in the synthesis of optically active PHB can now be calculated. The optical

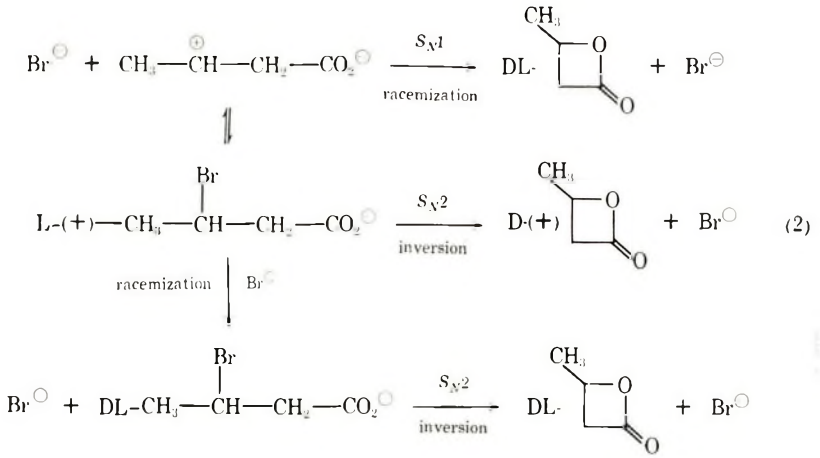

purity of the L-(+)-β-BBA was limited by the resolving agent, D-(+)-α-NEA, which was commercially available in only 96–97% optical purity. Because of this and procedural limitations the optical purity of the L-(+)-β-BBA prepared in this laboratory was 90–91%. Realizing that conversion of the acid to the β-lactone occurs with 18% racemization (i.e., a total of 18% of the optically active acid was converted to the racemic form), then the limiting value of the D-(+)-β-BL is approximately 74% optical purity (i.e., 0.82 × 0.90). The optical purity of the resulting PHB is thus limited by this value, and it would appear to be virtually impossible to synthesize polymer from the lactone and attain an optical activity equal to that of the naturally occurring polymer (taken to be 100% optically pure).

Synthesis of D-PHB

Although the above discussion suggests that 100% optically pure D-PHB most probably could not be synthesized by the present approach, it was, nevertheless, evident that it should be possible to obtain an optically active PHB. Since this had never before been accomplished, it was decided to undertake the synthesis in order to learn more about the nature of this interesting polyester and the mechanism of ring-opening polymerizations of lactones.

Starting with D-(+)-β-BL (approx. 73% optical purity) and a catalyst system of Et_3Al–H_2O (1:1) the synthesis of D-PHB was accomplished as described in the experimental section[1] using the procedure previously worked out in this laboratory for polymerization of the DL monomer. If this polymerization proceeded exclusively by breakage of the acyl–O bond of the lactone, the optical purity of the synthetic polymer should have been the same as that of the monomer, i.e., 73%.

Alper et al.[13] obtained optical rotatory dispersion (ORD) data for a *Rhizobium* sample ($\bar{M}$ = 128,000) and showed that its specific rotation at 300 mμ was +44° and rapidly decreased to 0° at 440 mμ, remaining slightly

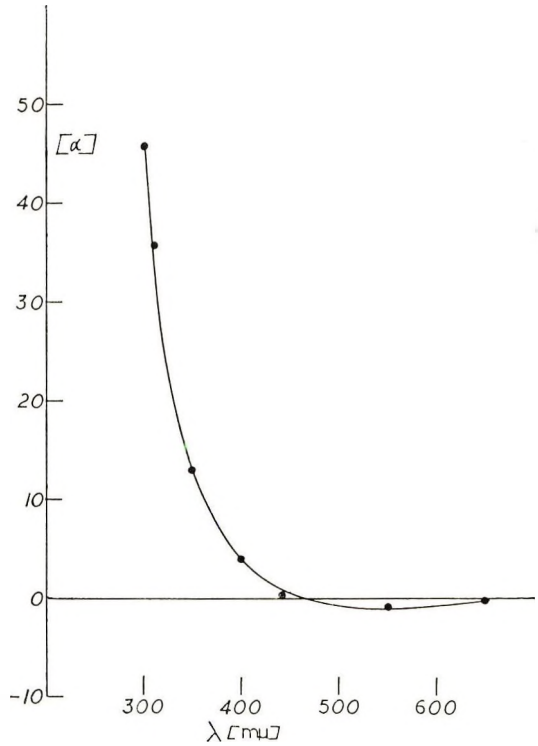

Fig. 3. ORD curve of naturally occurring poly-β-hydroxybutyrate.

negative (ca. −1°) past 440 mμ. Our ORD data for a *Bacillus cereus* sample ($\bar{M}_v$ = 900,000) showed the same plain curve with identical specific rotations at the indicated wavelengths. (Fig. 3).

In Figure 4 is plotted the ORD curve of our synthetic D-PHB. It can be seen that the shape of this curve is identical to that recorded in Figure 3; however, the rotatory power of this polymer is somewhat lower than observed with the bacterial polymers (i.e., [α] = +19° at 300 mμ compared to [α] = 44° for the natural polymer). If the observed rotation is proportional to optical purity, the maximum value that could be expected for a polymer obtained by polymerization of monomer that was only 73% optically pure would be a specific rotation at 300 mμ of approximately +31° (i.e., 0.73 × 44°).

Unfortunately, however, this assumption cannot be made. Physical properties of the natural polyester, including conformational aspects in solution, are described in recent papers by Marchessault and coworkers.[14,15] Optical rotatory dispersion of solutions of bacterial D-PHB show that the effect of molecular weight is not negligible, and that "the crossover point (wavelength where [α] = 0) seems to move continuously to higher wavelengths as molecular weight increases, although the experimental error is rather high in actually fixing this point." It should be mentioned here

that we encountered some difficulty in establishing a solvent ($CHCl_3$) baseline with respect to the ORD curve and thus could not actually fix the crossover point. As a point of reference we took the crossover point of the *Bacillus cereus* sample recorded by Alper and coworkers.[13]

The ORD data clearly indicates that we have successfully synthesized D-PHB. The polymer was fully characterized and showed that all the chemical and physical properties, excepting optical activity, were the same as those of our synthetic, crystalline DL-PHB prepared with the same

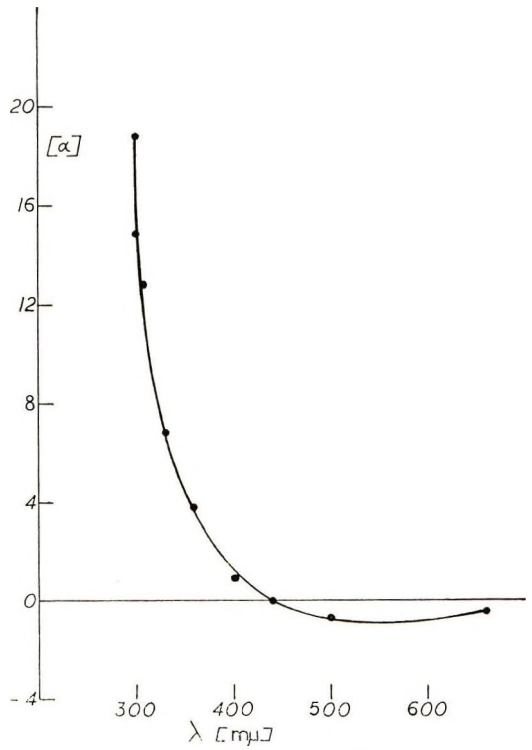

Fig. 4. ORD curve of poly-β-hydroxybutyrate synthesized from D-(+)-β-Butyrolactone (73% optical purity).

catalyst system.[1] The intrinsic viscosity of our synthetic D-PHB determined in $CHCl_3$ solution was $[\eta] = 0.60$ dl/g, which corresponded to a molecular weight within the range (0.5–11.45 dl/g) reported for the bacterial polymers isolated by Lundgren et al.[16] Compared to our naturally occurring D-PHB (Fig. 3), the synthetic polymer was lower in rotatory power, but again, essentially the same chemically and physically. Because of the inaccuracy in fixing a baseline and crossover point, it is conceivable that the specific rotations of the synthetic D-PHB could be higher at the indicated wavelengths.

Mechanism of Polymerization

Marchessault et al.[14,15] had shown that low molecular weight samples of PHB exhibited lower specific rotations at corresponding wavelengths. It is certain that the rotary power of our D-PHB is not at its maximum because of the lower optical purity of the starting monomer. During the polymerization little, if any, racemization takes place. This was proven experimentally by taking monomer of $[\alpha]_D^{23} = +29.45 \pm 0.05$ and polymerizing with Et_3Al–H_2O (1:1 mole ratio) over a period of 7 days at room temperature (35–40% conversion). Analyzing unreacted monomer showed it to have $[\alpha]_D^{23} = +28.85 \pm 0.05°$. The small decrease could reflect some preferential selectivity in the propagation step for D-β-BL. This phenomenon of selectivity has been reported in the polymerization of optically active propylene oxide with organomagnesium compounds.[17]

Consistent with the reactions suggested by Yamashita and coworkers,[18] initiation could occur by π-complexation with aluminum as in the scheme shown in eqs. (3)–(6), with subsequent localization to form a sigma bond between the ring oxygen and aluminum. The resulting oxonium ion is analogous to the propagating species proposed for the polymerizations of propylene oxide with Et_3Al–H_2O as catalyst,[19] and also for cyclic ester polymerization.[20]

Propagation involves attack by the ring oxygen of the monomer, β-BL, on the oxonium ion at the carbonyl carbon causing breakage of the acyl-oxygen bond. A new oxonium ion IV would thus be formed with retention of configuration in the monomer unit introduced into the growing chain. The observed stereoregularity of the resulting polymer can be explained by the proximity of the oxonium ion to the anion formed in the initial coordination at the catalyst surface. Thus, if the initiation involves coordination of a D monomer with aluminum, all subsequent propagation steps will be subject to the same steric influence of this unit leading to an isotactic sequence of D-PHB.

Initiation:

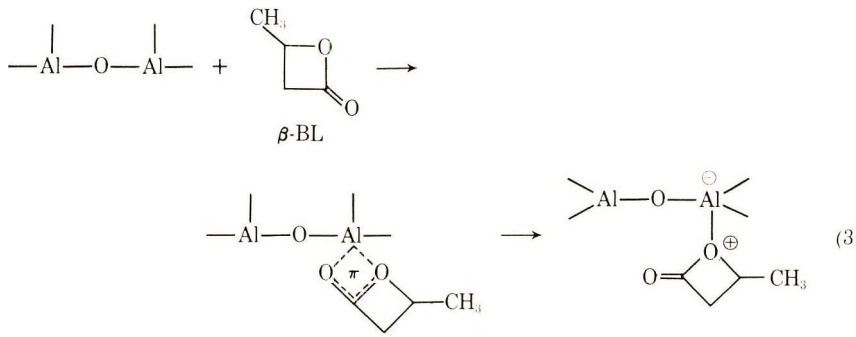

(3)

Propagation:

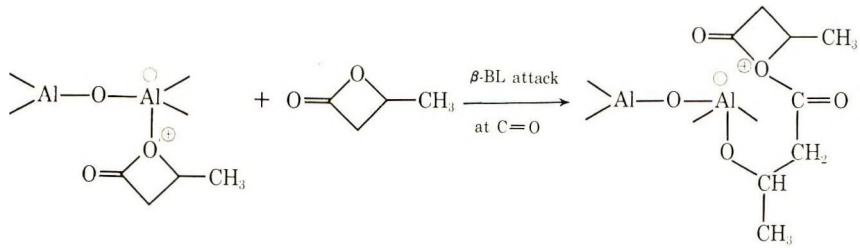

IV (4)

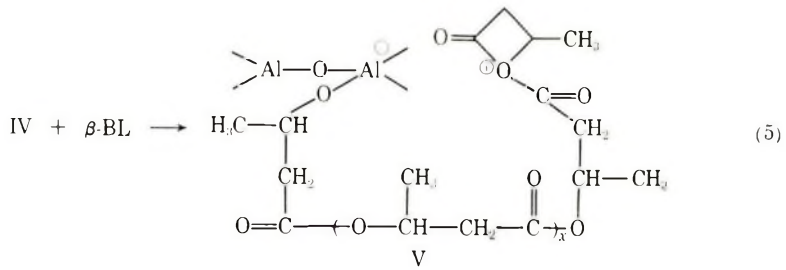

V (5)

Termination:

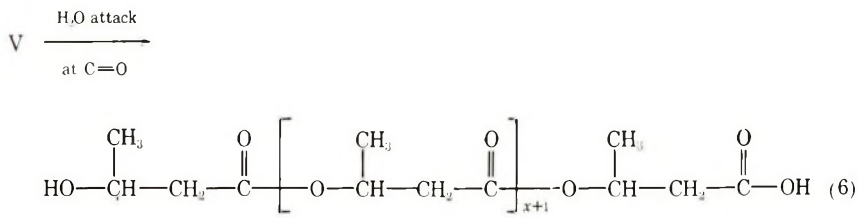

(6)

It is evident from the positive rotation at 300 mμ of the polymer synthesized from D-(+)-β-BL that propagation is mainly via a mechanism of the type described above since the configuration of the asymmetric center is retained. The high degree of crystallinity observed in both DL-PHB and synthetic D-PHB is also consistent with such a mechanism.

A probable reaction for termination of polymerization with added water is shown by eq. (6). Hydrolysis of both the aluminum-oxygen bond of the polymer and the oxonium cation would be expected. Thus, polymer V would be converted to a structure with hydroxyl and carboxyl endgroups. The presence of hydroxyl endgroups has been confirmed by infrared spectroscopy, but absorptions due to the carboxyl group were not identifiable, possibly because of other overlapping absorptions in the same region.

SUMMARY

Optically active crystalline D-poly-β-hydroxybutyrate, similar in all respects to the naturally occurring polymer, was synthesized in this laboratory by polymerization of optically active D-(+)-β-butyrolactone with

Et_3Al–H_2O (1:1) as catalyst and cocatalyst. The polymer was fully characterized, including optical rotary dispersion measurements which confirmed the same configuration as bacterial D-PHB. The specific rotation of the synthetic polymer at 300 mμ was somewhat low; however, it is not surprising because it was of lower molecular weight and synthesized from a monomer of only 73% optical purity.

The proposed mechanism for ring-opening polymerization of β-BL with this catalyst system, consistent with the above experimental observations, involves essentially attack of monomer at the carbonyl carbon of an oxonium ion propagating species with breaking of the acyl–oxygen bond to introduce new monomer units into the growing chain with retention of configuration at the asymmetric center.

Partial support of this work was provided by The Goodyear Tire and Rubber Co., Akron, Ohio.

References

1. D. E. Agostini, J. B. Lando, and J. R. Shelton, *J. Polym. Sci. A-1*, **9**, 2771 (1971). (Part I).
2. J. R. Shelton, J. B. Lando, and D. E. Agostini, *J. Polym. Sci. B*, **9**, 173 (1971).
3. J. A. Dale, D. L. Dull, and H. S. Mosher, *J. Org. Chem.*, **34**, 2543 (1969).
4. Y. Iwakura, K. Nazakubo, H. Kawasumi, and S. Kigawa, *J. Chem. Soc., Japan*, **72**, 406 (1951).
5. M. Raban and K. Mislow, in *Topics in Stereochemistry*, Vol. II, N. L. Allinger and E. L. Eliel, Eds., Interscience, New York, 1967, p. 199
6. J. L. Mateos and D. J. Cram, *J. Amer. Chem. Soc.*, **18**, 2756 (1969).
7. H. E. Zaugg, *Organic Reactions*, Vol. II, Wiley, New York, 1954, pp. 324–326.
8. E. Grunwald and S. Winstein, *J. Amer. Chem. Soc.*, **70**, 841 (1948).
9. W. A. Cowdrey, E. D. Hughes, C. K. Ingold, S. Masterman, and A. D. Scott, *J. Chem. Soc.*, **1937**, 1252.
10. E. D. Hughes, F. Juliusberger, A. D. Scott, B. Topley, and J. Weiss, *J. Chem. Soc.*, **1936**, 1137.
11. E. D. Hughes, C. K. Ingold, and S. Masterman, *J. Chem. Soc.*, **1937**, 1196.
12. E. D. Hughes, C. K. Ingold, and A. D. Scott, *J. Chem. Soc.*, **1937**, 1201.
13. R. Alper, D. G. Lundgren, R. H. Marchessault, and W. A. Cote, *Biopolymers*, **1**, 545 (1963).
14. R. H. Marchessault, K. Okamura, and C. J. Su, *Macromolecules*, **3**, 735 (1970).
15. J. Cornibert, R. H. Marchessault, H. Benoit, and G. Weill, *Macromolecules*, **3**, 741 (1970).
16. D. G. Lundgren, R. Alper, C. Schnaitman, and R. H. Marchessault, *J. Bacteriol.*, **89**, 245 (1965).
17. T. Tsuruta, S. Inoue, and Y. Yokota, *Makromol. Chem.*, **103**, 164 (1967).
18. Y. Yamashita, Y. Ishikawa, T. Tsuda, and S. Miura, *Kogyo Kagaku Zasshi*, **66**, 110 (1963).
19. R. O. Colclough and K. Wilkinson, *J. Polym. Sci. C*, **4**, 311, (1964).
20. R. W. Lenz, *Organic Chemistry of Synthetic High Polymers*, Interscience, New York 1967, p. 560.

Received April 19, 1971
Revised May 25, 1971

JOURNAL OF POLYMER SCIENCE: PART A-1 VOL. 9, 2801–2815 (1971)

Permeability of Membranes Containing Ionogenic Groups

J. KOPEČEK, J. VACÍK, and D. LÍM, *Institute of Macromolecular Chemistry, Czechoslovak Academy of Sciences, Prague 6, Czechoslovakia*

Synopsis

The present paper deals with the transport properties of membranes made of hydrophilic gels containing ionogenic groups. Introduction of ionogenic groups into a gel based on 2-hydroxyethyl methacrylate will affect the permeability of the investigated membranes for sodium chloride by an order or more. Dependences of the permeability on the content of ionogenic groups, three-dimensional network density, and pH were established. The permeability for NaCl was compared for that for bivalent salt ($MgSO_4$). It is shown, on the basis of independently determined distribution coefficients, that an increase in the permeability of ampholytic membranes in comparison with the neutral ones is primarily due to an increase in the diffusivity of the salt in the membranes with modified structure. It can also be concluded that an approximation of the free volume from the volume of the solvent in the membrane cannot be applied to the poly(2-hydroxyethyl methacrylate) gel.

INTRODUCTION

An interest taken by us in the further development of the knowledge acquired so far about hydrophilic gels has led to a systematic investigation of structures which, apart from basic hydrophilic and mechanical properties, are also characterized by functional groups capable of specific interactions.

After the biological tolerance of the above materials in a living organism has been established,[1] the preparation of "tailor-made" polymers for medical uses (for instance, in hemodialysis) necessitates the knowledge of the basic relations between the polymer structure and their transport properties. The knowledge of these relations is of great importance also in some other areas, such as, e.g., preparation of membranes for reverse osmotic separation.

The present paper deals with the transport properties of reinforced, poly(2-hydroxyethyl methacrylate) membranes crosslinked with ethylene dimethacrylate. The basic skeleton has been modified by introducing ionogenic groups. For this purpose, methacrylic acid and 2-(diethylamino)ethyl methacrylate were used as comonomers, which enabled four types of membranes to be obtained: neutral gel, gel containing acidic

groups, gel containing basic groups, and ampholyte containing both types of groups in approximately the same molar quantity. By varying the amount of ionogenic groups and crosslinking density, we prepared a set of membranes which allowed the relationship between the structure of this type of membranes and their transport properties to be determined over a wide composition range.

EXPERIMENTAL

Monomers

2-Hydroxyethyl methacrylate (HEMA) was prepared by alkaline reesterification of methyl methacrylate with ethylene glycol. The diester was removed from the water-diluted reaction mixture by several extractions with hexane, and the monoester was then extracted with ether. Purity was checked by the saponification number and gas chromatography; bp, 79°C/4 torr; $n_D^{20} = 1.4525$.

Ethylene dimethacrylate (EDMA), a Chemapol product, was freed from hydroquinone by shaking with 5% NaOH. On drying with annealed Na_2SO_4 it was redistilled *in vacuo* three times. Purity was checked by gas chromatography and infrared spectrometry (absence of the —OH groups); bp, 84°C/1 torr; $n_D^{20} = 1.4549$.

Methacrylic acid (MAA), a Chemapol product, was rectified, and its purity was checked by gas chromatography; bp, 59°C/10 torr; $n_D^{20} = 1.4314$.

2-(Diethylamino)ethyl methacrylate (DEAEMA) was prepared by alkaline reesterification of methyl methacrylate with 2-(diethylamino)-ethanol. The crude product was rectified. Purity was checked by gas chromatography; bp, 80°C/10 torr; $n_D^{20} = 1.4435$.

2,2′-Azobis(methyl isobutyrate) was obtained by saponification of 2,2′-azobisisobutyronitrile with hydrogen chloride in methanolic solution. The precipitated iminoether hydrochloride was hydrolyzed with lukewarm water. The crude product was recrystallized five times in petroleum ether, mp 30°C.

Preparation of Membranes

A nylon mesh 0.09 thick, was extracted with tetrachloromethane for 20 hr, dried, and ironed. After this treatment it was put between two polyethylene films, and the sandwich thus obtained was placed between two plane-parallel glass plates (10 mm), fixed in a metallic frame. The mixture of monomers was freed from dissolved oxygen by bubbling through with nitrogen and transferred by the pressure of nitrogen into the space between the two polyethylene films. On filling, the plane-parallel glass plates were placed between two thermostatted cells, whose surfaces adhered to the glass. The polymerization proceeded at 60°C for 15 hr. After the polymerization was completed, the individual mem-

TABLE I
Composition of the Starting Mixtures for the Preparation of Hydrophilic Membranes[a]

Membrane no.	[HEMA], mole/kg	[DEAEMA], mole/kg	[MAA], mole/kg	[EGDMA], mole/kg
41	6.44	—	—	0.040
42	6.27	—	—	0.124
43	6.14	—	—	0.210
44	5.51	—	1.34	0.040
45	5.41	—	1.32	0.125
46	5.26	—	1.34	0.210
47	5.01	0.990	—	0.040
48	4.88	0.990	—	0.123
49	4.75	0.980	—	0.202
50	5.17	0.576	0.590	0.041
51	5.02	0.587	0.605	0.127
52	4.89	0.577	0.597	0.211
53	6.44	—	—	0.021
54	5.54	—	1.319	0.021
55	5.03	0.929	—	0.021
56	5.22	0.510	0.593	0.021
57	6.06	—	0.299	0.125
58	5.81	—	0.648	0.126
59	5.58	—	1.004	0.126
60	4.89	—	2.041	0.126
61	5.83	0.275	—	0.125
62	5.38	0.562	—	0.126
63	4.98	0.835	—	0.125
64	4.59	1.080	—	0.125
66	5.95	0.138	0.156	0.124
67	5.62	0.287	0.290	0.126
68	5.25	0.443	0.482	0.128
69	4.42	0.866	0.779	0.127

[a] Polymerization at 60°C; [2,2'-azobis(methyl isobutyrate)] = 3×10^{-3} mole/kg; [butanol] = 2.15 mole/kg. Thickness of membranes swollen to equilibrium was 0.011–0.013 cm.

branes were put into redistilled water and left there for 3 to 4 weeks. The composition of the membranes is given in Table I.

Permeability Measurements

Measurements were carried out in a diffusometer made of Perspex and consisting of two cells of the same volume (50 ml). The membrane was fixed by means of a Teflon ring having conic section. This ring, together with two silicone rings, served as a seal between both cells of the diffusometer. The cells were fastened together with four brass screws. The liquid in both cells was stirred with a high-speed stirrer. The concentration changes in both cells were followed conductometrically (with a platinum electrode). The experiments were carried out at 25°C. The starting concentration was ~0.1%.

The results were evaluated according to the relationship[2]

$$Q_s = (DKc_2/\Delta x)[t - (\Delta x^2/6D)] \quad (1)$$

where Q_s is the total amount of salt (g/cm²) that diffused through a surface unit in time t(sec), c_2 is the starting concentration of salt (g/cm³, $c_2 \gg c_1$, where c_1 is the concentration of salt in the cell with lower concentration. In time $t = 0$, $c_1 = 0$), Δx is the membrane thickness (cm), D is the diffusion coefficient (cm²/sec), and K is the distribution coefficient of salt between the solution and the membrane. By plotting Q_s versus t it is possible to obtain the permeability $P = DK$ from the slope. The determination of diffusion coefficients from the intercepts on the t axis is not exact owing to the small membrane thickness; we therefore determined the distribution coefficients independently and calculated D from the known values of P and K (cf. below). The concentration polarization was neglected in the evaluations.

In permeability measurements at various pH, the procedure was similar to that used in the neutral region. The pH of solutions was maintained by the least possible amount of the universal Britton-Robinson buffer, which was determined by a blank test and in no case exceeded 40 ppm. An inert nitrogen atmosphere was maintained in both cells during measurements in the alkaline region in order to prevent the lowering of pH due to CO_2 absorption.

Determination of the Distribution Coefficients

Small blocks of gel prepared from the same starting mixture as the membranes under investigation were placed in a 5% NaCl solution at 25°C. On attaining equilibrium (after several weeks) they were taken out, and the NaCl solution which stuck to the surface was removed by a quick dipping of the sample in redistilled water. The sample was put into such an amount of redistilled water which allowed the volume of the sample to be neglected (1:200). On establishing equilibrium the concentration of sodium chloride in the washing water was determined conductometrically. From the known volume of the samples (see below) and the concentration of the salt solution the distribution coefficient K of the salt was determined as

$$K = \frac{\text{g NaCl/cm}^3 \text{ of the membrane}}{\text{g NaCl/cm}^3 \text{ of the solution}} \quad (2)$$

Determination of the Equilibrium Swelling Degree

The measurements were carried out on cylindric polymer samples (average volume 3 cm³) of the same composition as the membranes employed. The samples were swollen to equilibrium in water at 25°C, divided into three parts, and each of them was weighed several times. One part was dried at 45°C/5 torr to constant weight. The second part was swollen to equilibrium in NaCl solutions of various concentrations.

The degree of equilibrium swelling was again determined by weighing. The third part of the sample was used for the determination of the degree of equilibrium swelling at various pH. From the values thus determined, it was possible to calculate the weight swelling ratio in dependence on the concentration of the salt in solution, or on pH.

The volume degree of swelling (v_2) was calculated on the assumption of the additivity of the water and polymer volumes [for the polymer density the value for poly(2-hydroxyethyl methacrylate)[4] was used, i.e., 1.313],

$$v_2 = (m_2/\rho_2)/[(m_2/\rho_2) + (m_1/\rho_1)] \quad (3)$$

where v_2 is the volume fraction of the polymer in a gel swollen to equilibrium, m_2 is the weight of the dry polymer, ρ_2 is the density of the dry polymer, m_1 is the weight of water and ρ_1 is the density of water.

TABLE II

Dependence of the Equilibrium Degree of Swelling (Volume Fraction of the Polymer v_2) of Modified Hydrophilic Gels on the Concentration of NaCl and the Permeability of the Membranes Studied

	v_2					
Sample[a]	H_2O	1% NaCl	3% NaCl	5% NaCl	$P_{NaCl} \times 10^8$, cm²/sec	$P_{MgSO_4} \times 10^9$, cm²/sec
41	0.5599	0.5716	—	0.6296	12.3	1.76
42	0.5860	0.5958	—	0.6465	7.97	1.08
43	0.6163	0.6232	—	0.6646	4.44	1.69
44	0.6135	0.6180	—	0.6780	2.85	2.85
45	0.6290	0.6279	—	0.6744	1.92	1.73
46	—	—	—	—	1.20	0.405
47	0.6272	0.6464	—	0.7101	0.675	19.4
48	0.6417	0.6560	—	0.7108	0.753	5.05
49	0.6619	0.6733	—	0.7148	0.931	2.95
50	0.4506	0.4378	—	0.4572	31.9	—
51	0.4539	0.4426	—	0.4618	29.3	55.9
52	0.4538	0.4354	—	0.4543	27.8	31.8
53	0.5494	—	—	0.5516	14.5	—
54	0.6015	—	0.6390	0.6592	3.34	—
55	0.6119	—	0.6694	0.6870	0.892	—
56	0.4119	—	0.3914	0.4035	—	—
57	0.5959	—	0.6293	0.6485	4.82	—
58	0.6705	—	0.6463	0.6626	2.67	—
59	0.6245	—	0.7889	0.7963	2.79	—
60	0.6271	—	0.6578	0.6685	1.38	—
61	0.5882	—	0.5903	0.6038	1.23	—
62	0.6159	—	0.6675	0.6817	0.540	—
63	0.6395	—	0.6784	0.6960	0.375	—
64	0.6545	—	0.7055	0.7055	0.313	—
66	0.5492	—	0.5810	0.5969	8.48	1.26
67	0.5928	—	0.6240	0.6404	9.73	—
68	0.5939	—	0.6338	0.6529	7.64	2.12
69	0.5909	—	0.6301	0.6485	107	152

[a] For composition of samples see membranes in Table I.

The dependence of the equilibrium degree of swelling on the concentration of sodium chloride is shown in Table II.

Determination of the Titration Curves

Samples of polymers containing ionogenic groups were prepared by solution polymerization. In contrast with the preparation of membranes, no crosslinking agent (EDMA) was used in this case, so that a soluble polymer was obtained. The solution of the polymer was precipitated in an excess of diethyl ether, filtered off, washed, and dried *in vacuo*.

The dry sample (~0.1 g) was dissolved in a corresponding amount of ethanol which was neutralized in advance, and the necessary amount of preboiled distilled water was then added. The carboxyl groups were titrated with 0.1*N* NaOH, the amine groups were titrated with 0.1*N* HCl, both in an argon atmosphere. A potentiograph E 336 (Metrohm) with combined glass–calomel electrodes was employed for following the pH of the mixture.

RESULTS AND DISCUSSION

2-Hydroxyethyl methacrylate was the basic monomer employed in the preparation of membranes, both owing to the good properties which allowed its wide uses in various applications and also because the kinetics of polymerization and structure of the polymer have already been studied in detail.[3,4]

The basic skeleton of the poly(2-hydroxyethyl methacrylate) gel (crosslinked with ethylene dimethacrylate) was modified by copolymerization with monomers containing either acidic or basic groups. Methacrylic acid was selected as the carrier of acidic groups, and 2-(diethylamino)ethyl methacrylate served as the carrier of basic groups. The polymerization was carried out to 100% conversion. It follows from the determination of the soluble fractions and the analysis of the polymers formed (determination of the nitrogen content and titration of the —COOH groups) that all components are quantitatively incorporated in the three-dimensional network. Owing to the inequality of the copolymerization parameters in the case under consideration and also to their dependence on pH in the case of ionogenic monomers,[5] the distribution of the components along the chain will not be a statistical one. The characterization of membranes by the composition of the starting monomeric mixture gives the composition of the polymer formed, but cannot of course supply any data on the distribution of the individual components along the polymeric chain.

The first part of the work was devoted to an investigation of the effect of the network density upon the permeability of membranes for sodium chloride, in which for each group (i.e., neutral, ampholytic, acidic, and basic) the content of ethylene dimethacrylate was varied (Table I, membranes 41–55). The content of monomers containing ionogenic groups

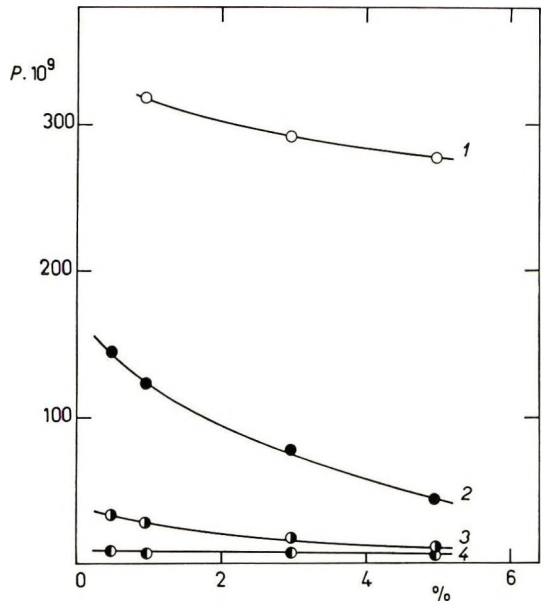

Fig. 1. Dependence of the permeability coefficient P (cm²/sec) of modified hydrophilic membranes (approximately 20 mole-% of ionogenic components) for NaCl on the network density (expressed in % by weight EDMA): (1) copolymer HEMA–EDMA DEAEMA–MAA; (2) HEMA–EDMA; (3) HEMA–EDMA–MAA; (4) HEMA–EDMA–DEAEMA.

was approximately 20 mole-%, the content of ethylene dimethacrylate varied from 0.5 to 5 wt-%. At 25°C, the permeabilities of the bove membranes vary up to 30 times (Fig. 1). The lowest permeability is observed with membranes carrying a permanent negative charge (copolymers containing methacrylic acid structure units) or a permanent positive charge [copolymers containing 2-(diethylamino)ethyl methacrylate]. This can be understood, since owing to Donnan's excluding effect the transport of the coion through the membrane will be slowed down, so that, with respect to the necessity of the conservation of electroneutrality, the diffusion of the salt as a whole will be slowed down. The highest permeability is shown by ampholytic membranes [gels containing units of methacrylic acid and 2-(diethylamino)ethyl methacrylate], since in this case the electric charge leads to an acceleration of the diffusion of both ions. The permeability of neutral membranes is situated between that of ampholytic membranes and membranes containing only one type of ionogenic groups. It is of interest to compare the slope of dependence of permeability on the content of the crosslinking agent (ethylene dimethacrylate) in the starting mixture. The steepest slope is observed with neutral membranes, where a change in the network density is most marked, since in this case the gel affects the permeating particle only by physical forces of a shorter range. The slope of the other types of mem-

branes containing ionogenic groups and in which coulomb interactions occur is much milder, since in this case the effect of the change of the free volume upon permeability will not be so pronounced (for a group of membranes having the same permanent charge).

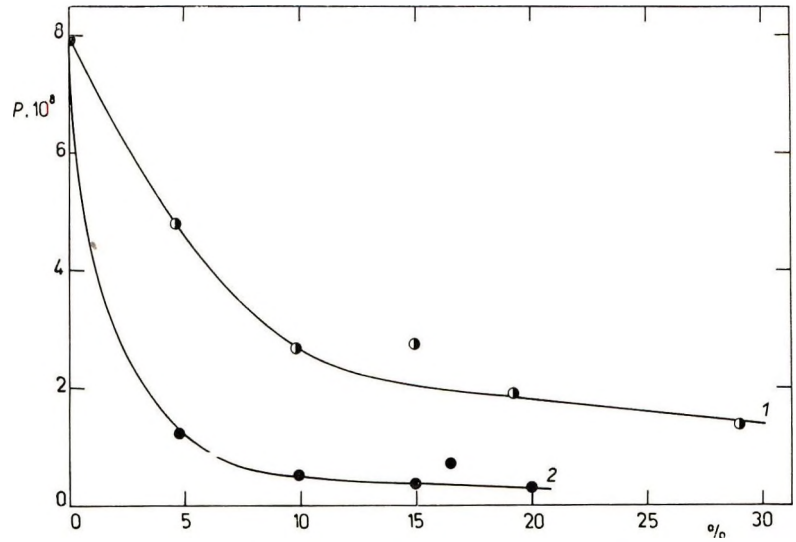

Fig. 2. Dependence of the permeability coefficient P (cm²/sec) of modified hydrophilic membranes for NaCl on the content of ionogenic groups (mole-%): (*1*) copolymer HEMA–3 wt-% EDMA–MAA; (*2*) HEMA–3 wt-% EDMA–DEAEMA.

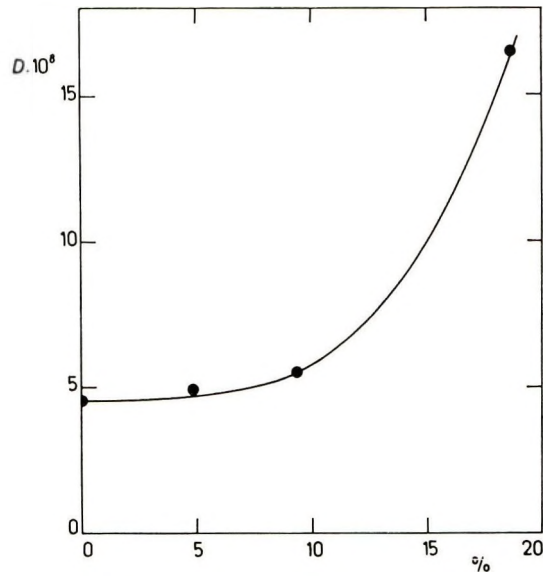

Fig. 3. Dependence of the permeability coefficient P (cm²/sec) of ampholytic membranes (copolymer HEMA–3 wt-% EDMA–MAA–DEAEMA) for NaCl on the content of ionogenic components (mole-%); [MAA] = [DEAEMA].

The dependence of permeability of acidic or basic membranes for sodium chloride on the content of ionogenic component (MAA or DEAEMA) in the membrane is characterized by a strong initial decrease (Fig. 2 and Table II), followed by a much milder decrease on attaining the limit concentration. On the other hand, in the case of ampholytic membranes the permeability is first constant (Fig. 3 and Table II), and starts rising after the limit concentration has been attained.

Permeability of Membranes for Magnesium Sulfate

The permeability for inorganic salts is known to be affected by the valency of the salt and the size of the hydrated volume of ions. It can be said, on the whole, that in contrast with NaCl the permeability for $MgSO_4$ is much lower (Table II and Fig. 4). Here again an increase in permeability is observed for ampholytic membranes, but there is no principal difference between the permeabilities of neutral and acidic membranes. These findings, and also the steep negative slope of the dependence of permeability of ampholytic membranes for $MgSO_4$ on the network density indicate that, owing to the large radius of hydrated ions[6] (4.21 Å for hydrated Mg^{2+} and 3.79 Å for hydrated SO_4^{2-}), the low value of the free volume manifests itself pronouncedly also in the membranes carrying a permanent charge. For larger particles, the effect of the pore distribution will prevail, and consequently, also the mechanical barriers

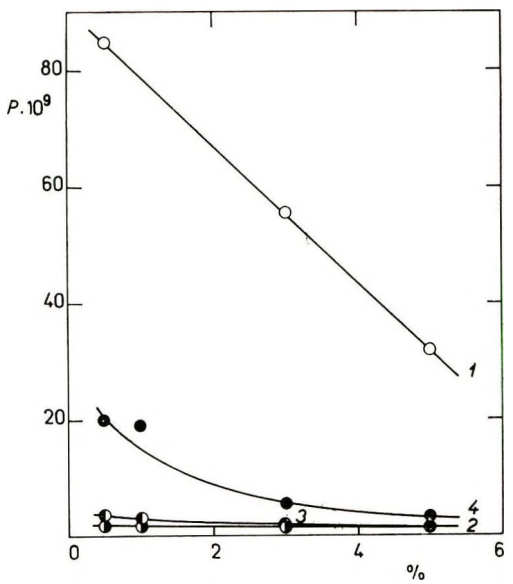

Fig. 4. Dependence of the permeability coefficients P (cm²/sec) of modified hydrophilic membranes (approximately 20 mole-% ionogenic groups) for $MgSO_4$ on the network density (expressed in wt-% EDMA): (*1*) copolymer HEMA–EDMA–DEAEMA–MAA; (*2*) HEMA–EDMA; (*3*) HEMA–EDMA–MAA; (4) HEMA–EDMA–DEAEMA.

to diffusion will prevail over the other influences, including the coulomb interactions.

The observed effect of the permeability of $MgSO_4$ through membranes containing basic groups is due to the lower pH of the $MgSO_4$ solutions, which leads to a change in the degree of ionization of the membrane. At lower network densities, this can be used to affect the permeability. If the network density is larger, the effect of the pore distribution will prevail (shift towards smaller values), as has been discussed above.

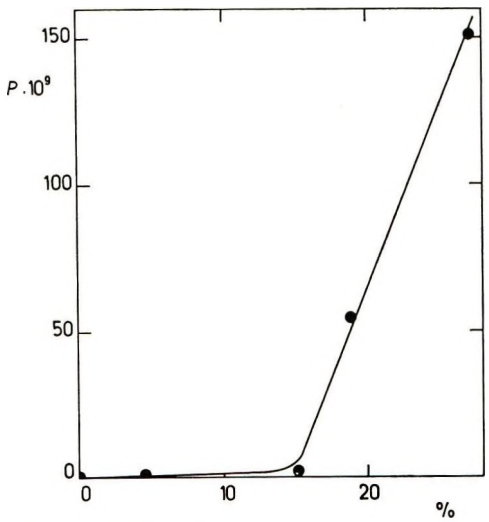

Fig. 5. Dependence of the permeability coefficient P (cm²/sec) of ampholytic membranes (copolymer HEMA–3 wt-% EDMA–MAA–DEAEMA) for $MgSO_4$ on the content of ionogenic groups (mole-%); [MAA] = [DEAEMA].

We have also investigated the dependence of permeability on the content of ionogenic components for ampholytic membranes (Table II and Fig. 5). The shape of the curve is similar to that in the case of permeation of NaCl, with the difference that the limit concentration of the ionogenic components, beyond which there is an increase in permeability, is more pronounced. The results can again be interpreted by an increase in the ion mobility in polymers having a higher content of ionogenic groups.

Dependence of Permeability on pH

As can be expected, the permeability of membranes containing ionogenic groups is strongly dependent on the degree of ionization. The above dependence has been investigated for all the three types of membranes containing ionogenic groups (membrane 59 as a representative of acidic membranes, membrane 61 as a representative of basic membranes, and membrane 69 as an ampholytic membrane, cf. Table I). As follows from the results, shown in Figure 6, the permeability for NaCl through a gel membrane containing basic units of methacrylic acid (membrane

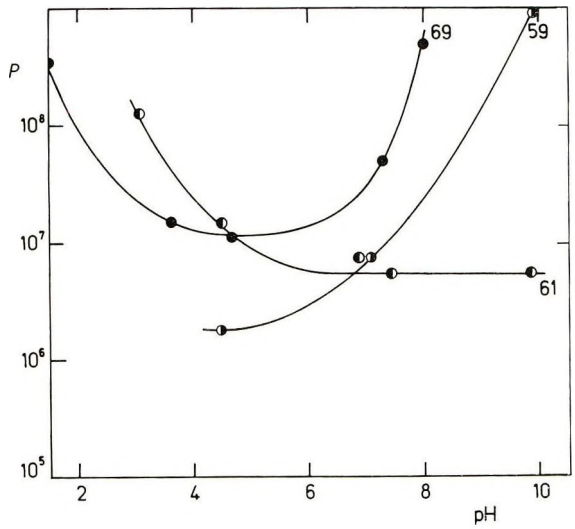

Fig. 6. Dependence of the permeability coefficient P (cm²/sec) of modified hydrophilic membranes for NaCl on pH. The curve numbers denote the number of the membrane composition (Table I).

59), increases in the alkaline region, whereas the permeability through a gel membrane containing basic units of 2-(diethylamino)ethyl methacrylate (membrane 61) increases in the acidic region. The permeability through an ampholytic membrane [membrane 69, gel containing approximately the same quantities of the methacrylic acid and 2-(diethylamino)ethyl methacrylate units] passes through a minimum and increases in both directions from the isoelectric point, whose position is in accordance with the results by Jacobson.[7] It can be assumed, on the basis of the results described above, that the ampholytic membranes studied by us are internal salts having the structure I:

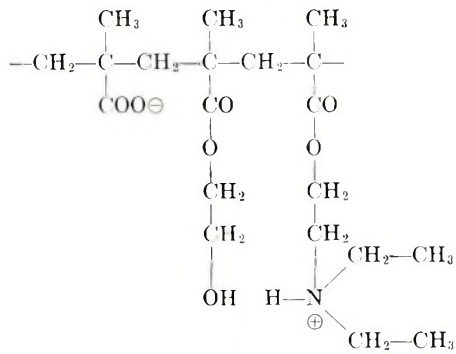

I

To be able to correlate the observed dependences of the permeability for NaCl on pH with the degree of ionization of modified hydrophilic gels, two samples of copolymers were prepared, an acidic and a basic one,

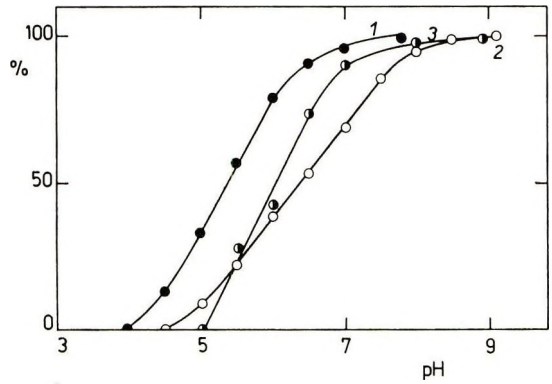

Fig. 7. Titration curves of the HEMA–MAA copolymer: (1) in $C_2H_5OH:H_2O$ = 1:20 mixture; (2) in $C_2H_5OH:H_2O$ = 1:1 mixture; (3) in a 1% solution of NaCl in a $C_2H_5OH:H_2O$ = 1:1 mixture. [HEMA] = 0.912 mole/kg; [MAA] = 0.146 mole/kg; [C_2H_5OH] = 18.84 mole/kg; [2,2′-azobis(methyl isobutyrate)] = 3.9×10^{-3} mole/kg; polymerization at 60°C.

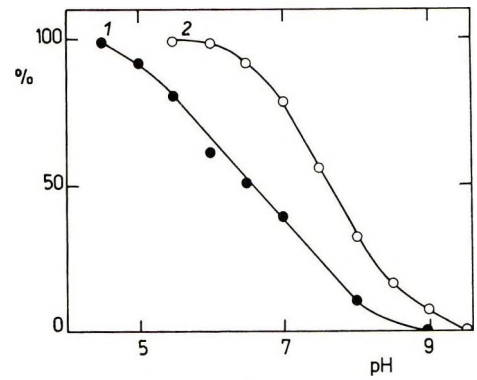

Fig. 8. Titration curves of the HEMA–DEAEMA copolymer: (1) in $C_2H_5OH:H_2O$ = 1:1 mixture; (2) in a 1% solution of NaCl in a $C_2H_5OH:H_2O$ = 1:1 mixture. [HEMA] = 0.797 mole/kg; [DEAEMA] = 0.130 mole/kg; [C_2H_5OH] = 18.92 mole/kg; [2,2′-azobis(methylisobutyrate)] = 3.9×10^{-3} mole/kg; polymerization at 60°C.

which in contrast with the investigated membranes were not crosslinked, and their titration curves were determined.

Owing to the solubility of the copolymer, the titrations were carried out in ethanol–water mixed solvent. To exclude the effect of ethanol on pH, the titrations were made in a series of ethanol–water mixtures (1:1, 1:5, 1:7, 1:10, and 1:20). The shape of the curves is essentially the same, with decreasing content of ethanol they are shifted to lower pH. The values obtained for the copolymer HEMA–EDMA–MAA in 1:1 and 1:20 mixed solvents are plotted in Figure 7. A titration in a 1% solution of NaCl was also carried out, in order to investigate the effect of the presence of an electrolyte on the ionization of the —COOH groups. Although perceptible, this effect is nevertheless considerably less pro-

nounced than described by Jadwin[8] in his thesis. Figure 8 shows titration curves of the copolymer HEMA–EDMA–DEAEMA. It also shows the effect of the presence of sodium chloride upon the quaternization of a tertiary amine group.

A conclusion can be drawn from the above measurements, that even at the pH of distilled water there is a partial ionization of ionogenic groups present in acidic or basic membranes, and the latter bear the responsibility for a decrease in the rate of permeation described above. The ampholytic membranes are internal salts, as also has been stated above.

Diffusion Coefficients

The transport of sodium chloride, which has been discussed above in terms of permeation coefficients, can be interpreted, at least for some of the membranes under investigation, by means of diffusion coefficients. As has been shown, the diffusion coefficients cannot be calculated by the time-lag method owing to the low value of $L = \Delta x^2/6D$. We therefore measured the distribution coefficient K independently and calculated the diffusion coefficient from the relationship $D = P/K$.

With respect to the dependence of the Donnan excluding effect on the concentration of the external electrolyte, the above method can be used for interpreting the data for neutral and ampholytic membranes only. The dependence of the diffusion coefficients upon the content of ionogenic components for ampholytic membranes is shown in Figure 9. If we assume that the distribution coefficient is independent of the network density (on the basis of the small dependence of the equilibrium degree of

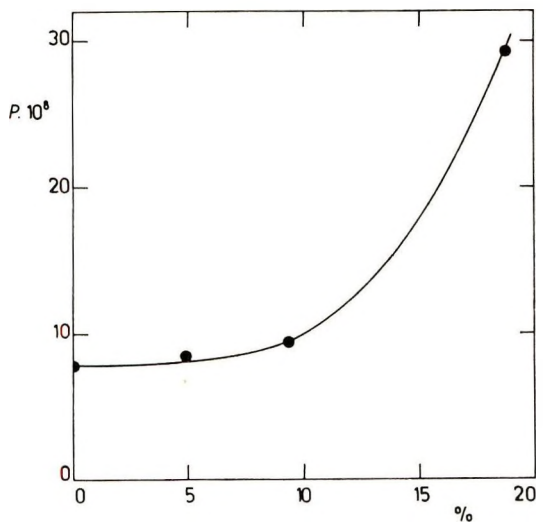

Fig. 9. Dependence of the diffusion coefficient D, (cm²/sec) of ampholytic membranes (copolymer HEMA–3 wt-% EDMA–MAA–DEAEMA) for NaCl on the content of ionogenic groups (mole-%); [MAA] = [DEAEMA].

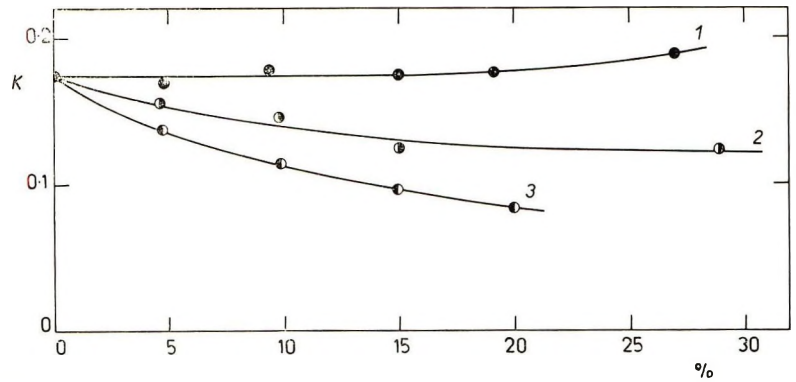

Fig. 10. Dependence of the distribution coefficient K for NaCl on the content of ionogenic groups in modified hydrophilic membranes (mole-%): (*1*) copolymer HEMA–3 wt-% EDMA–MAA–DEAEMA; (*2*) HEMA–3 wt-% EDMA–MAA; (*3*) HEMA–3 wt-% EDMA–DEAEMA.

swelling on the concentration of the crosslinking agent), then the course of the dependence of the diffusion coefficients on the network density for neutral and ampholytic membranes will be analogous to the course of the dependence of the permeation coefficients on the network density (curves *1* and *2* in Fig. 1; for neutral membranes $K_{NaCl} = 0.175$; for ampholytes with $\sim 20\%$ of ionogenic components; $K_{NaCl} = 0.177$).

With respect to the facts described above, it can be said that an acceleration of the transport of inorganic salts by ampholytic membranes compared with the neutral ones is due to an increase in their diffusivity, and not to a decrease in the concentration of the salt inside the membrane (decrease in solubility).

In the case of membranes containing only one type of ionogenic groups the transport of the salt will in the first place be affected by Donnan's excluding effect, which is shown particularly at low concentrations, used by the authors in the permeability measurements. Besides the influence described above, which is concentration-dependent, the influence of the polymer structure on the mobility of ions can also be observed. Measurements of distribution coefficients in the concentration range in which Donnan's effect can already be neglected yield a qualitative picture of this effect (Fig. 10).

Yasuda et al.[9–11] interpreted the diffusion data determined on a series of hydrophilic polymers in terms of the free volume theory.[12–14] From this theory, a relationship can be derived for the diffusion coefficient

$$D \sim \exp - \{v^+/v_f\} \tag{4}$$

where v^+ is the characteristic volume occupied by the permeating particle and v_f is the free volume in the polymer. Their assumption for the case of neutral membranes, namely, that the free volume is linearly dependent on the volume fraction of the solvent, does not apply to a gel based on

2-hydroxyethyl methacrylate. The crosslinking density has only little influence upon the degree of equilibrium swelling of hydroxyethyl methacrylate gels in water[4] (which has also been confirmed by measurements listed in Table II). In our opinion, this finding ought to be taken into consideration while applying the free volume theory of diffusion to the systems used by us. In this case, the free volume cannot be regarded as proportional to the volume fraction of the solvent; it will rather depend on the length of the polymeric segments. The length of the segments will considerably affect their mobility, so that it can be imagined that two differently crosslinked gels can have different free volumes, even in the case of not too different degrees of swelling. It can be assumed that similar conclusions will be generally valid in those cases where the gel is swollen in a thermodynamically poor solvent.

The authors are indebted to Mrs. L. Žižková for technical assistance.

References

1. M. Barvič, J. Vacík, D. Lím, and M. Zavadil, *J. Biomed. Mat. Res.*, **5**, 225 (1971).
2. J. Crank, *The Mathematics of Diffusion*, Oxford Univ. Press, London 1956.
3. J. Kopeček, J. Jokl, and D. Lím, in *Macromolecular Chemistry, Prague 1965 (J. Polym. Sci. C*, **16**), O. Wichterle and B. Sedláček, Eds., Interscience, New York, 1968, p. 3877.
4. J. Kopeček and D. Lím, *J. Polym. Sci. A-1*, **9**, 147 (1971).
5. T. Alfrey, H. Morawetz, and H. Pinner, *J. Amer. Chem. Soc.*, **74**, 438 (1952).
6. E. R. Nightingale, *J. Phys. Chem.*, **63**, 1381 (1959).
7. H. Jacobson, *J. Phys. Chem.*, **66**, 570 (1962).
8. T. A. Jadwin, Ph.D. Thesis, Department of Chemical Engineering, Massachusetts Institute of Technology, Boston, Massachusetts, May 1968.
9. H. Yasuda, C. E. Lamaze, and L. D. Ikenberry, *Makromol. Chem.*, **118**, 19 (1968).
10. H. Yasuda, L. D. Ikenberry, and C. E. Lamaze, *Makromol. Chem.*, **125**, 108 (1969).
11. H. Yasuda, A. Peterlin, C. K. Colton, K. A. Smith, and E. W. Merrill, *Makromol. Chem.*, **126**, 177 (1969).
12. M. H. Cohen and D. Turnbull, *J. Chem. Phys.*, **29**, 1049 (1958).
13. N. Hirai, and H. Eyring, *J. Polym. Sci.*, **37**, 51 (1959).
14. S. Rosenbaum, H. I. Mahon, and O. Cotton, *J. Appl. Polym. Sci.*, **11**, 2041 (1967).

Received December 31, 1970

JOURNAL OF POLYMER SCIENCE: PART A-1 VOL. 9, 2817–2834 (1971)

Friedel-Crafts Copolymerization of Thiophene and *p*-Di(chloromethyl)benzene. I. Products, Kinetics, and Mechanism of the Early Stages of the Reaction

N. GRASSIE, J. B. COLFORD,* and I. G. MELDRUM,† *Department of Chemistry, University of Glasgow, Glasgow W.2, Scotland*

Synopsis

The rate of polymerization of thiophene, at concentrations of catalyst ($SnCl_4$), and thiophene of the same order as was subsequently used in studying the reaction between thiophene and di(chloromethyl)benzene, is of the order of 10^{-2}%/hr at 30°C. There is no significant self-condensation of DCMB under the same conditions. Since the reaction between thiophene and DCMB is complete at 30°C in minutes rather than hours, it is assumed that self-condensation of thiophene or DCMB during the reaction between them will be negligible and should not influence the course of the reaction or the structure of the resulting polymer. Reaction at 30°C is much too fast for convenient study. A temperature of 0°C is more appropriate and was used in subsequent kinetic work. The first two products of the condensation of *p*-di(chloromethyl)benzene (DCMB) with thiophene have been identified by a combination of mass, infrared, and nuclear magnetic resonance spectroscopy as thenylchloromethylbenzene (TCMB) and dithenylbenzene (DTB). DCMB, TCMB, and DTB have been estimated quantitatively during the course of the reaction by gas-liquid chromatography (GLC), and it has been established that the rates of each of the two reaction steps is first-order with respect to the chloro compound (DCMB and TCMB respectively), thiophene, and $SnCl_4$. Rate constants for these two consecutive reactions were calculated to be $k_1 = 2.79 \times 10^{-4}$ l.²/mole²-sec, $k_2 = 6.37 \times 10^{-3}$ l.²/mole²-sec; the corresponding energies of activation are $E_1 = 7.93$ kcal/mole, $E_2 = 7.67$ kcal/mole. These rate constants are appreciably higher than values previously obtained for the corresponding DCMB–benzene reactions.

In an earlier paper[1] it was shown that a variety of heterocyclic, as well as carbocyclic, aromatic substances condense with *p*-di(chloromethyl)-benzene (DCMB) in the presence of Lewis acids to form polymeric resins with potential commercial applications. These materials have been called Friedel-Crafts polymers.[2] Evidence was presented[1] which suggests that, among the heterocyclics tested, thiophene gives the most thermally stable polymer and that it is stable to a temperature approximately 50°C higher than the corresponding benzene polymer prepared under com-

* Present address: Shell Research Ltd., Carrington Plastics Laboratory, Manchester, England.

† Present address: B. P. Research Centre, Sunbury-on-Thames, Middlesex, England.

parable conditions. It was not clear, however, whether the enhanced stability of the thiophene polymer is associated directly with the presence of thiophene units in the polymer structure or whether it is associated with a higher degree of branching or crosslinking in the polymer. As a first step towards a clarification of the situation, a comprehensive study of the kinetics of the polymerization and the structure of the benzene polymer was undertaken. This involved the separation and identification of a number of the lower molecular weight products of reaction of DCMB with benzene[3,4] and diphenylmethane[5] and of the self-condensation of benzyl chloride[6] and the evaluation by computer methods of the rate constants for a large number of steps in each of these reactions.[7–9] On the basis of these results, and again by the use of computer methods, information has been obtained about the structure of the ultimate insoluble, infusible polymer and its relationship to the polymerization conditions.[10]

This and the following paper[11] describe an extension of this kind of investigation to the thiophene/DCMB system which was chosen because of the earlier indications of greater stability in the resulting polymer.[1] It is well known that thiophene undergoes self-condensation in presence of certain Lewis acids and it soon became clear to us that the resulting polymer is relatively unstable, so that sequences of thiophene units formed in this way could seriously affect the stability of thiophene–DCMB copolymers. The first part of this paper is therefore devoted to a brief investigation of the self-condensation of thiophene and to determining suitable conditions for the thiophene–DCMB reaction to be studied. This is followed by a quantitative investigation of the products, kinetics and mechanism of the early stages of reaction. The second paper[11] is devoted to the later stages of the reaction.

EXPERIMENTAL

Reagents

p-Di(chloromethyl)benzene (Bush, Boake and Allen Ltd.) was recrystallized from methanol and dried in a vacuum oven at 60°C for 48 hr (mp 99°C). Thiophene (B.D.H. Ltd., reagent grade) was initially stored for a prolonged period over CaH_2. Before use it was subjected to the following sequence under vacuum. It was degassed by the freezing and thawing technique and distilled on to finely ground CaH_2 in a storage ampoule which was sealed off and intermittently agitated. After one week it was redistilled on to fresh CaH_2, stored for a further week, twice distilled under vacuum, and stored under vacuum in a sealed ampoule.

2-Methyl- and 3-methylthiophene (Ralph Emanuel Ltd., Puriss Grade) were distilled at atmospheric pressure and dried over CaH_2 for 48 hr.

Anhydrous stannic chloride (B.D.H. Ltd., reagent grade) and 1,2-dichloroethane (DCE) were similarly purified, except that freshly sublimed P_2O_5 was used instead of CaH_2 as drying agent.

Manipulation of Reagents

Since traces of water and other impurities can have a profound effect upon catalyzed reactions of this type,[3] strict precautions were taken to minimize contamination. In the manipulation of the reagents for the preparation of reaction mixtures, an all-glass apparatus with break-seals instead of stopcocks was used throughout, and since stannic chloride catalyzes the self-polymerization of thiophene, these two reagents were never allowed to come into contact with each other until the final stage of preparation of the reaction mixture. Reaction mixtures were prepared in ampoules which were sealed off under vacuum. The tediousness and time consumption associated with the use of break-seals was justified by the very high degree of reproducibility achieved.

Reaction Conditions

Preliminary experiments were carried out in a water thermostat at 30 ± 0.1°C. Later experiments at 0°C were carried out in a Towson and Mercer Ltd. "Minus Seventy" thermostat bath which could be controlled to ±0.5° C. Reactions were quenched by immersion of the ampoule in liquid nitrogen.

Analysis of Hydrogen Chloride

A reservoir containing approximately 20 ml of distilled water was sealed to the reaction ampoule and the water brought into contact with the reaction mixture by breaking the break-seal of the ampoule. The mixture was shaken vigorously for 15 min to ensure complete dissolution of the HCl in the water. The HCl was estimated by titration against standard alkali.

Quantitative GLC Analysis

Quantitative analysis was carried out by using a Microtek 2000R gas chromatograph with dual columns, flame ionization detector, and linear temperature programmer. In order to achieve good separation of products, samples were injected on to a 1% silicone gum (SE30) on 100/120 Embacel column which was then linearly programmed from 50°C to 250°C at 10°C/-min. Calibration of the flame ionization detector for each reaction product was carried out as described in a later section of this paper and these calibrations were checked at frequent intervals. A Pye 105 automatic preparative chromatograph was used with a 1.25% silicone gum (SE30) on 30/90 Gas Chrom column for the preparation of small amounts of pure products for these calibrations.

Spectral Measurements

Mass spectra were measured by using an LKB 900 combined gas chromatograph-mass spectrometer with an ionization voltage of 70 eV. NMR spectra were obtained by using a Perkin-Elmer R10, 60 mcps instrument or a Varian HA100 Mcps instrument. Infrared spectra were obtained on

Perkin-Elmer 225 and 257 spectrometers by using liquid films between NaCl disks.

Molecular Weight Measurements

The molecular weight of the thiophene polymer was measured in toluene solution at 65°C by using a Hewlett Packard 301A vapor-pressure osmometer.

RESULTS

Self-Condensation of Thiophene

Since Meyer[12] first reported the polymerization of thiophene catalyzed by sulfuric acid, the reaction has been shown to be catalyzed by a variety of acidic species and Friedel-Crafts type catalysts.[13] Gold'stein and his colleagues[14,15] have demonstrated spectroscopically that the polymer incorporates aliphatic carbon–hydrogen bonds, and Curtis and Armour and their colleagues[16–18] showed that both aromatic and aliphatic groups are present. It is clear, therefore, that complex structures exist in thiophene polymer.

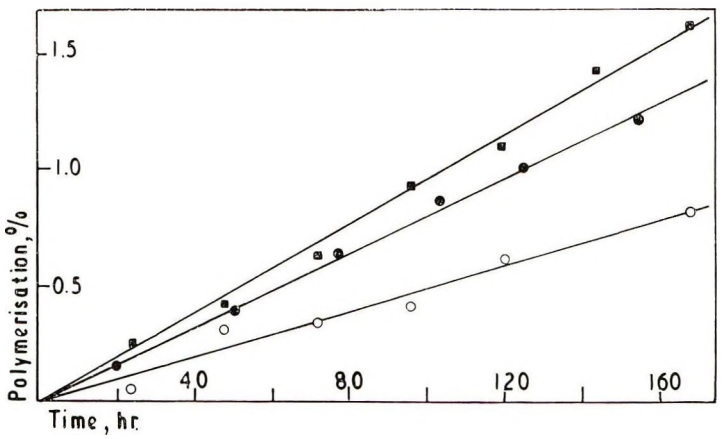

Fig. 1. Self polymerization of thiophene at 30°C: (○) 0.020 mole/l., $SnCl_4$ 2.52 mole/l. thiophene, *in vacuo;* (●) 0.018 mole/l., $SnCl_4$ 3.43 mole/l. thiophene, *in vacuo;* (■) 0.024 mole/l., $SnCl_4$ 5.50 mole/l. thiophene, in nitrogen.

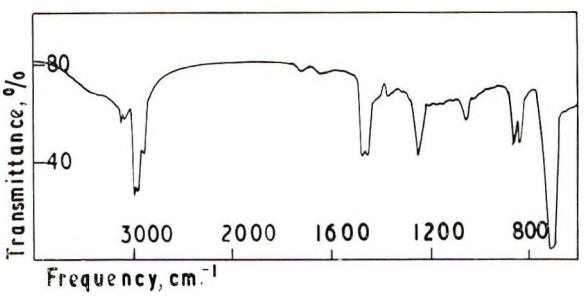

Fig. 2. Infrared spectrum of the polymer of thiophene.

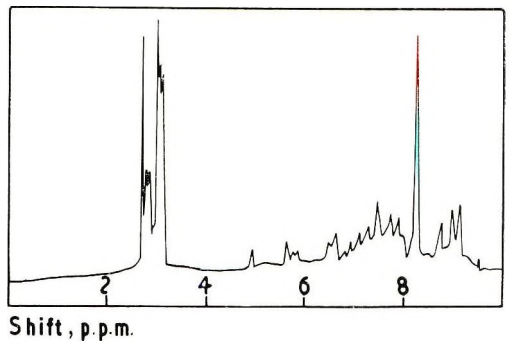

Fig. 3. Nuclear magnetic resonance spectrum of the polymer of thiophene.

and that if these were produced in significant concentrations during the DCMB–thiophene reaction they might influence both polymerization kinetic measurements and the stability of the resulting polymer. For this reason it was felt necessary to estimate the extent to which self-polymerization of thiophene is liable to occur under conditions comparable with those under which the DCMB–thiophene reaction is to be studied.

Figure 1 illustrates the course of three reactions carried out in solution under nitrogen and *in vacuo* at 30°C with thiophene and $SnCl_4$ concentrations of the magnitude used in the DCMB–thiophene work to be described. It is clear that the reaction curves are linear over the period and that the fastest rate observed is of the order of 1.5% conversion of thiophene in 160 hr. These rates are insignificant compared with rates which will be quoted in this and the following paper for the thiophene–DCMB reaction.

Analyses of the products of the polymerization under nitrogen were carried out. The molecular weight of the deep brown viscous oil was 343 ± 28. The ultraviolet spectrum shows a single absorption at 237 mμ which is evidence of thiophene nuclei. This was confirmed by bands at 850, 825, and 695 cm^{-1} in the infrared spectrum (Fig. 2) and at 2.7–3.2τ in the NMR spectrum (Fig. 3). Infrared absorption at 1455 cm^{-1} and NMR absorption at 5.5–9.2τ also confirm the presence of aliphatic carbon–hydrogen bonds.

Self-Condensation of DCMB

Similarly it is important to establish whether DCMB would undergo significant self-condensation under the reaction conditions, since this would make branching possible in the very early stages of reaction by way of the self-condensation product.

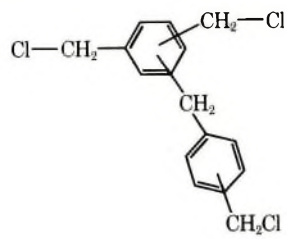

Mixtures of DCMB and stannic chloride of the appropriate concentration were mixed in DCE solution and allowed to stand at 30°C for prolonged periods. The most sensitive method of following reaction is by titration of the HCl formed against standard alkali. No reaction could be detected after several weeks. It may therefore be assumed that the self-condensation of DCMB will not contribute to the DCMB–thiophene reaction.

Reaction between Thiophene and DCMB

Some preliminary experiments were carried out in order to determine the best experimental conditions for polymerization to be carried out and to help devise convenient methods for studying the reaction. These experiments were carried out at 30°C under vacuum and the following observations were made.

Initially all reaction mixtures are clear and colorless. After a short time, however, a yellow color appears, which gradually deepens through orange to deep red. As the solutions darken, they also become opaque, and a solid is precipitated. Addition of water rapidly discharges the deep red coloration, giving a pale green solution. After washing and drying, the polymer is deep yellow. It is infusible and insoluble in all common solvents. The onset of coloration indicates the formation of complexes involving stannic chloride and aromatic nuclei. It has already been noted[13,14] that such complexes are formed between stannic chloride and thiophene and their formation was also accompanied by coloration of the reaction mixture. As addition of water causes hydrolysis of the stannic chloride, it would also be expected to cause coloration to be discharged.

At no point during the reaction was complete gelation observed. Close examination shows that loss of transparency as the reaction proceeds is due to the formation of microgel, i.e., discrete particles of gel which remain suspended in the solution. The formation of this insoluble gel accompanied by deep red coloration, which represents a late stage in the reaction, occurs at 30°C in minutes compared with hours for the corresponding benzene–DCMB system. Since for separation and analysis of the intermediate products a soluble product is required, and since an accurate measure of reaction time is necessary for kinetic measurements, it is clear that the reaction must be studied at much lower temperatures. For this reason, all subsequent experiments were carried out at 0°C.

Identification of Products of Reaction between Thiophene and DCMB

As in the previous work on the benzene–DCMB system,[3] it was found that for extents of reaction up to 15% of the theoretical evolution of hydrogen chloride the reaction mixture contains only the starting materials and the first two products. Relatively high concentrations of thiophene were used in the reaction mixtures in order to favor production of P_3, rather than higher products. Larger molecular products only appear in significant quantities beyond 15% conversion but they are too involatile to be eluted

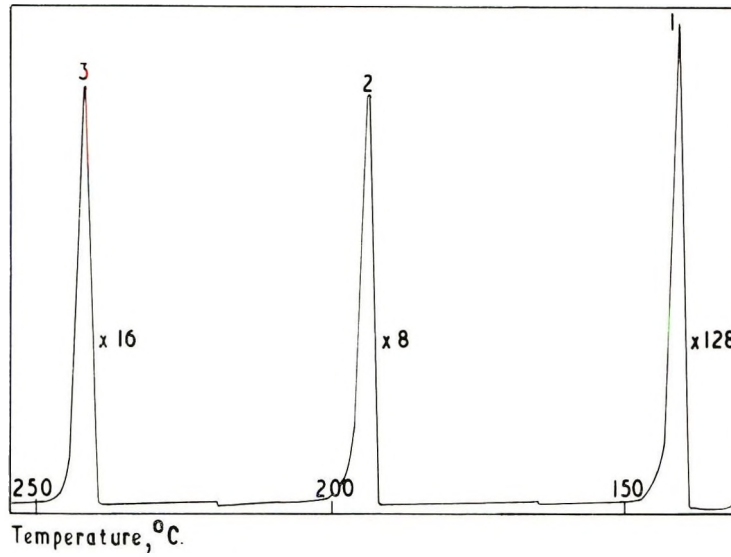

Fig. 4. A typical gas–liquid chromatogram of the early products of reaction of thiophene and DCMB at 0°C.

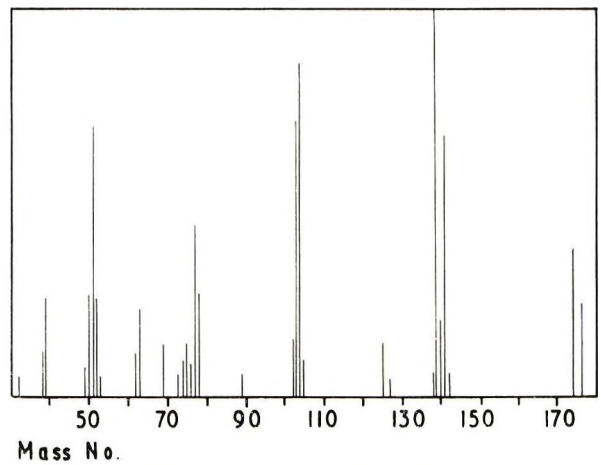

Fig. 5. Mass spectrum of P_1.

from the g.l.c. column. In the present experiments, therefore, reaction was never carried beyond 15%. Chromatograms with three well separated peaks were obtained as shown in Figure 4. Owing to their high volatility, thiophene and the solvent dichloroethane were eluted almost instantaneously from the column.

Peak 1 (P_1). The mass, infrared, and NMR spectra of P_1 are illustrated in Figures 5–7 and are identical with the spectra of pure DCMB. Peaks at 139, 125, and 104 in the mass spectrum are due to loss of a chlorine atom, a chloromethyl group, and two chlorine atoms respectively, while the pres-

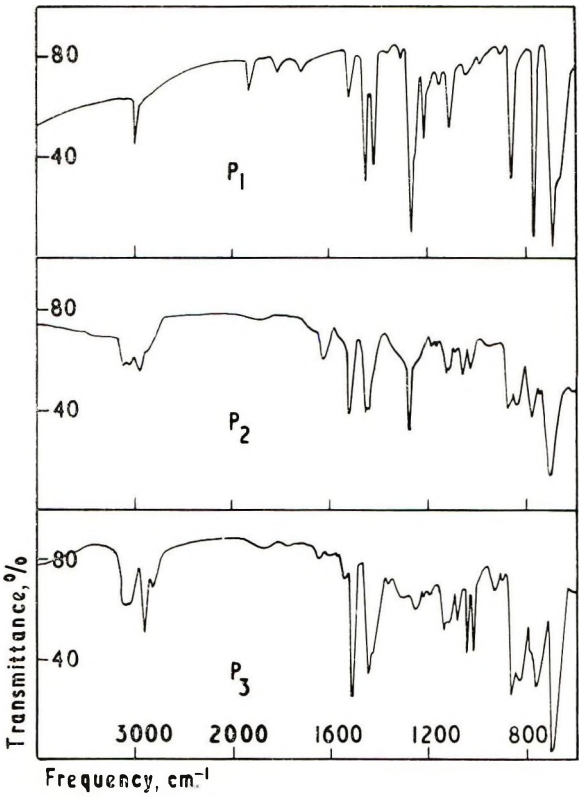

Fig. 6. Infrared spectra of P_1, P_2, and P_3.

ence of chloromethyl groups is confirmed by absorption at 675 cm^{-1} in the infrared spectrum. Peaks at 2.65 τ and 5.49 τ in the NMR spectrum are due to absorption by the aromatic and chloromethyl protons, respectively.

Peak 2 (P_2). The mass, infrared, and NMR spectra of P_2 are illustrated in Figures 6–8. The parent ion mass number at 222 could result from substitution of one chlorine atom in DCMB by thiophene to form thenylchloromethylbenzene (TCMB) in which T represents a thiophene nucleus.

$$T—CH_2—C_6H_4—CH_2Cl \quad (P_2)$$

Peaks at 187, 173, and 97 representing loss of Cl—, Cl—CH_2— and Cl—CH_2—C_6H_4— and a peak at 97 representing T—CH_2— support this structure for P_2. This identification is confirmed by infrared and NMR evidence. The complex array of peaks between 2.60 and 3.30 τ are due to resonance by the aromatic protons while resonances between 5.40 and 6.20 τ can be attributed to protons attached to aliphatic carbon atoms. The peak at 5.45 τ is assumed to be due to absorption by the chloromethyl group as in DCMB and those at 5.88 and 6.06 τ to the protons of the methylene bridge between thiophene and benzene nuclei. This shift to higher field is caused by replacement of the strong inductive deshielding effect of

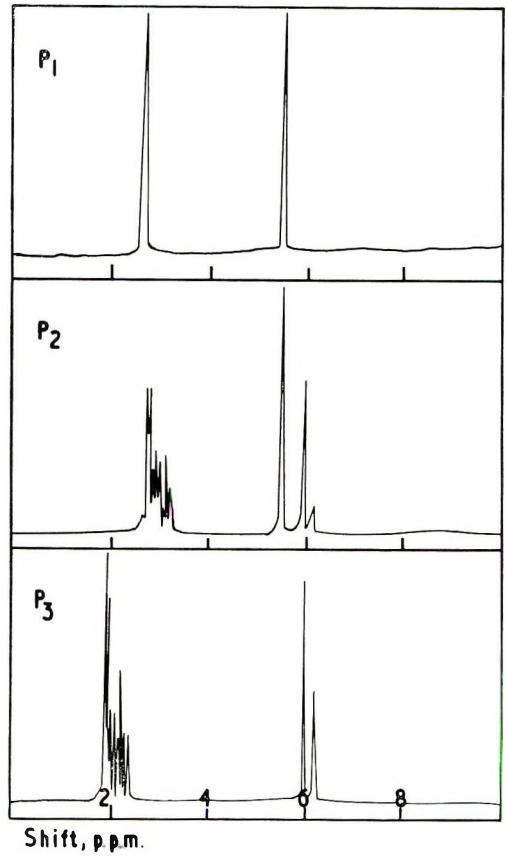

Fig. 7. Nuclear magnetic resonance spectra of P_1, P_2, and P_3.

the chlorine atom by the less effective anisotropic deshielding effect of the thiophene ring. The peak at 5.88 τ is attributed to the methylene groups substituted in the 2 position of thiophene and the peak at 6.06 τ is assigned to substitution in the 3 position. These assignments are confirmed by comparison of the NMR spectra of 2-methyl- and 3-methylthiophene (Fig. 9), which indicate that the deshielding effect of the thiophene nucleus is greater on substituents in the 2 position. The relative concentrations of 2- and 3-substituted nuclei were calculated from the relative intensities of the absorptions at 5.88 and 6.06 τ in Figure 7 and found to be in a ratio of approximately 3:1.

Both 2- and 3-substituted thiophene nuclei are confirmed by absorptions at 695 and 760 cm^{-1}, respectively, in the infrared spectrum. Although the relative intensities of these two peaks do not give quantitative information they do tend to confirm the greater tendency to 2-substitution indicated by NMR. Absorption at 675 cm^{-1}, which would be expected from the chloromethyl group, is probably represented by the shoulder on the peak at 695 cm^{-1}.

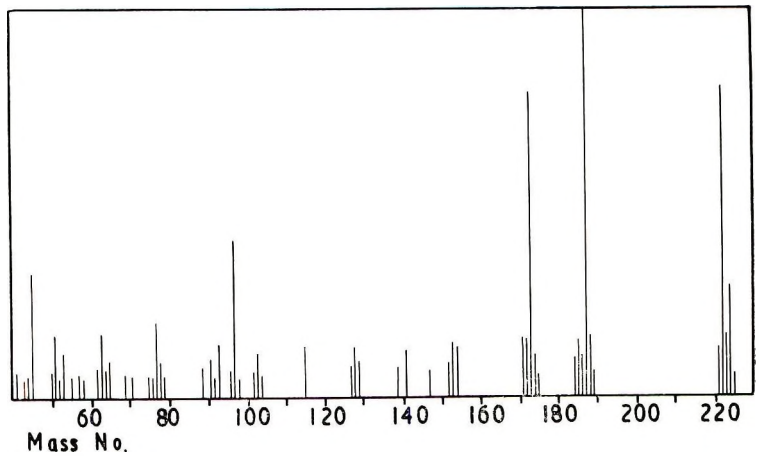

Fig. 8. Mass spectrum of P_2.

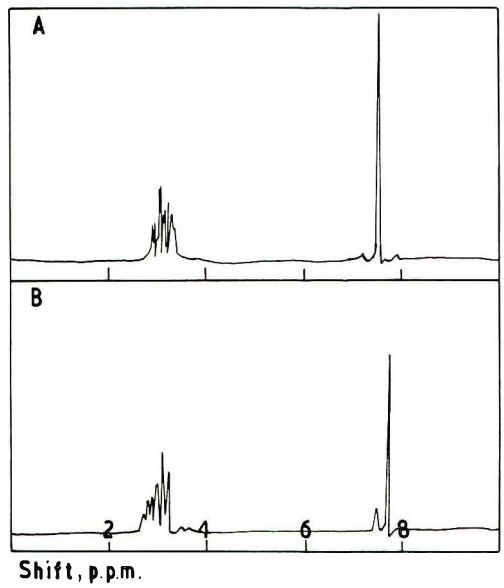

Fig. 9. Nuclear magnetic resonance spectra of A, 2-methyl thiophene; B, 3-methyl thiophene.

Peak 3 (P_3). The mass spectrum of P_3, illustrated in Figure 10, has a parent ion mass number of 270, while the cracking pattern indicates the loss of T—CH_2— and T—CH_2—C_6H_4— giving peaks at 173 and 97 respectively. This is consistent with the identification of P_3 as diethylbenzene (DTB):

$$T—CH_2—C_6H_4—CH_2—T \quad (P_3)$$

The infrared spectrum (Figure 6) is very similar to that of P_2 and indicates the presence of both 2- and 3-substituted thiophene nuclei. The peak at

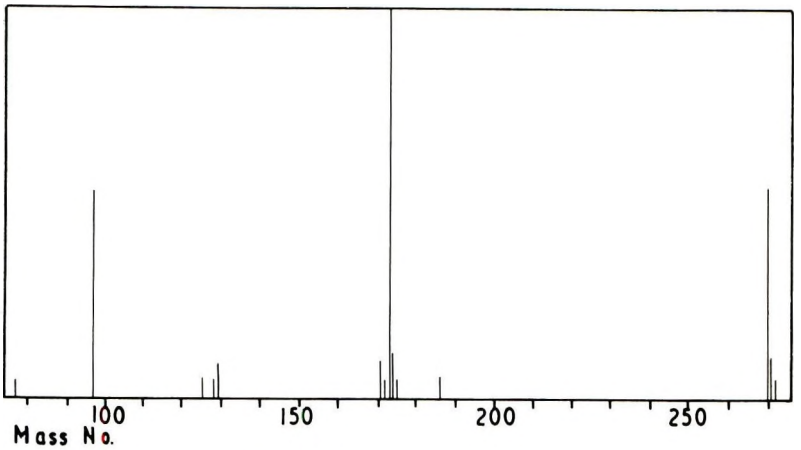

Fig. 10. Mass spectrum of P_3.

695 cm^{-1} is not as broad as the corresponding peak in the spectrum of P_2 and does not have the shoulder at 675 cm^{-1} which was taken as evidence for the chloromethyl group which should be present in P_2 but not P_3. The absence of chloromethyl groups is P_3 is confirmed by the absence of resonances at 5.46 τ in the NMR spectrum (Fig. 7). The superimposition of the benzene and thiophene resonances in the 2.60–3.40 τ region again prevent any detailed analysis. Absorptions due to the methylene bridge protons occur at 5.94 and 6.11 τ for 2- and 3-thiophene substitution respectively. The movement of both aromatic and methylenic absorptions to higher field can be accounted for by the complete removal of the strong inductive deshielding effect of the chlorine atoms. The concentrations of 2- and 3-substituted thiophene nuclei are in the ratio of approximately 2:1.

Quantitative Estimation of Products of Reaction between Thiophene and DCMB

The flame ionization detector of the gas chromatograph gives a response which depends upon the nature of the component being measured. It is therefore necessary to calibrate the detector for each component in order to be able to obtain relative concentrations of P_1, P_2, and P_3 in a reaction mixture directly from chromatograms of the type illustrated in Figure 4. These calibrations were carried out by using mixtures of known composition of pure P_1, P_2, and P_3 obtained by preparative GLC. Thus it was established that the peak areas per unit molar concentration of P_1, P_2, and P_3 were in the ratio 1:0.98:1.44. It follows that the relative molar ratio, a:b:c, of the three compounds is given by, a:b:c = area under peak 1/1:area under peak 2/0.98: area under peak 3/1.44.

By using this relationship the absolute concentrations of the three components were then determined by exactly the same methods as described previously for the DCMB–benzene reaction[3] with an estimated error of $\pm 5\%$.

Kinetics of the Reaction between Thiophene and DCMB

Typical reaction curves for P_1, P_2, P_3 and hydrogen chloride are illustrated in Figure 11. The P_1, P_2 and P_3 curves are of the general shape to be expected as a result of two consecutive reactions:

$$\mathrm{Cl{-}CH_2{-}C_6H_4{-}CH_2{-}Cl + T}$$
$$\downarrow$$
$$\mathrm{Cl{-}CH_2{-}C_6H_4{-}CH_2{-}T + HCl}$$
$$\downarrow \mathrm{T}$$
$$\mathrm{T{-}CH_2{-}C_6H_4{-}CH_2{-}T + HCl}$$

in which T represents a thiophene residue. A progressive decrease in the rate of consumption of P_1 should have been expected during the course of the reaction. That the P_1 curve in Figure 11 is linear rather than concave upwards is a strong indication that the aromatic nuclei in later products are more reactive than thiophene. The concentration of P_2 initially increases rapidly but levels off as the rate of formation of P_3 increases continuously to high conversion. The reaction curves for hydrogen chloride are not all well defined in the initial stages owing to the difficulty of measuring small

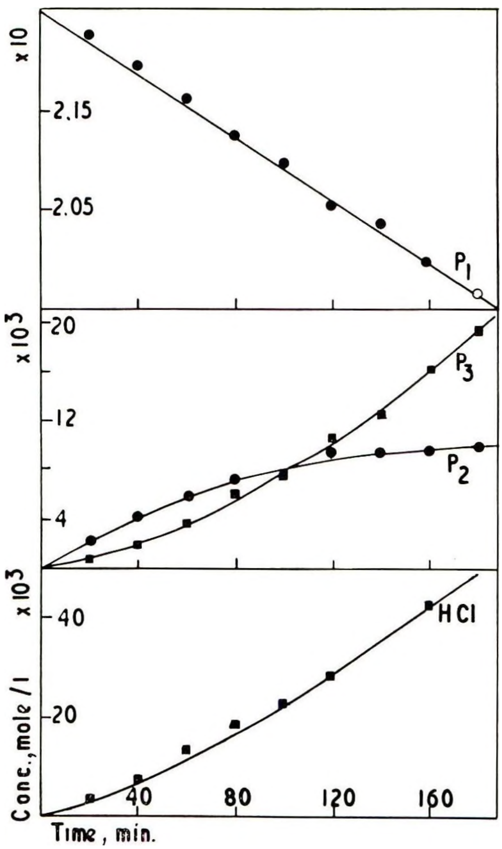

Fig. 11. Typical reaction curves for P_1, P_2, P_3, and hydrogen chloride (reaction 10, Table I).

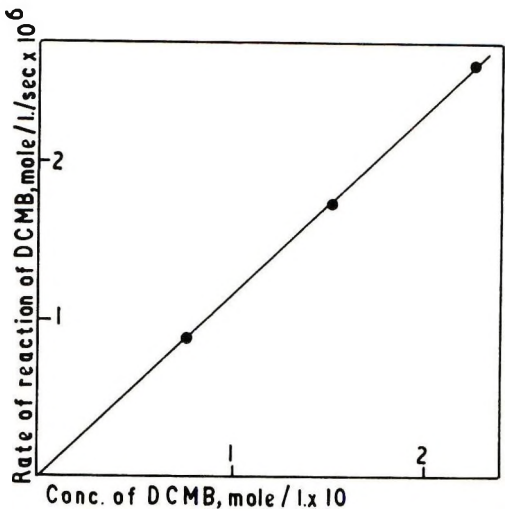

Fig. 12. Dependence of rate of reaction of DCMB on DCMB concentration (see Table I).

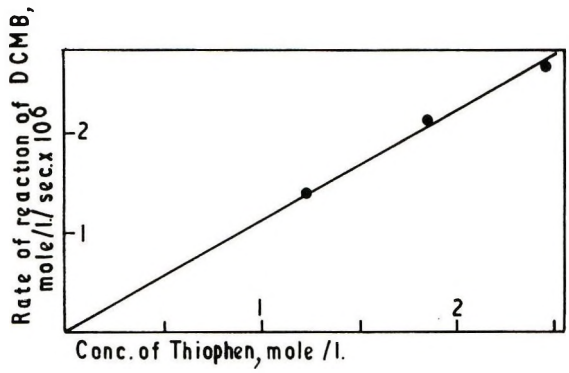

Fig. 13. Dependence of rate of reaction of DCMB on thiophene concentration (see Table I).

concentrations of hydrogen chloride. They do, however, tend to suggest an acceleration of rate in the early stages.

The rate of formation of P_2 is given by the slope of the P_1 curve in Figure 11 because initially the decrease in concentration of P_1 must be entirely due to the formation of P_2. By varying the initial concentrations of P_1, thiophene and stannic chloride in turn, the results in the fifth column of Table I were obtained. These results are represented in Figures 12–14 which demonstrate that the formation of P_2 from P_1 and thiophene is first-order with respect to each of the reactants, P_1, thiophene, and stannic chloride.

Since the concentration of thiophene in all these experiments was high compared with the concentration of P_1, it may be assumed that it does not change significantly during the initial stages of the reaction. Because

TABLE I
Kinetic Data Obtained at 0°C

Reaction	Concn of reactants, mole/l.			$-d[P_1]/dt$, mole/l.-sec $\times 10^6$	$d[P_3]/dt/[P]$, $sec^{-1} \times 10^4$	$k_1 \times 10^4$, $l.^2/mole^2$-sec	$k_2 \times 10^4$, $l.^2/mole^2$-sec
	P_1	Thiophene	$SnCl_4$				
10	0.225	2.46	0.0171	2.60	2.58	2.75	61.3
11	0.077	2.50	0.0171	0.85	2.67	2.58	62.5
12	0.153	2.48	0.0171	1.72	2.66	2.65	62.7
13	0.225	1.23	0.0168	1.38	1.36	2.97	65.8
14	0.224	1.85	0.0168	2.04	1.98	2.93	63.7
15	0.224	2.47	0.0088	1.45	1.37	2.97	63.0
16	0.224	2.46	0.0245	3.64	4.05	2.69	67.3

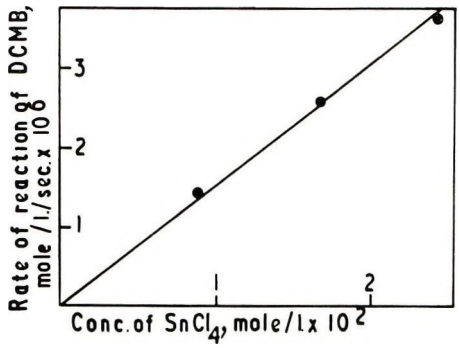

Fig. 14. Dependence of rate of reaction of DCMB on stannic chloride concentration (see Table I).

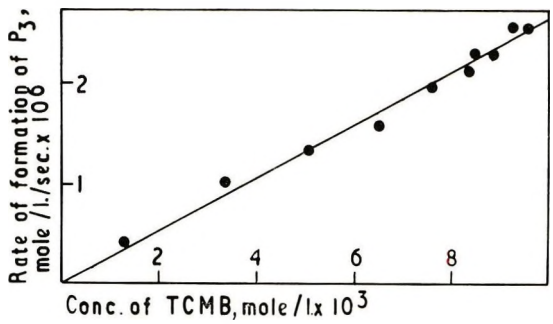

Fig. 15. Dependence of rate of formation of P_3 on DCMB concentration.

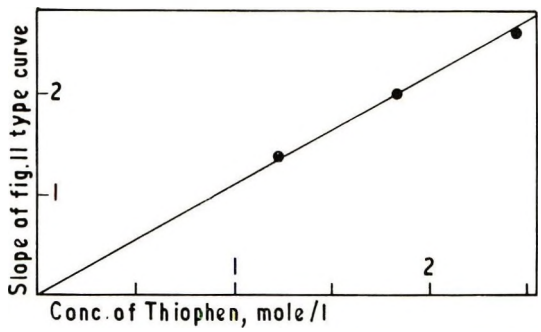

Fig. 16. Dependence of rate of formation of P_3 on thiophene concentration (see Table I).

stannic chloride is not consumed in the reaction its concentration will also remain constant. Thus plots of the changing slopes of the P_3 curves against the corresponding P_2 concentrations should illustrate directly the dependence of the rate of the second reaction on the concentration of P_2. A typical plot (deduced from P_2 and P_3 curves in Fig. 11) is illustrated in Figure 15, which demonstrates first-order dependence of the rate of the second reaction on the concentration of P_2. The slopes of these plots are

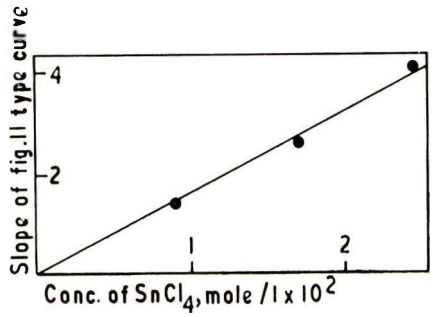

Fig. 17. Dependence of rate of formation of P_3 on stannic chloride concentration (see Table I).

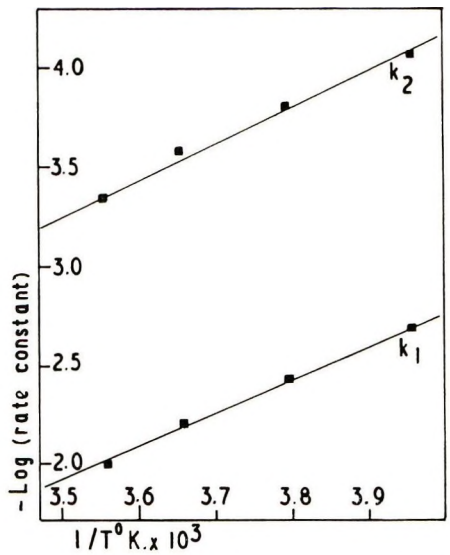

Fig. 18. Arrhenius plots of rate constants k_1 and k_2.

presented in the sixth column of Table I. Appropriate plots of these slopes against thiophene and stannic chloride concentration as in Figures 16 and 17 demonstrate first-order dependence of P_3 production on both these reagents. The overall reaction may therefore be represented by;

$$P_1 + T + SnCl_4 \xrightarrow{k_1} P_2 + HCl + SnCl_4$$

$$P_2 + T + SnCl_4 \xrightarrow{k_2} P_3 + HCl + SnCl_4$$

it follows that,

$$-d[P_1]/dt = k_1[P_1][T][SnCl_4]$$

$$d[P_3]/dt = k_2[P_2][T][SnCl_4]$$

By applying these rate equations to the data in Table I, values for k_1 and k_2 have been obtained as shown in the last two columns of Table I. Average values have been deduced as follows:

$$k_1 = 2.79 \times 10^{-4}\ l.^2/\text{mole}^2\text{-sec}$$

$$k_2 = 6.37 \times 10^{-3}\ l.^2/\text{mole}^2\text{-sec}$$

From Arrhenius plots of data obtained over the temperature range $-20°C$ to $+10°C$ (Fig. 18) energies of activation were obtained as follows:

$$E_1 = 7.93\ \text{kcal/mole}$$

$$E_2 = 7.67\ \text{kcal/mole}$$

DISCUSSION

Condensation reactions of this type are generally accepted as occurring in two steps.[19] The first step involves the formation of a complex between the catalyst and a chloromethyl group by interaction of the electropositive tin atoms with the electronegative chlorine atoms.

$$\text{Cl—CH}_2\text{—C}_6\text{H}_4\text{—}\overset{\delta^+}{\text{CH}_2}\text{- - -}\overset{\delta^-}{\text{SnCl}_5}$$

Reaction of the thiophene with this complex will then give

$$\text{Cl—CH}_2\text{—C}_6\text{H}_4\text{—CH}_2\text{—T} + \text{HCl} + \text{SnCl}_4$$

Grassie and Meldrum[3] have shown that in the corresponding DCMB/benzene reaction the establishment of an equilibrium concentration of the complex is rapid compared with the rate of the reaction of the complex with the aromatic molecule. The absence of any induction period in the formation of P_2 confirms that this is true in the present reaction. Grassie and Meldrum[3] have also demonstrated how first-order dependence upon all three reagents, which is observed in both the DCMB–benzene and DCMB–thiophene reactions, follows from this mechanism.

The values of k_1 and k_2 obtained in the present work at 0°C are appreciably greater than those obtained in the corresponding DCMB–benzene reaction at 30°C ($k_1 = 1.10 \times 10^{-4}\ l.^2/\text{mole}^2\text{-sec}$; $k_2 = 1.30 \times 10^{-3}\ l.^2/\text{mole}^2\text{-sec}$) thereby accounting for the greater overall rate of the thiophene reaction which necessitated the lower reaction temperature of 0°C compared with 30°C for the benzene reaction.[3] The greater reactivity of thiophene compared with benzene is accounted for by the presence of the sulfur atom in the thiophene ring, making the thiophene molecule more reactive to electrophilic reagents and thus to the positively charged carbon atom in the DCMB–$SnCl_4$ complex. The very much greater reactivity of the second chloromethyl group can be accounted for by the absence of a second strongly electronegative center in P_2. Thus the formation of the complex by the breaking of the C-Cl bond is greatly facilitated by the greater electron density on the chlorine atom. The acceleration in the production of hydro-

gen chloride in the early stages of the reaction can be accounted for qualitatively in terms of the greater reactivity of P_2 compared with P_1.

References

1. N. Grassie and I. G. Meldrum, *Europ. Polym. J.*, **4**, 571 (1968).
2. L. N. Phillips, *Trans. Plastics Inst.*, **32**, 298 (1964).
3. N. Grassie and I. G. Meldrum, *Europ. Polym. J.*, **5**, 195 (1969).
4. N. Grassie and I. G. Meldrum, *Europ. Polym. J.*, **6**, 499 (1970).
5. N. Grassie and I. G. Meldrum, *Europ. Polym. J.*, **6**, 513 (1970).
6. N. Grassie and I. G. Meldrum, *Europ. Polym. J.*, **7**, 629 (1971).
7. N. Grassie and I. G. Meldrum, *Europ. Polym. J.*, **7**, 17 (1971).
8. N. Grassie and I. G. Meldrum, *Europ. Polym. J.*, **7**, 613 (1971).
9. N. Grassie and I. G. Meldrum, *Europ. Polym. J.*, **7**, 645 (1971).
10. N. Grassie and I. G. Meldrum, *Europ. Polym. J.*, in press.
11. N. Grassie and J. B. Colford, *J. Polym. Sci. A-1*, **9**, 2835 (1971).
12. V. Meyer, *Ber.*, **16**, 1468 (1883).
13. J. Bruce, F. Challenger, H. B. Gibson, and W. E. Allenby, *J. Inst. Petrol. Technol.*, **34**, 226 (1948).
14. I. P. Gol'dshtein, E. N. Gur'yanova, and K. A. Kocheshkov, *Proc. Acad. Sci. USSR*, **144**, 456 (1962).
15. I. P. Gol'dshtein, Z. P. Il'ichera, N. A. Slovokhotova, E. N. Gur'yanova, and K. A. Kocheshkov, *Proc. Acad. Sci. USSR*, **144**, 490 (1962).
16. R. F. Curtis, D. M. Jones, G. Ferguson, D. M. Hawley, J. G. Sime, K. K. Cheung, and G. Germain, *Chem. Commun.*, **1969**, 165.
17. M. Armour, A. G. Davies, J. Upadhyay, and A. Vassermann, *J. Polym. Sci. A-1*, **5**, 1527 (1967).
18. R. F. Curtis, D. M. Jones, and W. A. Thomas, *J. Chem. Soc. C*, **1971**, 234.
19. G. A. Olah, S. J. Kuhn and S. R. Flood, *J. Amer. Chem. Soc.*, **84**, 1688 (1962).

Received March 15, 1971
Revised May 24, 1971

JOURNAL OF POLYMER SCIENCE: PART A-1 VOL. 9, 2835–2852 (1971)

Friedel-Crafts Copolymerization of Thiophene and *p*-Di(chloromethyl)benzene. II. Products of the Later Stages of the Reaction

N. GRASSIE and J. B. COLFORD,* *Department of Chemistry, University of Glasgow, Glasgow, W.2, Scotland*

Synopsis

Products of the copolymerization of thiophene and *p*-di(coloromethyl)benzene in presence of stannic chloride have been separated by using gel-permeation chromatography (GPC) and identified by using principally mass, infrared, and nuclear magnetic resonance spectroscopy. The GPC separation is not nearly as efficient as the separation of the products of the corresponding benzene–DCMB and diphenylmethane–DCMB reactions which have previously been described. A further complication which makes a kinetic analysis of this reaction more difficult is the occurrence of intramolecular condensation of certain of the earlier products leading to cyclic structures incorporating four aromatic rings. These investigations have made it possible to deduce some of the principal structural differences between the thiophene–DCMB and benzene–DCMB polymers which may have some bearing on the differences which have been found in their thermal stabilities.

In the previous paper[1] it was demonstrated how thenyl-chloromethylbenzene (TCMB) and dithenylbenzene (DTB), the first two products of the reaction between *p*-di(chloromethyl)-benzene (DCMB) and thiophene in presence of stannic chloride as catalyst, may be separated and estimated quantitatively by using gas–liquid chromatography (GLC). The mechanism of the formation of the products was shown to be strictly similar to the mechanism of formation of the first two products of the analogous DCMB–benzene reaction,[2] although the rate constants in the thiophene reaction are very much greater. As in the benzene[3] and diphenylmethane[4] reactions, it has been found possible, by using gel-permeation chromatography (GPC), to separate some of the later products of the thiophene reaction. The identification of these products and an investigation of the characteristics of their formation was undertaken in the expectation that by comparison with the benzene reaction further information would be revealed about the relationships between structure and stability in this class of polymers and in particular about the differences in stability between thiophene and benzene polymers.

* Present address: Shell Research Ltd., Carrington Plastics Laboratory, Manchester, England.

EXPERIMENTAL

Materials and their manipulation, experimental methods and techniques, apart from gel-permeation chromatography, were exactly as described in the previous paper.[1] The gel-permeation chromatographic separations were achieved exactly as described previously.[3]

RESULTS

A sequence of gel-permeation chromatograms obtained at successive stages of reaction are illustrated in Figure 1. As in the benzene reaction,[3] these chromatograms were constructed by plotting the weight of the product in each fraction against its elution ratio which is defined as the ratio of the elution volume of the fraction to the elution volume of DCMB which is common to all chromatograms. The ease with which peaks in a sequence of chromatograms were identified by means of their elution ratios is

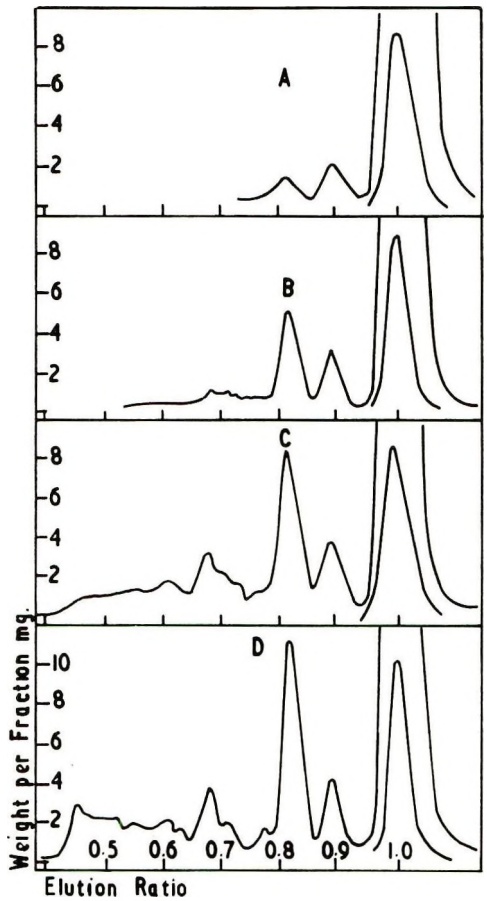

Fig. 1. Gel-permeation chromatograms of the products of reaction of thiophene with DCMB at 0°C: (*A*) 6 hr; (*B*) 18 hr; (*C*) 30 hr; (*D*) 48 hr.

TABLE I
Elution Ratios of Products

Reaction time, hr	Elution ratios (relative to P_1)									
	P_2	P_3	P_3	P_5	P_6	P_7	P_8	P_9	P_{10}	P_{11}
6	0.896	0.817								
13	0.889	0.817	0.770	0.705	0.685					
18	0.889	0.816	0.770	0.710	0.685		0.612			
24	0.888	0.815	0.770	0.705	0.678	0.645	0.612			
30	0.890	0.819	0.774	0.715	0.680	0.637	0.610			
36	0.896	0.818	0.778	0.713	0.680	0.635	0.608	0.554	0.523	0.457
41	0.890	0.817	0.778	0.714	0.681	0.630	0.610	0.552	0.513	0.454
48	0.889	0.817	0.771	0.713	0.681	0.641	0.615	0.550	0.523	0.445

TABLE II
Accuracy of Elution Ratios

Peak	Mean elution ratio	Maximum deviation from mean elution ratio	
1	1.000		
2	0.891	+0.005	−0.003
3	0.817	+0.002	−0.002
4	0.773	+0.005	−0.003
5	0.711	+0.004	−0.006
6	0.681	+0.004	−0.003
7	0.638	+0.007	−0.008
8	0.611	+0.003	−0.003
9	0.552	+0.002	−0.002
10	0.520	+0.003	−0.007
11	0.452	+0.005	−0.007

demonstrated by the data in Tables I and II. It is clear from Table I that the elution ratios may be arranged in columns which do not overlap in value. The accuracy with which the peaks are defined is demonstrated in Table II which provides clear justification for the use of elution ratios for the identification of peaks.

The separation of these products is not nearly as good as was achieved in earlier studies of the DCMB–benzene[3] and DCMB–diphenylmethane[4] reactions. Although good separation of products P_1, P_2, and P_3 was achieved, all other peaks in the chromatogram, except P_4 and P_5, overlap considerably. Thus, analyses were carried out as far as possible on the fractions recovered near the maxima of the peaks in order to minimize contamination. The total amount of material represented by each peak had to be deduced by extrapolation of its resolved parts, and because of the very small amounts of some of the products there is sometimes considerable potential error in the estimated amounts of products. However, the experimental conversion curves for the various products indicate that the errors were never so large as to prevent useful delineation of the changes in concentration of the products during the reaction.

Identification of Products of Reaction

Peaks 1, 2, and 3 (P_1, P_2 and P_3). By the methods previously described,[1] these materials were shown to be identical with the products separated from the early stages of the reaction by GLC and to be DCMB, TCMB, and DTB, respectively:

P_1: Cl—CH_2—C_6H_4—CH_2—Cl

P_2: Cl—CH_2—C_6H_4—CH_2—T

P_3: T—CH_2—C_6H_4—CH_2—T

where T represents a thiophene nucleus.

Peak 4 (P_4). Since the elution ratio should be expected to decrease with increasing molecular weight it is reasonable to consider structures of pro-

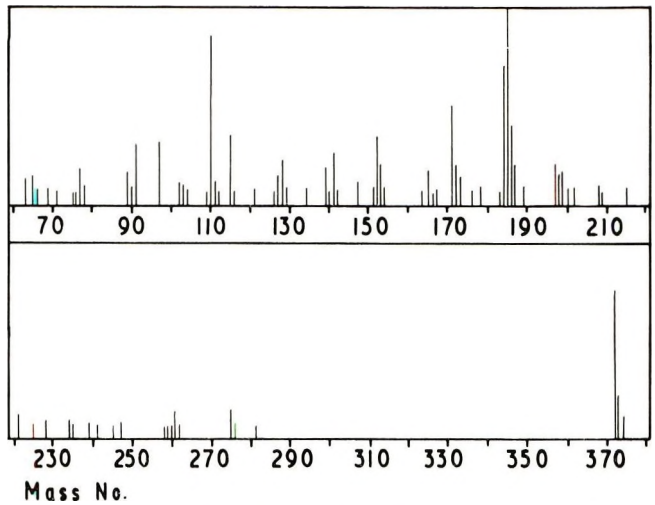

Fig. 2. Mass spectrum of P_4.

gressively increasing complexity on moving from right to left across the chromatograms illustrated in Figure 1. Thus, since P_4 occurs imperfectly resolved from P_3, it seems reasonable to expect that the molar volumes of P_3 and P_4 are comparable. The mass spectrum of P_4 (Fig. 2) gives a molecular weight of 372. This rules out the only other products, I and II, which, like P_3, have three aromatic rings. These would be formed by self-condensation of P_1 and by reaction of P_2 with P_1 and have molecular weights of 313 and 361, respectively.

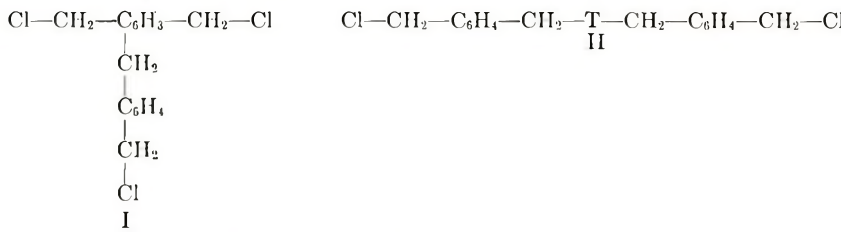

Similarly, III and IV, the most obvious products with four aromatic rings, must be eliminated as possible structures of P_4, since the molecular weights of both are 408.

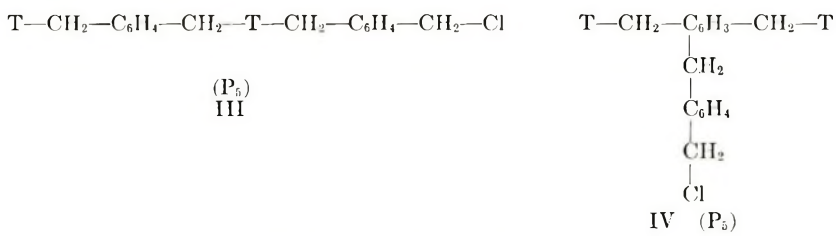

Because of their chloromethyl groups those compounds would also be expected to give rise to absorption at 675 cm^{-1} in their infrared spectra and at

5.46 τ in their NMR spectra. Although there is no strong absorption at 675 cm^{-1} in the infrared spectrum of P_4 (Fig. 3), there is a peak at 5.48 τ in its NMR spectrum (Fig. 4) which could be attributed to chloromethyl group protons. Comparison of the intensity of this peak with others in the spectrum clearly shows, however, that it is so small that it can only be accounted for in terms of a minor impurity. In any case, the large increase in

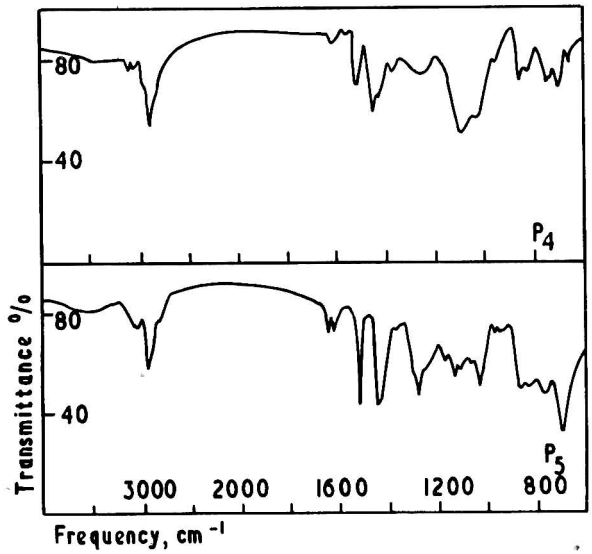

Fig. 3. Infrared spectra of P_4 and P_5.

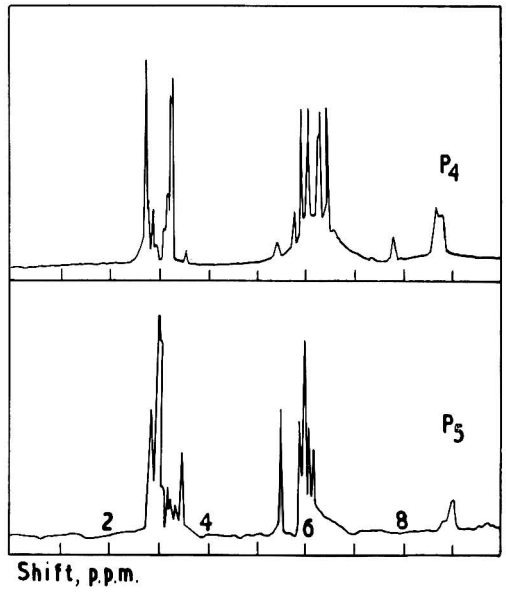

Fig. 4. Nuclear magnetic resonance spectra of P_4 and P_5.

molar volume in going from P_3 to either III or IV should be expected to cause a much greater decrease in elution ratio than that found for P_1.

The molecular weight of 372 found for P_4 suggests that this product could have been formed by elimination of hydrogen chloride from either II or IV. One possible product (V)

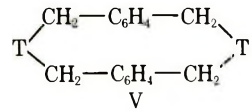

V

could be formed from III by intramolecular condensation. Studies with molecular models have revealed that this is possible, although it would not be possible for IV to undergo a comparable reaction. This compound has a molecular weight of 372, in agreement with mass spectral data, and peaks at 185, 171, and 110 suggest the presence of $—CH_2—T—CH_2—C_6H_4—^+$, $—T—CH_2—C_6H_4—^+$, and $—CH_2—T—CH_2—^+$ ions among the scission products. Minor differences between the masses of ionic species and m/e values can be accounted for by hydrogen transfer which is known to occur in aromatic systems.

Before trying to account for the major features of the NMR spectrum of P_4 it is necessary to consider the conformational features of V. Products of this type should be capable of existing in either of the two conformational forms illustrated in Figure 5.

The equatorial and axial hydrogens of the methylene bridges would be inequivalent in both these forms and those structural features could have a considerable effect on spectroscopic properties, making interpretation of spectra difficult. In both possible conformations of V the free rotation of benzene nuclei would be severely restricted. The effect of this would be that the planes of the benzene nuclei would be held parallel and at right angles to the planes of the thiophene nuclei. The overall effect of this should be

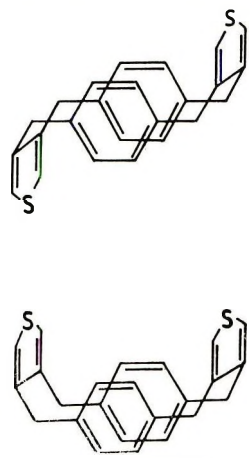

Fig. 5. Probable "boat" and "chair" conformations of P_4.

that in the NMR spectrum of V the deshielding effect which would normally be present in a linear or branched molecule of this type, due to the induced magnetic field at right angles to the plane of the aromatic rings, would be reduced because the fields induced in the benzene and thiophene rings would tend to cancel. Moreover the resultant induced field would be different for the chair and boat forms, as the planes of the thiophene rings are held at different angles in the two conformations. Thus the NMR spectrum of V could be reasonably complex, and a further complicating feature would arise from the possibility of the thiophene rings being substituted in different positions.

Although the NMR spectrum of P_4 (Fig. 4) is considerably more complex than those of P_2 and P_3 (Fig. 7 of Part I[1]) its principal features can be accounted for in the terms discussed above. Although the aromatic resonances occur in the same region as for P_3, namely 2.60–3.40 τ, the relative intensity of the absorptions at higher field is considerably greater as expected from the above discussion. Similarly, while there are absorptions due to methylenic protons at 5.94 and 6.07 τ as in P_3, additional absorptions at 6.25 and 6.39 τ are at considerably higher field than would have been expected from linear or branched molecules of types III and IV. A possible explanation is that four of the protons are held near to the plane of the resultant field, thus experiencing a shielding effect, while the other four are held at approximately right angles to the field and so experience a deshielding effect. The existence of four prominent peaks in this region could be accounted for by the different resultant fields produced by the two different conformations of the molecule. Other minor absorptions in this region of the spectrum may be associated with different positions of substitution in the thiophene ring. It is suggested that this evidence provides a strong indication that P_4 has the structure V, although it is clear that a more sophisticated spectral investigation is desirable.

The infrared spectrum of P_4 (Fig. 3) does not provide any additional evidence about its structure.

Peak 5 (P_5). P_5, like P_1, is a relatively minor product, and there is evidence to suggest that two imperfectly resolved peaks are involved. It was not possible to separate the two components so the spectral data refer to the mixture.

The infrared spectrum (Fig. 3) indicates that substitution in the aromatic rings is complex. The bands in the 900–625 cm^{-1} region are not very well resolved, and there is no clear evidence of chloromethyl absorption at 675 cm^{-1}, although 2- and 3-substituted thiophene nuclei are again confirmed by absorptions at 695 and 760 cm^{-1}.

The NMR spectrum (Fig. 4) gives strong evidence of chloromethyl groups with resonance at 5.50 τ. Absorption in the region 2.70–3.50 τ again confirms the presence of both benzene and thiophene nuclei while absorptions in the 5.90–6.20 τ region can be assigned to the protons of the methylene bridges between aromatic nuclei. The 5.92 and 6.09 τ peaks can be assigned to substitution in the 2 and 3 positions of the thiophene

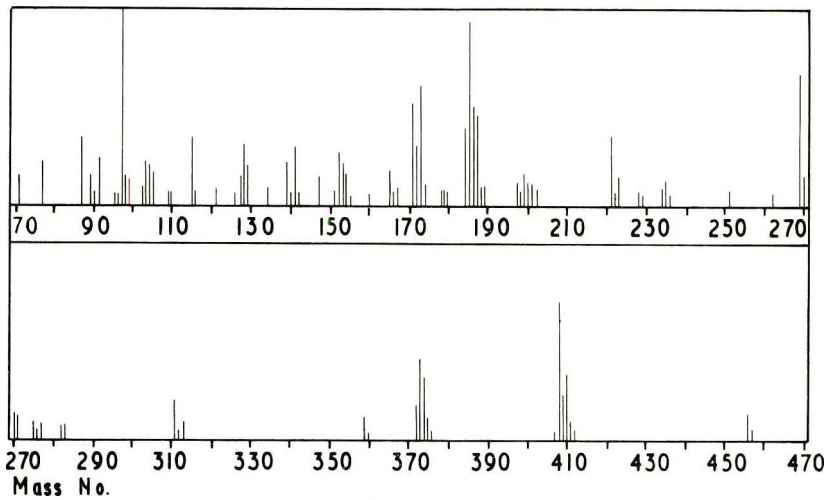

Fig. 6. Mass spectrum of P_5.

ring, respectively, while the large peak at 5.99 τ may be attributed to methylene groups linking two disubstituted nuclei in which the thiophene ring is 2,5-disubstituted. Similarly, the peak at 6.16 τ could be assigned to 2,4- or 3,4- substitution in the thiophene ring. This latter peak could also be due, however, to methylene groups linking disubstituted to trisubstituted benzene rings.

The mass spectrum of P_5 (Fig. 6) has a large peak at 408 which is assumed to be due to the parent ion. A very much smaller peak at 456 is probably due to impurity arising from inadequate separation of P_5 from P_6. Peaks at 373, 359, 311, 269, 221, 185, and 173 suggest the loss of Cl—, $ClCH_2$—, T—CH_2—, Cl—CH_2—C_6H_4—CH_2—, T—CH_2—C_6H_4—CH_2—, Cl—CH_2—

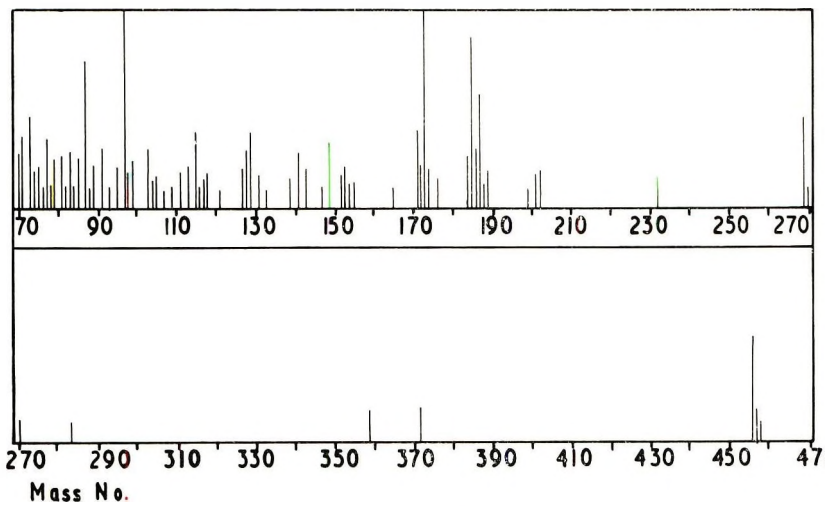

Fig. 7. Mass spectrum of P_6.

C_6H_4—CH_2—T—, and Cl—CH_2—C_6H_4—CH_2—T—CH_2— units from the molecule.

From this evidence it may reasonably be concluded that P_5 is a mixture of structures III and IV. Previous work[1,2] has shown that the thiophene nucleus is very much more reactive than the benzene nucleus, so it would be reasonable to expect the linear isomer, III, to predominate over the

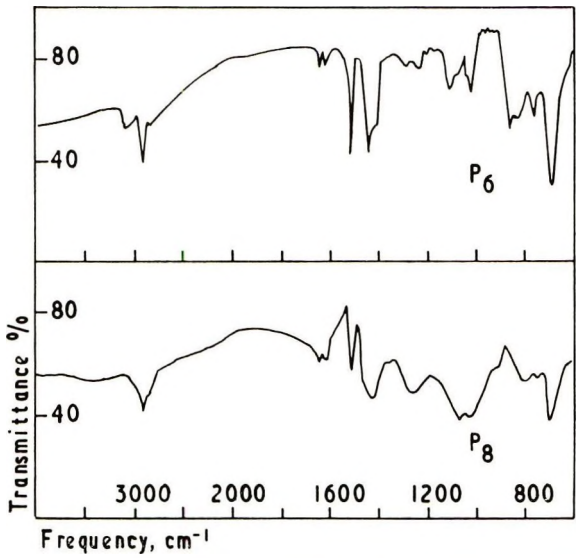

Fig. 8. Infrared spectra of P_6 and P_8.

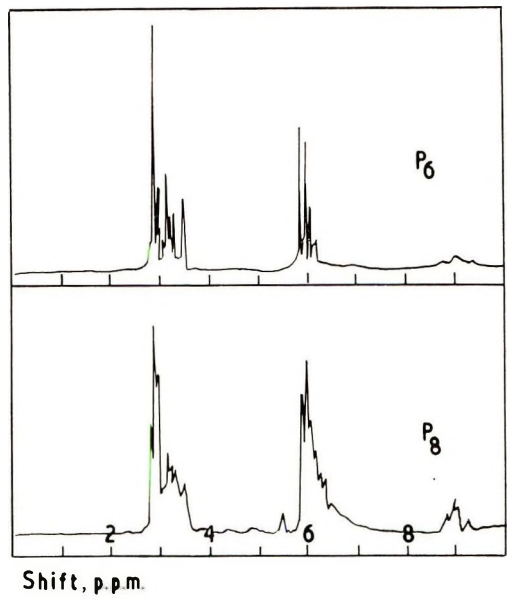

Fig. 9. Nuclear magnetic resonance spectra of P_6 and P_8.

branched isomer, IV. In addition, the methylene region of the NMR spectrum would be expected to be more complex if the isomers were present in comparable concentrations. From these latter pieces of evidence, together with the existence of P_4 which can only be derived from the linear isomer, it may be concluded that although P_5 consists of a mixture of III and IV, the linear isomer probably predominates.

P_5 could be formed by reaction of P_1 with an aromatic nucleus in P_3, by reaction of thiophen with II or by reaction of pairs of P_2 molecules. The first seems to be the most likely path, in view of the apparent absence of II among the reaction products and the relatively low concentration of P_2 during the reaction.

Peak 6 (P_6). The parent peak in the mass spectrum of P_6 (Fig. 7) is at mass number 456. The absence of absorption at 675 cm^{-1} in the infrared spectrum (Fig. 8) and at 5.50 τ in the NMR spectrum (Fig. 9) indicates that P_6 does not contain chloromethyl groups. This evidence suggests that it is a product containing five nuclei formed by reaction of P_5 with thiophene or P_2 with P_3. P_6 is therefore probably a mixture of VI and VII, which both have a molecular weight of 456.

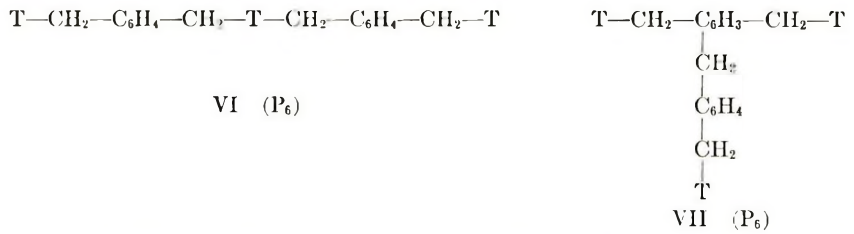

The methylene peaks in the region of 6.0 τ can be assigned similarly to those in the spectrum of P_5, and the same complex substitution pattern is confirmed by the various peaks and shoulders in the 650–770 cm^{-1} region of the infrared spectrum. Thus peaks at 700 and 765 cm^{-1} confirm the presence of both 2- and 3-monosubstituted thiophene nuclei and the peak at 755 cm^{-1} and the shoulders at 690 and 670 cm^{-1} indicate the presence of other types of substitution. For the same reasons as for P_5, it is believed that although both VI and VII are present, the linear form VI predominates. The proportion of aromatic to aliphatic protons, estimated from NMR spectra, was found to be 2.02, which agrees well with the value of 2.00 calculated for the molecular structure of P_6.

Peaks 7 and 8 (P_7 and P_8). The mass, infrared, and NMR spectra of P_7 are virtually indistinguishable from those of P_8 (Figs. 8–10), so it is concluded that they consist of two or more isomers. Chloromethyl groups are absent, so it seems necessary to account for this material in terms of the addition of at least one benzene and one thiophene nucleus to the five nuclei products comprising P_6. This is confirmed by a parent peak mass number of 642. Smaller peaks at 656 and 671 are believed to arise by combination of the parent ion with methylene fragments. The ratio of aromatic to aliphatic protons (1.78) in structures of this type having seven nuclei is in

good agreement with the value (1.83) calculated for the molecular formula. The absence of the intermediate product formed by reaction of P_1 with P_6 is perhaps surprising in view of the presence of P_5 among the products. It can be explained, however, in terms of the very much higher reactivity of the second chloromethyl group in P_1 compared with the first and is similar to the situation in the DCMB–benzene system previously described by Grassie and Meldrum.[3] The intermediate product will doubtless be present in the system but at a concentration too low for detection.

A large number of products having seven nuclei are possible. However, in view of the much greater reactivity of the thiophene nuclei compared with the benzene nuclei and the small concentration of trisubstituted benzene nuclei found in previous products it is reasonable to assume that the major branched isomer will be substituted in the central thiophene ring.

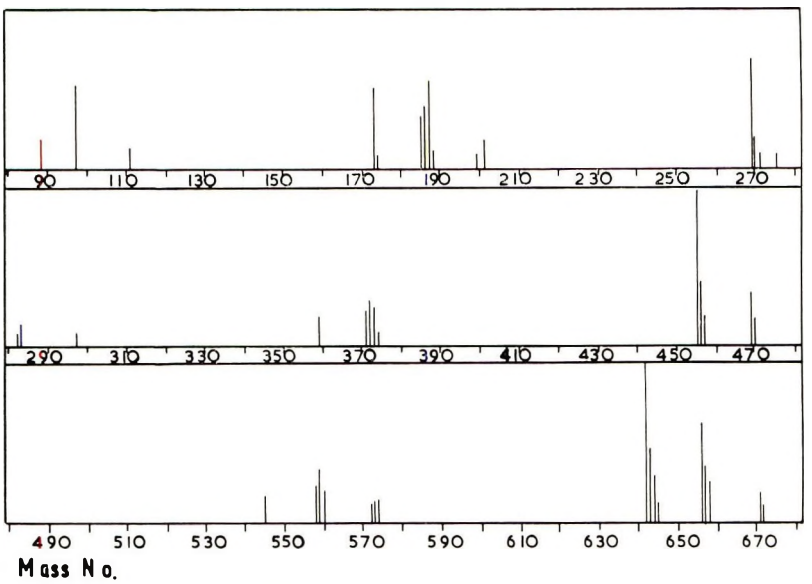

Fig. 10. Mass spectrum of P_8.

The infrared and NMR spectra of P_7 and P_8 are poorly resolved. However, peaks at 5.90, 5.98, 6.07, and 6.17 τ can be identified and accounted for as in the spectrum of P_6. There are, in addition, two small peaks at 6.25 and 6.34 τ which could be due to the appearance of trisubstituted benzene rings. However, they are also reminiscent of peaks in a similar position in the spectrum of P_4. Examination of mass and infrared spectra give no obvious clues as to whether or not the material of peaks P_7 and P_8 contains, as impurity, compounds incorporating P_4 rings substituted in either the thiophene or benzene nuclei. In view of the appreciable concentrations of P_4 which appear early in the reaction, however, it seems certain that such compounds do exist among the later reaction products.

On the basis of all this spectral evidence it is suggested that the principal constituents of P_7 and P_8 are represented by VIII and IX

$$T—CH_2—C_6H_4—CH_2—T—CH_2—C_6H_4—CH_2—T—CH_2—C_6H_4—CH_2—T$$

VIII (P_8)

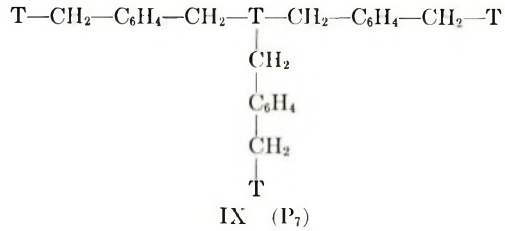

IX (P_7)

The elution ratio of the branched isomer should be expected to be larger than that of the linear isomer; thus P_7 and P_8 are likely to be IX and VIII, respectively. It must be emphasized, however, that a large number of branched isomers are possible and that although IX and VIII are believed to be the principal components of P_7 and P_8, they will inevitably contain considerable concentrations of impurities.

Peak 9 (P_9). The group of peaks at mass number 828 in the mass spectrum of P_9 in Figure 11 suggests that this product contains eleven aromatic nuclei, and the cracking pattern for P_9 can be interpreted in the same way as for previous products. Both infrared and NMR spectra are poorly resolved although similar to those of P_8. The relative intensities of the peaks at 5.90 and 5.99 τ indicate, however, that the proportion of mono- to di- or trisubstituted thiophene nuclei is slightly lower than for P_8. Although this is, at best, only a qualitative observation it does indicate that P_9, which un-

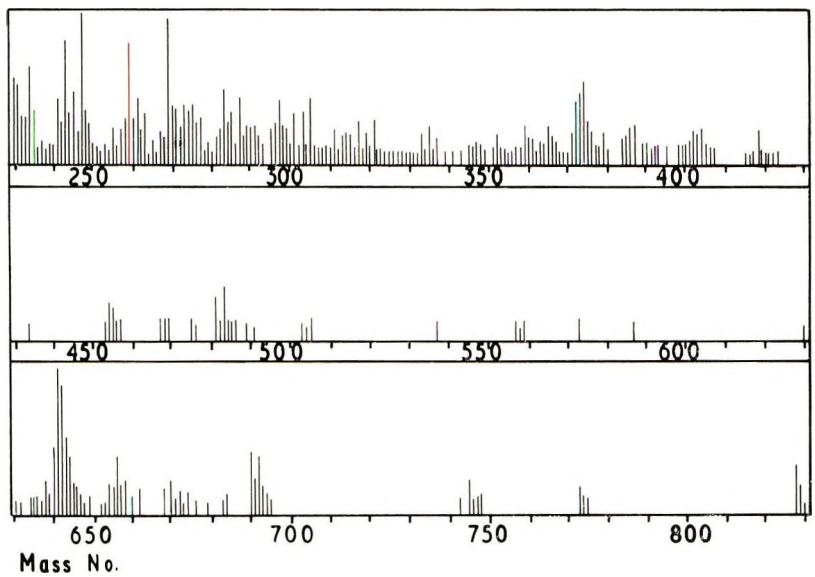

Fig. 11. Mass spectrum of P_9.

doubtedly consists of a complex mixture of isomers, still contains a fair proportion of linear material.

Peaks 10 and 11. It was not possible to obtain any peaks above mass number 600 in the mass spectra of P_{10} and P_{11}. It may therefore be concluded that the parent ion and subsequent high mass number scission products are too unstable to be recorded. Infrared and NMR spectra of these products were again very similar to those of P_8 but so poorly resolved that it was not possible to make even qualitative conclusions about preferred arrangements of nuclei. It may only be concluded that P_{10} and P_{11} are complex mixtures of linear and branched species with more than eleven aromatic nuclei.

Product Reaction Curves

The overlapping of P_7 and P_8 and of P_{10} and P_{11} was so great in some chromatograms that separation by extrapolation of their resolved parts was not feasible. It has been shown, however, that P_7 and P_8 are isomers and P_{10} and P_{11} have not been identified, so it seems reasonable to derive the

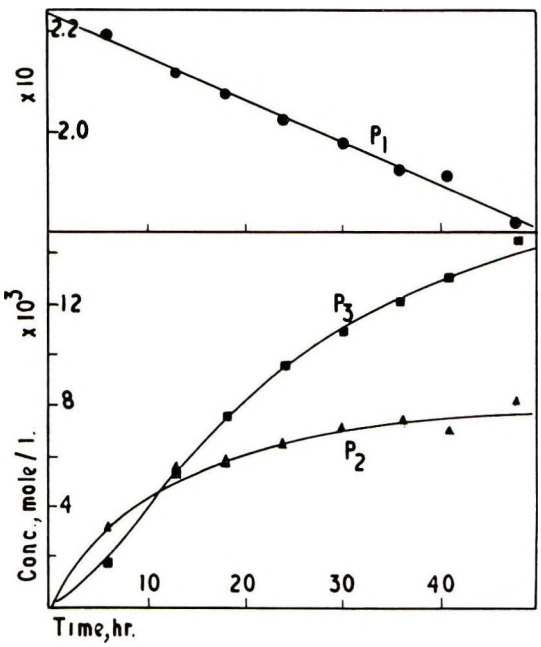

Fig. 12. Reaction curves for P_1, P_2, and P_3.

total amounts of P_7 and P_8 and of P_{10} and P_{11} and to treat them as single products in the construction of reaction curves. Concentrations of products obtained at various stages of reaction are presented in Table III and reaction curves derived from these results are illustrated in Figures 12 and 13.

TABLE III
Concentrations from Gel-Permeation Chromatograms[a]

Reaction time, hr	Concentrations of products, mole/l.								
	P_1	P_2	P_3	P_4	P_5	P_6	$P_{7,8}$	P_9	$P_{10,11}$
6	0.2190	0.0031	0.0017						
13	0.2118	0.0056	0.0055	0.0002	0.0005	0.0002			
18	0.2079	0.0057	0.0076	0.0006	0.0013	0.0008	0.0002		
24	0.2025	0.0064	0.0096	0.0008	0.0015	0.0018	0.0009		
30	0.1979	0.0071	0.0108	0.0008	0.0019	0.0027	0.0014	0.0004	0.0007
36	0.1927	0.0073	0.0121	0.0015	0.0024	0.0034	0.0023	0.0008	0.0014
41	0.1914	0.0069	0.0130	0.0016	0.0020	0.0034	0.0020	0.0014	0.0021
48	0.1825	0.0081	0.0144	0.0020	0.0027	0.0045	0.0040	0.0018	0.0030

[a] Initial concentrations of reactants: DCMB, 0.2239 mole/l.; thiophene, 0.2229 mole/l.; $SnCl_4$, 0.0170 mole/l.

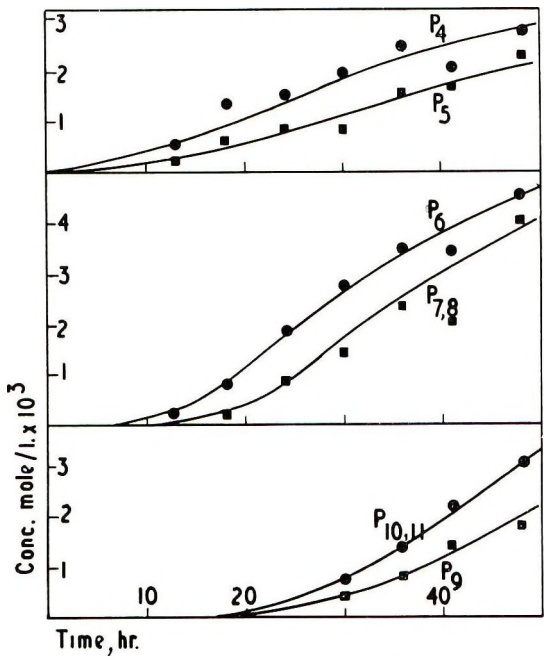

Fig. 13. Reaction curves for P_4, P_5, P_6, $P_{7,8}$, P_9, and $P_{10,11}$.

As previously found in the GLC study of the initial stages of reaction,[1] the reaction curve for DCMB is linear. The earlier parts of the reaction curves for P_2 and P_3 are also similar to those obtained from GLC data. Later, the rate of increase of the concentration of P_3 falls off in a similar manner to that of P_2 showing that in the later stages of the reaction its rate of reaction with chloromethyl compounds is becoming comparable with its rate of formation. On comparing the reaction curves for P_4 and P_5, it is perhaps surprising to find such a high proportion of P_4 so early in the reaction. If it is assumed that P_4 is produced exclusively by self-condensation of P_5, then the relative proportions of P_4 and P_5 would suggest that this self-condensation is a very facile reaction. This demonstrates that self-condensation of chloromethyl compounds may play an important role at all stages of the reaction. The reaction curves for P_4 and P_5 are very similar and both show only a very gradual increase in concentration as the reaction proceeds. This would seem to indicate that both are very reactive. The P_5 curve confirms that the second chloromethyl group in a DCMB molecule, which has become incorporated into a higher molecular weight product, is extremely reactive. Further evidence of relatively high reactivity is provided by the absence of chloromethyl compounds in detectable quantities among the products of higher molecular weight. The reaction curves for all other products are similar in form to that obtained for DTB although, as expected, with progressively longer induction periods. These curves were not well enough delineated or carried to high enough

conversion to determine kinetic relationships between the various components. Thus it was not possible to establish that the maximum rates of formation of the various compounds coincide with the maximum concentrations of their precursors. The reaction curves clearly demonstrate, however, the consecutive pattern of the series of reactions involved.

DISCUSSION

It is now possible to make a number of generalizations about the reaction between DCMB and thiophene, about the structure of the resulting polymer, and the possible relevance of these structural features to its thermal stability compared with that of the corresponding benzene polymer.

During the initial stages of the reaction the principal events are the formation of thenylchloromethylbenzene and dithenylbenzene by successive replacement of the two chlorine atoms in *p*-di(chloromethyl)benzene by thiophene. The second chloromethyl group in DCMB is very much more reactive than the first so that the concentrations of product molecules containing chloromethyl groups remains low throughout the reaction. As the concentrations of P_2 and P_3 increase, more complex products are formed. While the concentrations of DCMB and thiophene are still high, these more complex products will mostly result from the reaction of DCMB with an earlier product followed by reaction of thiophene with the free chloromethyl group. As the reaction proceeds, however, and the concentration of free thiophene is diminished, these pendant chloromethyl groups will tend to react increasingly with aromatic nuclei in product molecules to form highly complex branched and crosslinked structures. It is clear that chloromethyl groups will react preferably with thiophene rather than benzene nuclei. This will have at least two significant structural effects. Firstly, the early products of the reaction will tend to be very much less branched than in the benzene reaction. For example, it is to be expected that the concentration of III in P_5 is very much greater than the concentration of IV. Secondly, the bulk of chain branches will occur at thiophen rather than benzene nuclei. Another basic structure difference from the benzene polymer is concerned with the obvious facility of intramolecular reactions of the type which result in the formation of P_4 from P_5. Although P_4 was the only such cyclic compound isolated, it is clear that this kind of reaction will almost certainly occur in larger molecular products. This, together with the fact that P_4 will react further with DCMB so that these rings become incorporated into the polymer structure will lead to a final material incorporating very many more individual structural features than the benzene polymer. It may be that the less satisfactory GPC separation of the products of the thiophene reaction compared with the benzene reaction is due to a continuous background of substituted P_4 type products in the chromatogram. In any case the greater complexity of structural types due to the presence of two types of aromatic rings and the occurrence of cyclization reactions renders very much more difficult a computer-based kinetic

analysis of the system of the type which provided so much insight into the structure of the ultimate DCMB–benzene polymer.[5–8]

Since the incorporation of these cyclic structures will result in what is effectively a partial ladder structure the facility with which these structures are formed may account for the greater stability of the thiophene–DCMB compared with the benzene–DCMB polymer.

References

1. N. Grassie, J. B. Colford, and I. G. Meldrum, *J. Polym. Sci. A-1*, **9**, 2817 (1971).
2. N. Grassie and I. G. Meldrum, *Europ. Polym. J.*, **5**, 195 (1969).
3. N. Grassie and I. G. Meldrum, *Europ. Polym. J.*, **6**, 499 (1970).
4. N. Grassie and I. G. Meldrum, *Europ. Polym. J.*, **6**, 513 (1970).
5. N. Grassie and I. G. Meldrum, *Europ. Polym. J.*, **7**, 17 (1971).
6. N. Grassie and I. G. Meldrum, *Europ. Polym. J.*, **7**, 613 (1971).
7. N. Grassie and I. G. Meldrum, *Europ. Polym. J.*, **7**, 645 (1971).
8. N. Grassie and I. G. Meldrum, *Europ. Polym. J.*, in press.

Received March 15, 1971
Revised May 24, 1971

JOURNAL OF POLYMER SCIENCE: PART A-1 VOL. 9, 2853–2867 (1971)

Studies with Inorganic Precipitate Membranes. III.* Consideration of Energetics of Electrolyte Permeation through Membranes

FASIH A. SIDDIQI, N. LAKSHMINARAYANAIAH, and MOHAMMAD N. BEG, *Department of Pharmacology, University of Pennsylvania School of Medicine, Philadelphia, Pennsylvania 19014, and Department of Chemistry, Aligarh Muslim University, Aligarh, India*

Synopsis

The permeability of various electrolytes through parchment-supported ferrocyanide membranes of manganese, cobalt, silver, and cadmium has been measured at 10, 15, 20, 25, and 30°C. The order of permeability at a given temperature was $Cl^- > NO_3^- > CNS^- > CH_3COO^- > SO_4^{2-}$ for both monovalent and divalent cations. For any given anion, the cations followed the sequence $NH_4^+ > Li^+ > Ba^{2+} > Ca^{2+} > Mg^{2+} > Al^{3+}$. This sequence has been correlated with the size of the hydrated ion. Further, the data have been considered from the standpoint of the theory of rate processes and the values for the entropy of activation ($\Delta S'$) have been derived assuming an equilibrium distance of 3 Å in the membrane. The values of $\Delta S'$ were all negative and decreased with increasing valence of the ions. This was interpreted to mean electrolyte permeation with partial immobilization in the membrane.

INTRODUCTION

Zwolinski et al.[1] in 1949 examined the nonelectrolyte premeability data available in the literature for various plant and animal cells by applying the theory of absolute reaction rates.[2] Similarly Shuler et al.[3] considered the kinetics of membrane permeation for nonelectrolytes through collodion membranes. With the availability of thin lipid membranes,[4] Tien and Ting[5] measured their permeability to water and considered the permeation process from the standpoint of the theory of rate processes. In recent years, a number of investigators[6–8] have investigated the electrolyte permeability characteristics of parchment-supported inorganic precipitate membranes. In this paper, the electrolyte permeability of four inorganic membranes at different temperatures in a number of electrolytes is considered on the basis of the concepts of the theory of absolute reaction rates.

* The permeability and the charge density characteristics of parchment-supported membranes of silver chloride, silver phosphate, and silver tungstate are described in Parts I and II, see *Z. physik. Chem.* (Frankfurt), **72**, 298, 307 (1970).

EXPERIMENTAL

Preparation of Parchment-Supported Inorganic Membranes

Manganese, cobalt, silver, and cadmium ferrocyanide membranes were prepared following the procedures described elsewhere.[8] To precipitate these substances in the interstices of the parchment paper, 0.2*M* solution of potassium ferrocyanide was kept inside the glass tube, to one end of which was tied the parchment paper. This was suspended for 72 hr in a 0.2*M* solution of a suitable salt of magnanese (chloride), cobalt (chloride), silver (nitrate), or cadmium (chloride). The two solutions were interchanged later and kept for another 72 hr. The membranes were washed with deionized water for removal of free electrolyte.

Measurement of Membrane Potential

The apparatus used was similar to the one used by Siddiqi and Pratap.[8] The membrane was held between two half cells (capacity ca. 125 ml), each of which contained 125 ml of the electrolyte solution. Initially the concentrations C_1 and C_2 were 0.001 and 0.1*M*, respectively. In each half cell there were two firmly fixed platinized platinum electrodes to follow concentration changes on a conductivity bridge and an anion reversible Ag–AgCl electrode to measure the electrical potentials arising across the membrane. The whole cell was immersed in a water thermostat maintained at 25 ± 0.1°C. The various salt solutions (chlorides of Li^+, Na^+, K^+, NH_4^+, Ba^{2+}, Ca^{2+}, Mg^{2+}, and Al^{3+}) were prepared from B.D.H. AR-grade chemicals by use of deionized water. The solutions in both the chambers were kept well stirred by magnetic stirrers.

Exactly known weights or volumes of two test solutions were introduced (say at zero time), and the platinized platinum electrodes were connected to the conductance bridges to follow conductance change with time. No appreciable change in conductance was noted within the 5-hr period on the C_2 side (0.1*M*), and so we have assumed this concentration to be practically constant and followed only the conductance change on the C_1 side. The exact concentration of this solution was determined from a calibration curve where conductance was plotted against concentration. The Ag–AgCl electrodes were connected to a Pye precision vernier potentiometer to monitor the potential across the membrane with time.

Measurement of Electrolyte Permeability

The diffusion experiments were performed by the method of Austin et al.[9] based on the constant flow principle. The membrane in the form of a circular disk (functional area = 19.6 cm^2) was washed thoroughly to remove adsorbed electrolyte and fixed in the leak-proof all-glass cell which finally rested on a magnetic stirrer plate. The upper and lower portions of the cell were connected, past manometers, to reservoirs of 0.2*M* electrolyte solution and of doubly distilled water, respectively. On leaving the cell, the water passed two platinized platinum electrodes which were used to

follow the conductance change of the effluent. The rate of this flow was 180 ml/hr. Similarly the electrolyte flow was maintained usually at 300 ml/hr. The hydrostatic pressure on each side of the membrane was kept equal by adjusting the rates of flow of solution and water.

From calibration curves relating conductance to electrolyte concentration previously established for the conductivity cell, the concentration of the effluent was determined. This, combined with the rate of flow of the effluent, enabled permeability P in millimoles per hour to be calculated at any given temperature. The whole cell assembly was kept immersed in a water thermostat maintained constant to an accuracy of $\pm 0.1°C$. The experiments were carried out at 10, 15, 20, 25, and 30°C.

RESULTS AND DISCUSSION

The potential difference between Ag–AgCl electrodes placed on either side of the membrane is the algebraic sum of the electrode potential difference E_e (i.e., concentration potential) and the membrane potential E_m. E_e is obtained by calculation from the measured concentrations of the solutions C_1 and C_2 on the two sides of the membrane from the equation

$$E_e = (RT/Z_-F) \ln (C_2\gamma_2/C_1\gamma_1) \quad (1)$$

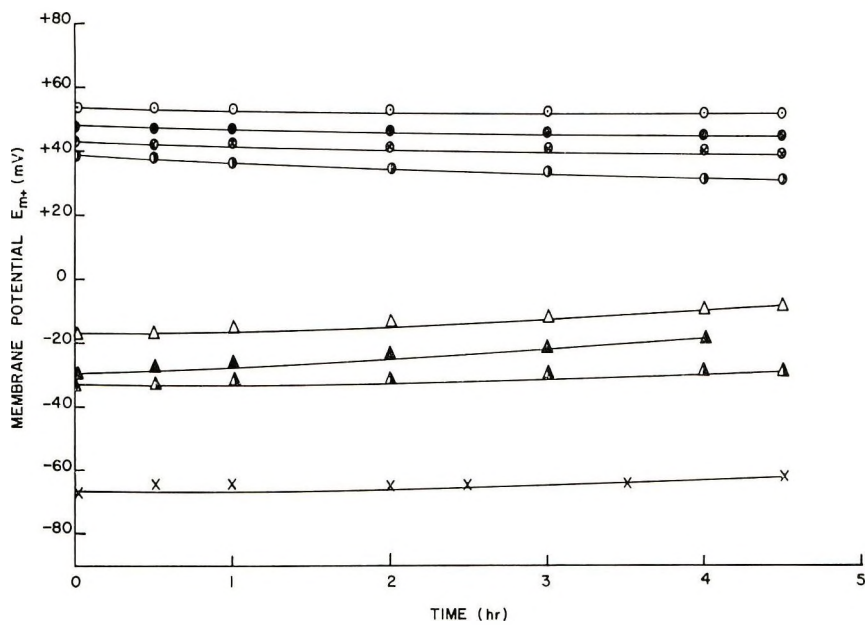

Fig. 1. Variation of membrane potential E_m with time occurring across a parchment-supported manganese ferrocyanide membrane when it separated 0.1 and 0.001M solutions of the same electrolyte. The electrolytes used were: chlorides of (⊙) Li^+; (●) Na^+; (⊕) K^+; (◑) NH_4^+; (▲) Ca^{2+}; (△) Ba^{2+}; (◭) Mg^{2+}; and (×) Al^{3+}.

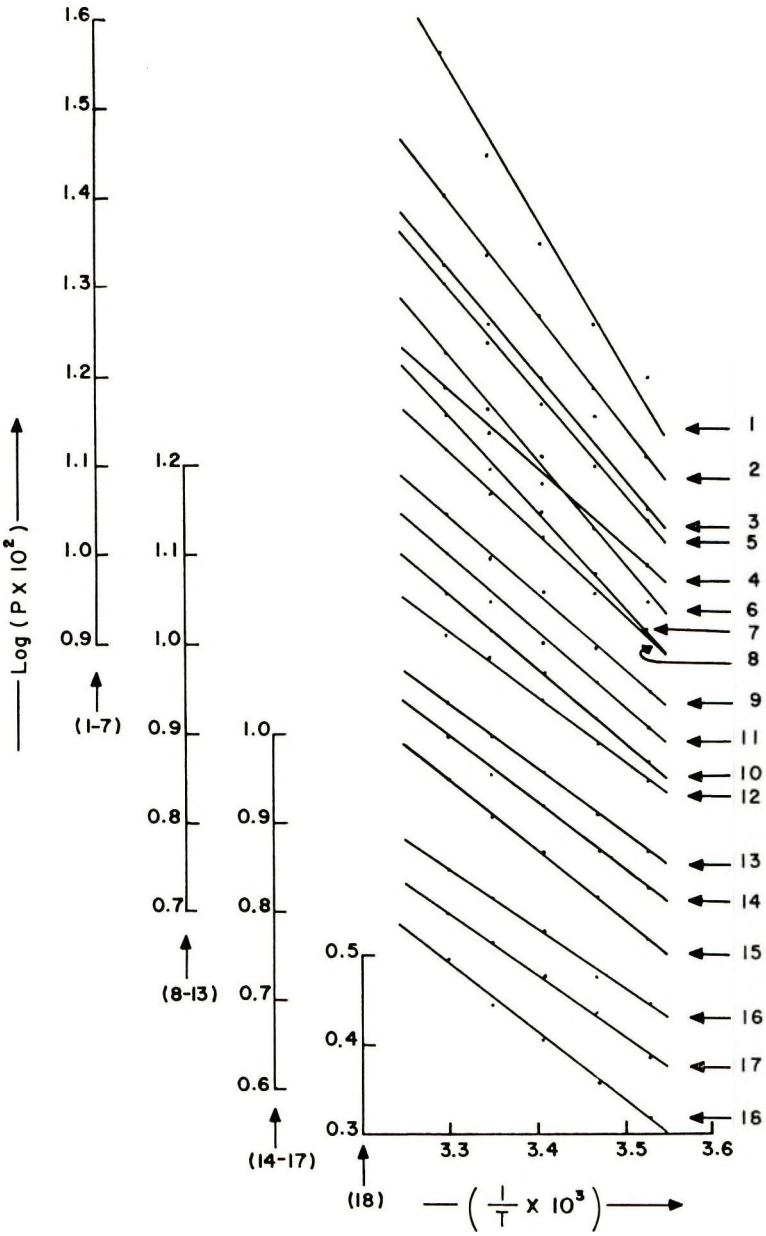

Fig. 2. Variation in permeability P (mmole/hr) of a manganese ferrocyanide membrane with temperature in presence of different electrolytes: (*1*) NH_4Cl; (*2*) NH_4NO_3; (3) NH_4CNS; (4) $(NH_4)_2SO_4$; (*5*) LiCl; (*6*) $LiNO_3$; (*7*) Li_2SO_4; (*8*) $BaCl_2$; (*9*) $Ba(NO_3)_2$; (*10*) $Ba(CH_3COO)_2$, (*11*) $CaCl_2$; (*12*) $Ca(NO_3)_2$; (*13*) $Ca(CH_3COO)_2$, (*14*) $MgCl_2$; (*15*) $Mg(NO_3)_2$; (*16*) $Mg(CH_3COO)_2$; (*17*) $MgSO_4$; (*18*) $AlCl_3$.

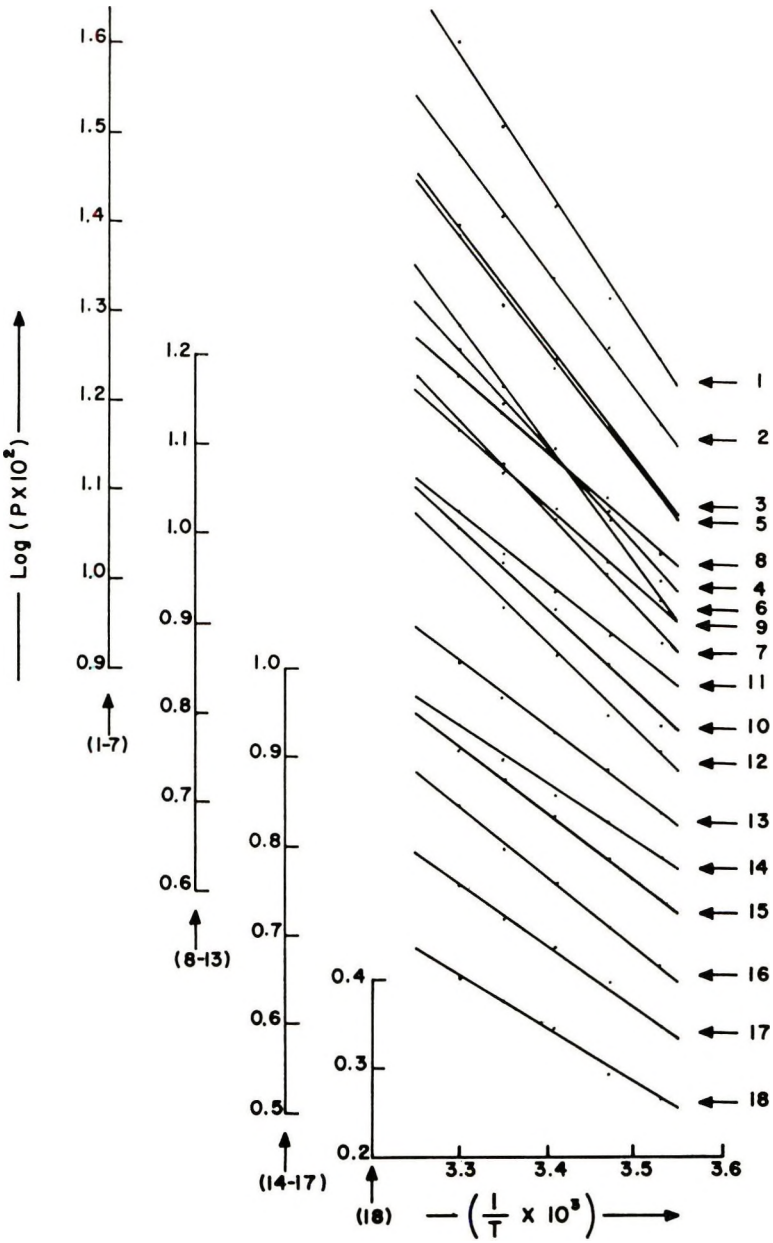

Fig. 3. Variation in permeability P(mmole/hr) of a cobalt ferrocyanide membran with temperature in presence of different electrolytes: (*1*) NH_4Cl; (*2*) NH_4NO_3; (*3* NH_4CNS; (*4*) $(NH_4)_2SO_4$; (*5*) LiCl; (*6*) $LiNO_3$; (*7*) Li_2SO_4; (*8*) $BaCl_2$; (*9*) $Ba(NO_3)_2$; (*10*) $Ba(CH_3COO)_2$; (*11*) $CaCl_2$; (*12*) $Ca(NO_3)_2$; (*13*) $Ca(CH_3COO)_2$; (*14*) $MgCl_2$; (*15*) $Mg(NO_3)_2$; (*16*) $Mg(CH_3COO)_2$; (*17*) $MgSO_4$; (*18*) $AlCl_3$.

where the γ are the activity coefficients of the electrolyte solutions. Since Z_- is always unity, E_e at 25°C is given by

$$E_e = 59.16 \log (C_2\gamma_2/C_1\gamma_1)$$

As E_e and $(E_c + E_m)$ measured directly are known, E_m can be obtained by subtraction.

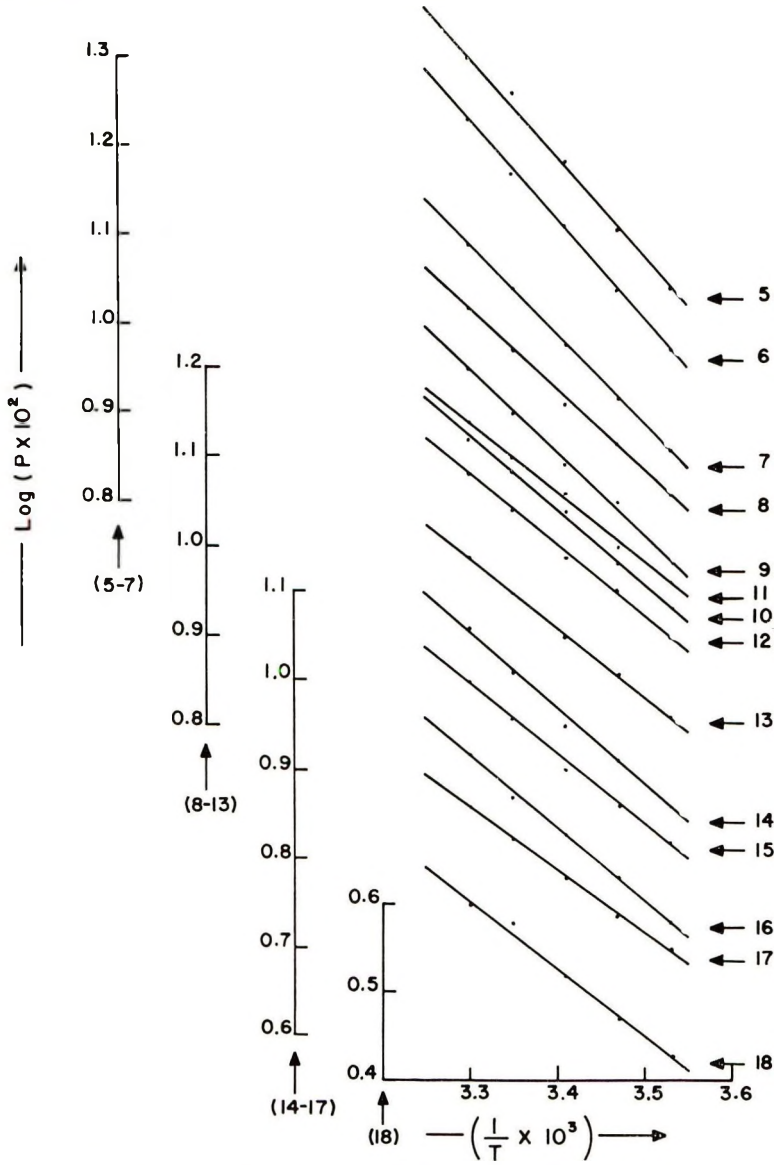

Fig. 4. Variation in permeability P (mmole/hr) of a silver ferrocyanide membrane with temperature in presence of different electrolytes: (*5*) LiCl; (*6*) $LiNO_3$; (*7*) Li_2SO_4; (*8*) $BaCl_2$; (*9*) $Ba(NO_3)_2$; (*10*) $Ba(CH_3COO)_2$; (*11*) $CaCl_2$; (*12*) $Ca(NO_3)_2$; (*13*) $Ca(CH_3COO)_2$; (*14*) $MgCl_2$; (*15*) $Mg(NO_3)_2$; (*16*) $Mg(CH_3COO)_2$; (*17*) $MgSO_4$; (*18*) $AlCl_3$.

The changes in E_m noted with time are shown in Figure 1 for various electrolytes diffusing through a manganese ferrocyanide membrane. Little change in the values of E_m with time is noted. Similar values for E_m (not

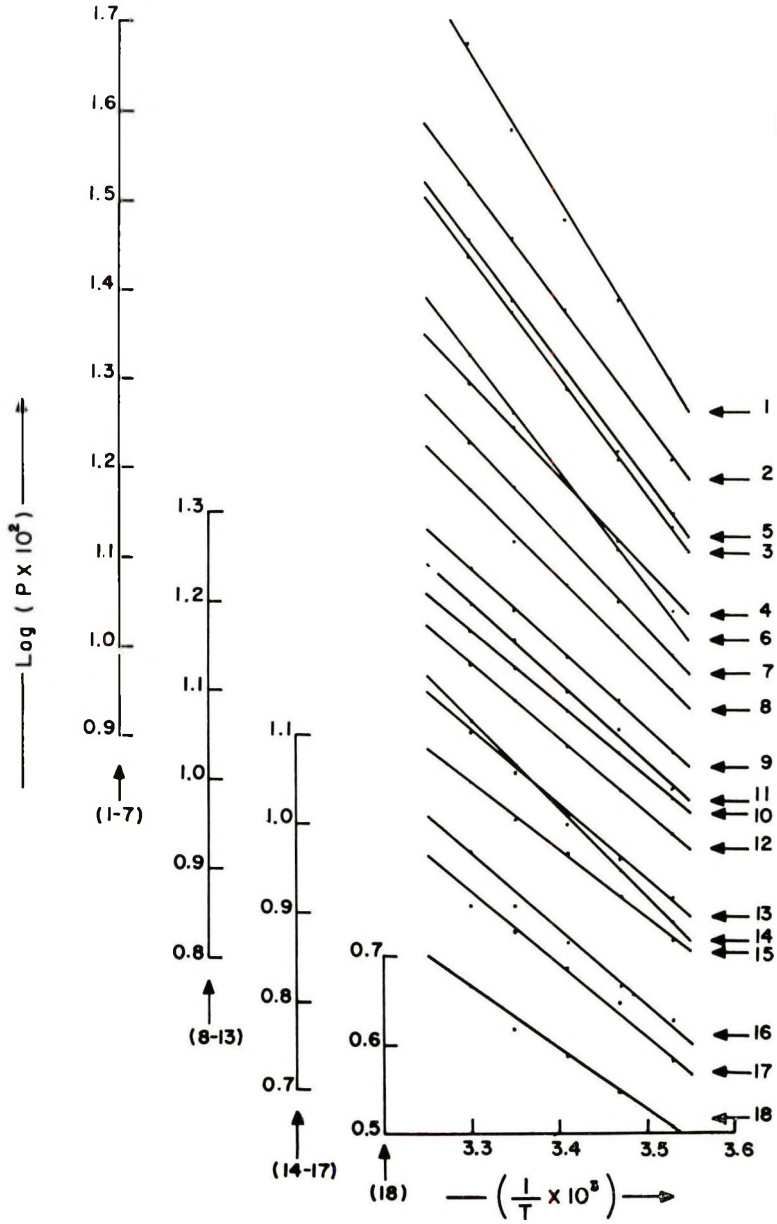

Fig. 5. Variation in permeability P(mmole/hr) of a cadium ferrocyanide membrane with temperature in presence of different electrolytes: (*1*) NH_4Cl; (*2*) NH_4NO_3; (*3*) NH_4CNS; (*4*) $(NH_4)_2SO_4$; (*5*) LiCl; (*6*) $LiNO_3$; (*7*) Li_2SO_4; (*7*) $BaCl_2$; (*9*) $Ba(NO_3)_2$; (*10*) $Ba(CH_3COO)_2$; (*11*) $CaCl_2$; (*12*) $Ca(NO_3)_2$; (13) $Ca(CH_3COO)_2$; (*14*) $MgCl_2$; (*15*) $Mg(NO_3)_2$; (*16*) $Mg(CH_3COO)_2$; (*17*) $MgSO_4$; (*18*) $AlCl_3$.

given) were observed with the other three membranes also. An interesting point with these values of E_m is the fact that in the case of (1:1) electrolytes, the values are all positive (i.e., dilute solution side C_1 taken positive). This means that the membrane is cation-selective. In the case of 2:1 and 3:1 electrolytes, E_m changes sign and therefore becomes anion-selective. This change in the selectivity character of the membrane is due to adsorption of multivalent ions leading to a state where a net positive charge is left on the membrane surface making it anion-selective. Adsorption of Al^{3+} makes the membrane more anion-selective than it is with the adsorption of other divalent cations. Such behavior is not peculiar to these systems. Rosenberg et al.[10] found in the case of thorium counterion, negative electroosmotic transport of water. The ion was so strongly adsorbed on a cation exchange membrane that it conferred anion selectivity to the membrane, and thus water was transferred in the opposite direction (i.e., to the anode chamber instead of to the cathode chamber). Similarly Schulz[11] found, in the case of sodium diphosphate, adsorption of the diphosphate anion on the surface of the anion exchange membrane, Permplex A-100. This reversed the charge on the membrane and also the direction of water flow. This surface-charge reversal occurred in every one of the membranes and electrolytes (2:1 and 3:1) used in this study.

In Figures 2–5 are given the plots of log P against $(1/T)$, where T is the absolute temperature at which the experiments were conducted, for the four membranes and different 1:1, 2:1, and 3:1 electrolytes.

The two important factors which control electrolyte permeability through a membrane are charge on the membrane and its porosity. Parchment paper, except for the presence of some stray and end carboxyl groups, contains very few fixed groups. Deposition of inorganic precipitates gives rise to a net negative charge on the membrane surface in the case of 1:1 electrolyte leading to the type of ionic distribution associated with the electrical double layer. However, as discussed above, use of 2:1 or 3:1 electrolytes leaves a net positive charge on the membrane and again results in the formation of the electrical double layer. Flow of electrolyte by diffusion, because of the presence of a net charge ($-ve$ or $+ve$) on the membrane, gives rise to the membrane potential, as opposed to the liquid junction potential ordinarily observed under similar conditions in the absence of the membrane, which regulates the flow of electrolyte by increasing the speed of the slow moving ion and also by decreasing the speed of the fast moving ion. This regulated rate of flow (i.e., premeability) measured for different electrolytes through the various membranes at any given temperature decreases in the order $Cl^- > NO_3^- > CNS^- > CH_3COO^- > SO_4^{2-}$ for both monovalent and divalent cations. For any given anion, the cations follow the sequence

$$NH_4^+ > Li^+ > Ba^{2+} > Ca^{2+} > Mg^{2+} > Al^{3+}$$

Electrolyte types follow the sequence 1:1 > 2:1 > 3:1.

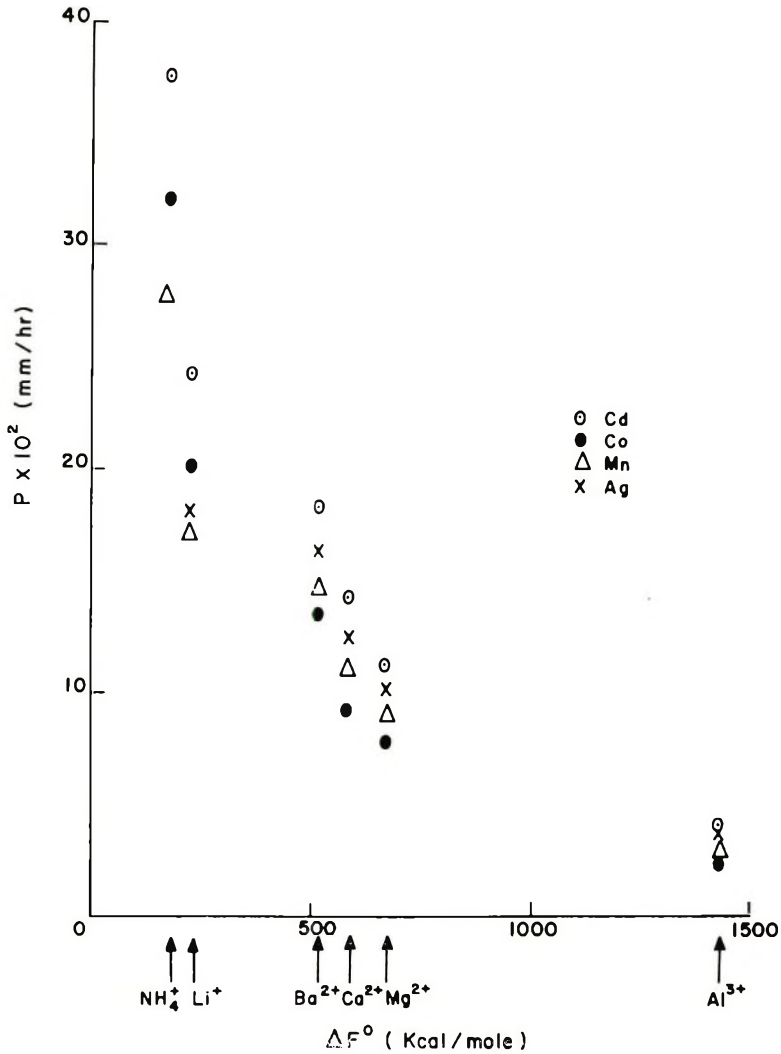

Fig. 6. Permeability P(mmole/hr) at 25°C of various electrolytes (chlorides) through different membranes plotted against the free energy ($\Delta F°$) of hydration of cations: (Δ) manganese ferrocyanide; (●) cobalt ferrocyanide; (×) silver ferrocyanide; (⊙) cadium ferrocyanide.

Membrane porosity in relation to the size of the species (hydrated) flowing through the membrane seems to determine the above sequence. Although the sizes of the hydrated electrolytes are not known with certainty, there are a few tabulations[12,13] of the number of moles of water associated with some electrolytes. However, in Figure 6, a plot of permeability of different electrolytes (chlorides) against free energy of hydration of cations[14] is given for the four membranes. It is seen that permeability decreases with increasing hydration energy, that is, greater size due to increase in hydration. This points to the fact that the electrolyte is diffusing along pores or

TABLE I

Experimental Activation Energy E_a and Other Thermodynamic Parameters Calculated from the Transition State Theory of Rate Processes for Electrolyte Diffusion through Membranes (Temperature = 25°C)

Electrolyte	Manganese ferrocyanide				Cobalt ferrocyanide			
	E_a, kcal	$\Delta H'$, kcal	$\Delta F'$, kcal	$\Delta S'$, e.u.	E_a, kcal	$\Delta H'$, kcal	$\Delta F'$, kcal	$\Delta S'$, e.u.
NH_4Cl	7.37	6.78	8.55	−6.0	7.55	6.96	8.58	−5.8
NH_4NO_3	6.07	5.48	8.72	−10.9	6.07	5.48	8.72	−10.8
NH_4CNS	5.53	4.94	8.83	−13.1	5.97	5.38	8.85	−11.6
$(NH_4)_2SO_4$	4.97	4.38	9.00	−15.5	5.07	4.48	9.01	−15.2
$LiCl$	5.50	4.91	8.85	−13.2	5.90	5.31	8.85	−11.9
$LiNO_3$	5.48	4.89	8.95	−13.6	5.80	5.21	8.99	−12.7
$LiSO_4$	4.79	4.20	9.05	−16.3	4.61	4.02	9.10	−17.1
$BaCl_2$	4.24	3.65	8.95	−17.8	3.96	3.37	9.08	−19.2
$Ba(NO_3)_2$	3.96	3.37	9.05	−19.1	3.96	3.37	9.18	−19.5
$Ba(CH_3COO)_2$	3.85	3.26	9.15	−19.8	3.95	3.36	9.32	−20.1
$CaCl_2$	3.76	3.17	9.11	−19.9	3.59	3.00	9.30	−21.1
$Ca(NO_3)_2$	3.59	3.00	9.20	−20.8	4.22	3.63	9.40	−19.4
$Ca(CH_3COO)_2$	3.40	2.81	9.31	−21.8	3.22	2.63	9.52	−23.1
$MgCl_2$	3.41	2.82	9.24	−21.5	2.95	2.36	9.41	−23.7
$Mg(NO_3)_2$	3.45	2.86	9.30	−21.6	3.33	2.74	9.44	−22.5
$Mg(CH_3COO)_2$	3.32	2.73	9.43	−22.5	3.21	2.62	9.55	−23.2
$MgSO_4$	3.22	2.63	9.50	−23.0	3.13	2.54	9.65	−23.9
$AlCl_3$	3.68	3.09	9.93	−22.9	2.86	2.67	10.10	−26.3

TABLE II

Experimental Activation Energy E_a and Other Thermodynamic Parameters Calculated from the Transition State Theory of Rate Processes for Electrolyte Diffusion through Membranes (Temperature = 25°C)

Electrolyte	Silver ferrocyanide				Cadmium ferrocyanide			
	E_a, kcal	$\Delta H'$, kcal	$\Delta F'$, kcal	$\Delta S'$, e.u.	E_a, kcal	$\Delta H'$, kcal	$\Delta F'$, kcal	$\Delta S'$, e.u.
NH_4Cl	—	—	—	—	7.65	7.06	8.56	−5.1
NH_4NO_3	—	—	—	—	6.36	5.77	8.70	−9.9
NH_4CNS	—	—	—	—	6.26	5.67	8.81	−10.5
$(NH_4)_2SO_4$	—	—	—	—	5.16	4.57	8.98	−14.8
LiCl	5.53	4.94	8.80	−13.0	6.36	5.77	8.79	−10.1
$LiNO_3$	5.49	4.90	8.93	−13.5	5.99	5.40	8.97	−12.0
Li_2SO_4	4.61	4.02	9.10	−17.1	4.79	4.20	9.07	−15.3
$BaCl_2$	4.24	3.65	8.85	−17.5	4.61	4.02	8.95	−16.5
$Ba(NO_3)_2$	4.15	3.56	8.95	−18.1	4.24	3.65	9.07	−18.2
$Ba(CH_3COO)_2$	3.95	3.36	9.03	−19.0	4.15	3.56	9.15	−18.8
$CaCl_2$	3.68	3.09	9.00	−19.8	4.24	3.65	9.11	−18.3
$Ca(NO_3)_2$	3.58	2.99	9.10	−20.5	3.68	3.09	9.20	−20.5
$Ca(CH_3COO)_2$	3.57	2.98	9.23	−21.0	3.58	2.99	9.31	−21.2
$MgCl_2$	3.96	3.37	9.13	−19.4	4.61	4.02	9.25	−17.6
$Mg(NO_3)_2$	3.59	3.00	9.21	−20.9	3.68	3.09	9.31	−20.9
$Mg(CH_3COO)_2$	3.59	3.00	9.34	−21.3	3.50	2.91	9.45	−21.9
$MgSO_4$	3.32	2.73	9.38	−22.3	3.49	2.90	9.50	−22.1
$AlCl_3$	3.41	2.82	9.72	−23.1	3.32	2.73	9.86	−23.9

channels of dimensions adequate to allow the substance to penetrate the membrane. The state of hydration of the penetrating electrolyte may be considered to exist in a dynamic condition so that at higher temperatures considerably higher fraction f of the total number of a given kind would possess excess energy ΔE according to the Boltzmann distribution $f = e^{-\Delta E/RT}$ (R is the gas constant). Under these circumstances, those ionic species which have lost sufficient water of hydration to be smaller than the size of the pore would enter the membrane. This way the permeability would increase with increase in temperature, subject however to the proviso that the membrane has undergone no irreversible change in its structure. That no such structural change is involved is evident from the linear

TABLE III
Thermodynamic Parameters $\Delta S'$ for Permeation of Various Substances through Different Systems[a]

Diffusion system		Entropy factor $\lambda[e^{\Delta S'/R}]^{1/2}$,		
Diffusing species	Medium	Å	$\Delta S'$, e.u.	Reference
Water	Water	11.0	9.5	
Phenol	Methyl alcohol	1.4	1.3	
Phenol	Benzene	1.4	1.3	2a[b]
$C_2H_2Br_4$	$C_2H_2Cl_4$	1.0	0	
Bromine	CS_2	0.4	−3.6	
Mannitol	Water	2.8	4.1	16b[b]
H_2	Butadiene–acrylonitrile membrane	182	16.0	
N_2	Butadiene–acrylonitrile membrane	130	14.7	
N_2	Butadiene–methyl methacrylate membrane	150	15.3	
Ar	Butadiene–methyl methacrylate membrane	93	13.4	
N_2	Butadiene–polystyrene membrane	24	7.8	2b,17[c]
Ar	Butadiene–polystyrene membrane	33	9.3	
H_2	Neoprene membrane	74	12.4	
N_2	Neoprene membrane	215	16.7	
Ar	Neoprene membrane	185	16.2	
H_2	Chloroprene membrane	150	15.3	
H_2	Silicone rubber membrane (sheet)	1.3	−3.4	
N_2	Silicone rubber membrane (sheet)	0.85	−5.0	
O_2	Silicone rubber membrane (sheet)	0.61	−6.3	18
He	Silicone rubber membrane (sheet)	0.87	−4.9	
Ar	Silicone rubber membrane (sheet)	0.83	−5.1	

TABLE III (*continued*)

Diffusion system		Entropy factor $\lambda[e^{\Delta S'/R}]^{1/2}$, Å	$\Delta S'$, e.u.	Reference
Diffusing species	Medium			
H_2	Glass membrane	4×10^{-2}	−17.1	3
He	Glass membrane	4×10^{-2}	−17.1	
Sucrose	Collodion membrane	1.1×10^{-2}	−22.2	
Lactose	Collodion membrane	4.3×10^{-2}	−16.8	
Mannitol	Collodion membrane	8.1×10^{-3}	−23.4	
Raffinose	Collodion membrane	2.4×10^{-2}	−19.1	
H_2O (sucrose) solution	Collodion membrane	1.2×10^{-2}	−21.8	
H_2O	*n*-Hexadecane liquid	2.8	−0.2	19
H_2O	Hexamethyltetracosane liquid	4.8	1.9	
H_2O	Polyethylene membrane	3.9×10^3	28.4	20
H_2O	Polypropylene membrane	25×10^3	35.8	
H_2O	Lipid bilayer membrane (oxidized cholesterol)	5.5×10^{-2}	−15.8	5
H_2O (Endosmosis)	Arbacia eggs (unfertilized)	14.4×10^3	3.16	1[d]
Propionamide	Arbacia eggs (unfertilized)	26.9×10^3	34	
Butyramide	Arbacia eggs (unfertilized)	12.1×10^4	40	
Nonelectrolyte (glycerol, glycols, thiourea)	Oxerythrocyte membrane	7.7	3.7	16b

[a] All results correspond to $\lambda = 3$ Å unless otherwise noted.
[b] Calculations correspond to $\lambda = 1$ Å.
[c] Calculations correspond to $\lambda^2 = 10^{-15}$ cm².
[d] Calculations correspond to $\lambda = 5$ Å.

plots of log P versus $(1/T)$ given in Figures 2–5. The slope of these lines which is equal to $(E_a/2.303R)$ gave the activation energy E_a required for the diffusion process. The values so derived are given in Tables I and II.

The theory of absolute reaction rates[2] has been applied to diffusion processes in membranes by several investigators.[1–3,15,16a] Following Zwolinski et al.,[1] we may write

$$P' = (\lambda^2 kT/dh)\, e^{-\Delta F'/RT} \tag{2}$$

where P' is the permeability,* k is the Boltzmann constant, d is membrane

* P', (cm/sec) is related to P (mmole/hr) by the relation

$$P' = P \times 10^{-6}/3{\cdot}6A\Delta C$$

where A is membrane area (19.6 cm²) and ΔC is the difference in the electrolyte concentration existing across the membrane (0.2 mole/l.). Introducing these values gives $P' = 7.1 \times 10^{-8} P$. The slopes of linear plots of log P vs $(1/T)$ and of log P' vs $(1/T)$ will be equal.

thickness, h is Planck constant, and λ is the average distance between equilibrium positions in the process of diffusion. $\Delta F'$ is the free energy of activation for permeability and is related by Gibbs-Helmholtz equation:

$$\Delta F' = \Delta H' - T\Delta S' \tag{3}$$

to enthalpy $\Delta H'$ and entropy $\Delta S'$ of activation for permeability. $\Delta H'$ is related to Arrhenius energy of activation E_a by the equation

$$E_a = \Delta H' + RT \tag{4}$$

As the values of d (manganese ferrocyanide membrane = 0.03556 cm; cobalt ferrocyanide = 0.03048 cm; silver ferrocyanide = 0.03810 cm; cadmium ferrocyanide = 0.02794 cm) and of the universal constants are known, values of $\Delta H'$, $\Delta S'$, and $\Delta F'$ can be calculated provided the value for λ is known. Different investigators[1-3,5,15] have used values ranging from 1 to 5 Å for λ. In this work, a value of 3 Å has been used in the calculations, and the values so derived for the different thermodynamic parameters are given in Tables I and II. For purposes of comparison, in Table III, are given the values of $\Delta S'$ determined by various investigators for a variety of systems.

The values of $\Delta S'$ (see Table III) are either positive or negative for membranes. There are a few values which are close to zero and correspond to liquid systems. According to Eyring and co-workers,[1,2] the values of $\Delta S'$ indicate the mechanism of flow; large positive $\Delta S'$ is interpreted to reflect breakage of bonds, while low values indicate that permeation has taken place without breaking bonds. The negative $\Delta S'$ values are considered to indicate either formation of covalent bond between the permeating species and the membrane material or that the permeation through the membrane may not be the rate determining step.

On the contrary, Barrer[15,17,18] has developed the concept of "zone activation" and applied it to the permeation of gases through polymer membranes. According to this zone hypothesis, a high $\Delta S'$, which has been correlated with high energy of activation for diffusion, means either the existence of a large zone of activation or the reversible loosening of more chain segments of the membrane. A low $\Delta S'$, then means either a small zone of activation or no loosening of the membrane structure on permeation. In view of these differences in the interpretation of $\Delta S'$, Shuler et al.,[3] who found negative $\Delta S'$ values for sugar permeation through collodion membranes, have stated that "it would probably be correct to interpret the small negative values of $\Delta S'$ mechanically as interstitial permeation of the membrane (minimum chain loosening) with partial immobilization in the membrane (small zone of disorder)." On the other hand, Tien and Ting,[5] who found negative $\Delta S'$ values for the permeation of water through very thin (50 Å thickness) bilayer membrane, stressed the possibility that the membrane may not be the rate-determining step. Based on additional experimental data, they came to the conclusion that the solution–membrane interface was the rate-limiting step for permeation.

The data of the present study (see Tables I and II) indicate that electrolyte permeation gives rise to negative values for $\Delta S'$, whose magnitude however depends on the value chosen for λ, the distance between equilibrium positions in the process of diffusion. The values of $\Delta S'$ for all the four membranes used in this study show similar behavior for the different electrolytes. It is in general found that as the valence of the individual ion is increased, the decrease in the value of $\Delta S'$ is increased. Since the membranes used in this study are fairly thick compared to bilayers, it is believed that the membrane and not the solution-membrane interface controlled the electrolyte permeation process. The negative values of $\Delta S'$ therefore, as suggested by Shuler et al.,[3] indicated electrolyte permeation with partial immobilization in the membrane, the partial immobility increasing in a relative manner with increase in the valence of the ions constituting the electrolyte.

The writing of this work has been supported in part by Public Health Service grant NB-08163-02. Thanks are due to Dr. S. M. F. Rahman, Head of the Chemistry Department, for providing laboratory facilities.

References

1. B. J. Zwolinski, H. Eyring, and C. E. Reese, *J. Phys. Chem.*, **53**, 1426 (1949).
2. S. Glasstone, K. J. Laidler, and H. Eyring, *The Theory of Rate Processes*, McGraw-Hill, New York, 1941, (a) p. 525; (b) p. 544.
3. K. E. Shuler, C. A. Dames, and K. J. Laidler, *J. Chem. Phys.*, **17**, 860 (1949).
4. N. Lakshminarayanaiah, *Transport Phenomena in Membranes*, Academic Press, New York, 1969, pp. 436–456.
5. H. T. Tien and H. P. Ting, *J. Colloid Interface Sci.*, **27**, 702 (1968).
6. W. U. Malik and F. A. Siddiqi, *Proc. Indian Acad. Sci.*, **A56**, 206 (1962); *J. Colloid Sci.*, **18**, 161 (1963).
7. W. U. Malik, H. Arif, and F. A. Siddiqi, *Bull. Chem. Soc. Japan*, **40**, 1746 (1967).
8. F. A. Siddiqi and S. Pratap, *J. Electroanal. Chem.*, **23**, 137 (1969).
9. A. T. Austin, E. J. Hartung, and G. M. Willis, *Trans. Faraday Soc.*, **40**, 520 (1944).
10. N. W. Rosenberg, J. H. B. George, and W. D. Potter, *J. Electrochem. Soc.*, **104**, 11 (1957).
11. G. Schulz, *Z. Anorg. Allgem. Chem.*, **301**, 97 (1959).
12. H. S. Harned and B. B. Owen, *The Physical Chemistry of Electrolyte Solutions*, 3rd ed., Reinhold, New York, 1958, p. 525.
13. R. A. Robinson and R. H. Stokes, *Electrolyte Solutions*, 2nd ed., Butterworths, London, 1959, p. 62.
14. Y. Marcus and A. S. Kertes, *Ion Exchange and Solvent Extraction of Metal Complexes*, Interscience, New York, 1969, p. 13.
15. R. M. Barrer and G. Skirrow, *J. Polym. Sci.*, **3**, 549 (1948).
16. W. D. Stein, *The Movement of Molecules across Cell Membranes*, Academic Press, New York, 1967, (a) pp. 70–89; (b) p. 89.
17. R. M. Barrer, *Trans. Faraday Soc.*, **38**, 322 (1942).
18. R. M. Barrer and H. T. Chio, in *Transport Phenomena in Polymeric Films* (*J. Polym. Sci. C*, **10**), C. A. Kumins, Ed., Interscience, New York, 1965, p. 111.
19. P. Schatzberg, in *Transport Phenomena in Polymeric Films* (*J. Polym. Sci. C*, **10**), A. Kumins, Ed., Interscience, New York, 1965, p. 87.
20. H. Yasuda and V. Stannett, *J. Polym. Sci.*, **57**, 907 (1962).

Received January 12, 1971

JOURNAL OF POLYMER SCIENCE: PART A-1 VOL. 9, 2869–2875 (1971)

Studies with Inorganic Precipitate Membranes. IV.* Evaluation of Apparent Fixed Charge on Membranes

FASIH A. SIDDIQI, N. LAKSHMINARAYANAIAH, and MOHAMMAD N. BEG, *Department of Pharmacology, University of Pennsylvania School of Medicine, Philadelphia, Pennsylvania 19104 and Department of Chemistry, Aligarh Muslim University, Aligarh, India*

Synopsis

Membrane potentials arising across four parchment-supported ferrocyanide membranes of manganese, cobalt, silver, and cadmium when they separate 1:1 electrolyte solutions of concentration C_1 and C_2 such that $C_1 = 10C_2$, have been measured. The data have been used according to the procedure prescribed by one of the theories of membrane potential due to Teorell and Meyers and Sievers to derive values for the quantity of charge present on the membranes. An alternative procedure employed by Altug and Hair has been considered and found to overestimate the value for the charge on the membranes.

Introduction

From the results discussed in Part III,[1] it is evident that parchment-supported inorganic precipitate membranes have the ability to generate potentials when they are used to separate electrolyte solutions of different concentration. This property is attributed to the presence of a net charge (negative in the case of 1:1 electrolytes and positive in the case of 2:1 or 3:1 electrolytes) on the membrane probably due to adsorption of anions or cations. The quantity of charge required to generate potentials, particularly when dilute solutions are used, is very small.[2a] This, of course, is dependent on the porosity of the membrane. If the membrane pores are too wide, any amount of charge on the membrane does little to generate good potentials. But if the membrane pores are narrow, a little charge on it can give ideal potentials according to the Nernst equation

$$E_{max} = (RT/F) \ln (a_1/a_2) \quad (1)$$

where a_1 and a_2 are the activities of the two solutions on either side of the membrane in an electrochemical cell of the type

$Hg–Hg_2Cl_2$	saturated KCl–agar	solution a_1	Membrane	solution a_2	saturated KCl–agar	$Hg_2Cl_2–Hg$

* The permeability and the charge density characteristics of parchment-supported membranes of silver chloride, silver phosphate, and silver tungstate are described in Parts I and II, see *Z. Physik. Chem.* (Frankfurt), **72**, 298,307 (1970).

E_m is the membrane potential and R, T, and F have their usual significance. In this paper the quantity of charge present on ferrocyanide membranes of manganese, cobalt, silver, and cadmium, when they are in contact with 1:1 electrolytes, is evaluated.

Experimental

The membranes were prepared as outlined in Part III.[1] The potential developed across the cell was measured by using a Pye precision vernier potentiometer (No. 7568). The concentration of solutions used in the above cell was always $C_1 = 10C_2$, where $C\gamma = a$ (γ is the activity coefficient).

Results and Discussion

The values of membrane potential measured across four ferrocyanide membranes with the use of various 1:1 electrolytes are given in Table I.

The fixed groups present in well characterized ion-exchange membranes can be easily estimated by titration. This procedure was used by Sollner et al.[3,4] to estimate the end groups and stray carboxyl groups present in the collodion material. Because of the difficulty in obtaining adequate amount of the material, Lakshminarayanaiah[5] in his studies with thin membranes of Parlodion, used two methods—the isotopic and the potentiometric—to evaluate the apparent fixed charge on the membrane material. In the present studies, the titration method proved inconvenient and very inaccurate, while the isotopic method was discarded in view of the strong ionic adsorption phenomenon exhibited by these systems. Consequently the potentiometric method was used. This method is based on the fixed charge theory of membrane potential proposed simultaneously by Teorell[6] and by Meyers and Sievers[7], the important features of which have been reviewed by Lakshminarayanaiah.[8,2b]

The membrane potential E_m in millivolts according to the theory, applicable to a highly idealized system is given by the equation (at 25°C)

$$E_m = 59.2\left[\log \frac{C_1(\sqrt{4C_2^2 + \bar{X}^2} + \bar{X})}{C_2(\sqrt{4C_1^2 + \bar{X}^2} + \bar{X})} + \bar{U}\log \frac{\sqrt{4C_1^2 + \bar{X}^2} + \overline{XU}}{\sqrt{4C_2^2 + \bar{X}^2} + \overline{XU}}\right] \tag{2}$$

where $\bar{U} = (\bar{u} - \bar{v})/(\bar{u} + \bar{v})$, $\bar{u}$ and $\bar{v}$ are the mobilities of cation and anion, respectively, in the membrane phase (overbars refer the parameter to the membrane phase). $\bar{X}$ is the charge on the membrane expressed in equivalents/liter of imbibed solution. In order to evaluate this parameter for the simple case of 1:1 electrolyte and membrane carrying a net negative charge of unity ($\bar{X} = 1$), theoretical concentration potentials E_m existing across the membrane were calculated as a function of C_2, the ratio (C_1/C_2) being kept at a constant value of 10 for different mobility ratio $(\bar{u}/\bar{v})$ and plotted as shown in Figure 1. The observed membrane potential values given in Table I for different membranes and KNO_3 electrolyte were plotted

TABLE I

Membrane potential observed in a membrane cell at 25°C

$Hg\text{-}Hg_2Cl_2$ | saturated KCl-Agar | (1:1) electrolyte solution (C_1) | Membrane | (1:1) electrolyte solution (C_2) | saturated KCl-Agar | Hg_2Cl_2-Hg (E_m in millivolts)

Membrane	Solution concn, mole/l.		E_m for 1:1 electrolytes, mV					
	C_1	C_2	KNO_3	$NaNO_3$	NH_4NO_3	KCl	NaCl	NH_4Cl
Manganese ferrocyanide	0.002	0.0002	32.5	38.5	39.0	37.0	40.0	41.5
	0.01	0.001	26.5	31.5	34.5	32.0	35.5	37.5
	0.02	0.002	20.5	26.5	29.0	18.0	22.5	28.5
	0.05	0.005	14.0	19.5	22.0	14.5	19.0	24.5
	0.10	0.01	11.5	17.5	18.5	12.0	12.5	21.5
	0.20	0.02	9.5	14.0	16.5	2.6	9.8	14.5
Cobalt ferrocyanide	0.002	0.0002	46.5	53.2		45.2	57.0	
	0.005	0.0005	45.0	47.2		43.5	42.0	
	0.01	0.001	43.1	41.5		41.5	39.5	
	0.02	0.002	36.5	32.5		35.5	30.0	
	0.05	0.005	26.0	29.0		24.2	25.0	
	0.10	0.01	25.5	27.0		22.0	23.5	
Silver ferrocyanide	0.002	0.0002	36.0	35.2				
	0.005	0.0005	34.3	34.2				
	0.01	0.001	32.8	31.5				
	0.02	0.002	30.9	27.4				
	0.05	0.005	27.3	24.4				
	0.10	0.01	22.1	24.6				
Cadmium ferrocyanide	0.002	0.0002	34.1	39.7		27.6		
	0.005	0.0005	32.8	39.4		26.3		
	0.01	0.001	32.0	35.4		25.3		
	0.02	0.002	31.9	31.9		24.5		
	0.05	0.005	30.5	31.2		22.3		
	0.10	0.01	30.3	30.0		20.4		

in the same graph as a function of $\log(1/C_2)$. The experimental curve for any given membrane was shifted horizontally and ran parallel to one of the theoretical curves. The extent of this shift gave log $\bar{X}$ and the parallel theoretical curve gave the value for $(\bar{u}/\bar{v})$. In Table II are given the values of $\bar{X}$ and $(\bar{u}/\bar{v})$ derived in this way for the different membranes and elec-

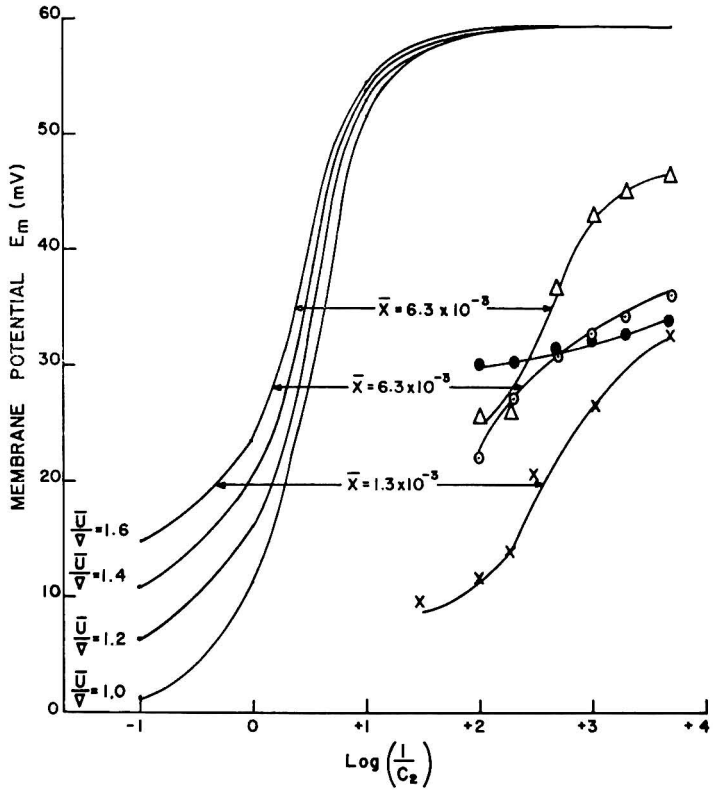

Fig. 1. Evaluation of membrane charge density $\bar{X}$ and the mobility ratio $\bar{u}/\bar{v}$ in the membrane phase. Smooth curves on the left are the theoretical concentration potentials for a cation selective membrane ($\bar{X}$ = 1), 1:1 electrolyte and constant solution concentration ratio (C_1/C_2) = 10 as a function of log ($1/C_2$). The different curves are for different mobility ratios ($\bar{u}/\bar{v}$). The experimental values of E_m for the four ferrocyanide membranes: (×) manganese, (Δ) cobalt, (⊙) silver, and (●) cadmium and KNO_3 electrolyte solution are plotted in the same graph against log ($1/C_2$). Shift of the experimental curve coinciding with one of the theoretical curves gave log $\bar{X}$, and the coinciding curve gave the mobility ratio.

trolytes. In a modification of this type of plotting, Altug and Hair[9] evaluated $\bar{X}$ for glass membranes, choosing the solution values for $\bar{u}$ and $\bar{v}$ and calculating the total membrane potential for different values for $\bar{X}$. The membrane potentials were plotted against log ($1/C_2$) giving now a family of theoretical curves for different values of $\bar{X}$ and constant value of $(\bar{u}/\bar{v})$. The theoretical curve with which the experimental curve overlapped gave

TABLE II

Values Derived for the Membrane Parameters $\bar{X}$ and $(\bar{u}/\bar{v})$

Membrane	Parameter	KNO_3	$NaNO_3$	NH_4NO_3	KCl	NaCl	NH_4Cl
Manganese ferrocyanide	$(\bar{X}) \times 10^3$, eq/l.	1.3	1.6	1.7	3.7	3.2	4.6
	$(\bar{u}/\bar{v})$	1.6	1.8	1.8	1.4	1.4	1.6
Cobalt ferrocyanide	$(\bar{X}) \times 10^3$, eq/l.	6.3	2.9		4.6	2.2	
	$(\bar{u}/\bar{v})$	1.6	1.8		1.6	1.8	
Silver ferrocyanide	$(\bar{X}) \times 10^3$ eq/l.	6.3	1.0				
	$(\bar{u}/\bar{v})$	1.6	>2.0				
Cadmium ferrocyanide	$(\bar{X}) \times 10^3$, eq/l.	2.1	3.2		0.3		
	$(\bar{u}/\bar{v})$	>2.0	>2.0		>2.0		

TABLE III

Apparent Transport Number of Counterion $(\bar{t}_+)$ and the Mobility Ratio $(\bar{u}/\bar{v})$ in the Membrane Phase Derived from Transport Number Values

KNO_3 concentration		Manganese ferrocyanide		Cobalt ferrocyanide		Silver ferrocyanide		Cadmium ferrocyanide	
C_1	C_2	$\bar{t}_+$	$\bar{u}/\bar{v}$	$\bar{t}_+$	$\bar{u}/\bar{v}$	$\bar{t}_+$	$\bar{u}/\bar{v}$	$\bar{t}_+$	$\bar{u}/\bar{v}$
0.002	0.0002	0.78	3.5	0.89	8.1	0.81	4.3	0.79	3.8
0.005	0.0005			0.88	7.3	0.79	3.8	0.78	3.5
0.01	0.001	0.73	2.7	0.87	6.7	0.78	3.5	0.77	3.4
0.02	0.002	0.66	1.9	0.82	4.6	0.76	3.3	0.77	3.4
0.05	0.005	0.63	1.7	0.75	3.0	0.73	2.7	0.76	3.3
0.10	0.01	0.61	1.6	0.70	2.3	0.69	2.2	0.76	3.3
0.20	0.02	0.59	1.4						

the value for $\bar{X}$. A similar procedure was used by Siddiqi and Pratap[10] (also see Beg and Saxena[11]) to determine the value for $\bar{X}$ for a parchment-supported silver iodide membrane. The value derived by them was 0.01 eq/l. The results of the present study given in Table II for the four parchment-supported membranes are all lower, and the values for the mobility ratio are all higher than unity, the value used by Siddiqi and Pratap for KCl solution. Since the mobility ratios in solutions of KNO_3, $NaNO_3$, NH_4NO_3, KCl, NaCl, and NH_4Cl are 1.03, 0.70, 1.03, 0.97, 0.66, and 0.95, respectively—all lower than the values given in Table II—use of this alternate procedure resorted to by Altug and Hair[9] would give values for $\bar{X}$ different from those given in Table II. A typical calculation made for KNO_3 solution and silver ferrocyanide membrane gave a value of about 2×10^{-2} eq/l. ($\bar{u}/\bar{v} = 1.03$) as opposed to a value of 6.3×10^{-3} eq/l. and ($\bar{u}/\bar{v} = 1.6$). Consequently, it is believed that the approach of Altug and Hair overestimated the value of $\bar{X}$. Further it is not realistic to use the solution mobility ratio in these calculations in view of the fact that the membrane potential data of Table I lead to values for mobility ratios for the membrane phase (KNO_3 solution) given in Table III. These values, which are all higher than 1.03 and decrease with increase in the concentration of the external solution, were derived from eqs. (3)–(5).

For 1:1 electrolyte, the counterion transport number $\bar{t}_+$ is given by[2c]

$$\bar{t}_+ = (E_m/2E_{max}) + 0.5 \tag{3}$$

$$(\bar{u}/\bar{v}) = (\bar{t}_+/\bar{t}_-) \tag{4}$$

$$\bar{t}_+ + \bar{t}_- = 1 \tag{5}$$

$\bar{t}_-$ is the coion transport number and E_{max} is given by eq. (1).

The trend noted in the data given in Table III was also observed in the case of other electrolytes and membranes. The important point emerging from this data is that the mobility ratio goes through a change, considerable in some cases, in the membrane phase. Usually in the case of cation selective membrane (value of $\bar{X}$ high) $(\bar{u}/\bar{v}) \rightarrow \infty$ in dilute solutions and only when the membrane is in equilibrium with concentrated solutions $(\bar{u}/\bar{v}) \rightarrow (u/v)_{solution}$. In view of this, the approach of Teorell and Meyer and Sievers is unreliable to use to evaluate $\bar{X}$ for ion-exchange membranes which have a high concentration of fixed groups. This point has been well illustrated by Lakshminarayanaiah[5] for phenolsulfonate membrane. It is not that unreliable for a membrane which has a low concentration of $\bar{X}$, as found in this study, due to the fact that the change in the values of the factor $(\bar{u}/\bar{v})$ is not as drastic as it is with membranes of high charge density.

The writing of this work has been supported in part by Public Health Service Grant NB-08163-02. Thanks are due to Dr. S. M. F. Rahman for providing laboratory facilities.

References

1. F. A. Siddiqi, N. Lakshminarayanaiah, and M. N. Beg, *J. Polym. Sci. A-1*, **9**, 2853 (1971).
2. N. Lakshminarayanaiah, *Transport Phenoemna in Membranes*, Academic Press, New York, 1969, (a) p. 196; (b) p. 203; (c) p. 199.
3. K. Sollner, C. W. Carr, and I. Abrams, *J. Gen. Physiol.*, **25**, 411 (1942).
4. K. Sollner and J. Anderman, *J. Gen. Physiol.*, **27**, 433 (1944).
5. N. Lakshminarayanaiah, *J. Appl. Polym. Sci.*, **10**, 1687 (1966).
6. T. Teorell, *Proc. Soc. Exptl. Biol. Med.*, **33**, 182 (1935); *Proc. Nat. Acad. Sci. U. S.*, **21**, 152 (1935).
7. K. H. Meyers and J. F. Sievers, *Helv. Chim. Acta*, **19**, 649, 665, 987 (1936).
8. N. Lakshminarayanaiah, *Chem. Rev.*, **65**, 491 (1965).
9. I. Altug and M. L. Hair, *J. Phys. Chem.*, **72**, 599 (1968).
10. F. A. Siddiqi and S. Pratap, *J. Electroanal. Chem.*, **23**, 147 (1969).
11. M. A. Beg and S. K. Saxena, *Kolloid Z-Z Polym.*, **243**, 67 (1971).

Received January 12, 1971

JOURNAL OF POLYMER SCIENCE: PART A-1 VOL. 9, 2877–2892 (1971)

Acid-Catalyzed Polymerization of 1,6-Anhydro-β-D-glucopyranose*

PAUL C. WOLLWAGE† and PAUL A. SEIB‡
The Institute of Paper Chemistry, Appleton, Wisconsin 54911

Synopsis

A number of 1,6-anhydrides were polymerized in the melt at 115°C by use of monochloroacetic acid as catalyst. In the early stages of polymerization (up to 40–50% monomer consumed), each monomer was found to disappear by a first-order rate process. The 1,6-anhydrides investigated and their relative rates of polymerization were: 1,6-anhydro-2-*O*-methyl-β-D-glucopyranose, 1.0; 1,6-anhydro-3,4-di-*O*-methyl-β-D-glucopyranose, 1.4; 1,6-anhydro-2-*O*-methyl-β-D-galactopyranose, 2.3; 1,6-anhydro-3-*O*-methyl-β-D-glucopyranose, 2.6; 1,6-anhydro-4-*O*-methyl-β-D-glucopyranose, 6.3; 1,6-anhydro-4-*O*-(β-D-glucopyranosyl)-β-D-glucopyranose, 9.0; 1,6-anhydro-β-D-galactopyranose, 17; 1,6-anhydro-β-D-glucopyranose, 37; 1,6-anhydro-β-D-mannopyranose, 91; and 1,6-anhydro-2-deoxy-β-D-arabino-hexopyranose, 240. The effect of substitution on the rate of polymerization suggests this reaction is mechanistically related to the acid hydrolysis of pyranosides. The results suggest that polymerization proceeds in two stages: (1) an initial build-up of dimer followed by (2) a slower growth to higher molecular weight material.

INTRODUCTION

The acid-catalyzed polymerization of 1,6-anhydrohexopyranoses in the melt provides a convenient method for the preparation of a variety of synthetic polysaccharides. This approach to the chemical synthesis of polysaccharides has been reviewed by Goldstein and Hullar.[1]

The optimum conditions for polymerization of 1,6-anhydro-β-D-glucopyranose (levoglucosan) (I) have been found[2] to occur in the melt at 115–120°C with monochloroacetic acid (MCA) as catalyst in a molar ratio of monomer to catalyst of 50:1. 1,6-Anhydro-β-D-galactopyranose (levogalactosan)[3] and 1,6-anhydro-β-D-mannopyranose (levomannosan)[1] have also been polymerized to give a galactan and mannan, respectively, under conditions used for the polymerization of I.

In their work on the mechanism of polymerization of 1,6-anhydrohexopyranoses, Schuerch and co-workers observed that 1,6-anhydro-2-*O*-methyl-β-D-galactopyranose (2-methyllevogalactosan) was very resistant

* Presented in part at the157th National Meeting of the American Chemical Society, Minneapolis, Minnesota, April 1969.

† Present address: St. Regis Technical Center, West Nyack, New York 10994.

‡ Present address: Department of Grain Science and Industry, Kansas State University, Manhattan, Kansas 66502.

to polymerization.[3] Similarly, trisubstituted derivatives of I, such as the trinitrate, the trimethanesulfonate, the tri-*p*-tolylsulfonate, the trimethyl ether, and the triacetate failed to polymerize with the use of several catalysts.[4] The unreactivity of 2-methyllevogalactosan and the trisubstituted derivatives of I led Schuerch and co-workers to postulate[2,3] that "some intermediate related structurally to 1,2-anhydroglucopyranose" was necessary for polymerization to occur. These workers suggested that when the reactive 1,2-anhydride forms, it rapidly reacts with a free hydroxyl group to give a glycosidic bond; however, blocking the 2-hydroxyl greatly decreases the rate of polymerization by preventing the formation of the reactive intermediate.

Another polymerization mechanism, which is similar to the acid-hydrolysis of glucopyranosides,[5] was postulated by Goldstein and Hullar.[1] Ring opening of the protonated molecule, which is aided by the 2-hydroxyl group in an undefined manner, gives a carbonium-oxonium ion that can react in three ways: (a) the ion can return to the protonated I, (b) the ion can react with a free hydroxyl group on another monomer molecule (ROH) to

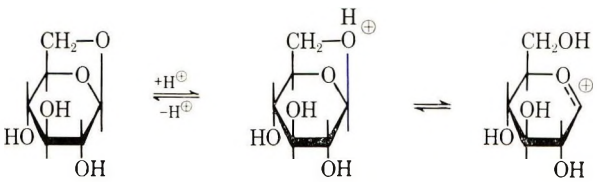

form a glycosidic bond and regenerate the protic catalyst, and (c) the carbonium-oxonium ion can react with the oxygen atom of the 1,6-anhydride

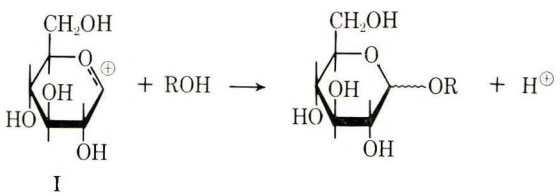

I

bridge of another monomer molecule to form a (1 → 6)-linkage and regenerate the ion directly. A similar reaction has been proposed for the polymerization of cyclic ethers,[6] which in the presence of acids, are believed to

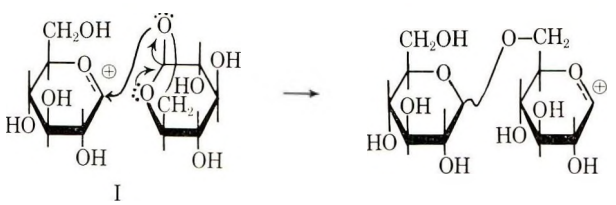

I

react via a trialkyoxonium ion mechanism.

Results and Discussion

In order better to understand the acid-catalyzed polymerization mechanism of I and to clarify the importance of the 2-hydroxyl group in the polymerization reaction, we have investigated the polymerization of a number of 1,6-anhydrides.

In this work the 1,6-anhydrides were heated at 115°C in sealed glass tubes with a molar ratio of monomer to MCA of 54:1 to 51:1. The disappearance of each monomer was followed by trimethylsilylation of the reaction mixture and quantitative analysis of the monomer's trimethylsilyl ether by gas-liquid chromatography (GLC).

In Figure 1 the weight fraction of unreacted monomer (F_M) for I is plotted against time, along with a semilogarithmic plot of the data. Similar plots for the polymerization of 1,6-anhydro-2-*O*-methyl-β-D-glucopyranose (2-methyllevoglucosan) are presented in Figure 2. These plots are typical for the polymerization of the 1,6-anhydrides studied. The remaining monomers investigated were: 1,6-anhydro-2-deoxy-β-D-arabino-hexopyranose (2-deoxylevoglucosan), 1,6-anhydro-β-D-mannopyranose (levomannosan), 1,6-anhydro-β-D-galactopyranose (levogalactosan), 1,6-anhydro-4-*O*-(β-D-glucopyranosyl)-β-D-glucopyranose (cellobiosan), 1,6-anhydro-4-*O*-methyl-β-D-glucopyranose (4-methyllevoglucosan), 1,6-anhydro-3-*O*-methyl-β-D-glucopyranose (3-methyllevoglucosan), 1,6-anhydro-2-*O*-methyl-β-D-galactopyranose (2-methyllevogalactosan), and 1,6-anhydro-3,-4-di-*O*-methyl-β-D-glucopyranose (3,4-dimethyllevoglucosan).

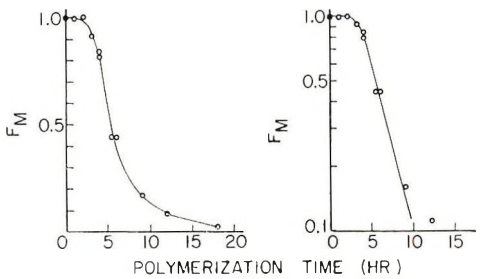

Fig. 1. Polymerization of levoglucosan (I).

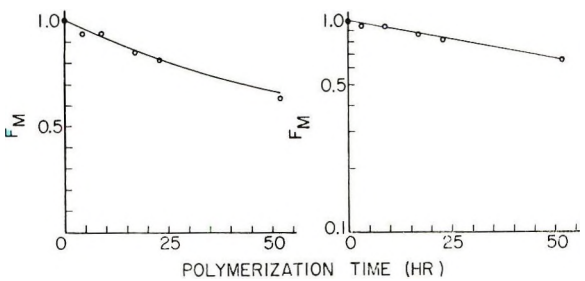

Fig. 2. Polymerization of 2-methyllevoglucosan.

The disappearance of a monomer followed one of two patterns as shown in Figures 1 and 2. One type of disappearance pattern is typified by the behavior of I. During the early stages of heating at 115°C, I disappears very slowly because of the heterogeneity of the reaction mixture. This heterogeneity results from the high melting point of I (mp 179–180°C). After a homogeneous melt is obtained, the major portion of monomer is consumed by a pseudo, first-order reaction. Levomannosan (mp 210–211°C) and levogalactosan (mp 223–224°C) behave the same as I. The remaining 1,6-anhydrides all had melting points below 115°C with the exception of 2-deoxylevoglucosan (mp 159–160°C), and their behavior during polymerization is represented by that of 2-methyllevoglucosan (Figure 2). The monomers with melting points less than 115°C formed a homogeneous melt almost immediately and, thus, no induction period appears in the plots. 2-Deoxylevoglucosan reacted so rapidly that it was not possible to observe an induction period.

With prolonged heating, the rate of disappearance of a monomer begins to deviate from first-order kinetics. This effect was observed for several 1,6-anhydrides whenever the monomer was heated beyond one half-life of the disappearance of the monomer. The polymerization reaction decelerates for two reasons. First, from loss of MCA, which becomes important at long polymerization times. The loss of MCA, which probably occurs through self-catalyzed esterification of sugar hydroxyl groups,[7] was followed titrimetrically during the polymerization of I. When 57% of I had disappeared, only 5% of MCA was consumed, whereas, at 98% disappearance of I 42% of MCA was consumed. The second reason for the deceleration of the polymerization reaction is due to the decrease in reactivity of the 1,6-anhydro bridge with substitution on the ring hydroxyls. This factor will be discussed subsequently.

To determine if polymerization had occurred upon heating the various 1,6-anhydrides with MCA, polymerizations were examined chromatographically after approximately one half-life ($F_M = 0.5$) had elapsed. At this time all reaction products were amber-colored glasses. Thin-layer and paper chromatography showed the presence of oligomers, but no products with a mobility higher than the original monomer were detected. Compounds of high mobility would be expected if the 1,6-anhydride is disappearing by dehydration as well as polymerization.

The principal reaction products ($R_G = 0.7$–0.8) formed from I at $F_M = 0.5$ were in the same zone of the paper chromatogram as cellobiosan ($R_G = 0.7$) and 1,6-anhydro-4-*O*-(α-D-glucopyranosyl)-β-D-glucopyranose (maltosan) ($R_G = 0.7$). Smaller amounts of products were detected near the starting line ($R_G = 0$–0.35). Analysis by GLC of the trimethylsilylated reaction mixture confirmed the presence of cellobiosan and maltosan. The reactions of the other 1,6-anhydrides gave only polymeric products as evidenced by paper, thin-layer, and gas-liquid chromatography.

Polymers from the slowest and fastest reacting monomers, respectively, were isolated and partially characterized. The slowest reacting monomer,

2-methyllevoglucosan, was heated 16 days at 115°C, and 36% of the product was precipitated from a 1.2% (w/v) aqueous solution by the addition of five volumes of acetone. The polymeric material had a number-average molecular weight of 1030 as determined by vapor-pressure osmometry. The specific rotation of the polymer was +79.2°, indicating the presence of both α- and β-D-glycosidic linkages.[1] The synthetic 2-methyl-D-glucan was hydrolyzed to give a syrup which contained only 2-*O*-methyl-D-glucopyranose as evidenced by paper chromatography. The fastest reacting monomer, 2-deoxylevoglucosan, was heated for 4 hr at 115°C and gave a 57% yield of polymeric material which was precipitated from an 0.43% (w/v) aqueous solution by the addition of three volumes of acetone. Hydrolysis of the polymeric substance followed by acetylation of the polymer hydrolyzate gave crystalline 1,3,4,6-tetra-*O*-acetyl-2-deoxy-α-D-arabino-hexopyranose.

Since all monomers in a homogeneous melt containing MCA disappear initially by a first-order process to give compounds of higher molecular weight, a comparison of the rates of disappearance gives a measure of each monomer's tendency to form a polysaccharide. The pseudo first-order rate constants of the model compounds have been determined graphically from the slopes of the linear portion of the semilogarithmic plots. These rate constants are estimated to be accurate to within a factor of two and are given in Table I along with the relative rates with reference to the slowest reacting monomer, 2-methyllevoglucosan. It should be noted that in the comparison of the polymerization rates, it has been assumed that the densities of all monomer melts are identical.

The data in Table I may be used to postulate a mechanism for the polymerization of I. As proposed by Goldstein and Hullar,[1] the first step (Fig. 3) in the reaction mechanism is a rapid, equilibrium-controlled, protonation of I at the oxygen atom between the C-1 and C-6 atoms to form the conjugate acid. The conjugate acid then undergoes heterolytic cleav-

TABLE I
Pseudo First-Order Rate Constants for the Acid-Catalyzed Polymerization of 1,6-Anhydrides

1,6-Anhydride	Pseudo rate constant k, hr^{-1}	Relative rate[a]
2-Deoxylevoglocosan	2.1	240
Levomannosan	0.78	91
Levoglucosan	0.32	37
Levogalactosan	0.15	17
Cellobiosan	0.077	9.0
4-Methyllevoglucosan	0.054	6.3
3-Methyllevoglucosan	0.022	2.6
2-Methyllevogalactosan	0.020	2.3
3,4-Dimethyllevoglucosan	0.012	1.4
2-Methyllevoglucosan	0.0086	1.0

[a] Rate with respect to 2-methyllevoglucosan.

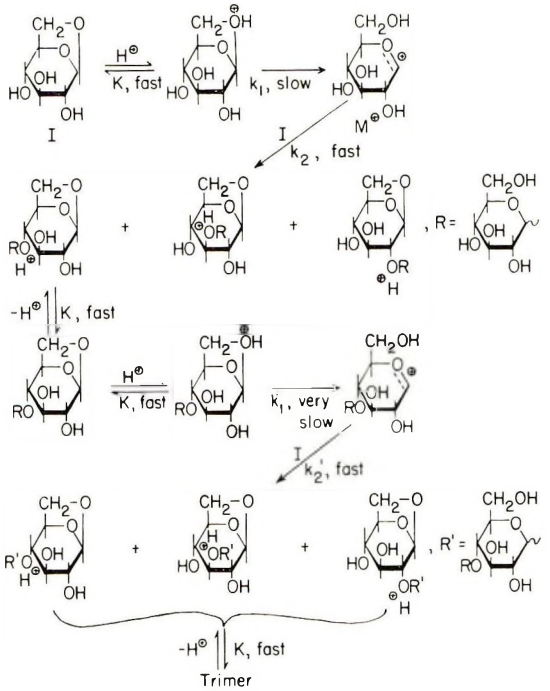

Fig. 3. Proposed mechanism for the acid-catalyzed polymerization of levoglucosan (I).

age, probably without anchimeric assistance by the 2-hydroxyl group, in the rate-controlling step to give a carbonium-oxonium ion intermediate ($M^{\oplus}$) which most likely exists in the half-chair conformation. This intermediate reacts rapidly with a hydroxyl group to produce a dimer along with the regeneration of the protic catalyst. Dimers are the only product at the onset of polymerization, since only monomer molecules are present to provide a hydroxyl group. However, as polymerization proceeds, oligomers will provide an increasingly greater proportion of hydroxyl groups for $M^{\oplus}$ to react with. The oligomers, which contain a 1,6-anhydro bridge, will slowly begin to undergo a series of reactions analogous to the monomer; thus, polymerization will continue.

The observance of pseudo first-order kinetics for the disappearance of the major portion of I and the other 1,6-anhydrides can be explained by one of two limiting cases. In the first case, the reactivity of the 1,6-anhydro bridge remains constant and is independent of the polymer chain length.* In the second case, the 1,6-anhydro bridge of a dimer or higher molecular weight oligomer is much less reactive than the 1,6-anhydro bridge of the monomer. For both cases, monomer disappears initially to give only

* Flory[8] established that the rate of esterification of aliphatic acids is independent of chain length. However, this axion may not hold in polymerizations where steric or conformational factors change with increasing molecular weight.

dimers. However, with a build-up of the dimer fraction in the first case, monomer will also begin to disappear by its hydroxyl groups reacting by way of opening of the 1,6-anhydro bridge on dimer molecules; such a route for the disappearance of monomer molecules would be negligible in the second case where k_1' is very much smaller than k_1 (Fig. 3).

The data in Table I clearly show that increasing substitution on a 1,6-anhydride decreases the rate of monomer disappearance. In other words, the polymerization of 1,6-anhydrohexopyranoses proceeds by the second limiting case defined in the preceding paragraph, where $k_1' \ll k_1$. The rate of disappearance of monomer then is dependent, to a first approximation, on the concentration of protonated monomer $[MH^+]$ according to the following expression:

$$dM/dt = -2 \cdot k_1 [MH^+] \tag{1}$$

where dM/dt denotes the rate of monomer disappearance (mole/l.-hr), k_1 is the rate constant for the rate-controlling step (hr^{-1}), and $[MH^+]$ denotes the concentration of conjugate acid of monomer (mole/l.). The factor two in eq. (1) arises because reaction of one conjugate acid molecule consumes two monomer molecules. Since the amount of conjugate acid is controlled by a rapid, equilibrium-controlled protonation of monomer, the concentration of conjugate acid $[MH^+]$ is equal to the product of $K[H^+][M]$, where K is the equilibrium constant (l./mole, $[H^+]$ is the concentration of acid (mole/l.) and $[M]$ is the monomer concentration (mole/l.). Substitution of the product $K[H^+][M]$ for $[MH^+]$ in eq. (1), and replacement of the constants K, k, $[H^+]$, and 2 with k_{pseudo}, we obtain

$$dM/dt = -k_{pseudo}[M] \tag{2}$$

where $k_{pseudo} = 2kK[H^+]$. Since the reactivity of the 1,6-anhydro bridge has been shown to decrease with substitution on the hydroxyl groups of the 1,6-anhydride, eq. (2) must eventually lose its validity as F_M goes to a smaller and smaller value. At very small F_M values, $M^{\oplus}$ can react only with the hydroxyl groups of oligomers and hence the factor of two in eq (1) will become unity.

Although the two possible explanations for the first-order disappearance of monomer could not be distinguished by the shapes of the curves in the pseudo, first-order plots presented in this work,* evidence indicates that I disappears in a manner in which oligomers undergo ring-opening of their 1,6-anhydro bridges much more slowly than for I. Direct evidence for this assertion is provided by the fact that cellobiosan reacts at approximately one-fourth the rate of I (Table I). Methyl substitution on the 4-

* In principle, the two cases should be distinguishable kinetically. For the case of constant reactivity, the plot of ln F_M versus time should be linear for all values of F_M.[8] For the other case, the plot should be linear initially but eventually becomes curvilinear. Although a discontinuity was found in the plots presented in Figure 1, another factor, catalyst consumption at longer reaction times was also operating to slow down the reaction.

hydroxyl of I is almost equally detrimental as glucopyranosyl substitution to the reactivity of the 1,6-anhydro bridge. Methylation of the 4-hydroxyl is approximately one-third as detrimental to the reactivity of the 1,6-anhydro bridge as substitution on the 2- or 3-hydroxyls (Table I). Since (1 → 3)-linked and especially (1 → 2)-linked dimers would be expected[1] to constitute at least one-half of the 1,6-anhydrodisaccharides formed in the polymerization of I, the rate of dimer disappearance would be less than the rate of disappearance of cellobiosan. The slower rate of polymerization of dimer (and oligomer) over monomer permits an initial build-up of oligomer and, thus, helps to explain the rather low molecular weight of isolated D-glucans.[9] This polymerization pathway is similar to that postulated by Abe and Prins,[9] who after studying molecular weight distributions of D-glucans obtained by the acid-catalyzed polymerization of I, concluded the first step of the reaction is the rapid dimerization of I followed by a slower reaction of dimers to give polymeric material.

This decrease in the reactivity of ether derivatives of I (1/4 to 1/37 as reactive as I) is not due to inductive or field effects since a methoxyl and hydroxyl group have identical Charton polar-substituent constants.[10] The phenomenon may be explained as follows. The rate-controlling step of the reaction is the heterolysis of the 1,6-anhydride's conjugate acid to form a carbonium-oxonium ion ($M^{\oplus}$) in a half-chair conformation. The conversion of the 1-C chair to the half-chair conformation requires rotation of the C-2 to C-3 and C-4 to C-5 bonds. An increase in the size of the groups attached to these positions will increase the hindrance to this conformational change[11] and will raise the energy of the transition state. On the other hand, the ground state energy of the methyl ether derivatives of I is probably close to that of I, since the conformational energies of a hydroxyl and an *O*-alkyl group are practically identical.[12,13] The net effect is a larger energy requirement to the half-chair transition state for the ether derivatives of I, and therefore, these derivatives react more slowly than I. Similar reasoning would explain the sluggish reactivity of 2-methyllevoglactosan.

This explanation of the polymerization of I and its derivatives is similar to the hypothesis of Edward,[11] who first used this argument to account for differences in the rates of acid hydrolyses of pyranosides. The hypothesis of Edward probably applies to the polymerization of I since the mechanism of the acid hydrolysis of pyranosides is the same as shown in Figure 3, except $M^{\oplus}$ adds a molecule of water instead of monomer. As might be expected, the methyl ethers of methyl D-glucopyranosides hydrolyze more slowly than the parent compounds. De and Timell[14] found that the 2-, 3-, 4-, and 6-*O*-methyl derivatives of methyl β-D-glucopyranosides are hydrolyzed somewhat more slowly than the unsubstituted compound (Table II). These workers attribute these decreases to an increased hindrance when these molecules assume their transition state. The rotational effects should be additives; thus, the permethylated glucopyranosides hydrolyze even more slowly relative to the unsubstituted glucopyranosides[15] than do the

TABLE II
Pseudo First-Order Rate Constants for the Acid-Hydrolysis of Methyl β-D-Glucopyranoside and Several of Its Ether Derivatives

Pyranoside	Pseudo rate constant, $\times 10^{-2}$, hr^{-1}
Methyl β-D-glucoside[a]	3.75
2-Methyl ether	3.13
3-Methyl ether	3.39
4-Methyl ether	2.98
6-Methyl ether	2.33
Methyl β-D-glucoside[b]	6.9
Tetramethyl ether	2.3
Levoglucosan[c]	4.14
Trimethyl ether	0.6

[a] Data of De and Timell.[14] In 0.5*M* sulfuric acid solution at 70°C, 0.025*M* glucopyranoside solution, polarimetry.

[b] Data of Haworth and Hirst.[15] In 0.01*M* hydrochloric acid at 95–100°C, polarimetry.

[c] Data of Freudenberg, et al.[16] In 0.5*M* sulfuric acid at 70°C, 0.2*M* glucopyranoside solution, polarimetry.

monomethyl derivatives. The trimethyl ether of I is also hydrolyzed more slowly than I[16] (Table II).

A reduction in eclipsing interaction at the C-2 to C-3 bond has been used to explain, in part, the enhanced acid-lability of methyl 2-deoxy-α-D-arabinohexopyranoside and methyl 3-deoxy-α-D-ribohexopyranoside. It has been estimated that rotational effects account for a factor of 20 in an overall difference of 2000 between the rates of hydrolysis of methyl 2-deoxy-α-D-arabinohexopyranoside and methyl α-D-glucopyranoside.[17] This same factor apparently explains why 2-deoxylevoglucosan polymerizes 6.5 times faster than levoglucosan.

Formation of the postulated 1,2-anhydro intermediate[2,3] in the polymerization mechanism for I seems unlikely for three reasons. First, the ability of 2-deoxylevoglucosan to form polymer indicates that such an intermediate is not required, provided anchimeric assistance by a hydroxyl group can be ruled out (see below). Second, formation of a 1,2-anhydro intermediate from I should lead to differences in the stereochemistry of the glycosidic linkages formed during the polymerization of I and its 2-methyl ether. The heterolyses of the conjugate acid of I and its 2-methyl ether are the rate-limiting steps of the polymerization reactions. The reactive intermediate formed from I may be partly or totally converted to a protonated 1,2-anhydro intermediate; however, this conversion would occur after the rate-controlling step. Even if a hydroxyl group on the C-2 atom leads eventually to a 1,2-anhydro intermediate and a methoxyl group blocks 1,2-anhydro formation, there should be little difference in the rates of reaction of I and its 2-methyl ether. Since anomerization does not occur under the conditions of polymerization,[2] the optical rotations of the soluble polymer can yield useful information on the structure of the reacting inter-

mediate. If I reacts through a 1,2-anhydro intermediate and its 2-methyl ether does not, the D-glucan should contain more β-linkages than the 2-*O*-methyl-D-glucan, particularly since Brigl's anhydride, 3,4,6-tri-*O*-acetyl-1, 2-anhydro-α-D-glucopyranose, has been shown to react with alcohols in the presence of trace amount of acids to give a predominance of β-D-glycopyranosides.[18,19] However, the specific rotation of the D-glucan ($[\alpha]_D$ = +91 ± 5°)[2] indicates that it contains approximately the same or fewer β-linkages than the 2-*O*-methyl-D-glucan ($[\alpha]_D$ = +79.2°) isolated in this laboratory.

Finally, anchimeric assistance by a hydroxyl and not a methoxyl in the heterolytic cleavage of the conjugate acid is probably not the reason why 2-substituted 1,6-anhydrides polymerize slowly. As seen in Table I, the 3-methyl and the 3,4-dimethyl ethers of I react almost as slowly as the 2-methyl ether even though the former derivatives contain free hydroxyls at the C-2 atom. Furthermore, the more rapid polymerization of levomannosan compared to I is difficult to rationalize stereochemically if anchimeric assistance by a 2-hydroxyl group is important in the formation of the transition state. The 2-hydroxyl group in levomannosan cannot assume a 1,2-*trans* diaxial orientation with the leaving group (0-6) on the C-1 atom. Therefore, assistance probably does not occur in levomannosan, yet it polymerizes more rapidly than I, wherein the assisting and leaving groups are locked in an optimal position for assistance.

In conclusion, in the melt (115°C) polymerization of 1,6-anhydro-β-D-glucopyranose with monochloracetic acid as catalyst it was found that replacement of any of the hydroxyl groups in 1,6-anhydro-β-D-glucopyranose by a methoxyl group or by a glucopyranosyl group at the C-4 atom decreases the rate of disappearance of the 1,6-anhydride whereas replacement of the 2-hydroxyl group by a hydrogen atom results in acceleration of the polymerization rate. This effect of hydroxyl group substitution or removal on the rate of polymerization suggests the reaction is mechanistically related to the acid-catalyzed hydrolysis of pyranosides. The polymerization of 1,6-anhydro-β-D-glucopyranose proceeds in two states:[9] (1) an initial build-up of dimer, followed by (2) a slower growth to higher molecular weight material. The polymerization data for several 1,6-anhydrides; namely, 1,6-anhydro-2-deoxy-β-D-arabino-hexopyranose, 1,6-anhydro-2-*O*-methyl-β-D-glucopyranose, and 1,6-anhydro-β-D-mannopyranose, do not support the hypothesis[2,3] that a 1,2-anhydro intermediate is required in the polymerization mechanism of 1,6-anhydro-β-D-glucopyranose.

EXPERIMENTAL

Compound Preparation

1,6-Anhydro-β-D-*arabino*-β-D-hexopyranose (2-Deoxylevoglucosan). This product was prepared as described by Seib;[20] mp 159–160°C.

1,6-Anhydro-β-D-mannopyranose (Levomannosan). The procedure of Wollwage and Seib was employed to prepare levomannosan;[21] mp 210.5–

211.5°C, $[\alpha]_D^{26}$ − 129° (*c* = 1.70, water); lit.[22] mp 210–211°C, $[\alpha]_D$ − 127.6° (*c* = 1.50, water).

1,6-Anhydro-β-D-glucopyranose (I) (Levoglucosan). The method of Coleman[23] was used to synthesize I, mp 179°C, $[\alpha]_D^{25}$ − 66.0° (*c* = 3.40, water); lit.[24] mp 179–180°, $[\alpha]_D$ − 66.2° (*c* = 2.0, water).

1,6-Anhydro-β-D-galactopyranose (Levogalactosan). This compound was obtained by the procedure of Gasman and Johnson,[25] mp 220–223°C; lit.[1] mp 223–224°C.

1,6-Anhydro-4-*O*-(β-D-glucopyranosyl)-β-D-glucopyranose (Cellobiosan). Cellobiosan was synthesized by the method of Montgomery et al.;[26] mp 98–102°C (hygroscopic), $[\alpha]_D^{25}$ − 74° (*c* = 2.08, water); lit.[26] mp 122°C (semicrystalline hygroscopic material), $[\alpha]_D^{25}$ − 75.0° (*c* = 2, water).

Anal. Calcd for $C_{12}H_{20}O_{10}$; C, 44.45%; H, 6.22%. Found: C, 44.67%; H, 6.31%.

1,6-Anhydro-4-*O*-methyl-β-D-glucopyranose (4-Methyllevoglucosan). This compound was previously obtained by the authors,[21] mp 67–68°C, $[\alpha]_D^{25}$ − 65.4° (*c* = 3.21, acetone).

1,6-Anhydro-3-*O*-methyl-β-D-glucopyranose (3-Methyllevoglucosan). The second method described by Reeves[27] was employed to obtain 3-methyllevoglucosan, mp 65–67°C, $[\alpha]_D^{30}$ − 59.0° (*c* = 1.00, acetone); lit.[27] mp 63–64°, $[\alpha]_D^{25}$ − 64.5 (*c* = 0.52, acetone).

1,6-Anhydro-2-*O*-methyl-β-D-galactopyranose (2-Methyllevogalactosan). The method of Gasman and Johnson[25] was used to prepare this compound, mp 114–116°C; lit.[2] mp 115–116°C.

1,6-Anhydro-3,4-di-*O*-methyl-β-D-glucopyranose (3,4-Dimethyllevoglucosan). This product was prepared as previously described;[21] mp 41–43°C, $[\alpha]_D^{28}$ −49.7° (*c* = 2.11, acetone); lit.[28] $[\alpha]_D^{24}$ −44 ± 2° (*c* = 1.36, methanol).

1,6-Anhydro-2-*O*-methyl-β-D-glucopyranose (2-Methyllevoglucosan). This compound had mp 93–94°, $[\alpha]_D^{25}$ −72.7° (*c* = 1.45, acetone), in agreement with the literature[29] value.

Polymerization

Prior to polymerization, monomers were finely powdered and dried to constant weight. Polymerizations were performed in pyrex tubes, of 8 mm diameter having a length of approximately 15 cm and sealed at one end. Monomer, 16–30 mg (40–60 mg I), was introduced through a glass funnel which extended to the bottom of the tube. The catalyst, monochloroacetic acid (MCA), which was purified by sublimation (mp 61–64°C) was dissolved in anhydrous benzene and an aliquot of solution delivered into the polymerization tube with a Hamilton (1–10 μl) syringe (no. 701, ±1% accuracy and precision, Hamilton Co., Whittier, Calif.). The benzene was evaporated in 1 hr at room temperature under reduced pressure (≈93 mm Hg). Titration, using standardized sodium hydroxide solution, of the tube contents after benzene removal showed that 95–97% of the

catalyst remained. The open end of the polymerization tube was sealed over a flame and the tube placed in an oil bath maintained at 115 ± 1°C.

Gas-Liquid Chromatography

After polymerization, the reaction mixture was dissolved in water containing a known amount of methyl α-D-mannopyranoside, which was used as an internal standard for the GLC determination of monomer. *O*-Hydroxymethyl-phenyl-β-D-glucopyranoside (salicin) was used as internal standard for cellobiosan. The polymerizate and internal standard mixture were first trimethylsilylated with the commercial silylating agent, TRI-SIL (Pierce Chemical Company, Rockford, Ill.) before injection into the gas-chromatograph.

All analyses were performed on an Aerograph Hy-Fi gas chromatograph (Model A-600-B) equipped with a hydrogen flame, ionization detector. The column (5 ft) employed was housed in $^1/_8$-in. stainless steel tubing and contained 5 wt-% SE-30 on 60/80 mesh Chromosorb W. Dry nitrogen was used as the carrier gas at a pressure of 11–12 lb; the hydrogen flow rate to the detector flame was approximately 30 ml/mm.

The silylated mixture of 1–3 μl was injected into the gas chromatograph three times to give three chromatograms. The fraction of monomer remaining in the polymerization reaction was calculated by using the equation

$$F_M = f(V_{IS})(C_{IS})(1/W_{M_0})(A_M/A_{IS}) \quad (3)$$

where F_M is the weight fraction of monomer in the reaction mixture, f is a response factor for internal standard relative to monomer, V_{IS} is the volume

TABLE III
Retention Times and Response Factors for Trimethylsilylated 1,6-Anhydrides

1,6-Anhydride	Retention time, min[a]	Response factor[b]
Levoglucosan	5.2	1.04 ± 0.01
Levomannosan	4.6	1.01 ± 0.02
Levogalactosan	4.3	1.05 ± 0.01
2-Deoxylevoglucosan[c]	2.8	1.13 ± 0.01
2-Methyllevoglucosan	3.5	1.37 ± 0.01
3-Methyllevoglucosan	3.2	1.32 ± 0.02
4-Methyllevoglucosan	3.7	1.40 ± 0.01
2-Methyllevogalactosan	3.2	1.33 ± 0.01
3,4-Dimethyllevoglucosan	2.4	1.45 ± 0.01
Methyl α-D-mannoside	7.6, 12.0[c]	—
Cellobiosan[d]	6.5	1.23 ± 0.01
Salicin[d]	4.6	—

[a] Column temperature 170–175°C; injection port temperature 250°C.

[b] Response factors were determined at three levels of monomer concentration; these were approximately 25, 50 and 75 wt-%.

[c] Column temperature 164–167°C; injection port temperature 250°C.

[d] Column temperature 260–265°C; injection port temperature, 325°C.

of internal standard solution (ml), C_{IS} is the concentration of internal standard solution, W_{M_0} is the weight of initial monomer, and $\langle A_M/A_{IS} \rangle$ the ratio of areas, average gas chromatographic responses, for monomer and internal standard. The value of f is calculated from gas chromatographic responses of monomer and internal standard in mixtures of known composition. In Table III the retention times and the response factors are given for all monomers.

The area under monomer and the internal standard curves were integrated manually with a Technicon integrator/calculator (Model AAG). Mixtures of monomer and catalyst which were not heated to 115°C were used as controls to check the reliability of the GLC determinations in each polymerization run. The reproducibility in two separate polymerization runs on levoglucosan was found to be ±3% up to 6 hr reaction time (F_M = 0.45).

Catalyst Loss

A small loss of MCA occurred (3–5%) on evaporation of the benzene prior to polymerization, while after prolonged polymerization time, a major loss was observed. To determine how much catalyst was lost at these times, reaction mixtures were dissolved in water, and the solutions titrated with standard sodium hydroxide solution. The endpoints were determined[30] with a Beckman glass electrode pH meter (Model H-2). In Table IV the results for catalyst loss are presented.

TABLE IV
Loss of MCA Catalyst During Evaporation of Benzene and During Polymerization of Levoglucosan

Polymerization time, hr	F_M	MCA Loss, %
—[a]	1.00	5
—[a]	1.00	3
3.0	0.92	6
4.0	0.82	4
4.7	0.68	6
6.1	0.43	9
16.0	0.02	43
16.0	0.02	47
16.0	0.02	46

[a] Loss MCA during benzene removal from levoglucosan.

Polymer Detection

The polymerizates of all 1,6-anhydrides having a F_M of 0.5 were qualitatively examined by paper, thin-layer, and gas-liquid chromatography. All polymerizates gave spots at the origin and spots for oligomers. Paper chromatograms were developed for 8 days in a mixture of butyl acetate, pyridine, ethanol, and water (8:2:2:1) by the descending method. Detec-

tion of the compounds on the chromatogram was accomplished with silver nitrate by using the dip procedure.[31] Thin-layer plates (200 × 100 mm) coated to a thickness of 1 mm with silica gel G (Brinkmann Instruments) were developed twice with a mixture of ethyl acetate and methanol (2:1). The components of the polymerizate were visualized by spraying the plate with a 10% solution of sulfuric acid in methanol followed by charring on a hot plate.

Large-Scale Polymerization of 2-Methyllevoglucosan for $\bar{M}_n$ and $[\alpha]_D$ Determination

2-Methyllevoglucosan (0.320 g) was heated for 16 days at 115°C with a mole ratio of monomer to MCA of 52:1, and the dark amber-colored product was dissolved in approximately 10 ml of water. When acetone (50 ml) was added to the aqueous solution, an amber-colored substance precipitated. After centrifugation, the precipitate was washed with acetone (50 ml) on the centrifuge. Thin-layer chromatography (developer ethyl acetate–methanol 2:1) showed that only polymeric material was present (all material remained at the starting line). The precipitated polymer was dissolved in several milliliters of water and the solution lyophilized. The yield of 2-methyl-D-glucan was 0.116 g (36%), $[\alpha]_D^{25}$ + 79.2° (c = 1.91, water), $\bar{M}_n$ 1030 (by vapor pressure osmometry, ArRo Laboratories, Inc., Joliet, Illinois).

Acid Hydrolysis of 2-*O*-Methyl-D-Glucan and 2-Deoxy-D-Glucan

2-*O*-Methyl-D-Glucan. 2-Methyllevoglucosan (0.0456 g) was heated for 12 days at 115°C with MCA as catalyst at a mole ratio of monomer to catalyst of 51:1. The polymerizate was dissolved in distilled water (15 ml) and the solution dialyzed in 3 liters of distilled water for 2 hr. The dialyzate was evaporated to dryness to give a material weighing 0.028 g. Thin-layer chromatography of this material [developer, ethyl acetate–methanol (2:1)] showed dialysis was incomplete in removing all the monomer from the polymerizate. The material was further fractionated by dissolving it in methanol (1 ml) and adding acetone (20 ml) to precipitate a light amber-colored substance which was removed by centrifugation. The precipitate was washed with acetone (20 ml) on the centrifuge and was dried; yield 0.006 g (13%). Thin-layer chromatography showed only high molecular weight material which remained on the starting line.

The precipitated polymer was hydrolyzed by refluxing in 0.2M sulfuric acid (20 ml) for 72 hr. The hydrolyzate was cooled to room temperature, deionized by passage through Amberlite MB-3 (H^+, OH^-) resin, and the effluent concentrated to sirup. The major component indicated by paper chromatography was 2-*O*-methyl-D-glucopyranose (R_G 1.8) along with four minor components. Chromatograms were developed in a mixture of ethyl acetate, pyridine, and water (8:2:1) and compounds detected by silver nitrate–sodium hydroxide–sodium thiosulfate.[31]

2-Deoxy-D-Glucan. 2-Deoxylevoglucosan (0.0228 g), was heated for 4 hr at 115° with MCA present in the mole ratio of monomer to catalyst, 52:1. The product was dissolved in 3 ml of hot (80°C) water and the polymer was precipitated by the addition of acetone (10 ml). The precipitated substance was separated by centrifugation, twice washed with acetone (20 ml) on the centrifuge, and dried; yield 0.013 g (57%). Thin-layer chromatography of this substance (developer, ethyl acetate–methanol 2:1) showed only polymeric material which remained on the starting line.

The polymer was hydrolyzed in 0.5*M* sulfuric acid (10 ml) at room temperature for 2 hr followed by $^1/_2$ hr at 50°. The hydrolyzate was diluted with water (10 ml), neutralized by passage through Amberlite MB-3 (H^+, OH^-) resin, and the effluent evaporated to a sirup. The major component identified by TLC [developer, ethyl acetate–methanol (2:1)] was 2-deoxy-D-arabino-hexose (R_G 2.0).

The polymer hydrolyzate was acetylatedin the usual manner using pyridine (0.2 ml) and acetic anhydride (0.16ml). The sirupy acetylated product (13 mg) was anomerized with acid by the procedure outlined by Bonner[32] to give principally the α-pyranose form. To the sirup dissolved in 0.1 ml of a mixture of acetic acid and acetic anhydride (1:1) was added 5 ml of 0.5*M* sulfuric acid solution. The reaction mixture was allowed to stand at room temperature and was neutralized with an aqueous sodium hydrogen carbonate at 4°C. This mixture was stirred for 30 min and was extracted three times with chloroform (30 ml). The chloroform phase after successive washings with aqueous sodium hydrogen carbonate and water, and drying over sodium sulfate was evaporated to give a sirup (10 mg). Crystallization occurred from a mixture of isopropanol and petroleum ether (bp 30–60°C) to give 5 mg of product, mp 107–109°C. A mixed-melting point with authentic material (mp 108–109°C) obtained by the procedure of Bonner was undepressed.

This paper is a portion of a thesis submitted by P. C. Wollwage in partial fulfillment of the requirements of The Institute of Paper Chemistry for the degree of Doctor of Philosophy from Lawrence University, Appleton, Wisconsin. June 1969.

References

1. I. J. Goldstein and T. I. Hullar, *Adv. Carbohyd. Chem.*, **21**, 431 (1966).
2. J. S. Carvalho, W. Prins, and C. Schuerch, *J. Amer. Chem. Soc.*, **81**, 4054 (1959).
3. A. Bhattacharya and C. Schuerch, *J. Org. Chem.*, **26**, 3101 (1961).
4. A. J. Mian, E. J. Quinn, and C. Schuerch, *J. Org. Chem.*, **27**, 1895 (1962).
5. J. N. BeMiller, *Adv. Carbohyd. Chem.*, **22**, 25 (1967).
6. J. Furukawa and T. Saegusa, *Polymerization of Aldehydes and Oxides*, Vol. 3, Interscience, New York, 1963, Chaps. III–V.
7. A. Kailan and S. Rosenblatt, *Monatsh.*, **68**, 109 (1936); *Chem. Abstr.*, **30**, 74298, (1936).
8. P. J. Flory, in *High Molecular Weight Organic Compounds*, R. E. Burk and O. Grummitt, Eds., Interscience, New York, 1949, p. 231.
9. H. Abe and W. Prins, *Makromol. Chem.*, **42**, 216 (1961).
10. M. Charton, *J. Org. Chem.*, **29**, 1222 (1964).
11. J. T. Edward, *Chem. Ind.* (London), **1955**, 1102.

12. J. A. Hirsch, in *Topics in Stereochemistry*, Vol. 1, N. L. Allinger and E. L. Eliel, Eds., Interscience, New York, 1967, p. 199.

13. E. L. Eliel, N. L. Allinger, S. J. Angyal, and G. A. Morrison, *Conformational Analysis*, Interscience, New York, 1965, Chap. 7.

14. K. K. De and T. E. Timell, *Carbohyd. Res.*, **4**, 72 (1967).

15. W. N. Haworth and E. L. Hirst, *J. Chem. Soc.*, **1930**, 2615.

16. K. Freudenberg, W. Kuhn, W. Dürr, F. Bolz, and G. Steinbrunn, *Ber.*, **63A**, 1510 (1930); *Chem. Abstr.*, **25**, 1496.

17. W. G. Overend, C. W. Rees, and J. S. Sequeira, *J. Chem. Soc.*, **1962**, 3429.

18. J. P. Teresa, *Anales Real Soc. Espan. Fis. Quim*, **508**, 79 (1954); *Chem. Abstr.*, **49**, 3027e.

19. E. Hardegger and J. Pascual, *Helv. Chim. Acta*, **31**, 281 (1948); *Chem. Abstr.*, **42**, 4148b.

20. P. A. Seib, *J. Chem. Soc. C*, **1969**, 2552.

21. P. C. Wollwage and P. A. Seib, to be published.

22. A. E. Knauf, R. M. Hann, and C. S. Hudson, *J. Amer. Chem. Soc.*, **63**, 1447 (1941).

23. G. H. Coleman, in *Methods in Carbohydrate Chemistry*, Vol. II, R. L. Whistler and M. L. Wolfrom, Eds., Academic Press, New York, 1963, p. 397.

24. E. M. Montgomery, N. K. Richtmyer, and C. S. Hudson, *J. Amer. Chem. Soc.*, **65**, 3 (1943).

25. R. C. Gasman and D. C. Johnson, *J. Org. Chem.*, **31**, 1830 (1966).

26. E. M. Montgomery, N. K. Richtmyer, and C. S. Hudson, *J. Amer. Chem. Soc.*, **65**, 1848 (1943).

27. R. E. Reeves, *J. Amer. Chem. Soc.*, **71**, 2116 (1949).

28. R. W. Jeanloz, A. M. C. Rapin, and S. Hakomori, *J. Org. Chem.*, **26**, 3939 (1961).

29. P. C. Wollwage and P. A. Seib, *Carbohyd. Res.*, **10**, 589 (1969).

30. W. J. Blaedel and V. W. Meloche, *Elementary Quantitative Analysis: Theory and Practice*, Row, Peterson and Co., New York, 1957, p. 330.

31. W. E. Trevelyan, D. P. Procter, and J. S. Harrison, *Nature*, **166**, 444 (1950).

32. W. A. Bonner, *J. Org. Chem.*, **26**, 908 (1961).

Received June 7, 1971.

JOURNAL OF POLYMER SCIENCE: PART A-1 VOL. 9, 2893–2900 (1971)

Synthesis of Phosphorus-Containing Poly-*O*-Acylamideoximes from Polyacrylonitrile

CHARLES E. CARRAHER, JR., and LONG-SHYONG WANG,
Chemistry Department, University of South Dakota, Vermillion, South Dakota 57069

Synopsis

The synthesis of phosphorus-containing poly-*O*-acylamideoximes from polyacrylonitrile has been accomplished by the reaction sequence:

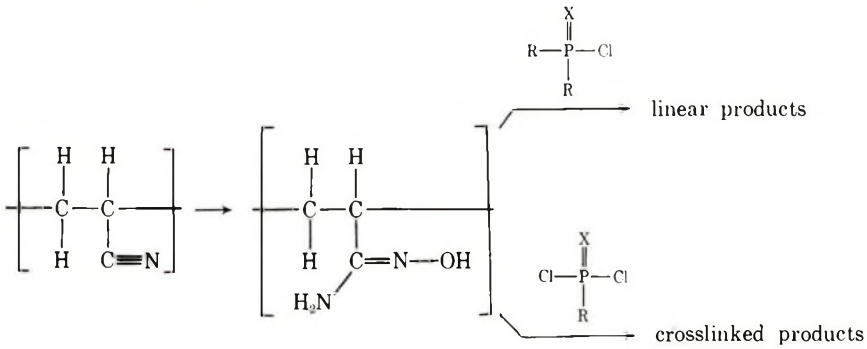

Reaction is believed to occur at the NH_2 nitrogen as well as at the oxime group, but reaction is not believed to occur at both groups in the amide oxime unit. Inclusion of the phosphorus moiety occurs in the medium to high range.

Introduction

The modification of polymer chains via reaction with functional groups connected on the chain is an area of intensive study.[1] We have recently been interested in the modification of readily obtainable, inexpensive polymers to products with properties different from those of the original polymer.[2,3] The purpose is to obtain products which might be commercially desirable.

Bloomstrom[4] and Donaruma[5] have announced the synthesis of poly-*O*-acylamideoximes of the form II by reaction of amideoximes with acid chlorides (I).

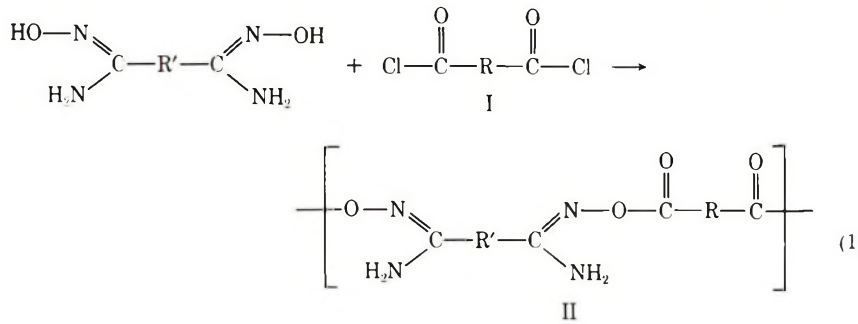

(1)

Another area of our research has been concerned with the production of poly(phosphonate esters), poly(phosphate esters) and polyphosphonamides by reaction of dihalophosphonates and dihalophosphates such as shown in eq. (2) via a Schotten-Baumann type condensation.[6-9] The similarities between the reactivity of acid chlorides of (I) and phosphorus-containing acid chlorides (III) is clearly established.[9]

The present work is a straightforward extension of the work reported above.

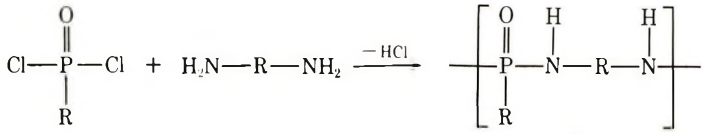

III IV (2)

Polyacrylonitrile is converted to polyacrylamideoxime by reaction with hydroxylamine. This is subsequently condensed with di- or monochlorophosphonates or -phosphates to give linear or crosslinked products. A brief outline of the reaction sequences given in eqs. (3).

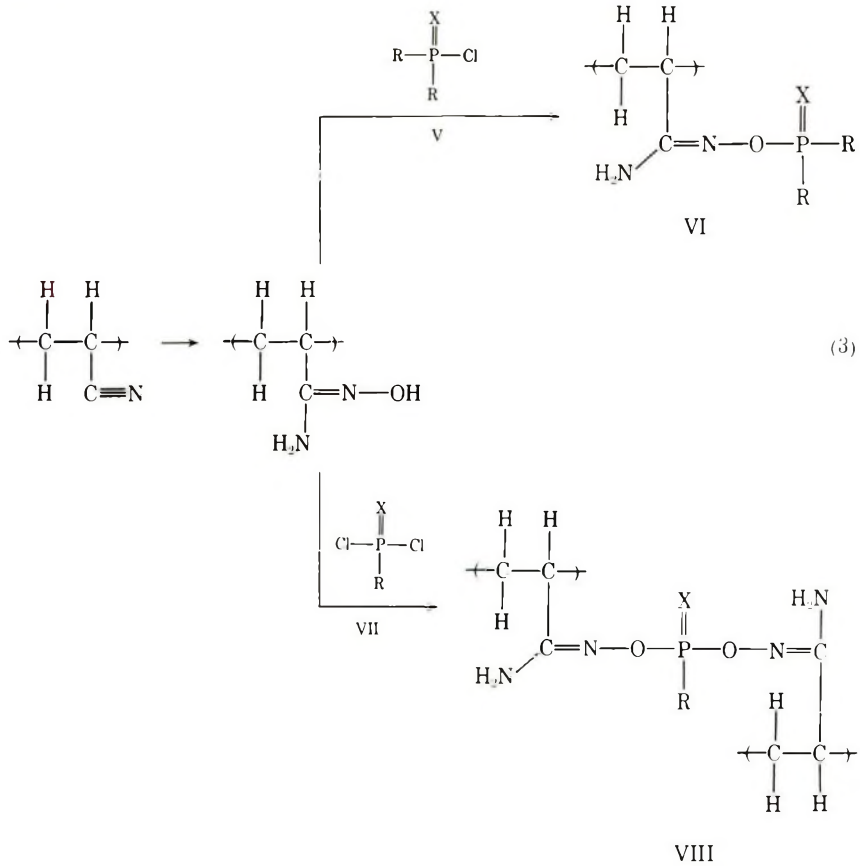

(3)

A brief review of some previous modifications of polyacrylonitrile has been given by Fettes.[1]

This is the initial report of the condensation of phosphorus reactants of V and VII with amideoximes.

Experimental

Polyacrylonitrile was prepared by using a slurry method.[10a] It exhibited a limiting viscosity number of 8.20 dl/g in dimethylformamide, which corresponds to a $\bar{M}_w$ of 1.1×10^6 as determined by light-scattering photometry in dimethylformamide.

Polyacrylonitrile was converted to polyacrylamideoxime by reaction at the nitrile with hydroxylamine. The procedure given by Sorenson and Campbell was used initially.[10b] The infrared spectrum of the product showed the presence of a large amount of unreacted nitrile as calculated from the height of the C≡N band at about 2250 cm^{-1}.

The following procedure was followed to obtain a product which did not exhibit detectable nitrile bands in the infrared region. Polyacrylonitrile (50 g) in 500 ml dimethylformamide was added to a 1-liter three-necked flask equipped with a thermometer, condenser, and stirrer. The reaction mixture was brought to 75°C and maintained there for the remainder of the reaction. Hydroxylamine hydrochloride (105 g, 1.5 mole) and sodium carbonate (75 g, 0.7 mole) were added to the flask. After 3 hr the reaction mixture was filtered to remove insoluble salts. The filtrate was added to 1

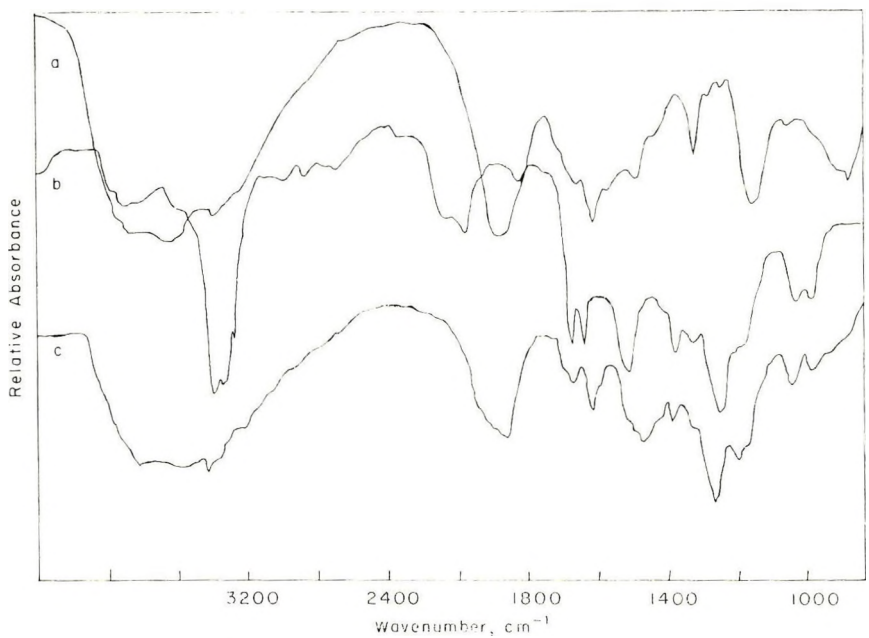

Fig. 1. Infrared spectra of (*a*) polyacrylamideoxime; (*b*) diethyl chlorophosphate; (*c*) condensation product of polyacrylamideoxime and diethyl chlorophosphate.

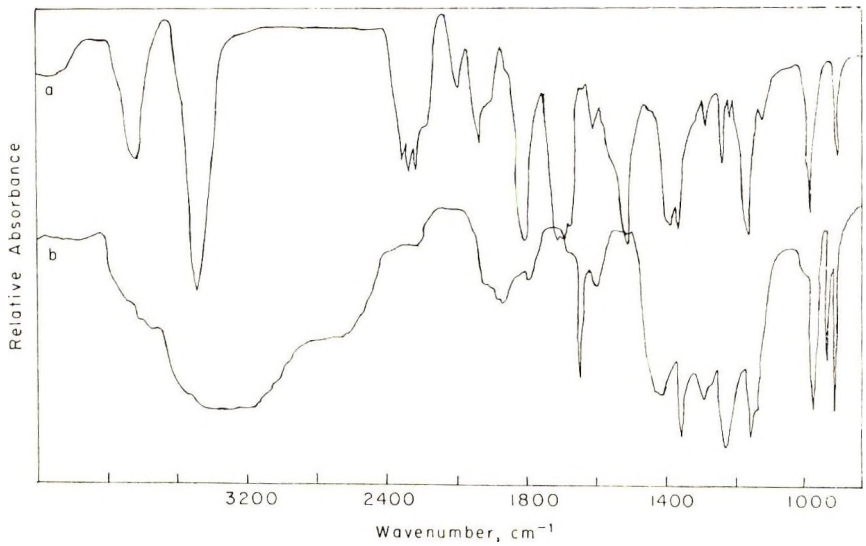

Fig. 2. Infrared spectra of (*a*) phenylphosphonic dichloride and (*b*) condensation product of phenylphosphonic dichloride with polyacrylamideoxime

liter of methanol to bring about precipitation of the product. The polymer was washed with portions of methanol and dried. The yield of product is about quantitative (98%).

Synthesis of phosphorus containing poly-*O*-acylamideoximes was accomplished by the interfacial technique. Aqueous solutions of polyacrylamideoxime containing sodium hydroxide (amount equal to the theo-

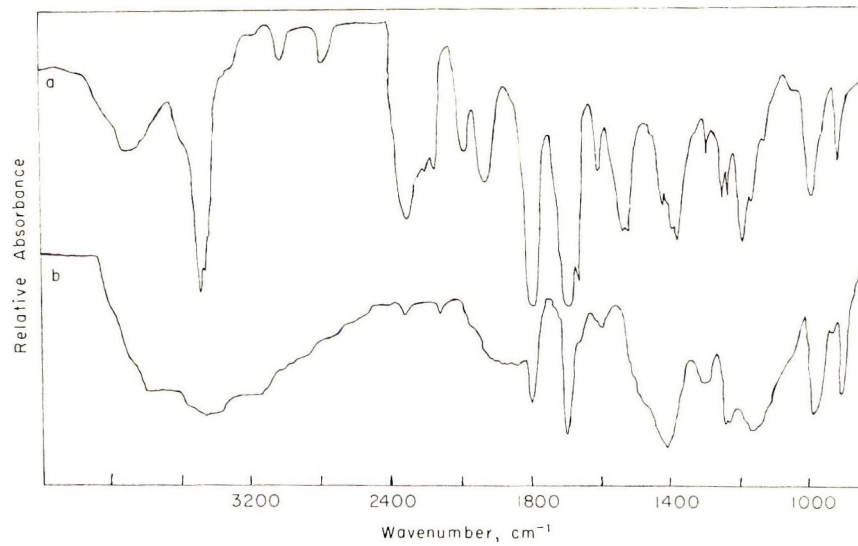

Fig. 3. Infrared spectra of (*a*) diphenyl chlorophosphate and (*b*) condensation product of diphenyl chlorophosphate with polyacrylamideoxime.

retical molar amount of potential HCl) were added to rapidly stirred solutions composed of a water-immiscible solvent containing the phosphorus-containing reactant. The product precipitated from the reaction mixture. It was separated by suction filtration and washed repeatedly with portions of water and then dried and weighed. The materials obtained were white, generally glassy-like in texture. Infrared spectra were obtained on KBr pellets by using the Beckman IR-12 instrument (over the range of 200–900 cm^{-1}) and Perkin-Elmer 237-B spectrophotometer. Representative spectra appear in Figures 1–3.

Softening ranges were determined by using a Fisher-Johns melting point apparatus at a heating rate of 5C°/min. Most of the products did not exhibit melting ranges but rather changed color to a red or brown. The temperature where color change began to occur is shown in Table I.

Amount of phosphorus reactant included in the product was determined for some of the products (Table I). The aqueous phase (combined with the wash water) was evaporated under vacuum. Water was then added to the solid residue, dissolving the salt, unreacted NaOH, and hydrolyzed acid chloride but not the polyacrylamideoxime, which takes several hours to go into solution. The mixture was filtered and the solid unreacted polymer weighed. From knowledge of the unreacted polymer the amount of phosphorus reactant incorporated in the product was calculated. An

TABLE I
Product Properties as a Function of Phosphorus Reactant[a,b]

Phosphorus reactant	Yield, %[c]		% Inclusion of phosphorus reactant, %[d]	Color change temperature, °C
	10 sec reaction time	20 sec reaction time		
Diethyl chlorothiophosphate	29	29	28	138
Diethyl chlorophosphate	50	48	42	144
Phenylphosphonic dichloride	97[e]	—	—	[f]
Phenyl dichlorophosphate	62[g]	72	50	180
Diphenyl chlorophosphate	67	69	—	136
Dimethyl chlorothiophosphate	43	—	43	196

[a] Reaction conditions: acid chloride (0.0025 mole) in 50 ml chloroform is added to stirred solutions of polyacrylamideoxime (0.0025 mole) in 50 ml of water with added sodium hydroxide (0.0025 mole) at 27°C and 17,500 rpm stirring rate (no load).

[b] In systems employing diacid chlorides, 0.0050 mole of sodium hydroxide was used while in those systems employing double the amounts of acid chloride a mole amount equal to the maximum theoretical amount of hydrogen chloride based on the acid chloride was used.

[c] Theoretical yield is calculated by using the formula units illustrated in structure VI for monochloro reactants and structure VIII for dichloro reactants.

[d] Based on reactions run for 20 sec stirring time. See Experimental Section for method of calculation.

[e] Yield increased to 99% when amount of dichloride was doubled.

[f] Melted at 140–144°C. Probably also degraded at this point.

[g] Yield increased to 78% when amount of phenyl dichlorophosphate was doubled.

independent determination of phosphorus included in the product was made by hydrolyzing the phosphorus acid chloride and determining the amount of unreacted acid chloride. This value was in good agreement with the value reported in Table I.

RESULTS AND DISCUSSION

The synthesis of phosphorus-containing poly-*O*-acylamideoximes appears to be general (Table I). Monochloro phosphorus-containing reactants produce linear products which exhibit solubility in such solvents as formic acid but which are insoluble in such solvents as acetone, chloroform, carbon tetrachloride, hexane, benzene, water, and 2-chloroethanol. These products also dissolve in concentrated H_2SO_4 and HCl, but presently there is question whether the products undergo degradation in these solvents. Dichloro phosphorus reactants produce crosslinked products which exhibit insolubility in all tried solvents.*

Previous polycondensations with acid chlorides (I) were reported to occur at the N-OH rather than the NH_2 group.[4,11] The authors have not been able to find satisfactory proof of this. It is possible that reaction could occur at the NH_2 as well as the NOH group. Such aminations are well known. In the present situation the authors have not been able to differentiate between reaction at either site. The poor solubility properties have made it difficult to conduct NMR studies of the products. Eloy and co-workers[11] report the formation of both acylated products in the study of acyl derivatives of formamidoxime. Under one set of reaction conditions the

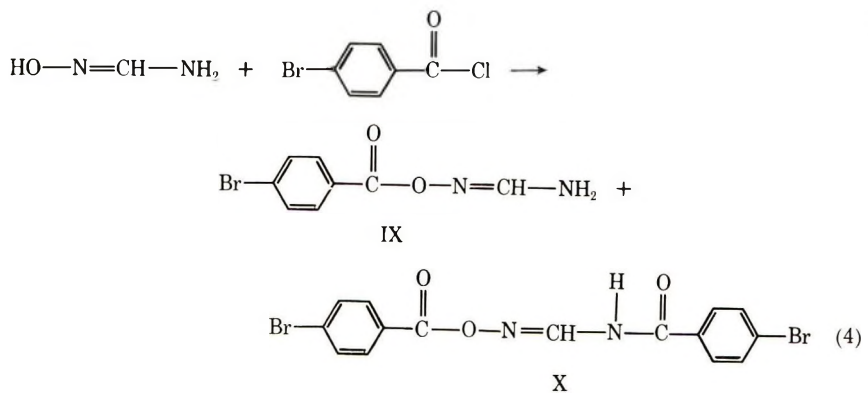

(4)

ratio of IX/X was about 3/1. Thus it is proper to consider that the products contain a mixture of the NOH and NH_2 phosphorylated products.

* While insolubility is a crude sensing tool it is nevertheless often used as a parameter verifying crosslinking.

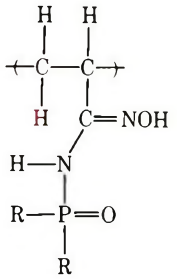

XI

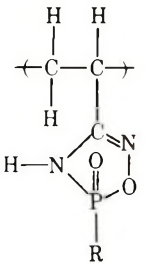

XII

Further, it is possible that such cyclic units as XII might be included in products formed from reaction with dichloro reactants.

It is also possible that the products contain units of XIII, where phosphorylation occurred at both the NOH and NH_2 sites. To evaluate the possible importance of this, double the amount of phenylphosphonic

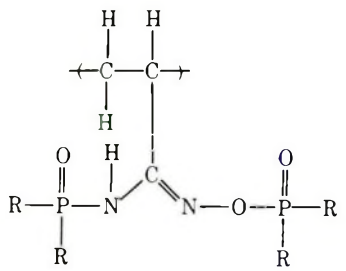

XIII

dichloride was added in a reaction. A 97% yield of product was obtained with a 1:1 molar ratio of the reactant to the number of repeating amideoxime units. With a 2:1 molar ratio, the product yield increased to only 99%. Then reaction occurs at one site or the other within a unit because of electronic (intrinsic) reasons, steric reasons, or both. Thus units of form XIII do not make a large contribution to the overall structure of the product.

An increase in the concentration of phosphorus reactant does increase the product yield. This is shown by an increase from 62% to 78% in product yield for diphenyl chlorophosphate in going from an equal molar reaction system to system employing a double molar amount of the phosphorus reactant (Table I).

The amount of phosphorus component was calculated as described in the experimental section and appears in Table I. An inclusion of one phosphorus molecule per repeating amideoxime unit would give a 50% phosphorus inclusion value. The medium to high inclusion values for phosphorus indicate a large amount of assimilation of the phosphorus moiety in the polymer chain. Precipitation of the product should signal the conclusion of active assimilation of the acid chloride. Thus, the medium to high

values of phosphorus moiety inclusion attests (tentatively) to the great reactivity between the amideoxime and acid chloride.

The synthesis of the P–O–N=C group has previously been unknown. Because of the rapidity of precipitation of the product from the reaction mixture (thus isolating it from water and base) little can be inferred about the hydrolytic stability of such a group.

Yield is constant as time increases. The values shown in Table I are for 10 and 20 sec stirring times.

Phosphorus-containing poly-*O*-acylamideoximes have been synthesized in medium to good yield. Inclusion of the phosphorus moiety is in the medium to high range. Reaction is believed to occur both at the NH_2 and oxime group. It is presently not believed to occur at both groups in the amideoxime unit.

This paper is taken in part from the thesis submitted by L.-S. Wang.

References

1. E. Fettes, Ed., *Chemical Reactions of Polymers*, Interscience, New York, 1964.
2. C. Carraher and L. Torrie, *J. Polym. Sci. A-1*, **9**, 975 (1971).
3. C. Carraher and J. Piersma, *Makromol. Chem.*, in press.
4. D. Bloomstrom, U.S. Pat. 3,044,994 (1952).
5. L. Donaruma, *J. Org. Chem.*, **26**, 577 (1961).
6. C. Carraher and D. Winthers, *J. Polym. Sci. A-1*, **7**, 2417 (1969).
7. C. Carraher and D. Posey, *J. Polym. Sci. A-1*, **7**, 2436 (1969).
8. C. Carraher and P. Billion, *Makromol. Chem.*, **128**, 143 (1969).
9. C. Carraher, *Inorg. Macromol. Rev.*, in press.
10. W. Sorenson and T. Campbell, *Preparative Methods of Polymer Chemistry*, Interscience, New York, 1961, (a) pp. 168–169; (b) p. 171.
11. F. Eloy, R. Lenaers, and C. Moussebois, *Helv. Chim. Acta*, **45**, 437 (1962).

Received April 7, 1971
Revised May 6, 1971

JOURNAL OF POLYMER SCIENCE: PART A-1 VOL. 9, 2901–2911 (1971)

Radiation-Induced Reaction of Ethylene–Cyclohexane–Carbon Tetrachloride System

MASAMORI YAMABE* and HARUMICHI SHIMIZU, *Tokyo Metropolitan Isotope Research Center, Setagaya-ku, Tokyo, Japan*

Synopsis

The γ-ray-induced reaction of ethylene with carbon tetrachloride in cyclohexane was carried under a pressure of 30 kg/cm^2 and at a temperature of 20°C. The liquid and the solid products were obtained. Their structures were discussed on the basis of infrared absorption spectra and differential thermal analysis curves. The liquid product is considered to be ethylene–carbon tetrachloride telomer. The solid product consists of three components, differing slightly in molecular structure and molecular weight. To clarify the reaction process, some runs with the ethylene–cyclohexane–(ethylene–carbon tetrachloride telomer) system were also carried out. In this system, only solid product was obtained. Thus, it is concluded that the reaction proceeds stepwise, the first step being the telomerization reaction and the second the graft polymerization of ethylene onto the telomer produced in the first step.

INTRODUCTION

It is well known that ethylene in solution as well as in the gaseous phase can be polymerized with γ-ray irradiation. Henley and Chong,[1] for instance, have reported this type of polymerization of ethylene dissolved in water, ethanol, benzene or carbon tetrachloride. Medvedev *et al.*[2] reported polymerization of ethylene dissolved in several kinds of organic solvents. According to this report, the G value of ethylene consumption obtained with methanol, cyclohexane, or n-heptane solution of this monomer is several times as large as that obtained with the gaseous monomer. When the solvent is carbon tetrachloride, for which the G value of radical formation is much larger and consequently the rate of the initiation of the reaction should be much larger than the other solvents, the G value of ethylene consumption is only about the same as that obtained with ethylene in gaseous phase. The product in this case is of relatively low molecular weight; it is usually called ethylene–carbon tetrachloride telomer, Cl_3C-$(CH_2$-$CH_2)_n Cl$, where n is a small integer (usually less than 5).

This is certainly attributable to the strong effect of chain transfer to this solvent. If carbon tetrachloride diluted with another organic liquid is used as the solvent, it is possible that this effect is reduced, increasing the G value of ethylene consumption to at least the same order as in the cases

* Present address: Mitsubishi Petrochemical Co., Ltd., Chiyoda-ku, Tokyo, Japan.

in which the other organic solvents are used, and the molecular weight of the product may be controlled by the concentration of carbon tetrachloride in the solvent.

Takehisa *et al.*[3] have thoroughly studied the telomerization of ethylene and carbon tetrachloride under widely varied reaction conditions. They showed that if the carbon tetrachloride/ethylene molar ratio is reduced, the average molecular weight of the resulting telomer increases to some extent. This is evidence of a decrease of the chain transfer effect.

On the other hand, a catalytic reaction between ethylene and the telomer was reported by Ovakimyan et al.[4] According to their experiments, ethylene reacts with the telomer on the carbon atom closest to the $—CCl_3$ group to form a grafted side chain.

From these results it can be expected that if a mixed solvent including carbon tetrachloride is used, both telomerization and grafting reactions will take place, and the product will be the telomer of a larger molecular weight, a telomer with long side chains, or a mixture of these two types of molecules; if the reaction conditions are suitable, polyethylene having functional groups at ends of the molecule can be obtained.

In the present experiments, radiation-induced reaction of the ethylene–carbon tetrachloride–cyclohexane system have been carried out. The main purpose of the present experiments is to find a way to increase the G value of ethylene consumption and to obtain a polyethylene with one or more functional groups at the ends of the molecule. Some runs with the ethylene–(ethylene–carbon tetrachloride telomer)–cyclohexane system have also been made to clarify the mechanism of the reaction in the former system.

EXPERIMENTS

Reagents

Cyclohexane and carbon tetrachloride were reagent-grade materials, stored in glass reservoirs with calcium chloride desiccant and were used immediately after distillation. Ethylene of nominal purity of 99.9% (gaseous impurities were evaluated by gas chromatography to be 0.025 mole-%) was used without further purification. Ethylene–carbon tetrachloride telomer was prepared by the method described in the following section.

Procedure

A glass tube containing 40 ml of the solvent mixture (cyclohexane with carbon tetrachloride or cyclohexane with the telomer) of a given molar ratio was placed in an autoclave of a nominal volume of 100 ml. To eliminate oxygen in the mixed solvent, nitrogen stream was fed through the autoclave for 20 min at a flow rate of 100 ml/min.

As a comparison, one run was carried out after deaeration three times under freezing with liquid nitrogen. As these two methods of oxygen elimination gave the same results, the first method was used for all runs.

For irradiation, a 3000-Ci ^{60}Co source (Tokyo Metropolitan Isotope Research Center) was used. The dose rate was about 0.15 Mrad/hr, and the total dose was 0.15–7.2 Mrad. In all cases, irradiation was carried out at a constant temperature of 20°C.

After irradiation, unreacted ethylene was introduced into a vacuum system of known volume and was estimated from the increase in pressure of the system. Ethylene consumption could thus be easily calculated. The reaction mixture in the autoclave was poured into a glass beaker with 100 ml of methanol. A white, waxy solid coagulated slowly. After 24 hr the solid was filtered, washed with methanol, and dried overnight *in vacuo*. This solid product was weighed and analyzed as described in the next section.

The filtrate was distilled on a water bath at 50°C under a reduced pressure of 40 mm Hg to eliminate low-boiling material. The remainder was termed liquid product and treated as described below.

The telomer used was prepared as follows. Ethylene was dissolved in carbon tetrachloride and the solution was equilibrated under an ethylene pressure of 30 kg/cm^2 and at a constant temperature of 20°C. After the irradiation to a dose of 7.0 Mrad with ^{60}Co γ-rays, ethylene remained was purged and unreacted carbon tetrachloride was distilled out at 50°C and 40 mm Hg.

As shown in Figure 1, which shows programmed temperature gas chromatogram of the telomer, the $n = 3$ component was most abundant, and the quantity of residual carbon tetrachloride was almost negligible.

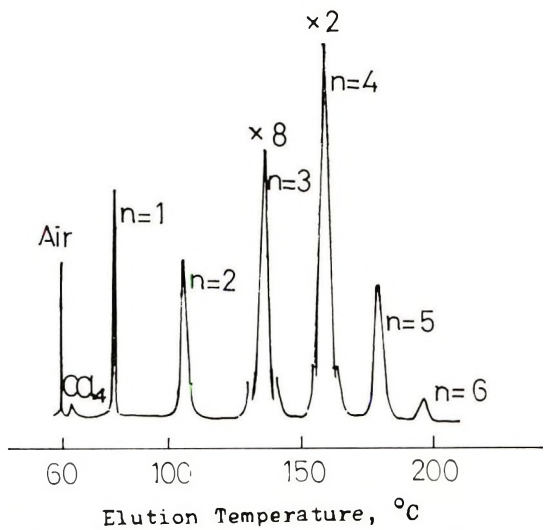

Fig. 1. Programmed-temperature gas chromatogram of the telomer. Column packing, PEG succinate; rate of temperature elevation, 5°C/min.

Analysis and Measurement

The molecular weight of the solid products was measured by ebullioscopic method. Chlorine content was determined by the combustion method.

Infrared absorption spectra of the solid and liquid products and of the telomer were obtained with a JASCO type IRS infrared spectrophotometer (Japan Spectroscopic Co., Ltd.). Melting behavior of the solid products was determined with a Shimadzu Model DTA-10 differential thermal analysis apparatus (Shimadzu Ltd.). For DTA work, each specimen was tested after twice being completely melted and recooled in a sample cell to prevent effects of thermal hysteresis and unevenness.

RESULTS

Yield of the Products

Radiation-induced reaction in the system with carbon tetrachloride gave both solid and liquid products, except in the case of higher concentrations of carbon tetrachloride, where only liquid products were obtained. The liquid products were formed even in the earliest stage of the reaction, and the rate of the formation depended largely on the concentration of carbon tetrachloride. The yield of the liquid products increased rapidly to its maximum value, then decreased slowly.

The solid products appeared after an induction period, the length of which depended on the concentration of carbon tetrachloride. The rate

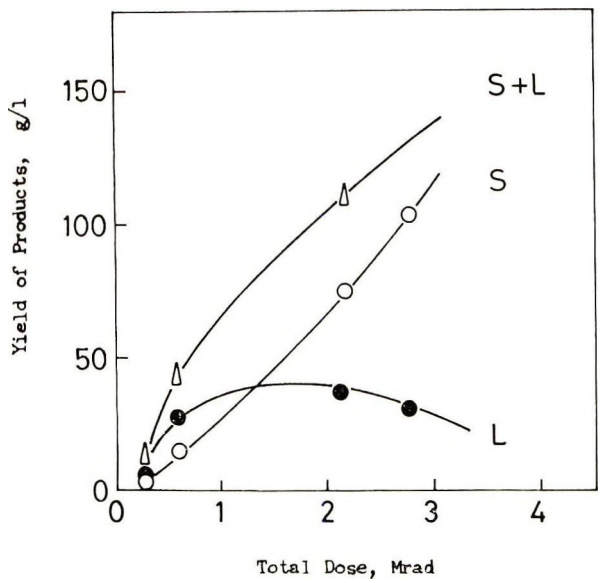

Fig. 2. Effect of total dose on yield of products (CCl_4 content, 2.66 mole-%): (L) liquid product; (S) solid product.

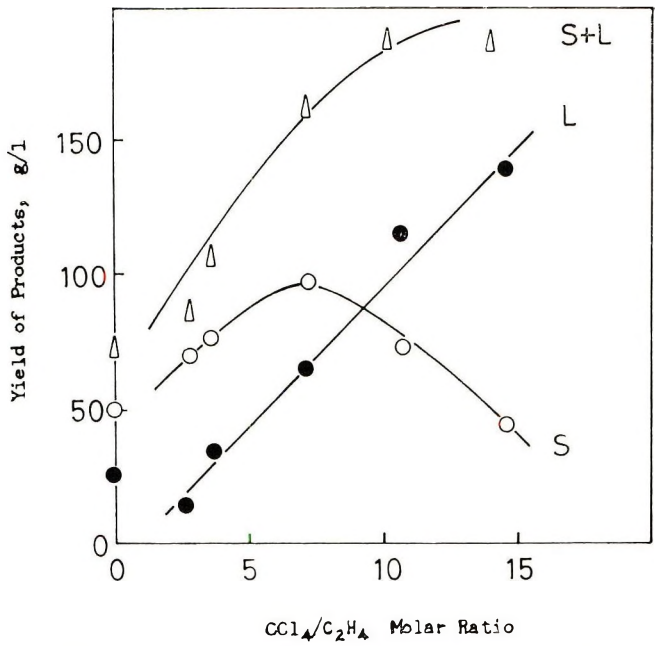

Fig. 3. Effect of CCl_4 content on yield of products (total dose, 2.12 Mrad): (L) liquid product; (S) solid product.

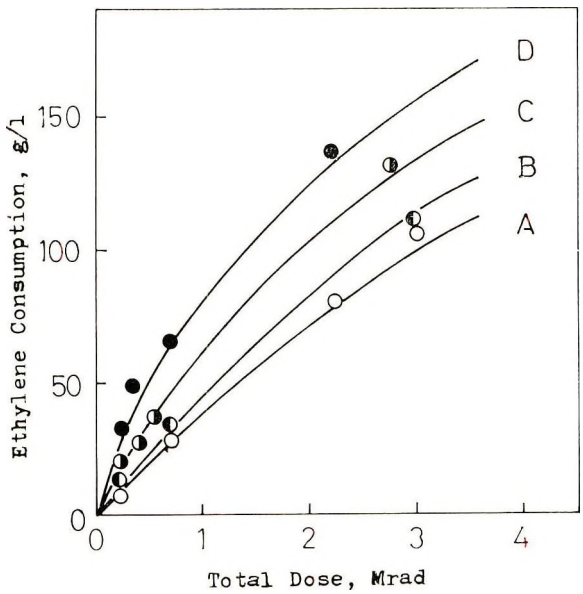

Fig. 4. Effect of total dose on ethylene consumption at various CCl_4 contents: (*A*) 0.00 mole-%; (*B*) 1.31 mole-%; (*C*) 2.62 mole-%; (*D*) 5.49 mole-%.

of the formation of the solid products immediately reached a large value. Figure 2 represents typical results.

Effect of the initial concentration of carbon tetrachloride on the yield is shown in Figure 3. An increase in the initial concentration of this component gives rise to an increase in the yield of the liquid products and to a decrease in the yield of solid products.

Either of the two following assumptions can explain these results. The first is that the value n of the telomer increases to a large value to cause the solid products. The second is the assumption of a stepwise reaction. The telomer is produced first, followed by grafting reaction of ethylene on it.

Ethylene consumption versus dose plots such as Figure 4 make it possible to calculate the initial rate and the initial G value of ethylene consumption. Table I shows the results.

TABLE I
Effects of Total Dose and CCl_4 on Radiation Polymerization of Ethylene in Cyclohexane

CCl_4, mole-%	Total dose, Mrad	Products, g/l.		Conversion, %[a]	$G(-C_2H_4) \times 10^{-3}$[b]
		Solid	Liquid		
0	0.74	19.5	16.5	17.9	1.8
0	2.22	50.3	29.2	40.3	1.4
0	6.06	145.5	3.0	76.2	0.9
1.31	2.11	70.8	13.0	42.4	1.5
1.31	3.16	97.0	16.5	56.2	1.4
1.31	5.52	145.5	16.5	81.7	1.1
2.66	2.18	74.5	37.5	52.7	1.9
2.66	2.75	105.5	29.7	68.3	1.8
2.66	5.62	149.5	20.2	85.9	1.2
5.49	2.14	99.0	67.0	84.2	2.9
5.49	2.54	129.0	47.5	89.6	2.5
5.49	5.72	184.3	44.5	115.8	1.5

[a] Conversion (%) is calculated by the equation: $\% = (W_p/W_e) \times 100$, where W_e is the initial quantity of ethylene (g/l.).

[b] G is calculated as follows: $G = (W_p N/MST) \times 100$, where W_p is the products formed in T hours (g/l.); N is Avogadro's number; S is the dose rate absorbed in solvent, 0.71×10^{22} eV/l.-hr; T is irradiated time, (hr); and M is the molecular weight of ethylene (28.0).

The G values fall in the range 1000–3000, larger than that obtained by Medvedev et al.[2] with some kinds of simple solutions.

The reaction in the system with the telomer also gave both solid and the liquid products. The system with telomer gave solid products from the earliest stage of the reaction with no induction period. The yield of solid products increases linearly with irradiation dose. The liquid product decreases slowly from the initial amount of telomer added. Figure 5 shows typical results. The liquid product from this system is somewhat different from that of the system with carbon tetrachloride.

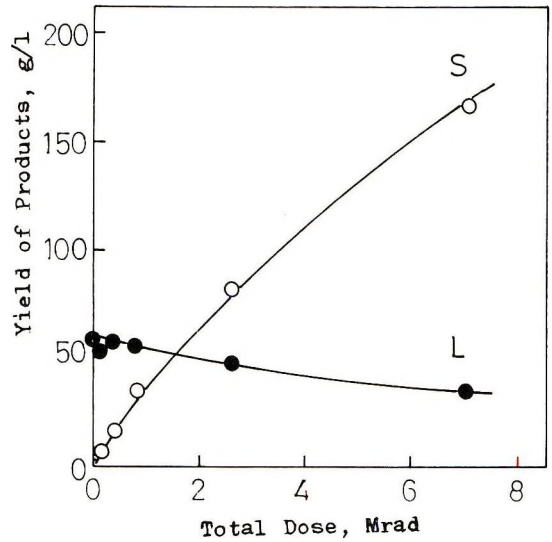

Fig. 5. Effect of total dose on yield of products (telomer/cyclohexane molar ratio, 0.025): (L) liquid product. (S) solid product.

The procedure of preparation of the liquid product is the same one as that of the telomer except for filtering of the solid product. The "liquid products" in this case therefore contain the telomer in addition.

Properties of the Products

Figure 6*a* shows some of the melting endothermic curves of the solid products obtained with the reaction of the system with carbon tetrachloride. Each of these endothermic curves has three endothermic peaks, suggesting that the solid products are mixtures of three components of different molecular types. These peaks are named A, B, and C from the lowest peak temperature to the highest. The components which are represented by these peaks are also named A, B, and C, respectively.

The solid products were fractionated and the melting endothermic curves were tested on each fraction. A product of the solid products can be dissolved in toluene at 50°C. The portion which remained undissolved (fraction 1) gives a endothermic melting curve with a single peak, which corresponds to the C peak. The portion dissolved can be fractionally precipitated by adding methanol and/or cooling the solution. Each fraction (fraction 2, 3, 4, or 5) gives an endothermic curve with its specific peak.

Every fraction except fraction 4 gives a single peak, and fraction 4 gives a pair of peaks, one of which corresponds to the A and the other to the B peaks. Fractions 2 and 3 seem to belong to the B part and fraction 5 to the A.

A mixture of the fractions which do not belong to the same part gives an endothermic curve with two melting peaks, each of which corresponds to the melting peak of the respective fraction. On the contrary, a mixture

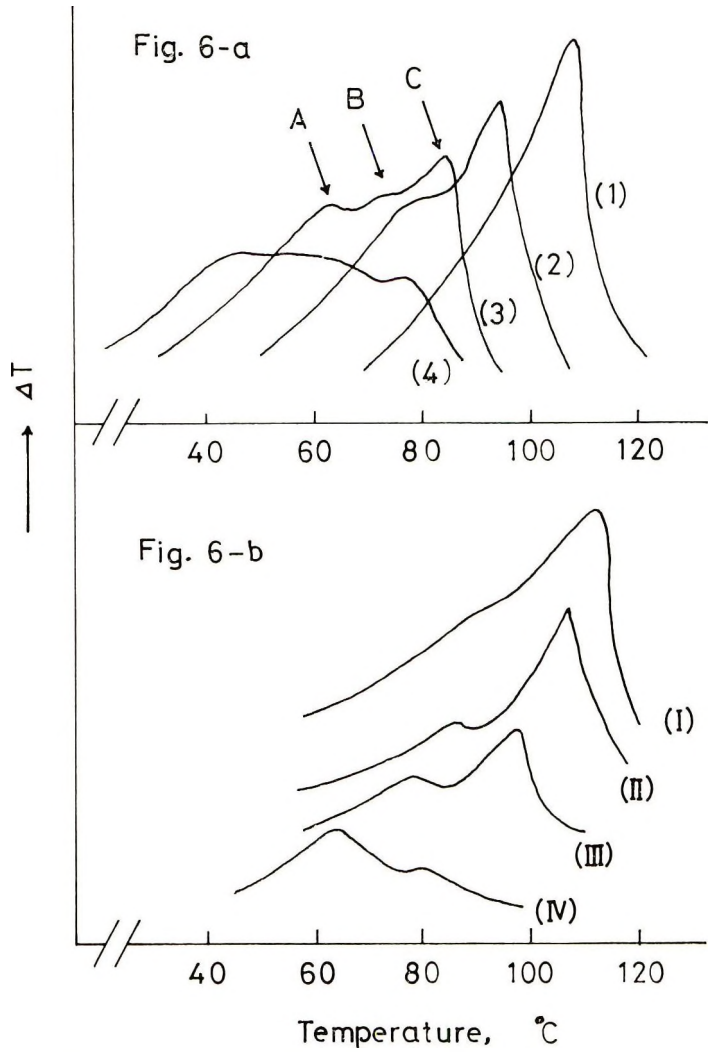

Fig. 6. Melting endothermic curves of several solid products in the systems with (*a*) CCl_4 and (*b*) with telomer. A, B, or C denote A, B, or C peaks, respectively. Initial concentration of CCl_4: (*1*) 0; (*2*) 1.31 mole-%; (*3*) 2.66 mole-%; (*4*) 5.49 mole-%. Initial concentration of telomer: (I) 2.44 mole-%; (II) 2.44 mole-%; (III) 3.35 mole-%; (IV) 100 mole-%. Irradiation dose: 0.15 Mrad for (I), 2.65 Mrad for others.

of fractions 2 and 3 which belong to the same part B, gives an endothermic melting curve with a single, somewhat broader peak. From these results it can be concluded that those three peaks in the endothermic curves of the solid products show the melting peaks of a fraction which has a different molecular structure. Figure 7 shows the results above mentioned.

Figure 6*b* shows the melting endothermic curves of the solid products obtained by reaction of the system with the telomer of different concentrations. Curve I shows only one peak, which corresponds to the C peak

in the cases of the system with carbon tetrachloride (Fig. 6*a*). Curves II and III show a second relatively small peak which corresponds to the B peak. A peak which corresponds to the A peak is not found in this case.

Figure 8 shows infrared absorption spectra of the products in the system with carbon tetrachloride under different reaction conditions. Spectra of the telomer and of a film made of commercial polyethylene is also shown for comparison. The main difference between spectra of the products

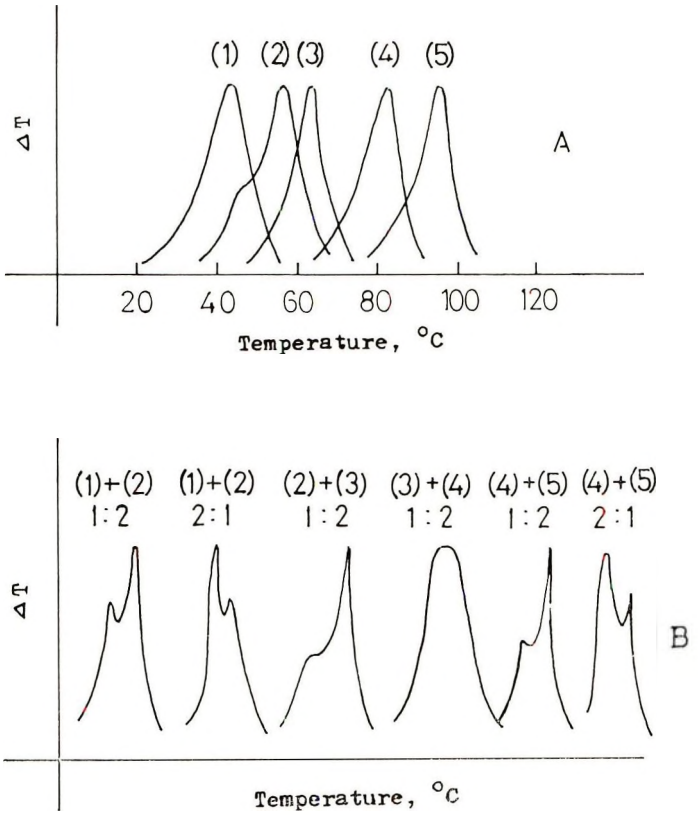

Fig. 7. Melting endothermic curves of (*A*) fractions of solid product and (*B*) of the mixtures of two fractions.

and the spectrum of commercial polyethylene is the absorption due to C-Cl bonds. The absorption peaks appeared at 775, 695, and 650 cm^{-1}. The former two peaks are considered to be absorptions due to $-CCl_3$ group and the last one to $-CH_2Cl$ group.

Although these spectra show little quantitative information, it is evident that the structure of the solid products varies continuously between two extremes, commercial polyethylene and the telomer.

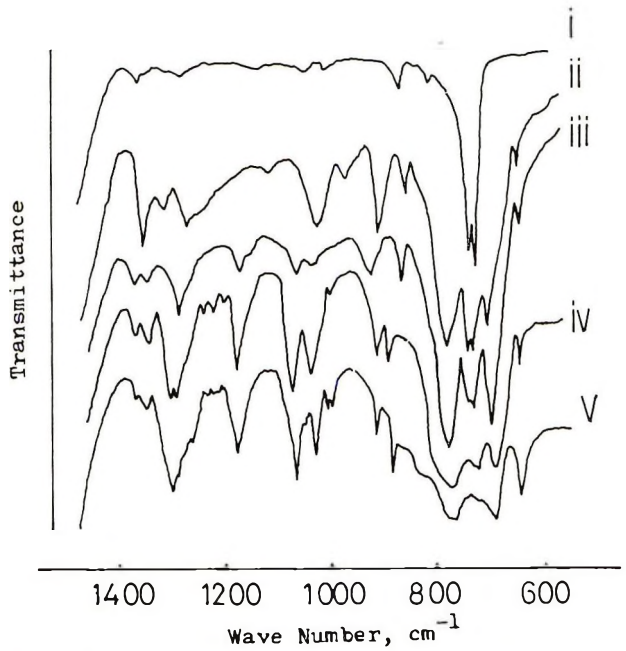

Fig. 8. Infrared absorption spectra of several specimens: (i) commercial polyethylene film; (ii) solid product of the system with 1.31 mole-% CCl_4, total dose, 2.16 Mrad: (iii) solid product of the system with 5.49 mole-% CCl_4, total dose 2.16 Mrad; (iv) liquid product of the system with 5.49 mole-% CCl_4, total dose 2.16 Mrad; (v) telomer.

DISCUSSIONS

In the γ-ray-induced reaction of the ethylene–carbon tetrachloride–cyclohexane system, the increase in the concentration of carbon tetrachloride gives rise to an increase in the rate of ethylene consumption. The cause seems to be a high G value of radical formation of carbon tetrachloride.

In the earliest stage of the reaction of the system with carbon tetrachloride, only liquid products appear. The molecular weight and infrared absorption spectra of the liquid products have shown that these have almost the same molecular structure as that of the telomer.

The molecular weight of the products was estimated by the two different methods, ebullioscopic measurement and evaluation from chlorine content. Assuming that each molecule of the products contained 4 chlorine atoms as in the case of the telomer, molecular weight was calculated from the chlorine content. As shown in Table II, the results of these calculations were in good agreement with values obtained with ebullioscopic method. This shows that each molecule of the products contains 4 chlorine atoms as in the case of the telomer, and that it can be assumed, therefore, that the telomer-like structure remains to the end of the reaction.

From infrared absorption spectra, little information can be derived about the structure of the solid products, but the results of differential thermal

TABLE II
Average Molecular Weight of Products

Sample	CCl_4, mole-%	M_n (by ebullioscopy)	Cl content, %	M_n (calcd from Cl %)
Solid product	1.31	1300	17.78	1250
"	2.62	800	20.29	720
"	5.49	700	21.20	680
"	3.09	500	27.38	530
"	10.45	450	31.22	450
Liquid product		300	44.37	320
Telomer	100.00	250	70.88	210

analysis give interesting information. As mentioned above, each of the DTA curves has three endothermic peaks showing that the solid products consist of three components, and one of these components does not migrate completely with the other. This means that the structure of one component is different from that of the others. Any of these three types of molecular structure should be considered to be one of above mentioned ones or their variations. Appearance of three peaks in the melting endothermic curves of the solid products shows that both of the above mentioned structures exist in the system with carbon tetrachloride. The C peak is the largest when the initial concentration of carbon tetrachloride is the lowest. In this case, it is sufficient remaining ethylene that forms a long side chain or side chains onto the telomer. In the system with the telomer, only the C part is formed at the earliest stage of the reaction, when a high concentration of ethylene is in contacts with the telomer. Then the B part appears at the stage when the concentration of ethylene becomes low. The A part is formed only in the system with carbon tetrachloride. The yield of this part is large when the initial concentration of carbon tetrachloride is high. In this case the quantity of unreacted ethylene is very small, that is, almost all ethylene has reacted with carbon tetrachloride and converted to the telomer. In the case of the system with the telomer where ethylene is in contact only with the telomer, the A part does not appear at all. These facts lead to the following conclusions: that the C part is of molecular structure having one or more long polyethylene branches; that the B part is also of branched structure but the side chains are much shorter than those of the C part, and that the A part may have a telomer-like structure.

According to the results of Ovakimyan et al.,[4] the reaction of ethylene onto the telomer proceeds as shown in eqs. (1)–(3).

$$Cl_3C{-}CH_2(CH_2{-}CH_2)_{n-1}{-}CH_2Cl + R\cdot \rightarrow Cl_3C{-}\dot{C}H{-}(CH_2{-}CH_2)_{n-1}{-}CH_2Cl + RH \quad (1)$$

$$Cl_3C{-}\dot{C}H{-}(CH_2{-}CH_2)_{n-1}{-}CH_2Cl + m(CH_2{-}CH_2) \rightarrow Cl_3C{-}\underset{\displaystyle (CH_2{-}CH_2)m\cdot}{\underset{|}{CH}}{-}(CH_2{-}CH_2)_{n-1}{-}CH_2Cl \quad (2)$$

$$Cl_3C—\underset{\displaystyle (CH_2—CH_2)_m\cdot}{\overset{\displaystyle |}{CH}}—(CH_2—CH_2)_{n-1}—CH_2Cl + R'H \rightarrow$$

$$Cl_3C—\underset{\displaystyle (CH_2—CH_2)_{m-1}—CH_2—CH_3}{\overset{\displaystyle |}{CH}}—(CH_2—CH_2)_{n-1}—CH_2Cl + R'\cdot \quad (3)$$

Here R· and R'· represent radicals of some kind.

In the present experiments, in which the reaction is induced by γ-radiation, the position on which ethylene will react cannot be definitely determined, but it is sure that this type of the grafting reaction takes place and that the quantity of ethylene present will strongly affect the length of the resulting side chains. Thus it can be concluded that the C part is a component consisting of the telomer with one or more long side chains and that the B material is that with one or more shorter side chains.

About the structure of the A part a possibility can be pointed out that this component is essentially telomer which is of somewhat larger molecular weight than that prepared by Takehisa et al.[3] Our conclusion is as follows: the molecular structure of the solid product is not clear but there are at least two possibilities. The first is that it has the same structure as the telomer but much longer carbon chain; the second is that there is a branched structure formed by graft polymerization of ethylene onto the telomer. The product with the latter structure may be called polyethylene accompanied with a telomerlike structure at one end.

From the results of the present experiments, it can be concluded that the radiation-induced reactions in the ethylene–carbon tetrachloride–cyclohexane system consist of two successive steps; the first step is telomerization, and the second is grafting reaction of ethylene onto the telomer

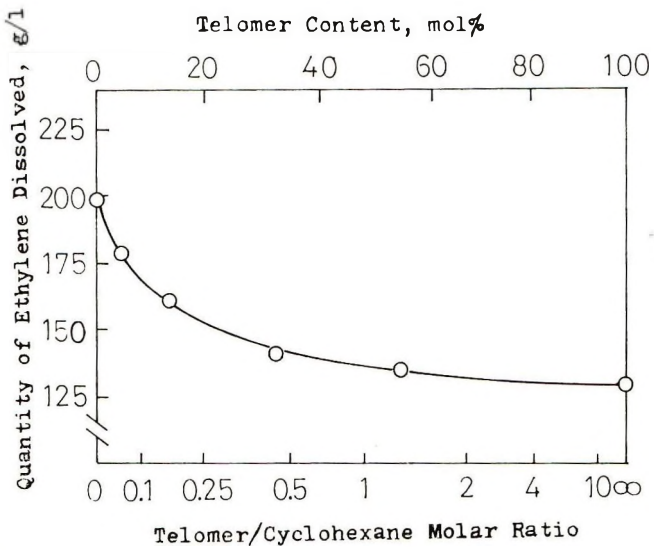

Fig. 9. Effect of telomer content on ethylene solubility. Ethylene pressure, 30 kg/cm²; Temperature, 20°C.

molecule. It can be concluded that the length of the side chain is affected by the quantity of ethylene in the reaction system.

In the case of the system with the telomer, solubility of ethylene must be noticed; as shown in Figure 9, solubility of ethylene in the mixed solvent is quite different for different telomer concentrations. As all experiments with the telomer were carried out under the same initial pressure of ethylene, a discussion of the results should consider the solubility of ethylene in the mixed solvent.

In these cases, predominantly grafting reaction takes place, resulting in the B and the C components. The first step [eq. (1)] of the stepwise reaction does not occur, and the component A consequently is not produced.

Kinetic studies of this kind of reaction have been made by several authors. Wiley et al.[5] have reported a results of a kinetic study for radiation-induced polymerization of ethylene in alkyl chlorides. Mellow and Burton[6] have reported that for telomerization reaction of ethylene and chloroform.

In the present experiments, unfortunately, reaction conditions are much more complicated than in the cases of these authors. Beside the initial reactants, ethylene and carbon tetrachloride, the liquid product of the first step of the reaction, probably the telomer, is considered to be one of reactants of the second step. The third strongly affects the solubility of ethylene in the reaction mixture. Furthermore, the effect of the solid product, which can be dissolved in the reaction mixture resulting a viscous liquid, is not known at all. The solubility of ethylene may be reduced more than that shown by the curve in Figure 9.

Of the data necessary for kinetic treatment only ethylene pressure and temperature in the reaction vessel can be followed in the course of the reaction. Ethylene concentration in the reaction mixture can not be known.

Initial data can of course be given, but these will represent only data for kinetic treatment of the first step, i.e., the telomerization reaction.

For these reasons, a study of kinetics is difficult in these reaction systems. Therefore, solution of this problem will require some further experiments with more simplified reaction conditions.

CONCLUSIONS

In the γ-ray-induced reaction of the ethylene–carbon tetrachloride–cyclohexane system, the initial rate of ethylene consumption is affected by the initial concentration of carbon tetrachloride.

This reaction proceeds stepwise. The product of the earlier stage is a liquid product, which is concluded to be the telomer. The solid product is formed some time after the period in which the telomerization reaction occurs predominantly. Therefore, this period is long when the initial concentration of carbon tetrachloride is high.

The results of thermal analysis show that the solid product consists of three components. The highest-melting one has (a) long side chain(s) formed in the second step of the reaction, which is a grafting of ethylene

onto the telomerlike structure. When the telomer is used instead of carbon tetrachloride, only the second step of the reaction occurs, and a purer product of this structure can be obtained.

The authors wish to thank Dr. G. Meshitsuka and Dr. Y. Shinozaki, Tokyo Metropolitan Isotope Research Center, for their valuable advice and encouragement.

References

1. E. J. Henley and C. Chong, *J. Polym. Sci.*, **36**, 511 (1959).
2. S. S. Medvedev et al., *Vysokomol. Soedin.*, **2**, 904 (1960).
3. M. Takehisa, M. Yasumoto, and Y. Hosaka, *Kogko Kagaku Zasshi*, **65**, 531 (1962).
4. G. B. Ovakimyan and M. A. Byesproevanny, *Khim. Nauk Prom.*, **2**, 13 (1957).
5. R. H. Wiley, N. T. Lipscomb, and C. F. Parrish, *J. Polym. Sci. A*, **2**, 2503 (1964).
6. F. W. Mellows and M. Burton, *J. Phys. Chem.*, **66**, 2168 (1962).

Received November 25, 1969
Revised April 30, 1971

JOURNAL OF POLYMER SCIENCE: PART A-1 VOL. 9, 2915–2932 (1971)

Radical Copolymerizations of β-Propiolactone with Acrylonitrile and with Styrene

SHITOMI KATAYAMA, HIDEICHI HORIKAWA, and OSAMU TOSHIMA, *Faculty of Science and Technology, Akita University, Akita, Japan*

SYNOPSIS

Radical copolymerizations of β-propiolactone (denoted 2) with acrylonitrile (denoted 1) and with styrene (also denoted 1) and the structures of the resulting copolymers were studied. The bulk copolymerization with acrylonitrile by α,α′-azobisisobutyronitrile at 50°C gave polyesteracrylonitriles of high enough molecular weight to form tough and transparent films, with the monomer reactivity ratios, $r_1 = 0.84$, $r_2 = 0.00$, and the structure of the copolymers was

$$-\!\!\left[\left(CH_2\underset{\displaystyle CN}{CH}\right)_x\left(CH_2\underset{\displaystyle CN}{CH}CO_2CH_2CH_2\right)_y\right]\!\!-$$

Radical copolymerization with the same initiator in *N,N*-dimethylformamide gave polyesteracrylonitriles of the same structure as that of the bulk polymer, blended with β-propiolactone homopolymer which was due to the competing anionic homopolymerization of β-propiolactone. Th reactivity ratios on the bulk copolymerization with styrene were $r_1 = 6.2$ and $r_2 = 0.0$ with benzoyl peroxide at 80°C, and $r_1 \cong 32$, $r_2 = 0$ with α,α′-azobisisobutyronitrile at 50°C. Polyesterstyrenes of intrinsic viscosity up to 0.83 were obtained.

INTRODUCTION

Several studies on the copolymerization of β-propiolactone with vinyl and related monomers have been reported, but most of them deal with ionic copolymerizations, and no high molecular weight copolymers were obtained. β-Propiolactone has been homopolymerized and copolymerized by radiation,[1–3] however, these reactions were considered to be of radiation induced ionic polymerizations. Magoffin and Hagemeyer[4] tried copolymerizations of β-propiolactone with a few vinyl monomers in the presence of radical initiators, but they reported nothing about the structures and properties of the resulting copolymers, nor did they indicate whether the monomers really copolymerized. Thus far no evident proof of the radical polymerizability of β-propiolactone has been reported.

In this study the authors have tried to clear the radical copolymerizability of β-propiolactone by discussing the monomer reactivity ratios on copolymerizations and studying the structures and a few properties of the resulting copolymers.

EXPERIMENTAL

Materials

Acrylonitrile was distilled in a nitrogen atmosphere after passing through silica gel in a long cylinder; bp 77.0–77.3°C/760 mm. β-Propiolactone (supplied by Daiseru Company, Ltd., Japan) and styrene were dried over an excess of anhydrous sodium sulfate overnight and distilled in a vacuum in a nitrogen atmosphere; β-propiolactone bp 59.0°C/18 mm, styrene bp 50–51°C/26–27 mm. Commercially available best quality α,α′-azobisisobutyronitrile and benzoyl peroxide were used as initiator as received. *N*,*N*-Dimethylformamide was kept in an excess quantity of anhydrous sodium sulfate and further dried with a small amount of calcium hydride for distillation in a nitrogen atmosphere, bp 68.2°C/40 mm. Chloroform was washed with concentrated sulfuric acid, aqueous sodium hydroxide, and then water, dried with potassium carbonate and distilled before use. Benzene was dried with metallic sodium and distilled. Methanol was dried over calcium oxide and distilled.

Polymerization Procedures

The monomer mixture of the compositions f_1 (mole fraction of acrylonitrile or styrene) and f_2 (mole fraction of β-propiolactone) was placed in an ampoule followed by solvent and then the initiator in a nitrogen atmosphere. The glass ampoule was sealed in a nitrogen atmosphere and placed in a constant temperature bath. The polymerization was carried out without agitation under the conditions listed in Table I. Polyesteracrylonitrile polymerized in *N*,*N*-dimethylformamide was precipitated in water, washed with methanol, and dried *in vacuo* at room temperature for several days. Polyesteracrylonitrile polymerized without solvent was dissolved in *N*,*N*-dimethylformamide and treated by the same method as above. The reacted mixture of β-propiolactone with acrylonitrile in chloroform was

TABLE I
Polymerization Conditions*

Experiment no.	Initiator (0.5 g)	Solvent	Polymerization temperature, °C	Polymerization time, hr
		With acrylonitrile		
I	AIBN	None	50	42
II	AIBN	DMF (300 ml)	50	42
		With styrene		
III	AIBN	None	50	48
IV	BPO	None	80	48

* Every quantity is for one mole of the total monomer mixture.

precipitated in methanol. Polyesterstyrene was dissolved in chloroform, and the solution was poured into strongly agitated benzene in a high speed mixer. The trace of resulting insoluble material was removed by filtration. The benzene solution was concentrated to one tenth its volume by vacuum evaporation, and the concentrated solution was poured into a tenfold volume of methanol to give polyesterstyrene powder.

Separation of β-Propiolactone Homopolymer from Polymer Mixtures

For polymers from acrylonitrile copolymerized with β-propiolactone (I and II), both of the following two methods were performed in order to separate poly-β-propiolactone homopolymer.

Reprecipitation. A 1-g portion of polymer was dissolved in 10 ml of *N*,*N*-dimethylformamide. The solution was poured into strongly agitated chloroform in a high speed mixer. The precipitate was filtered, washed with hot chloroform, and dried *in vacuo* at room temperature for a few days.

Extraction. A 1-g portion of polymer and 100 ml of chloroform were placed in a flask equipped with a condenser and refluxed for 5 hr. The insoluble material was filtered, washed with hot chloroform, and dried at room temperature for a few days. The extracted polymer residue was retreated by the same method.

For polymers from styrene copolymerized with β-propiolactone (III and IV), the already mentioned aftertreatment on the described polymerization procedure itself was a method of separating poly-β-propiolactone homopolymer.

Polymer Characterization and Analysis

Compositions of the polyesteracrylonitriles (I and II) were calculated from the elementary analytical data for carbon and nitrogen, and those of polyesterstyrenes (III and IV) were calculated from the carbon contents. Though most of the polyesteracrylonitriles did not melt in the sense of flow or softening, they showed optical birefringence. The temperature at which this birefringence disappeared was observed through a pair of crossed polaroids and defined as the crystalline melting point. Polyesterstyrenes did not show birefringence, so only the flow temperatures were observed with a microscope. Solution viscosities in *N*,*N*-dimethylformamide for polyesteracrylonitriles and in chloroform for polyesterstyrenes were measured at 30°C by using Ubbelohde viscometers. Potassium bromide tablets of polymer powder were used for infrared measurement, powder for x-ray diffraction, and dimethyl sulfoxide solution for NMR studies. Films were prepared from polyesteracrylonitriles by bulk polymerization, heating the *N*,*N*-dimethylformamide solution on a glass plate at 80°C in a vacuum below 5 mm Hg for 3 hr. Films of polyesterstyrenes were prepared by heating the chloroform solution on a glass plate at 40°C for 1 hr. Film formation was attempted for blended polymers of high molecular weight poly-β-propiolactone with polyacrylonitrile or with polystyrene under the

same conditions as mentioned above. A film of poly-β-propiolactone itself could be formed by heating a chloroform solution on a glass plate at 40°C at atmospheric pressure for 1 hr.

RESULTS AND DISCUSSION

Polymerizability

As shown in Figure 1, in the copolymerizations I, III, and IV, all of which were performed without solvent, the polymer yield increased with increasing f_1 value. On the other hand, in copolymerization II which was carried out in *N*,*N*-dimethylformamide, the polymer yield was over 75% over the whole f_1 range; the high yield is due to the competing ionic polymerization of β-propiolactone as will be discussed later. The polymer yield of I (AN–βPL) curves far over the curve of the theoretical 100% yield of acrylonitrile homopolymer for the total monomer feed, while the polymer yields of III and IV (ST–βPL) curve far below the curve of the theoretical 100% yield of styrene homopolymer for the total monomer feed. Thus the rate of

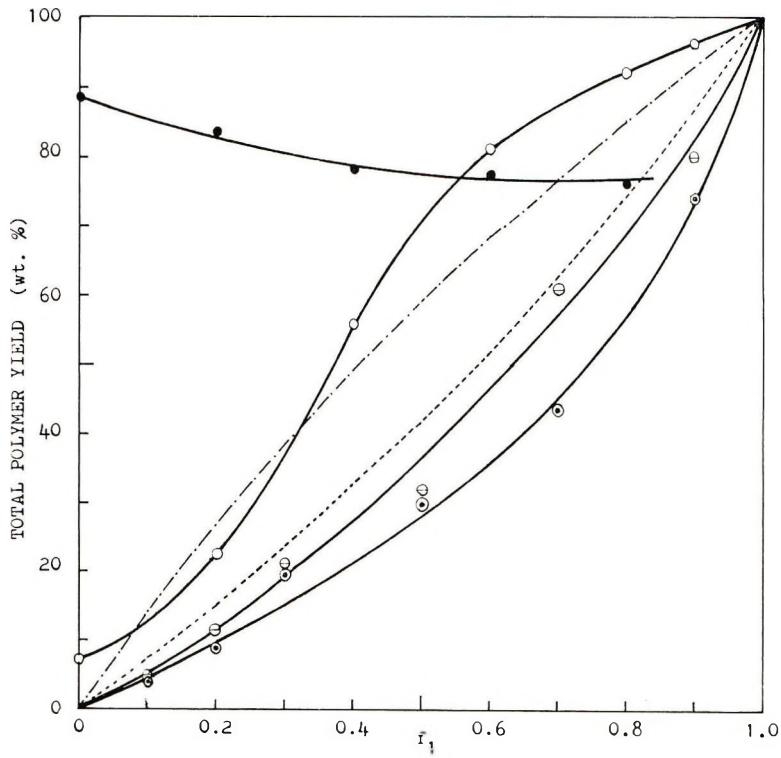

Fig. 1. Total polymer yield vs. initial monomer feed for the copolymerizations: (○) AN–βPL with AIBN without solvent at 50°C for 42 hr (I); (●) AN–βPL with AIBN in DMF at 50°C for 42 hr (II); (⊙) ST–βPL with AIBN without solvent at 50°C for 48 hr (III); (⊖) ST–βPL with BPO without solvent at 80°C for 48 hr (IV); (---) theoretical 100% yield of AN per total feed, (–.–) theoretical 100% yield of ST per total feed.

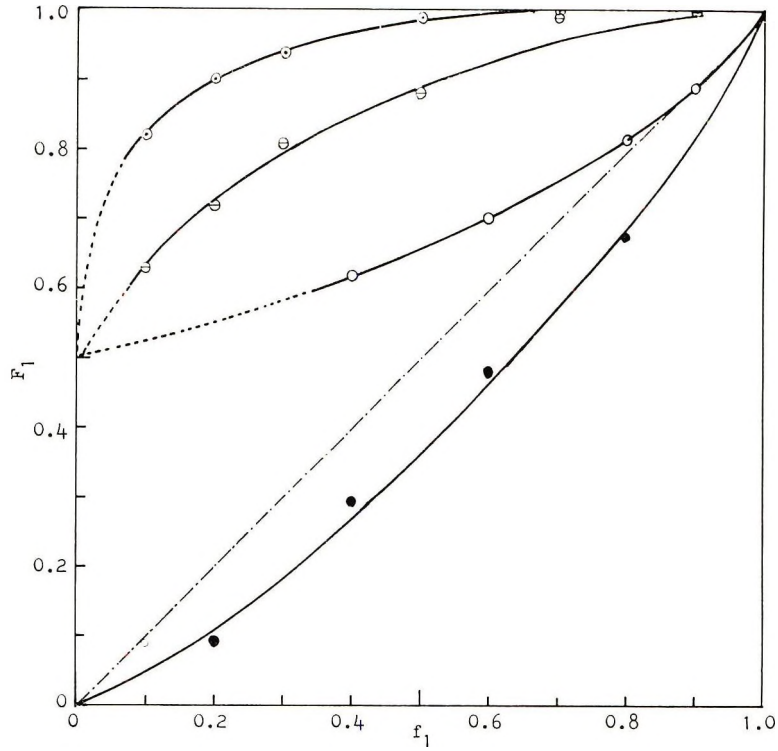

Fig. 2. Polymer composition vs. initial monomer feed for the copolymerizations: (○) AN–βPL with AIBN without solvent at 50°C (I); (●) AN–βPL with AIBN in DMF at 50°C (II); (⊙) ST–βPL with AIBN without solvent at 50°C (III); (⊖) ST–βPL with BPO without solvent at 80°C (IV).

polymerization of system I is much greater than those of III and IV. The yield of the copolymer in IV was higher than that of the copolymer in III, i.e., a higher temperature gave a higher yield. The 6.92% yield at $f_1 = 0$ of I is due to the small contribution of ionic homopolymerization of β-propiolactone. A homopolymerization of β-propiolactone without solvent or initiator but with 2.50 g of hydroquinone per mole of β-propiolactone gave 2.17% of poly-β-propiolactone. Another homopolymerization under the same conditions but with the addition of 0.001% of acrylic acid gave 5.93% of poly-β-propiolactone. Probably a trace of impurity such as acrylic acid may have caused an ionic homopolymerization of β-propiolactone. Homopolymerizations of β-propiolactone with and without 0.500 g of α,α′-azobisisobutyronitrile in 300 ml of chloroform per 1 mole of β-propiolactone gave no polymer. Copolymerizations by the same condition gave no polymer either. Thus chloroform worked as an inhibitor. Copolymerizations, at $f_1 = 0.2$, 0.5, and 0.7 with 0.500 g of hydroquinone per mole of the total monomer without solvent or initiator gave no polymer. These results indicate that the copolymerization proceeds by a radical mechanism instead of an ionic mechanism. β-Propiolactone cannot homopolymerize

radically, so that its rate constant k_{22} should equal zero. Actually, as shown in Figure 2 and Table II, the monomer reactivity ratios r_2 for the bulk polymerizations I, III, and IV are all zero, which is well understood since $r_2 = k_{22}/k_{21} = 0$. A homopolymerization of β-propiolactone without initiator in 300 ml of *N*,*N*-dimethylformamide gave 83.22% of poly-β-propiolactone. Copolymerizations under the same condition per mole of the total monomers gave only poly-β-propiolactone homopolymer. The apparent monomer reactivity ratios of II in Table II, $r_1 = 0.45$ and $r_2 = 1.25$ are thus understood to be due to the competing ionic homopolymerization of β-propiolactone. The $r_1 = 0.84$ of acrylonitrile and $r_1 = 6.2$ at 50°C, $r_1 = 32$ at 80°C of styrene show that acrylonitrile copolymerizes better than styrene. In order to discuss this difference in polymerizability, the Alfrey-Price *e*, *Q* values would be helpful. It would be impossible to obtain *e*, *Q* values if the r_2 were absolute zero. The r_2 in Table II is, however, considered to be the zero with experimental errors. With the aid of the basic *e*, *Q* values of styrene, $e = -0.8$, $Q = 1.0$, and those of acrylonitrile–styrene copolymerization, $e = 1.2$, $Q = 0.44$; *e*, *Q* values of β-propiolactone obtained are $e = -1.0$, $Q = 0.26$ at 50°C from the r_1 values of I and III in Table II. These *e*, *Q* values give small values of r_2 of I and III near zero within the experimental errors. The better copolymerizability of β-propiolactone with acrylonitrile than with styrene is explained well by the *e*, *Q* values: (a) electron-rich (negative *e* value) β-propiolactone and its radical like electron-poor (positive *e* value) acrylonitrile and its radical; (b) β-propiolactone (with lower resonance stability, *Q*) likes acrylonitrile whose *Q* values is nearer to that of β-propiolactone than that of styrene is.

TABLE II
Monomer Reactivity Ratios

Experiment no.	Comonomer	r_1	r_2	r_1r_2
I (at 50°C without solvent)	Acrylonitrile	0.84	0.00	0.00
II (at 50°C in DMF)[a]		0.45	1.25	0.56
III (at 50°C with AIBN)	Styrene	6.2	0.0	0.0
IV (at 80°C with BPO)		32	0	0

[a] Apparent values. Values of the monomer reactivity ratios accurate to only two digits.

Solution Viscosity and Melting Point or Flow Temperature

As shown in Figure 3, the intrinsic viscosities of all copolymers increase almost linearly with increasing f_1. The bulk copolymerization of acrylonitrile (I) gave very high viscosities of the resulting copolymers, while the copolymerization of acrylonitrile in *N*,*N*-dimethylformamide (II) and the copolymerizations of styrene (III and IV) gave lower viscosities. The higher temperature copolymerization of styrene (IV) gave lower viscosities than the lower temperature copolymerization (III). As shown in Figure 4,

the melting points of copolymers obtained in experiments I and II increased with increasing f_1 and F_1 values. The melting points of the copolymers polymerized without solvent (experiment I) were higher and increased smoothly with increasing f_1 and F_1, while those of the copolymers polymerized in *N*,*N*-dimethylformamide rose discontinuously from low to high melting points at $f_1 = 0.5$ and $F_1 = 0.3$–0.5. This is because the former polymers are pure copolymers and the latters are copolymers blended with

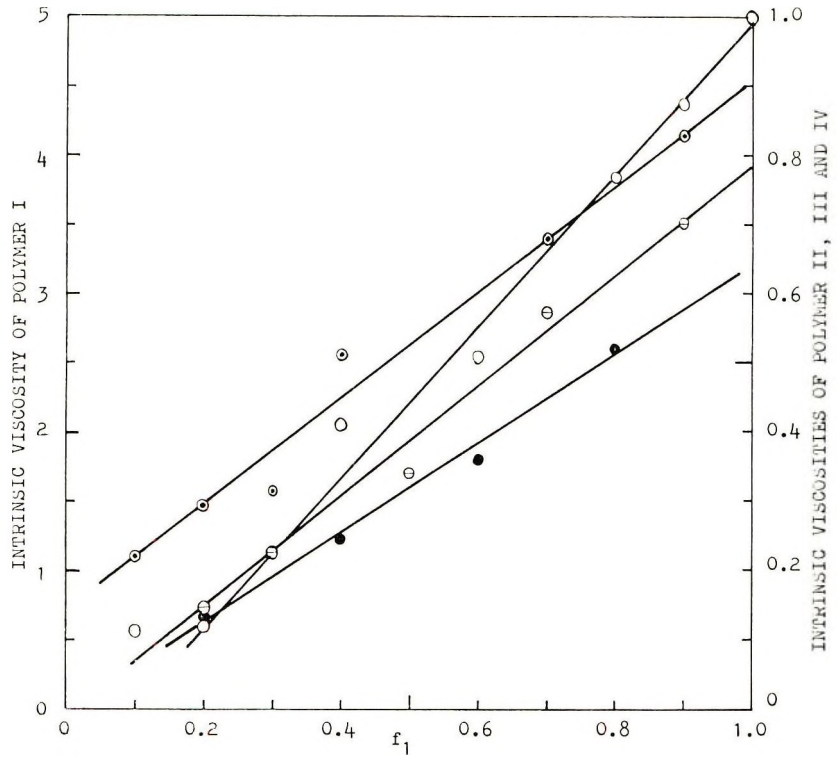

Fig. 3. Solution viscosity vs. monomer feed for the copolymerizations: (○) AN–βPL with AIBN without solvent at 50°C (I); (●) AN–βPL with AIBN in DMF at 50°C (II); (⊙) ST–βPL with AIBN without solvent at 50°C (III); (⊖) ST–βPL with BPO without solvent at 80°C (IV).

poly-β-propiolactone homopolymer. On the copolymerization of acrylonitrile in *N*,*N*-dimethylformamide (II) at an initial monomer feed $f_1 < 0.5$, excess of β-propiolactone gave much poly-β-propiolactone homopolymer by a competing ionic polymerization mechanism lowering the melting points of the resulting polymer mixtures, while in the range of $f_1 > 0.5$ the radical copolymerization surpassed the ionic polymerization to give copolymers blended with much less poly-β-propiolactone homopolymer. The flow temperatures of the copolymers of styrene (III and IV) were between 120 and 130°C.

Separation of Poly-β-propiolactone Homopolymer from Polymer Mixtures

As shown in Table III, poly-β-propiolactone homopolymer was almost completely removed from blended polymers of polyacrylonitrile and poly-β-propiolactone homopolymer both by reprecipitation and extraction, while poly-β-propiolactone units still remained in full amounts in the extracted residues of the copolymers I and II. The infrared absorption spectra of the extracted polymers from the copolymers I showed a nitrile band at 2260 cm^{-1}, while those from the copolymers II showed no nitrile band. The F_1 values of the latter copolymers increased after reprecipitation and ex-

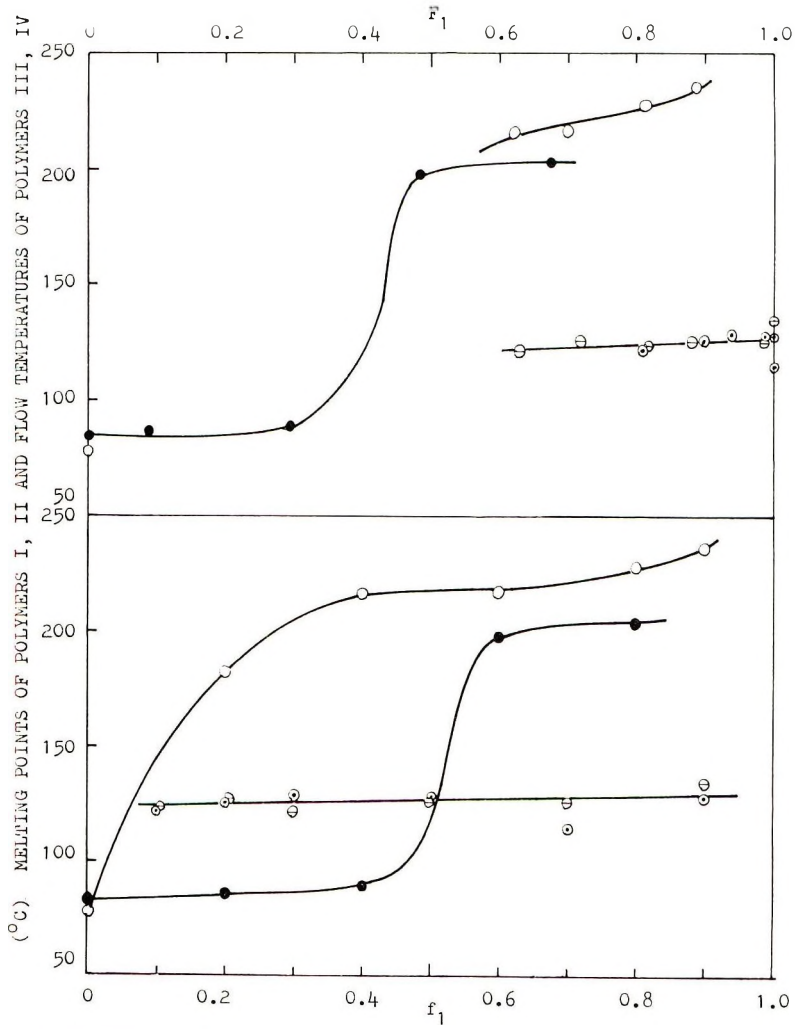

Fig. 4. Melting point and flow temperature vs. monomer feed and polymer composition of copolymers: (○) AN–βPL with AIBN without solvent at 50°C (I); (●) AN–βPL with AIBN in DMF at 50°C (II); (⊙) ST–βPL with AIBN without solvent at 50°C (III); and (⊖) ST–βPL with BPO without solvent at 80°C (IV).

traction, while in the former copolymers there were almost no changes of F_1 values. Thus Table III and Figure 6 prove that the polymers by the bulk polymerization I are pure copolymers and the polymers polymerized in *N*,*N*-dimethylformamide (experiment II) are copolymers blended with poly-β-propiolactone. Copolymers of styrene (III and IV) are also chemically combined copolymers, since poly-β-propiolactone homopolymer therein was removed on precipitation.

TABLE III
Changes of Polymer Composition after Reprecipitation and Extraction by Chloroform

Polymer no.	Original polymer, F_1	Polymer after reprecipitation			Polymer after extraction		
		Insoluble		Soluble, F_1	Insoluble		Soluble, F_1
		wt-%	F_1		wt-%	F_1	
Blend polymer[a]	0.900	88.8	0.990	0.00	87.6	0.991	0.00
	0.500	45.0	0.965	0.00	44.4	0.984	0.00
	0.200	17.9	0.977	0.00	18.6	0.992	0.00
I	0.815	89.6	0.803	0.871	94.4	0.801	0.977
	0.700	77.1	0.783	0.387	69.6	0.715	0.665
II	0.672	74.9	0.910	0.00	75.6	0.916	0.00
	0.484	58.9	0.798	0.00	59.3	0.817	0.00
	0.295	52.3	0.502	0.02	61.4	0.420	0.00
	0.087	Trace	—	—	Trace	—	—

[a] Prepared by precipitation in water of blended polymers of polyacrylonitrile ($[\eta]$ = 1.20) and poly-β-propiolactone ($[\eta]$ = 0.49) dissolved in *N*,*N*-dimethylformamide.

In Figure 5, the conversion of each monomer for a given monomer feed is shown calculated from the data in Figures 1 and 2 and Table III. Acrylonitrile and styrene have increasing conversion curves with increasing f_1 value in all copolymerizations (I, II, III, and IV). On the pure radical copolymerizations (I, III, and IV), β-propiolactone shows linear increasing conversion starting from zero, with increasing f_1. Meanwhile, an application of the general treatment of rates of copolymerization[5] gives eqs. (1) and (2)

$$R_1 = -d[M_1]/[M_1]dt = (I^{1/2}/YK)(r_1f_1 - f_1 + 1) \quad (1)$$

$$R_2 = -d[M_2]/[M_2]dt = (I^{1/2}/YK)f_1 \quad (2)$$

where I is the overall rate of initiation, Y is a function of f_1,

$$Y = (Af_1^2 + Bf_1 + C)^{1/2}$$

where A, B, and C are constants consisting of rate constants of copolymerization, and K is a constant related by $[M_1]_0 + [M_2]_0 = K$, in which $[M_1]_0$ is the initial monomer concentration of acrylonitrile or styrene and $[M_2]_0$ is that of β-propiolactone. K is technically taken as constant and r_2 is experimentally zero to give the above relations. Now known from the equation (2i):

$$\lim_{f_1 \to 0} R_2 = 0 \quad (3)$$

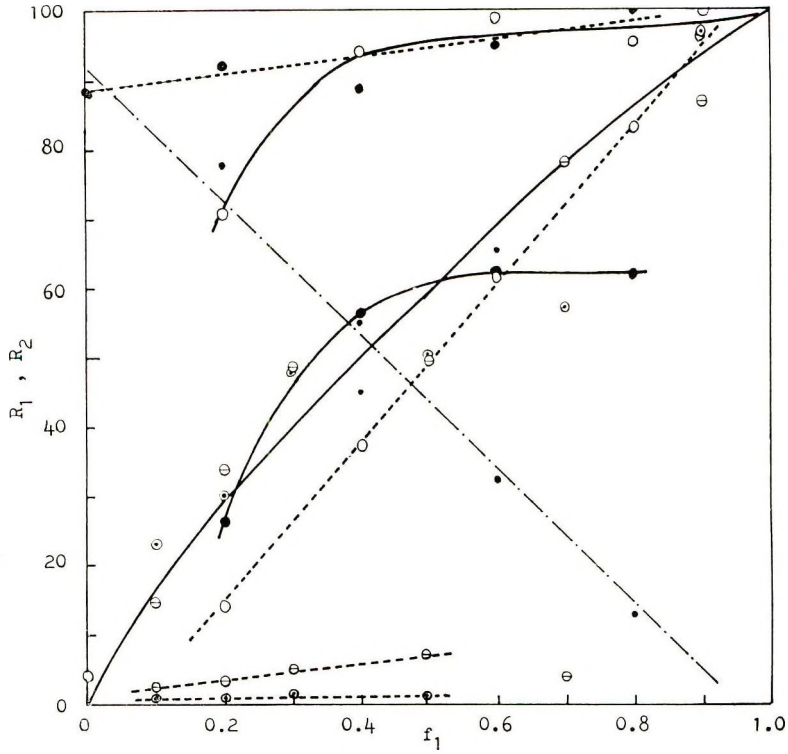

Fig. 5. Conversion of each monomer to polymer for the corresponding monomer feed, vs. monomer feed for the copolymerizations: (○) AN–βPL with AIBN without solvent at 50°C (I); (●) AN–βPL with AIBN in DMF at 50°C (II); (⊙) ST–βPL with AIBN without solvent at 50°C (III); (⊖) ST–βPL with BPO without solvent at 80°C (IV); (——) R_1, the conversion of AN or ST per corresponding initial monomer (AN or ST) feed; (--) R_2, the conversion of βPL per initial βPL feed; (–·–) the conversion of βPL to poly-β-propiolactone homopolymer for copolymerization II.

which is consistent with the experimental result, $r_2 = 0$. From Figure 5, it will experimentally be concluded:

$$\lim_{f_1 \to 0} R_1 = 0 \tag{4}$$

At $f_1 = 0$, R_1 equals $I^{1/2}/(KC^{1/2}) = I^{1/2}/(Kk_{t22}^{1/2}/k_{p21})$, so either I should be zero or k_{t22} should be infinitely large, since K and k_{p21} are definite. The former is correct, since the latter is not possible so far as a steady-state holds.

From eqs. (1) and (2), the eqs. (5) and (6) are derived:

$$\lim_{f_1 \to 1} R_1 = (I^{1/2}/YK)r_1 \tag{5}$$

$$\lim_{f_1 \to 1} R_2 = I^{1/2}/YK \tag{6}$$

where

$$Y = (A + B + C)^{1/2} = k_{t11}^{1/2}/k_{p12}$$

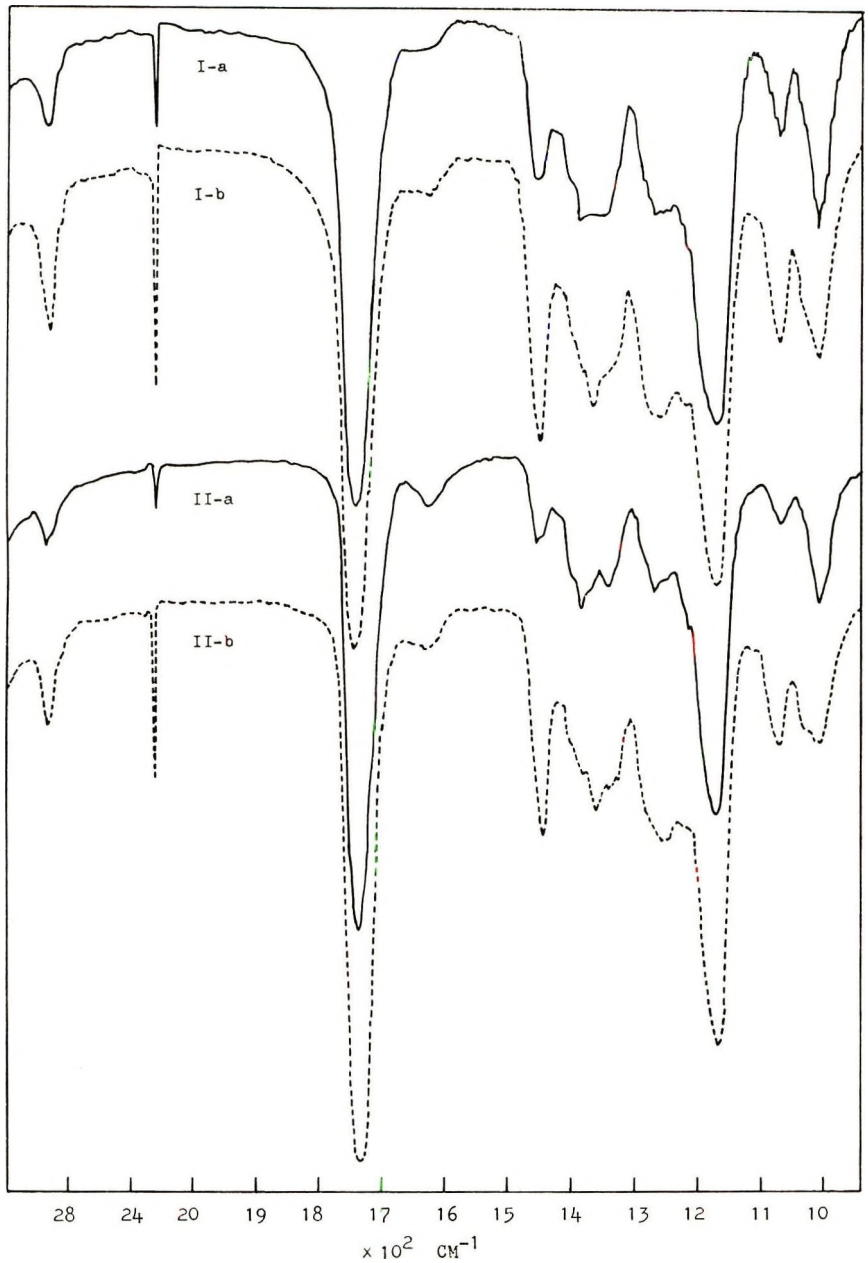

Fig. 6. Infrared absorption spectra of copolymers: (I-a) without solvent with 0.5 g AIBN/mole total monomers, (f_1 = 0.600, F_2 = 0.700); (I-b) residue of copolymer I-a extracted with hot chloroform (F_2 = 0.715); (II-a) in 300 ml DMF with 0.5 g AIBN/mole total monomers (f_1 = 0.600, F_1 = 0.484); (II-b) residue of copolymer II-a extracted with hot chloroform (F_1 = 0.817).

According to the eqs. (5) and (6), the R_1 value should be r_1-fold the R_2 value, which is well satisfied in copolymerizations I, III, and IV. Thus copolymerizations I, III, and IV all follow the radical polymerization mechanism. In copolymerization II, which has a contribution from ionic polymerization, the conversion of poly-β-propiolactone homopolymer decreased with increasing f_1 value. The conversion of acrylonitrile, however, follows a curve like that of the copolymerization I, which indicates that acrylonitrile itself is copolymerized radically. On separating the radical component like this, a rough r_1 value is calculated to be 1–1.3 for copolymerization II, a value which is near that of copolymerization I.

Structures of the Copolymers

As shown in Figure 6, both copolymers before and after extraction have characteristic ester absorptions at 1745 cm^{-1} (C=O) stretching) and 1170 cm^{-1} (C–O stretching). The relative intensities of the both absorptions over that of the nitrile band at 2260 cm^{-1} are greater after extraction.

As shown in Figure 7, polyacrylonitrile has a triplet at 7.95 (methylene) and a quartet at 6.9 (methyne), and poly-β-propiolactone has a triplet at 7.4 (α-methylene) and another triplet at 5.7 (β-methylene). If the copolymer I is a physical mixture of polyacrylonitrile and poly-β-propiolactone, it should have additive chemical shifts of the two polymers, i.e., three triplets and one quartet. The copolymer I has a chemical shift at 8.5, which is of a methylene group linked with the adjacent two carbon atoms. As the spectrum of copolymer I was taken at 80°C at a low concentration but at high viscosity (because copolymer I was difficult to dissolve in dimethyl sulfoxide), the spin-spin splitting of the chemical shifts are quite vague. At such a high concentration of dimethyl sulfoxide, the carbon 13 satellite signals appear at 8.6 and 6.3, and the spinning side band signals appear at 7.9 and 7.0. The signal at 7.95 is a chemical shift of a methylene at the β-position to a nitrile. This methylene is also adjacent to a carbon atom but not to an oxa or carbonyl group. The signal at 6.45 is probably a triplet overlapped with a carbon 13 satellite at 6.3. This triplet is probably due to a methyne adjacent to nitrile and carbonyl groups. The triplet at 5.7 is due to a methylene at the α-position to a carboxyl oxa linkage.

For the free radical-initiated ring opening of β-propiolactone there are formally eight possibilities of ring opening, but five are ruled out by the fact that the copolymer had only ester linkages but no ether or ketonic carbonyl, and by the organochemical assumptions that the fission of alkyl-alkyl linkage is quite difficult and that an oxy carbonyl radical ($-OCO\cdot$) is too unstable. Then the three types of ring opening shown in eqs. (7)–(9) are most likely.

(7)

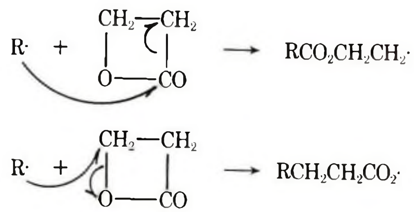

(8)

(9)

The structure of the resulting copolymer (for example, for copolymerization I) should, accordingly, be one of the three: A, B, or C.

$$\text{-[-OCOCH}_2\text{CH}_2\text{CH}_2\underset{\text{CN}}{\text{CH}}\text{-]-}_x$$

A

$$\text{-[-CO}_2\text{CH}_2\text{CH}_2\text{CH}_2\underset{\text{CN}}{\text{CH}}\text{-]-}_x$$

B

$$\text{-[-CH}_2\text{CH}_2\text{CO}_2\text{CH}_2\underset{\text{CN}}{\text{CH}}\text{-]-}_x$$

C

Now that the structure of the copolymer has been determined to be of the structure B, the ring-opening mechanism of β-propiolactone is by the mechanism (9). The NMR spectra could not be explained by the structures A and C.

Beer's law was applied to the infrared absorption spectra of copolymers from systems I and II and the blended mixtures of polyacrylonitrile and poly-β-propiolactone. Equation (10) can be easily derived by taking optical densities $D_{C=O}$ (the carbonyl stretching of the ester band at 1745 cm^{-1}) and $D_{C\equiv N}$ (the stretching of the nitrile cyano group at 2260 cm^{-1}) and the corresponding molecular extinction coefficients $\kappa_{C=O}$ and $\kappa_{C\equiv N}$.

$$D_{C=O}/D_{C\equiv N} = \kappa_{C=O}\, F_2/\kappa_{C\equiv N}\, F_1 \qquad (10)$$

As shown in Figure 8, eq. (10) holds good in every case. From each gradient of the three straight lines, the following molecular extinction coefficient ratios are given: $\kappa_{C=O}/\kappa_{C\equiv N}$ for copolymer I, 152; for copolymer II, 69.5; for blend polymer, 56.3.

From the above result it is known that physical blending does not decrease the intensity of the stretching vibration of the cyano group, while α-carboxy-substituted nitrile of the structure B decreases the intensity to a great extent as was pointed out by Bellamy.[6] The molecular extinction coefficient ratio of the copolymer II is between those of the copolymer I and the blend polymer. This is consistent with the fact that the copolymer II is a mixture of the copolymer of the structure B and poly-β-propiolactone.

On the basis of the chemical structure of the copolymer as discussed above, the corresponding physical or crystalline structure should naturally be different from the additive structure of polyacrylonitrile and poly-β-

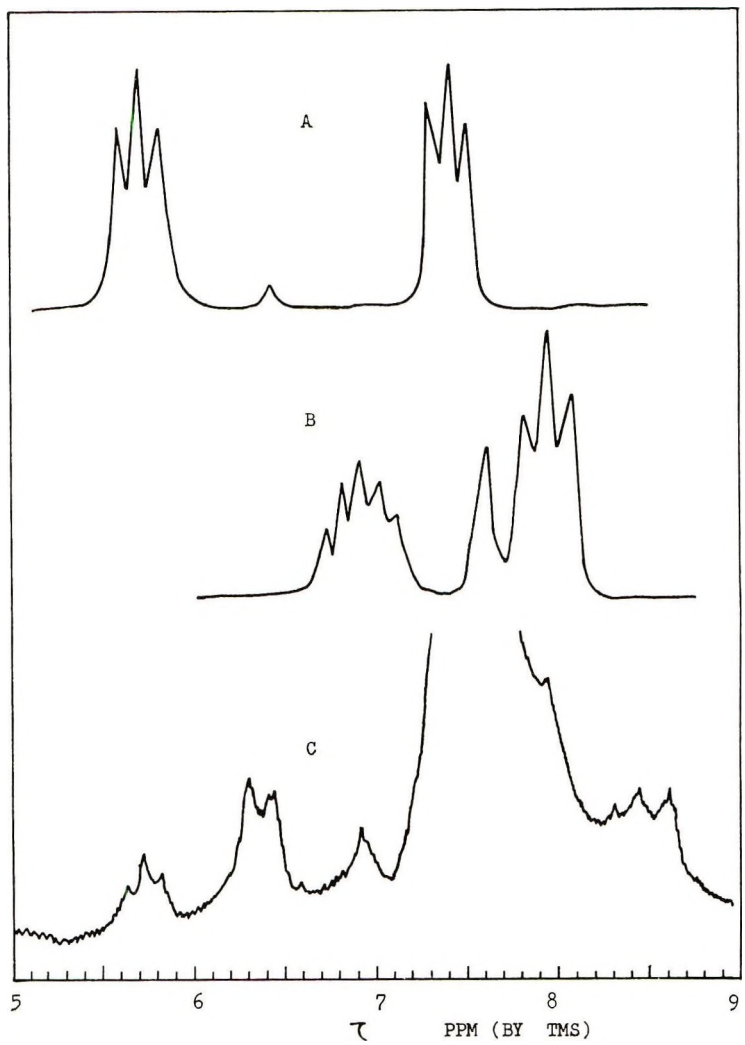

Fig. 7. Nuclear magnetic resonance of a copolymer I compared with those of polyacrylonitrile and poly-β-propiolactone: (*A*) --- poly-β-propiolactone, (*B*) polyacrylonitrile, and (*C*) copolymer I ($f_1 = 0.400$, $F_1 = 0.610$) polymerized without solvent with 0.5 g AIBN/mole total monomers.

propiolactone, in the case of the copolymers I and II. In the case of the copolymerizations III and IV which have high monomer reactivity ratios r_2 and the products of which have a smaller quantity of combined β-propiolactone units, the x-ray diffraction patterns were all amorphous, just like that of polystyrene. As shown in Figure 9, the copolymer IA polymerized without solvent ($f_1 = 0.600$, $F_1 = 0.700$) showed two peaks, one at 17.1° which is the same peak as that of polyacrylonitrile, and the other at 23.0° which should be a new peak due to the chemical structure B. Although 23.0° is almost the same angle as one of the peaks of poly-β-propiolactone,

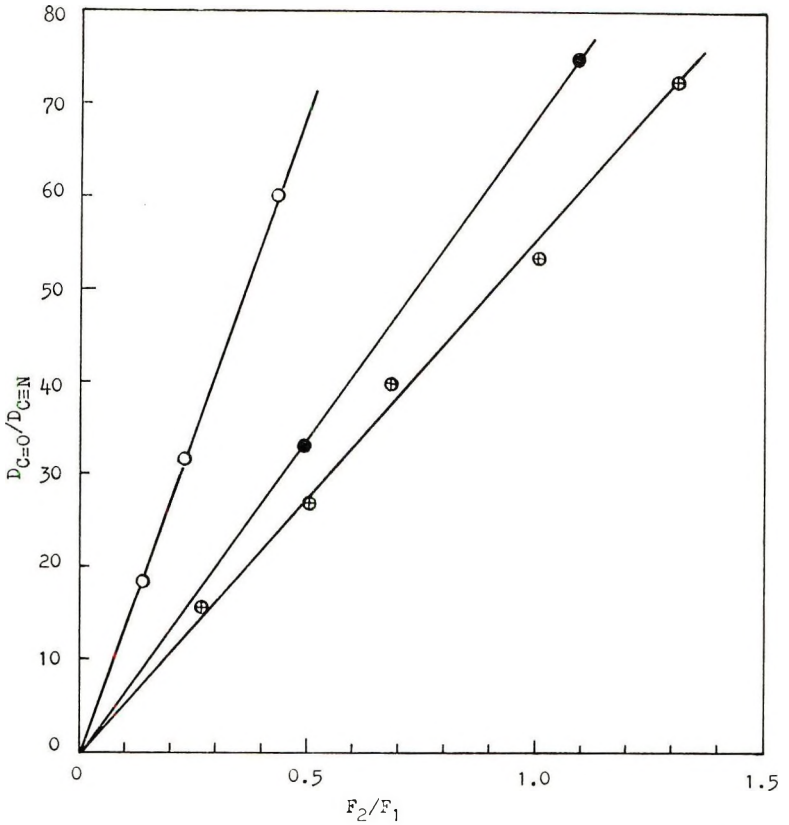

Fig. 8. Optical densities of (⊕) blended mixture of polyacrylonitrile and poly-β-propiolactone; (○) copolymers polymerized without solvent with 0.5 g AIBN/mole total monomers; (●) copolymer obtained in 300 ml DMF with 0.5 g AIBN/mole total monomers.

the typical highest peak at 21.0° of poly-β-propiolactone is not observed at all, so that this peak at 23.0° should be considered to be a new peak attributed to structure B. Copolymer IB ($f_1 = 0.800$, $F_1 = 0.815$) had only one peak at 17.1°, which is the same peak as that of polyacrylonitrile. The loss of the 23.0° peak in the copolymer IB is due to the smaller sequence length of the alternating units B. Copolymer IIA polymerized in *N*,*N*-dimethylformamide ($f_1 = 0.800$, $F_1 = 0.672$) had peaks at 17.0° which is attributed to the polyacrylonitrile unit, 21.0° which is attributed to the poly-β-propiolactone unit, 22.2° (a new peak), and 23.1°, which is either a new peak as mentioned for copolymer IA or a peak of the poly-β-propiolactone unit. The copolymer IIB had three peaks, at 21.0°, 23.1°, and 30.1°, all of which are quite the same as those of poly-β-propiolactone, which, as can be well understood from its small F_1 value, is due to the high content of poly-β-propiolactone homopolymer. The above results proved that the copolymers I are chemically united copolymers containing alternating copolymer units B without poly-β-propiolactone units.

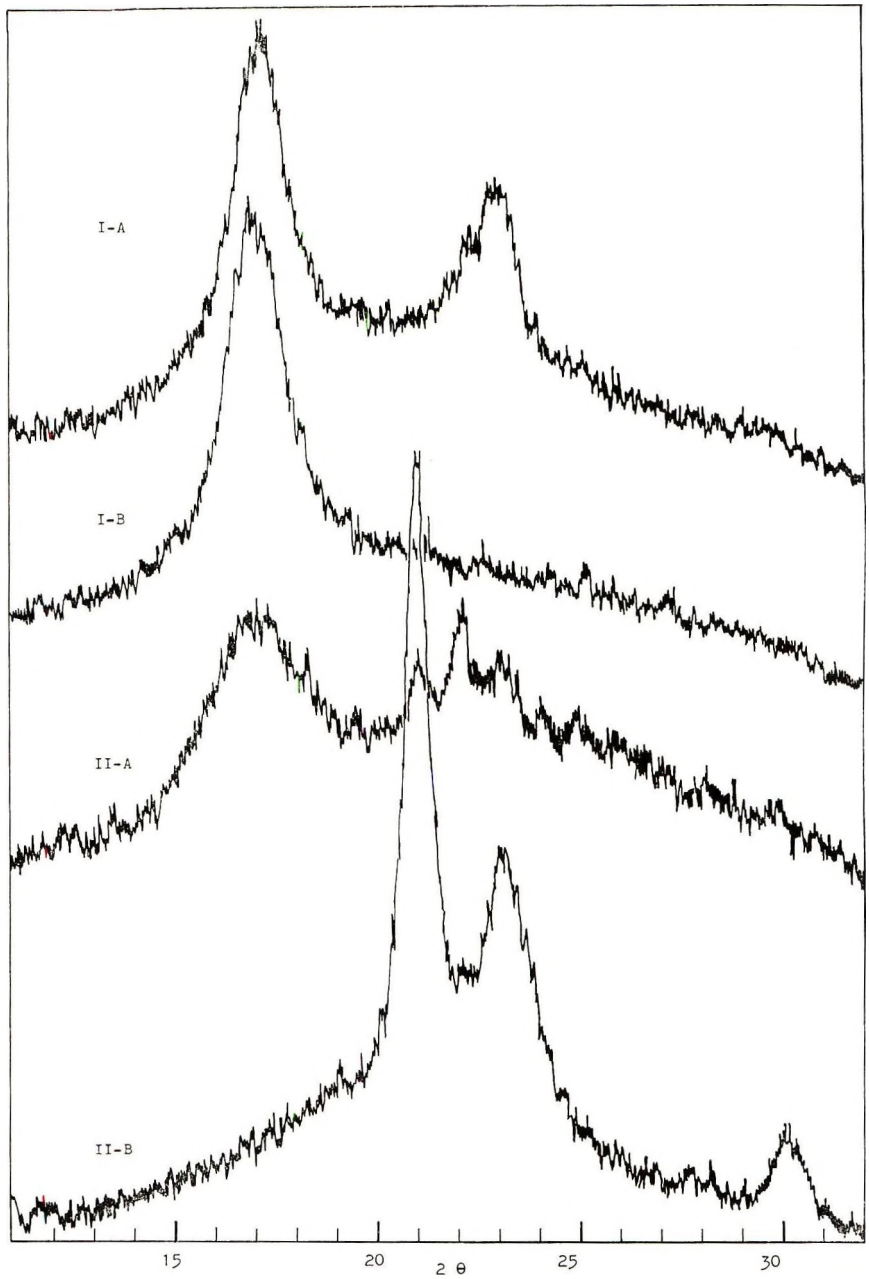

Fig. 9. X-ray diffraction patterns of copolymers obtained under various conditions: (I-A) without solvent with 0.5 g AIBN/mole total monomers ($f_1 = 0.600$, $F_1 = 0.700$); (I-B) without solvent with 0.5 AIBN/mole monomer ($f_1 = 0.800$, $F_1 = 0.815$); (II-A) in 300 ml DMF with 0.5 g AIBN/mole total monomers ($f_1 = 0.800$, $F_1 = 0.672$); (II-B) in 300 ml DMF with 0.5 g AIBN/mole monomer ($f_1 = 0.200$, $F_1 = 0.087$).

The films prepared from the blended mixtures of polyacrylonitrile or polystyrene with poly-β-propiolactone homopolymer were all opaque and very brittle. The polyacrylonitrile or polystyrene and poly-β-propiolactone phases were separated. The copolymers I, III and IV formed transparent films, and the copolymers I especially, formed quite tough films, which, however, gradually became brittle on keeping in air for about a week. This weakening may be due to a kind of depolymerization sometimes observed with polymers containing ester or ether linkages with small numbers of carbon atoms.

CONCLUSION

The result thus far discussed can be reduced to a simple conclusion, namely, the behavior on the free-radical copolymerization of acrylonitrile and β-propiolactone can be explained by a copolymerization mechanism, and the structure of the copolymer resulting may be as shown for the case of copolymerization of acrylonitrile with β-propiolactone:

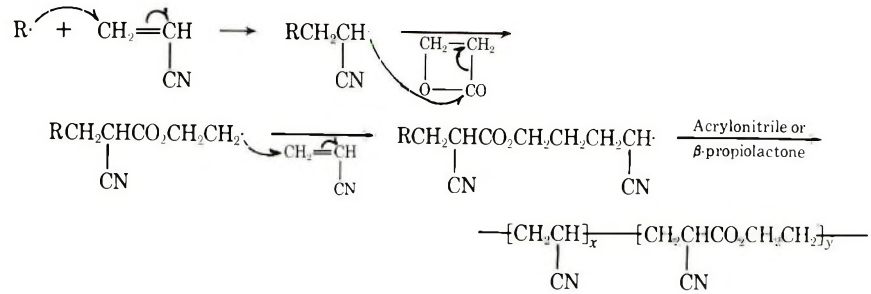

The initiation preferably gives acrylonitrile radicals but not β-propiolactone radicals. A propagating terminal acrylonitrile radical attacks the acyl group of β-propiolactone to cleave the acyl–alkyl linkage. The radicalophilic property of the acyl group of β-propiolactone may be due to the distorted π-bond because of the ring strain and of the distorted *p*-electrons of the neighboring oxygen atom.

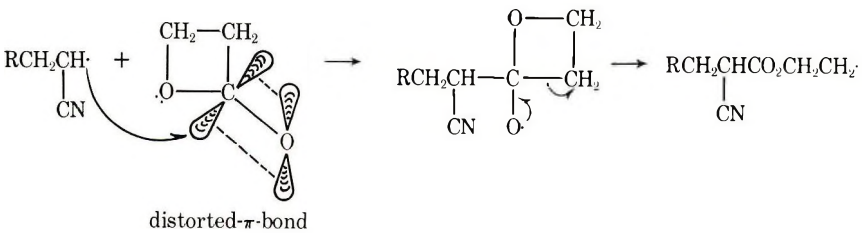

The resulting β-propiono acyl radical is unstable and splits from the α-carbon, similar to the mechanism of Kolbe's decarboxylation reaction.

Details of the competing ionic homopolymerization of β-propiolactone, will be discussed in a subsequent paper in this journal.

References

1. K. Hayashi, Y. Kitanishi, M. Nishi, and S. Okamura, *Makromol. Chem.*, **47**, 230, 237 (1961).
2. C. David, F. Provoost, and G. Verdyn, *Polymer*, **4**, 341 391 (1963).
3. M. Magat, *Bull. Inst. Text. France*, **No. 103**, 1175 (1962).
4. J. E. Magoffin and H. J. Hagemeyer, Jr., U.S. Pat. 2,487,885 (Nov. 15, 1949).
5. C. Walling, *J. Amer. Chem. Soc.*, **71**, 1930 (1949).
6. L. J. Bellamy, *The Infra-red Spectra of Complex Molecules*, Wiley, New York, 1958, p. 266.

Received July 20, 1970
Revised May 12, 1971

JOURNAL OF POLYMER SCIENCE: PART A-1 VOL. 9, 2933–2948 (1971)

Cationic Polymerization of Cyclic Dienes. X. Cationic Polymerization of 1-Vinylcyclohexene and 3-Methyl-1,3-pentadiene*

KAZUO HARA, YUKIO IMANISHI, TOSHINOBU HIGASHIMURA,
Department of Polymer Chemistry, Kyoto University, Kyoto, Japan, and MIKIHARU KAMACHI, *Department of Polymer Chemistry, Osaka University, Toyonaka, Japan*

Synopsis

1-Vinylcyclohexene (VCH), which has one of the double bonds in the ring and the other outside the ring, was synthesized and polymerized by cationic catalysts. The reactivity of VCH was very large in the polymerizations catalyzed by boron trifluoride etherate (BF_3OEt_2) and stannic chloride–trichloroacetic acid complex. Similar to other cyclic dienes, the polymerization of VCH was a nonstationary reaction having a very fast initiation step. The polymerization proceeded by either a 1,2- or a 1,4-propagation mode in which vinyl group was always involved. Particularly when BF_3OEt_2 was used as a catalyst, an intramolecular proton or an intramolecular hydride ion transfer reaction took place, resulting in the formation of methyl groups in the polymer. The degree of polymerization of polymer formed was about 10. This indicates the preponderance of monomer transfer reaction. To investigate the reason for the high reactivity of cyclic dienes, cationic copolymerizations of VCH and 3-methyl-*cis*/*trans*-1,3-pentadiene (*cis*/*trans*-MPD) was carried out. The relative reactivity of monomers decreased in the order VCH > *trans*-MPD > *cis*-MPD. On the other hand, the resonance stabilization of monomers decreased in the order VCH > *trans*-MPD > *cis*-MPD. Therefore, it could be considered that the monomer reactivity is mainly determined by the stability of carbonium ion intermediate. The relative stability of carbonium ion must be VCH > *trans*-MPD > *cis*-MPD. Thus the influence of the conformation of ion on its stability was clearly demonstrated.

INTRODUCTION

The investigations on the cationic polymerization and copolymerization of cyclic conjugated dienes have shown that the cyclic dienes such as cyclopentadiene,[2–8] 1,3-cyclohexadiene[4,9] and 1,3-cyclooctadiene[10] are reactive. The high reactivity of cyclic dienes has been explained in terms of the stability of the cycloalkenyl cation.[7,8]

It seems interesting to investigate the reactivity of conjugated dienes in connection with their structure. Conjugated dienes constitute a group of compounds having different structures (cyclic or linear, *cis* or *trans*, substituted or unsubstituted, etc.) and seem suitable for the study of struc-

* For the previous paper of this series, see Imanishi et al.[1]

ture–reactivity relationships. In the present investigation cationic copolymerization of 1-vinylcyclohexene, which has one of the double bonds in the ring and the other outside the ring, and its linear analog, 3-methyl-*cis*/*trans*-1,3-pentadiene was carried out. 1,3-Cyclohexadiene, which has two double bonds in the ring, was also chosen for comparison, and the influence of the position and the geometric structure of double bond on the reactivity was investigated. It was also attempted to elucidate how the stability of monomer and alkenyl cation is affected by being cyclic.

EXPERIMENTAL

Reagent

1-Vinylcyclohexene was synthesized from 1,2-dibromoethane as a starting material by the procedure described shown schematically

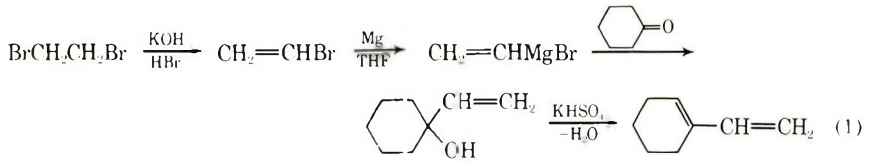

(1)

It was purified by preparative gas chromatography (bp 141–142°C, lit.[13] mp 143–144°C).

1,3-Cyclohexadiene was synthesized from cyclohexanol as a starting material by the procedure reported previously (bp 79–80°C).[9]

3-Methyl-*cis*/*trans*-1,3-pentadiene was synthesized from vinyl chloride as a starting material by the procedure of eq (2).

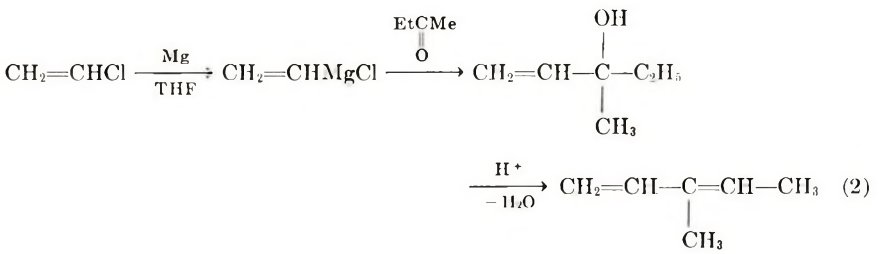

(2)

The fraction boiling at 73–75°C was collected and subjected to gas chromatography (column PEG 400 1.5 m + DNP 1.5 m, column temperature 60°C, carrier gas H_2, 1 kg/cm²). Three peaks were observed at the retention time from air 1.1, 2.75, and 4.5 min. The second peak (substance a) and the third peak (substance b) were collected separately by preparative gas chromatography and subjected to NMR spectroscopy (CCl_4 as solvent, at room temperature) (Fig. 1). The chemical shift of two methyl groups is different in substance a (τ 7.8 ppm and 8.9 ppm), while it is identical in substance b (τ 8.3 ppm). The relationship between the conformation of α,β-unsaturated carbonyl compound and the proton chemical shift[14] sug-

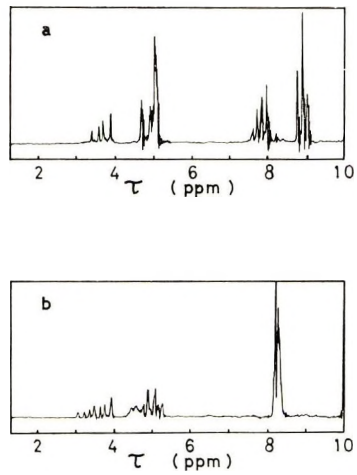

Fig. 1. NMR spectra of substances a and b obtained by preparative gas chromatography of 3-methyl-*cis*/*trans*-1,3-pentadienes. Carbon tetrachloride solution, TMS as an internal standard.

gests that substance a is the *cis* isomer and substance b is the *trans* isomer of 3-methyl-1,3-pentadiene.

A mixture of substances a and b was subjected to the Diels-Alder reaction with maleic anhydride under the reaction condition described by Craig et al.[15] Substance b was consumed many times as fast as the substance a. In view of the high reactivity of the s-*cis* conformation of conjugated dienes in the Diels-Alder reaction,[15] substance a is confirmed to be the *cis* isomer of 3-methyl-1,3-pentadiene and substance b to be the *trans* isomer.

The extent of conjugation between two double bonds of the conjugated dienes was estimated by mass spectrometry.

Commercial 1-methylcyclohexane (guaranteed reagent) was used for mass spectrometry without further purification.

4-Vinylcyclohexene was donated by Mitsubishi Monsanto Chemicals Co. It contained 1,5-cyclooctadiene (less than 2%) as an impurity.

Methylene chloride, dichloroethane, *n*-hexane, and toluene were used as solvents.

Boron trifluoride etherate, stannic chloride, and trichloroacetic acid (TCA) were used as catalysts. They were purified as usual.[5,16]

Procedure

The polymerization was carried out in the usual manner. At suitable time intervals an aliquot of the solution was withdrawn by a syringe and mixed with acetone to stop the polymerization. The acetone-insoluble fraction was filtered, vacuum-dried, and weighed. This procedure determines the gravimetric conversion. In other cases the consumption of mono-

mer was determined by gas chromatography, while the polymerization was carried out in the presence of an added internal standard.

The polymerization of 4-vinylcyclohexene by a Ziegler-type catalyst was carried out as described in the literature.[17]

The structure of the polymers was analyzed by infrared and NMR (CCl_4 or benzene-d_6 as solvent, at room temperature) spectroscopy.

POLYMERIZATION OF 1-VINYLCYCLOHEXENE

Homopolymerization of 1-Vinylcyclohexene

1-Vinylcyclohexene was polymerized under various combinations of solvent and catalyst.

The influence of the initial catalyst concentration $[C]_0$ on the time–conversion curve is shown in Figure 2. In this experiment the conversion

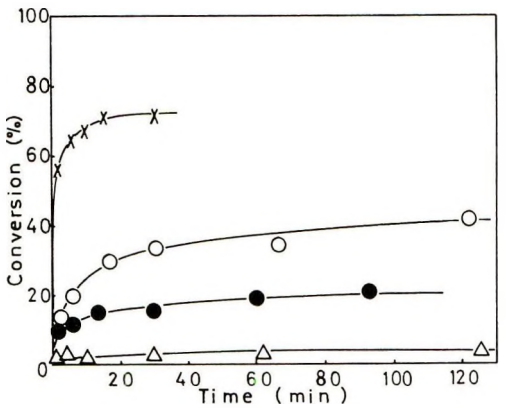

Fig. 2. Effect of catalyst concentration $[C]_0$ on the polymerization of 1-vinylcyclohexene by $SnCl_4$TCA in methylene chloride at 0°C: (×) 19.3 mmole/l.; (○) 9.6 mmole/l.; (●) 4.8 mmole/l.; (△) 1.9 mmole/l. $[M]_0$ = 1.63 mole/l.

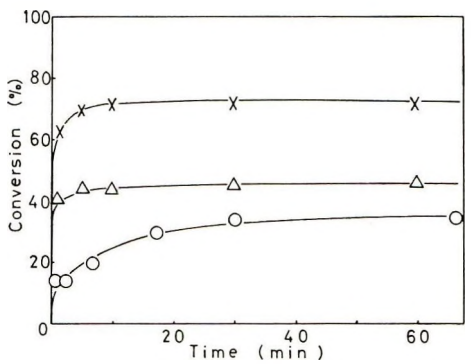

Fig. 3. Effect of monomer concentration $[M]_0$ on the polymerization of 1-vinylcyclohexene by $SnCl_4$TCA in methylene chloride at 0°C; (×) 0.81 mole/l.; (△) 1.22 mole/l.; (○) 1.62 mole/l. $[C]_0$ = 9.6 mmole/l.

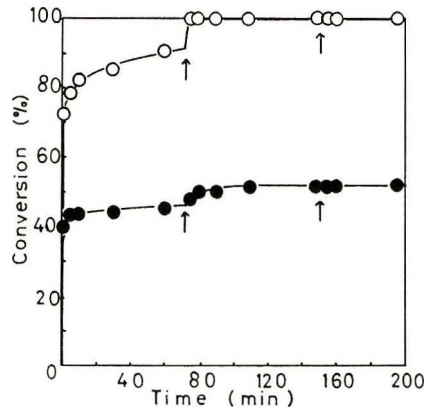

Fig. 4. Formation of acetone-soluble product in the polymerization of 1-vinylcyclohexene by $SnCl_4$TCA in methylene chloride at 0°C: (○) consumption of monomer determined by gas chromatography; (●) yield of acetone-insoluble product. The addition of catalyst is indicated by arrow. $[M]_0 = 1.22$ mole/l., $[C]_0 = 9.6$ mmole/l.

was determined by gravimetry. The polymerization rate was very large at the initial stage of polymerization, but slowed down rapidly at high conversions. Acetone-insoluble polymer was not produced beyond a certain conversion. The same trend was found for the $SnCl_4$TCA–toluene system and the BF_3OEt_2–toluene system. The final conversions (Y_∞) in Figure 2 were plotted against $[C]_0$. Obviously Y_∞ is proportional to $[C]_0$.

The influence of the initial monomer concentration $[M]_0$ on the time–conversion curve is shown in Figure 3. The conversion determined by gravimetry increased until it reaches a certain conversion, the same being observed in Figure 2. Y_∞ was bigger at smaller $[M]_0$. The product $[M]_0 Y_\infty$, however, was independent of $[M]_0$ and always about 0.55 mole/l.

To investigate further the influence of $[M]_0$ and to check the formation of acetone-soluble polymer, the conversion determined by gravimetry was compared with that determined by gas chromatography. As seen in Figure 4, the monomer consumption was always larger than the conversion to acetone-insoluble polymer. The acetone-insoluble polymers were filtered and the filtrate was evaporated to dryness; the infrared spectrum of the residue (acetone-soluble product) was nearly identical to that of polymer (acetone-insoluble product). The acetone-soluble fraction probably consists of oligomers of 1-vinylcyclohexene, although the nature of this fraction was not investigated further.

Structure of Poly-1-vinylcyclohexene

Poly-1-vinylcyclohexene is a white powder which is soluble in aromatic hydrocarbons and halogenated hydrocarbons. The molecular weight of the polymer as determined by ebulliometry of the toluene solution is about 1200 (DP about 11) and almost unaffected by the polymerization conditions.

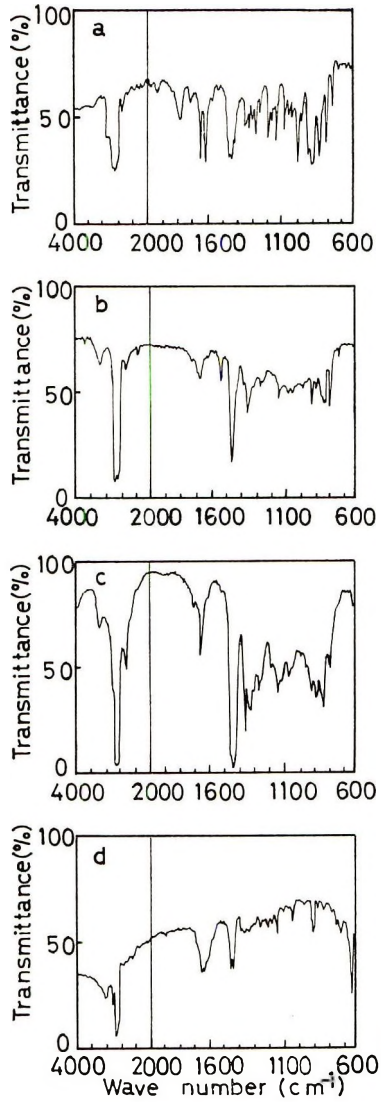

Fig. 5. Infrared spectra of poly(1-vinylcyclohexene) and related compounds. (*a*) 1-vinylcyclohexene; (*b*) poly-1-vinylcyclohexene produced by $SnCl_4$TCA in CH_2Cl_2 at 0°C; (*c*) poly-1-vinylcyclohexene produced by BF_3OEt_2 in CH_2Cl_2 at 0°C; (*d*) poly-4-vinylcyclohexene produced by $Al(i\text{-}Bu)_3$–$TiCl_3$ in toluene at 80°C.

Figure 5 shows infrared spectra of poly-1-vinylcyclohexene and related compounds. The following are the characteristic absorptions of 1-vinylcyclohexene: 3090 cm^{-1} (double bond), 1650 and 1610 cm^{-1} (conjugated double bond), 990 and 900 cm^{-1} (vinyl double bond), 800 cm^{-1} (trisubstituted ethylene). In the infrared spectrum of poly-1-vinylcyclohexene, the absorption at 990, 900 and 1610 cm^{-1} disappeared and the absorption at 800 cm^{-1} remained unchanged in the polymer, and only one absorption

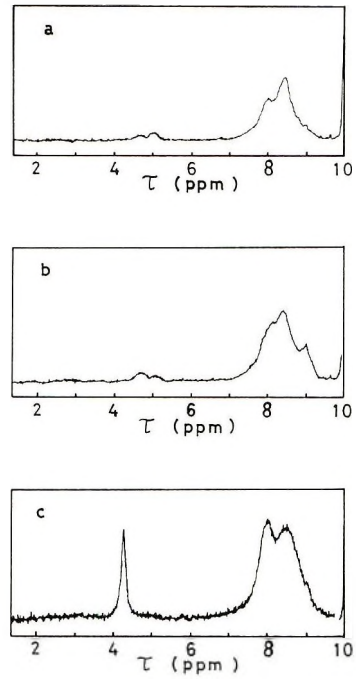

Fig. 6. Nuclear magnetic resonance spectra of poly-1-vinylcyclohexene and poly-4-vinylcyclohexene: (a) poly-1-vinylcyclohexene produced by $SnCl_4$TCA in toluene at 0°C; (b) poly-1-vinylcyclohexene produced by BF_3OEt_2 in toluene at 0°C; (c) poly-4-vinylcyclohexene produced by Al (i-Bu)$_3$–$TiCl_3$ in toluene at 80°C.

appeared at 1670 cm^{-1} (unconjugated trisubstituted ethylene) in the 1600-cm^{-1} region. These facts indicate that the vinyl-type double bond participates in the cationic polymerization of 1-vinylcyclohexene [1,2- or 1,4-polymerization, (III) or (IV)], and that the polymerization by only the cyclohexene ring [3,4-polymerization, (VII)] is ruled out. On the other hand, there appeared in the polymer a new absorption at 640 cm^{-1} which was absent in the monomer. This absorption vanishes after the bromination of the polymer. So, it could be an exo-type trisubstituted double bond resulting from either 1,4-polymerization (IV) or isomerization polymerization (VI). The above considerations receive further support from infrared spectrum of poly-4-vinylcyclohexene. In the Ziegler-type polymerization of 4-vinylcyclohexene the participation of cyclohexene ring is hardly possible.[18] In fact, the infrared spectrum showed absorptions at 650, 1650, and 3050 cm^{-1} which were ascribed to the double bond due to cyclohexene ring (I).

In Figure 6, NMR spectra of poly-1-vinylcyclohexene and related compounds are shown. Poly-4-vinylcyclohexene produced by Ziegler-type catalyst is expected to have the structure I, and the NMR spectrum showed peaks at τ 8.5 ppm (CH_2), 8.0 ppm (CH_2 at allyl position), and 4.26 ppm (olefin H). However, the peak area ratio of olefin proton against other

protons is about 1/7 instead of 1/5 for I. This could be because of the transannular polymerization resulting in the structure II.

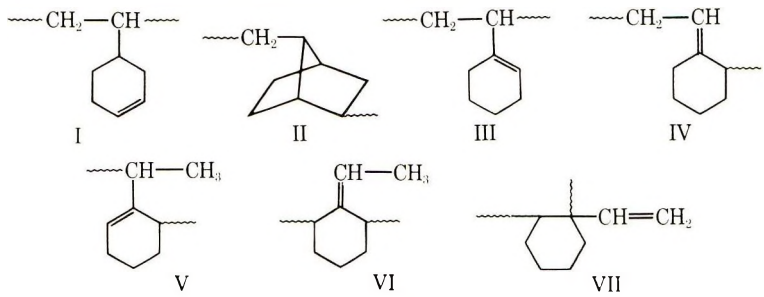

The effect of catalyst on the structure of poly-1-vinylcyclohexene obtained in the cationic polymerization is very marked. That is, the polymer produced by $SnCl_4$–TCA showed absorptions at τ 8.45–8.50 ppm, 8.00 ppm, and 5.00 ppm. This is consistent with structure IV. On the other hand, the polymer obtained by BF_3OEt_2 showed an absorption at τ 9.00 ppm. Because this absorption is correlated with the infrared absorption at 1380 cm^{-1} (Fig. 5), the polymer must contain methyl groups which cannot be explained by incorporation of the catalyst fragment into the polymer. The polymer produced by BF_3OEt_2 also showed NMR absorptions at τ 8.40–8.45 ppm, 8.15 ppm, and 4.65 ppm. All of these findings are consistent with the structure V. The fact that in the infrared spectrum (Fig. 5) the absorption at 1380 cm^{-1} is strong when the absorption at 840 cm^{-1} is weak supports the above considerations.

Polymerization Mechanism

The cationic polymerization of 1-vinylcyclohexene appears to be a nonstationary-state polymerization, as judged by Figures 2 and 3, where the initiation reaction is very fast and the numbers of propagating species decrease as a result of termination reactions. This sort of nonstationary-state polymerization has been observed in the cationic polymerization of cyclopentadiene,[2–8] 1,3-cyclohexadiene,[9] and 1,3-cyclooctadiene,[10] so it might be characteristic of the cationic polymerization in which a cycloalkenyl (VIII) or a semi-cycloalkenyl cation (IX) is involved.

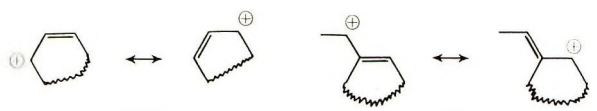

It is known that this sort of fast initiation reaction always accompanies an incomplete conversion of monomer.[2–10] Often, the conversion of monomer was inversely proportional to the initial monomer concentration.[2–10] It has been proposed that catalysts are consumed in the reaction with diene molecules which is of higher order with reference to diene con-

centration.[5] Also in the present investigation, the conversion of monomer to acetone-insoluble material decreased with increasing initial monomer concentration. This phenomenon may not be a problem of molecular weight distribution, because higher monomer concentrations usually lead to higher molecular weight polymers which are less soluble. The following mechanism may explain the available data. A part of catalysts initially added reacts with a part of monomer in a higher-order reaction. In this reaction, catalyst molecules are not completely destroyed as in the cyclopentadiene polymerization,[5] but give catalytically less active species. They start chains but terminate soon to form the acetone-soluble material. The rest of catalysts reacts with monomer in a usual lower-order reaction to give the acetone-insoluble material.

The polymer produced was proved to have various structures (III, IV, V, VI). The mechanism shown may explain the occurrence of various structures in the polymer.

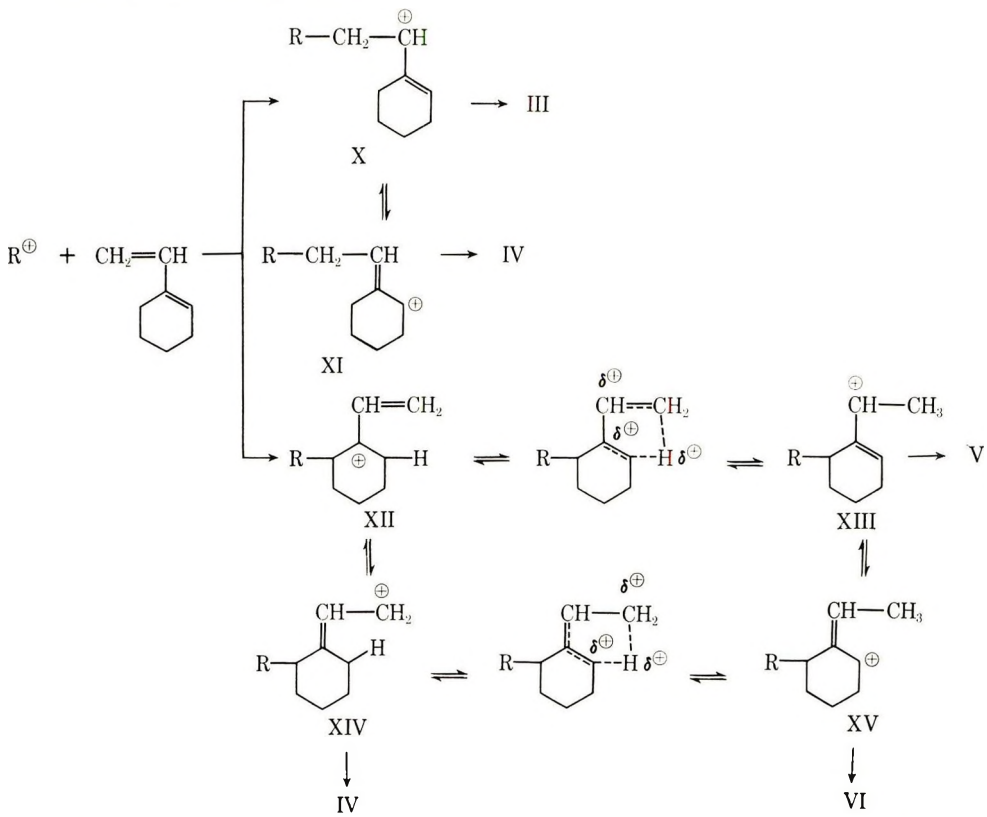

The addition of a propagating cation $R^{\oplus}$ to the vinyl group of 1-vinylcyclohexene gives the equilibrating cations X and XI. The repetition of the vinyl addition of X and XI leads to the structures III and IV, respectively. The addition of a propagating cation $R^{\oplus}$ to carbon 2 of 1-vinylcyclohexene gives the equilibrating cations XII and XIV. The repeti-

tion of the C_2 addition of XII is sterically inhibited, but that of XIV leads to the structure IV. The intramolecular proton migration of XII results in the formation of the equilibrating cations XIII and XV. The intramolecular hydride ion migration[19] of XIV results in the formation of the equilibrating cations XIII and XV as well. The further addition of the cations XIII and XV to 1-vinylcyclohexene gives the structures V and VI, respectively. Thus, the occurrence of methyl group in the polymer is explained, although intramolecular proton migration in XII and intramolecular hydride migration in XIV remains speculation.

According to this mechanism the occurrence of the methyl group is related to addition of a propagating cation to C_2 of 1-vinylcyclohexene. Since this mode of addition reaction is sterically more difficult than the addition to the vinyl group, it occurs only when the counteranion is sufficiently small such as the anion derived from BF_3OEt_2. This would explain the counterion effect.

COPOLYMERIZATION OF 1-VINYLCYCLOHEXENE

Cationic Copolymerization among 1-Vinylcyclohexene, 1,3-Cyclohexadiene, and 3-Methyl-1,3-pentadienes

1-Vinylcyclohexene, in which one of the conjugated double bonds is inside the ring and the other outside the ring, was copolymerized with 1,3-cyclohexadiene, in which both of the conjugated double bonds are inside the ring. The copolymer composition curve was obtained by following the monomer consumption by gas chromatography (Fig. 7). By cross-section method the monomer reactivity ratio was determined:

$$r_{VCH} = 2.52 \pm 0.72$$

$$r_{CHD} = 0.12 \pm 0.09$$

1-Vinylcyclohexene was more reactive than 1,3-cyclohexadiene. In the polymerization of 1-vinylcyclohexene the vinyl group is always involved,

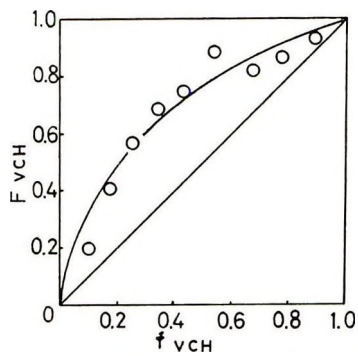

Fig. 7. Copolymerization of 1-vinylcyclohexene and 1,3-cyclohexadiene by $SnCl_4$TCA in methylene chloride at 0°C: (○) experimental results; (——) calculated for r_{VCH} = 2.52, r_{CHD} = 0.12.

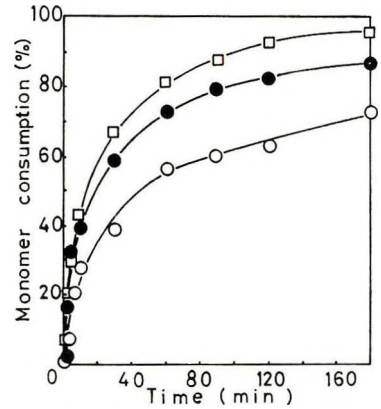

Fig. 8. Copolymerization of 1-vinylcyclohexene and 3-methyl-*cis*/*trans*-1,3-pentadienes by BF_3OEt_2 in methylene chloride at 0°C: (□) consumption of 1-vinylcyclohexene, $[M]_0$ = 0.41 mole/l.; (●) consumption of 3-methyl-*trans*-1,3-pentadiene, $[M]_0$ = 0.36 mole/l.; (○) consumption of 3-methyl-*cis*-1,3-pentadiene, $[M]_0$ = 0.10 mole/l. $[C]_0$ = 39.6 mmole/l.

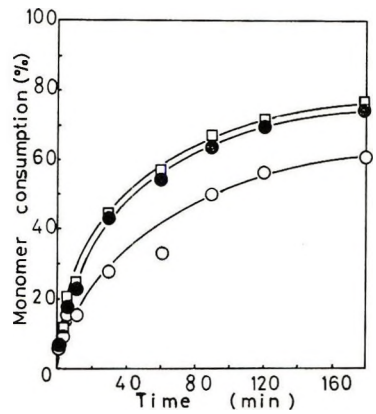

Fig. 9. Copolymerization of 1,3-cyclohexadiene and 3-methyl-*cis*/*trans*-1,3-pentadienes by BF_3OEt_2 in methylene chloride at 0°C: (□) consumption of 1,3-cyclohexadiene, $[M]_0$ = 0.53 mole/l.; (●) consumption of 3-methyl-*trans*-1,3-pentadiene, $[M]_0$ = 0.36 mole/l.; (○) consumption of 3-methyl-*cis*-1,3-pentadiene, $[M]_0$ = 0.10 mole/l. $[C]_0$ = 39.6 mmole/l.

whereas in the polymerization of 1,3-cyclohexadiene an endo-cyclic double bond is involved. So, presumably for steric reasons, 1-vinylcyclohexene is more reactive than 1,3-cyclohexadiene.

Whether a conjugated double bond is inside the ring or outside the ring seems to play an important role in determining the reactivity of conjugated dienes. To test this the reactivity of cyclic conjugated diene should be compared with that of linear conjugated diene. Here, the cationic copolymerization of 1-vinylcyclohexene with its linear analog, 3-methyl-*cis*/*trans*-1,3-pentadiene was carried out and the relative reactivities were compared. Copolymerizations were carried out at 0°C in methylene

chloride solution using BF_3OEt_2 or $SnCl_4TCA$ as catalyst. The relative rate of monomer consumption is shown in Figure 8.

The relative reactivity of three monomers in the BF_3OEt_2-catalyzed polymerization is

$$\text{1-VCH} > \text{3-MPD}(\textit{trans}) > \text{3-MPD}(\textit{cis})$$

The same result was also obtained in the $SnCl_4TCA$-catalyzed polymerization.

The reactivity of 1,3-cyclohexadiene, where two double bonds are inside the ring, was compared with 3-methyl-*cis*/*trans*-1,3-pentadiene. The results of copolymerization are shown in Figure 9. The relative reactivity of three monomers in the BF_3OEt_2-catalyzed polymerization is

$$\text{CHD} > \text{3-MPD}(\textit{trans}) > \text{3-MPD}(\textit{cis})$$

The same result was also obtained in the $SnCl_4TCA$-catalyzed polymerization.

Extent of Conjugation between Two Double Bonds of Diene

A single bond between two double bonds of conjugated dienes assumes double bond character because of conjugation. Therefore, this sort of single bond is more resistant to fragmentation than a normal single bond. If the ease of fragmentation of the relevant single bond is quantitatively measured, the information on the extent of conjugation between two double bonds is obtained. Since the conjugation seems to play an important role to determine the reactivity of monomer, the ease of fragmentation of the single bond was judged quantitatively by mass spectrometry and correlated with the extent of conjugation.

The results of mass spectrometry on 1-vinylcyclohexene, 3-methyl-*cis*/*trans*-1,3-pentadiene, and the related compounds are shown in Figures 10 and 11. In the series of Figure 10, the pattern of the mass spectrum is similar for four kinds of compounds. Therefore, a comparison of mass

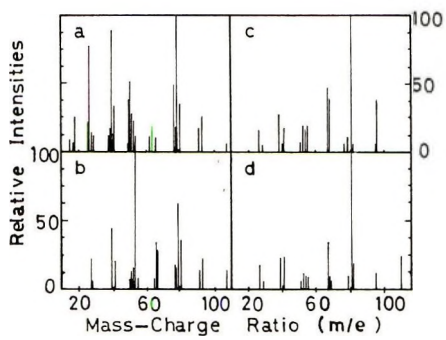

Fig. 10. Mass spectra of 1-vinylcyclohexene and related compounds. (*a*) 1-vinylcyclohexene, 80 eV; (*b*) 4-vinylcyclohexene, 80 eV; (*c*) 1-methylcyclohexene, 80 eV; (*d*) 1-ethylcyclohexene, 70 eV.[20]

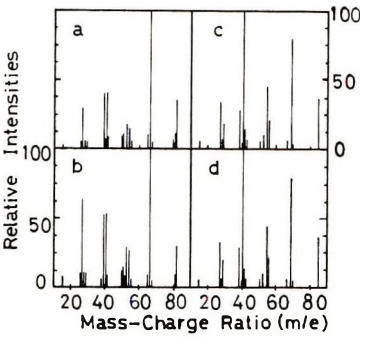

Fig. 11. Mass spectra of 3-methyl-cis/trans-1,3-pentadienes and related compounds: (*a*) 3-methyl-*trans*-1,3-pentadiene, 80 eV; (*b*) 3-methyl-*cis*-1,3-pentadiene, 80 eV; (*c*) 3-methyl-*trans*-2-pentene, 70 eV;[21] (*d*) 3-methyl-*cis*-2-pentene, 70 eV.[22]

spectra of the four compounds is meaningful. The same is true for the series of Figure 11.

In the series of Figure 10, the fragmentation of the relevant single bond gives an ionic species having a mass number 81. The ratio of pattern coefficient of mass number 81 against that of parent ion was calculated so

TABLE I
Ease of Fragmentation of a Single Bond as Judged by Relative Peak Strength in Mass Spectrometry

Compound	Pattern coeff. of mass no. 81 / Pattern coeff. of parent ion	Compound	Pattern coeff. of mass no. 55 / Pattern coeff. of parent ion
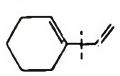	40.5	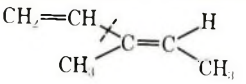	17.4
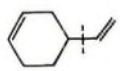	77.3	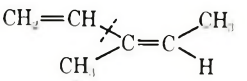	21.2
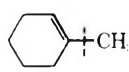	277	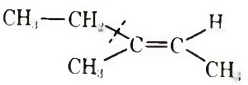	122.5[a]
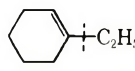	412[b]	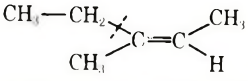	123[c]

[a] Data of American Petroleum Institute Research Project 44.[21]
[b] Data of American Petroleum Institute Research Project 44.[20]
[c] Data of American Petroleum Institute Research Project 44.[22]

as to compare among the four compounds the ease of fragmentation of the single bond. The same was done with ionic species having a mass number 55 for the series of Figure 11. As the measurement of mass spectrum was performed at the ionization potential 80 eV, the ionic species of mass numbers 81 or 55 are most probably the primary fragment ions. The results are listed in Table I.

Values in Table I show that 1-vinylcyclohexene and 3-methyl-*cis/trans*-1,3-pentadiene give ionic species having mass numbers 81 and 55, respectively, less easily than the related compounds. In other words, the single bond in those conjugated dienes is more difficult to break because of conjugation.

What we want to know is the comparison of the extent of conjugation between 1-vinylcyclohexene and 3-methyl-*cis/trans*-1,3-pentadienes. For that purpose, different series of compounds (Figs. 10 and 11) having very different peak patterns need be compared. To overcome this difficulty, the ratio of the value for diene compound against that for monoene compound was calculated and compared.

$$\frac{\text{1-vinylcyclohexene}}{\text{1-ethylcyclohexene}} = \frac{40.5}{412} = 0.098$$

$$\frac{\text{3-methyl-}trans\text{-1,3-pentadiene}}{\text{3-methyl-}trans\text{-2-pentene}} = \frac{17.4}{122.5} = 0.14$$

$$\frac{\text{3-methyl-}cis\text{-1,3-pentadiene}}{\text{3-methyl-}cis\text{-2-pentene}} = \frac{21.2}{123} = 0.17$$

These figures measure the variation of conjugation accompanied with going from monoene to diene. If it is admitted to assume that no large difference of stability exists among the monoene compounds, the extent of stabilization by conjugation decreases in the order

$$\text{1-VCH} > \text{3-MPD } (trans) > \text{3-MPD } (cis)$$

On the other hand, the reactivity of monomer in cationic polymerization at 0°C in methylene chloride by BF_3OEt_2 or $SnCl_4$TCA decreases in the order

$$\text{1-VCH} > \text{CHD} > \text{3-MPD}(trans) > \text{3-MPD}(cis)$$

Therefore, the monomer which is more stabilized in the initial state shows higher reactivity in cationic polymerization. This suggests that the difference of carbonium ion stability is more significant than the difference of monomer stability. The carbonium ion stability is likely to decrease in the order

$$\text{1-VCH} \simeq \text{CHD} > \text{3-MPD}(trans) > \text{3-MPD}(cis)$$

With regard to 1-vinylcyclohexene, the experimental data on the carbonium ion stability is not available. However, with regard to 1,3-cyclohexadiene and 3-methyl-*cis/trans*-1,3-pentadiene, the pK_{BH^+} values for the corresponding alkenyl cations can be deduced by calculation.[23,24]

$pK_{BH^+} = -10.2$

$pK_{BH^+} = -13.5$

The pK_{BH^+} values show that the cycloalkenyl cation is more stable than the linear alkenyl cation, and this may be responsible for the high reactivity of cyclic dienes in cationic polymerization.

The different stabilities between carbonium ions derived from two isomers of 3-methyl-1,3-pentadiene show that the rotation around a single bond of the carbonium ion is not free. Olah et al.[25] reported for a similar carbonium

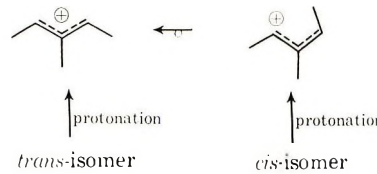

ion that the rotation around a single bond requires a free energy of activation 23.6 kcal/mole.

The cooperation of Dr. S. Nozakura of Osaka University on the polymerization of 4-vinylcyclohexene is gratefully acknowledged. The authors thank Prof. K. Hirota of Osaka University for allowing them to use Hitachi RMu-7HR mass spectrometer.

References

1. Y. Imanishi, K. Matsuzaki, T. Yamane, S. Kohjiya, and S. Okamura, *J. Macromol. Sci.-Chem.*, **A3**, 249 (1969).
2. Z. Momiyama, Y. Imanishi, and T. Higashimura, *Kobunshi Kagaku*, **23**, 56 (1966).
3. Y. Imanishi, S. Kohjiya, Z. Momiyama, and T. Higashimura, *Kobunshi Kagaku*, **23**, 119 (1966).
4. Y. Imanishi, T. Yamane, Z. Momiyama, and T. Higashimura, *Kobunshi Kagaku*, **23**, 152 (1966).
5. Y. Imanishi, S. Kohjiya, and S. Okamura, *J. Macromol. Sci.-Chem.*, **A2**, 471 (1968).
6. Y. Imanishi, K. Hara, S. Kohjiya, and S. Okamura, *J. Macromol. Sci.-Chem.*, **A2**, 1423 (1968).
7. S. Kohjiya, Y. Imanishi, and S. Okamura, *J. Polym. Sci. A-1*, **6**, 809 (1968).
8. C. Aso, O. Ohara, and T. Kunitake, *Kobunshi Kagaku*, **27**, 97 (1970).
9. Y. Imanishi, T. Yamane, S. Kohjiya, ad S. Okamura, *J. Macromol. Sci.-Chem.* **A3**, 223 (1969).
10. Y. Imanishi, K. Matsuzaki, S. Kohjiya, and S. Okamura, *J. Macromol Sci.-Chem.*, **A3**, 237 (1969).
11. R. Asami and T. Yamamoto, paper presented at the 20th annual meeting of the Japan Chemical Society, Tokyo, April 1967, Abstract 4P309.
12. M. S. Kharasch, M. C. McNab, and F. R. Mayo, *J. Amer. Chem. Soc.*, **55**, 2521 (1933).
13. P. A. Robins and J. Walker, *J. Chem. Soc.*, **1952**, 642.
14. J. W. Emsley, J. Feeney, and L. H. Sutcliffe, *High Resolution Nuclear Magnetic Resonance Spectroscopy*, Vol. 2, Pergamon Press, Oxford, 1966, pp. 735–740.
15. D. Craig, J. J. Shipman, and R. B. Fowler, *J. Amer. Chem. Soc.*, **83**, 2885 (1961).
16. Y. Imanishi, T. Higashimura, and S. Okamura, *J. Polym. Sci. A*, **3**, 2455 (1965).
17. W. Marconi, S. Cesca, and G. Della Fortuna, *J. Polym. Sci. B*, **2**, 301 (1964).

18. F. Danusso, in Macromolecular Chemistry, Paris 1963 (*J. Polym. Sci. C*, **4**) M. Magat, Ed., Interscience, New Yok, 1963, p. 1487.

19. C. Aso, T. Kunitake, and S. Shinkai, *Kobunshi Kagaku*, **26**, 280 (1970).

20. Mass spectral data, American Petroleum Institute Research Project 44, Carnegie Institute of Technology, Serial No. 1287, April 30, 1956.

21. Mass spectral data, American Petroleum Institute Research Project 44, Carnegie Institute of Technology, Serial No. 277, April 30, 1949.

22. Mass spectral data, American Petroleum Institute Research Project 44, Carnegie Institute of Technology, Serial No. 104, February 29, 1948.

23. N. C. Deno, *Progr. Phys. Org. Chem.*, **2**, 129 (1964).

24. N. C. Deno, J. Bollinger, N. Friedman, K. Hafer, J. D. Hodge, and J. J. Houser, *J. Amer. Chem. Soc.*, **85**, 2998 (1963).

25. J. M. Bollinger, J. M. Brinich, and G. A. Olah, *J. Amer. Chem. Soc.*, **92**, 4025 (1970).

Received February 9, 1971
Revised May 18, 1971

JOURNAL OF POLYMER SCIENCE: PART A-1 VOL. 9, 2949–2955 (1971)

Preparation and Polymerization of *N*-(1,1-Dimethyl-3-hydroxybutyl) acrylamide and *N*-(1,1-Dimethyl-3-hydroxybutyl)methacrylamide

DONALD I. HOKE,
The Lubrizol Corporation, Cleveland, Ohio 44117

Synopsis

The syntheses of *N*-(1,1-dimethyl-3-hydroxybutyl)acrylamide and the corresponding methacrylamide by reduction of the oxobutyl acrylamides are described. These monomers are colorless liquids which are soluble in water and many organic solvents. They polymerize readily to form homopolymers and copolymers with other vinyl monomers. The preparation of polymers containing these repeating units by reduction of polymers of diacetone acrylamide and diacetone methacrylamide is also described.

INTRODUCTION

A number of *N*-hydroxyalkylacrylamides have been reported, primarily in the patent literature. In general, this class of compounds has been synthesized by the reaction of acrylyl chloride with an amino alcohol. The reduction of *N*-(1,1-dimethyl-3-oxobutyl)acrylamide (diacetone acrylamide, I) now provides a convenient route to an *N*-hydroxyalkylacrylamide. Since I can be prepared by reaction of acrylonitrile with acetone, mesityl oxide, or diacetone alcohol,[1] the use of the acid chloride is avoided.

RESULTS AND DISCUSSION

Monomer Preparation

I can be reduced directly by use of a selective chemical reducing agent or indirectly by catalytic hydrogenation. Of the two common reagents for selective reduction of carbonyl groups, aluminum isopropoxide and sodium borohydride, the latter is far superior. Only low yields of impure product are obtained from the reduction of I with aluminum isopropoxide. Sodium borohydride reduced I and diacetone methacrylamide(II) to *N*-(1,1-dimethyl-3-hydroxybutyl)acrylamide(III) and *N*-(1,1-dimethyl-3-hydroxybutyl)methacrylamide(IV), respectively.[2] In each case, high yields of pure product are obtained when excess sodium borohydride is used. If the reduction is incomplete, the product contains starting material which cannot be readily separated by distillation.

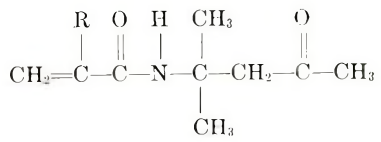

I, R = H
II, R = CH_3

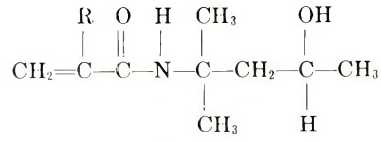

III, R = H
IV, R = CH_3

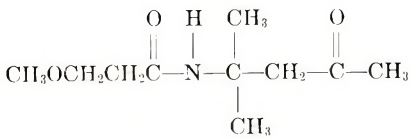

V

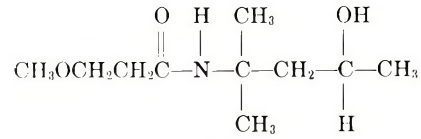

VI

III was also prepared by catalytic hydrogenation. To avoid reduction of the carbon–carbon double bond of I, it was blocked by conjugate addition of methanol to I. This adduct, *N*-(1,1-dimethyl-3-oxobutyl)-3-methoxypropionamide(V), was prepared in high yield by the reaction of I with excess refluxing methanol using a strong base as catalyst.[3]

Initial efforts to prepare alcohol adducts of I resulted in only 40–60% yields of impure products. A study of this reaction by use of gas chromatographic analysis to follow the reaction showed that at 65–70°C methanol adds rapidly to I. At a methanol:I ratio of 1:1–2:1 an 85% yield of V was formed in 1 hr. An additional hour of heating resulted in lowering of the yield to 75%. As the methanol:I ratio was increased, the rate of addition decreased, but the yield increased. At a ratio of 8:1 a 95% yield of 95% pure material was obtained in 6 hr.

Sodium hydroxide or sodium methoxide are equally effective as catalysts. The rate of addition of the methanol to I is proportional to the base concentration. Quaternary ammonium hydroxides give reaction rates which are approximately double those obtained with sodium hydroxide.

Catalytic reduction of V at 60–80°C gave a high yield of *N*-(1,1-dimethyl-3-hydroxybutyl)-3-methoxypropionamide(VI) in 4 hr. After reduction, methanol was eliminated by dropping VI onto hot sodium hydroxide pellets in a vertical tube under vacuum. At temperatures of 100–200°C

TABLE I
Characteristic Infrared Bands of II–VI

Absorption band, cm^{-1}	Assignment
3300	NH, OH
1715	C=O
1670	C(O)NH (amide I)
1625	C=C
1540	C(O)NH (amide II)
1120	C—O
980, 920	CH_2=

TABLE II
Nuclear Magnetic Resonance Characteristics of II–VI[a]

Chemical shift, δ		Assignment
1.23	(Doublet)	CH_3COH
1.43	(Not resolved)	$(CH_3)_2C$
1.48		CH_2COH
1.88	(Singlet)	$=C(CH_3)C(O)N$
2.08	(Singlet)	$CH_3C=O$
2.40	(Triplet)	$—CH_2C(O)NH$
3.00	(Singlet)	$CH_2C=O$
3.35	(Singlet)	$CH_3O—$
3.63	(Triplet)	$CH_2O—$
4.17	Multiplet	CHOH
5.22, 5.68		$CH_2=$
5.48, 6.10		$CH_2=CH—$
4.67	(Variable)	OH
8.00	(Variable)	NH

[a] All samples were run in $CDCl_3$ at ambient temperature with tetramethylsilane as the reference. The instrument was a Varian Model A-60.

only 30–50% yields of III were obtained, despite almost quantitative recoveries of methanol.

The diacetone methacrylamide used in this study was prepared by the reaction of diacetone alcohol with methacrylonitrile in the presence of sulfuric acid.

The characteristic infrared bands and NMR chemical shifts of II–VI are given in Tables I and II.

Polymerization

III and IV polymerize readily in solution, emulsion or bulk. Both homopolymers form brittle films which are insoluble in water. Polymers having good analyses with $[\eta]^{30°C}_{DMF} = 0.1–2$ were obtained.

The homopolymers of III and IV do not become highly plasticized and weak when immersed in water as does poly-I. The glass transition temperatures and decomposition temperatures are given in Table III.

TABLE III
Glass Transition Temperatures and Decomposition Temperatures of the Homopolymers of III and IV

Homopolymer	T_g, °C[a]	T_{dec} °C[a,b]
III	110	227
IV	197	272

[a] Determined with a differential scanning calorimeter, an accessory to the DuPont 901 thermal analyzer.

[b] Temperature at onset of decomposition.

The homopolymers of III and IV are soluble in methanol, ethanol, chloroform, dimethylformamide and wet acetone. They swell in benzene and dry acetone and are insoluble in aliphatic hydrocarbons.

Copolymers of III were prepared by using solution and emulsion techniques. (Table IV).

TABLE IV
Copolymers of *N*-(1,1-Dimethyl-3-hydroxybutyl)acrylamide(III)

Comonomer	Comonomer, % In charge	Comonomer, % In polymer[a]	Polymerization Technique	Initiator	Temp, °C	Yield, %
Vinyl acetate	10	15	Benzene solution	AIBN	80	—
	25	22	Benzene solution	AIBN	80	—
	50	41	Benzene solution	AIBN	80	52
	75	57	Benzene solution	AIBN	80	49
	90	78	Benzene solution	AIBN	80	34
Ethyl acrylate	10	7	Emulsion	$S_2O_8^=$	60	96
	20	21	Emulsion	$S_2O_8^=$	60	87
	25	31	Emulsion	$S_2O_8^=$	60	92
	36	37	Benzene solution	AIBN	60	95
Styrene	25	14	Benzene solution	AIBN	80	54
	50	47	Benzene solution	AIBN	80	16
Acrylic acid	25	31	Water solution[b]	$S_2O_8^=$/ $S_2O_5^=$	25	92
IV	25	25[c]	Emulsion[d]	$S_2O_8^=$/ $S_2O_5^=$	25	100
	50	50[c]	Emulsion[d]	$S_2O_8^=$/ $S_2O_5^=$	25	100
	75	75[c]	Emulsion[d]	$S_2O_8^=$/ $S_2O_5^=$	25	100

[a] Calculated from nitrogen analysis.
[b] Polymer precipitated.
[c] Determined from yield.
[d] Monomers soluble at start of polymerization.

Homopolymers of III and IV and some of their copolymers were also prepared by reduction of polymers derived from I and II with sodium borohydride in ethanol. This is illustrated in the experimental section by the reduction of poly-I but is applicable to any copolymer system in which the comonomer moiety is not altered by nor interferes with the reduction.

EXPERIMENTAL

The hydroxyl analyses were obtained by reaction of the sample with acetic anhydride in pyridine followed by titration with alcoholic alkali.[5]

The carbonyl analyses were obtained by oximation of the carbonyl compound with hydroxylamine hydrochloride in the presence of 2-di-

methylaminoethanol. Excess base was then titrated with aqueous perchloric acid.[6]

The gas chromatographic analyses were obtained by use of a dual-column instrument. The initial column temperature was 50–70°C. After sample injection, using acetone as the solvent, the columns were heated at 20–40°C/min to 220°C and held isothermally at that temperature. The 8-ft columns were packed with 20% FFAP on 80–100 mesh Aeropak 30(Varian-Aerograph).

N-(1,1-Dimethyl-3-oxobutyl)-3-methoxypropionamide(V)

Sodium hydroxide 172 g (4.3 mole) was dissolved in a solution of 7.273 kg (43 moles) of I in 11.161 kg (348.8 moles) of methanol. The solution was heated under reflux for 6 hr. After cooling to room temperature, 95% of the base was neutralized with 50% sulfuric acid. The remaining base was neutralized with a slight excess of acetic acid. The temperature during neutralization was held at 25–30°C. The precipitated salts were removed on a filter. The methanol, water, and acetic acid were removed under vacuum to give 8150 g (94%) of a light yellow liquid having a purity of 95%. Distillation of the yellow liquid through an 8-in. Vigreux column gave a colorless liquid (V), bp 100°C/0.1 mm, mp 26–30°C, n_D^{25} 1.4605 (reported[7] bp 98°C/0.6 mm, n_D^{22} 1.4610). The purity was 97% by gas chromatographic analysis.

ANAL. Calcd for $C_{10}H_{19}NO_3$: N, 6.96%. Found: N, 6.91%.

N-(1,1-Dimethyl-3-hydroxybutyl)acrylamide(III)

Reduction of I with Sodium Borohydride. A solution of 37.8 g (1.0 mole) of sodium borohydride in 1 liter of water was added to a stirred solution of 338 g (2.0 mole) of I in 1 liter of water. The temperature slowly rose to 45°C. After stirring for 2 hr, the excess sodium borohydride was destroyed by acidifying the solution to pH 4 with 5% sulfuric acid (caution: gas evolution). Aqueous sodium hydroxide was then added to adjust the solution to pH 8. The product was extracted with five 200-ml portions of chloroform. After drying the extracts over Drierite and filtering, the chloroform was removed on a rotary evaporator. The residue was distilled through an 8-in. heated Vigreux column in the presence of 1 g 4,4′-methylene-bis-2,6-di-*tert*-butylphenol to obtain III as a colorless liquid in 65–90% yields, bp 116°C/0.3 mm, n_D^{25} 1.4782. The purity by gas chromatographic analysis was 98–99%.

ANAL. Calcd for $C_9H_{17}NO_2$: N, 8.19%; hydroxyl, 9.95%. Found: N, 8.09%; hydroxyl, 9.95%.

Reduction of I with Hydrogen. A solution of 201 g (1.0 mole) of *N*-(1,1-dimethyl-3-oxobutyl)-3-methoxypropionamide(V) in 100 ml of methanol containing 3 g of Raney nickel was heated to 65–70°C on a Parr hydrogenation apparatus. The solution was shaken with hydrogen (initial

pressure 60–70 psi) for 4 hr. At this point, hydrogenation stopped, and the pressure drop showed almost theoretical uptake of hydrogen. The catalyst was separated by filtration, and the methanol was then removed on a rotary evaporator. A pale yellow liquid of 95% purity (GC) was obtained in 95–100% yield. Distillation with a molecular still gave an almost colorless product, but attempts to purify this product by fractional distillation failed.[4] Analyses and the infrared and NMR spectra showed this liquid to be VI.

ANAL. Calcd for $C_{10}H_{21}NO_2$: N, 6.83%; hydroxyl, 8.44% Found: N, 6.90%; hydroxyl, 8.37%.

The apparatus for elimination of methanol consisted of a vertical glass tube 2 cm in diameter and 50 cm long filled with sodium hydroxide pellets. This tube was wrapped with an electrical heating tape. The temperature was measured with thermocouples between the heating tape and the glass tube. An addition funnel was inserted into the top of the tube, and a two neck round bottom flask was connected to the bottom of the tube. The second neck of this flask was connected to a vacuum pump, and the pressure in the system was reduced to 6 mm. A Dry Ice trap between the flask and pump was used to collect low boiling material.

The glass tube was heated to 110–140°C, and a solution of 1.2 g 2,6-di-*tert*-butyl-*p*-cresol in 41.5 g (0.2 mole) VI was dropped into the tube over a period of 40 minutes. An orange polymeric deposit remained in the tube. The liquids in the flask (21.5 g) and Dry Ice trap (8.6 g) were analyzed by gas chromatography. These analyses showed that almost a quantitative yield of methanol was obtained, but only a 35% yield of III was obtained.

Diacetone Methacrylamide(II)

Methacrylonitrile (134 g, 2.0 mole) was weighed into a 1-liter resin flask fitted with a stirrer, thermometer, addition funnel, and an internal cooling coil. The nitrile was cooled to 0°C, and 429 g (4.2 mole) of 96% sulfuric acid was added while keeping the temperature at 0–5°C. Diacetone alcohol (232 g, 2.0 mole) was then added over a 100-min period at 6–15°C. After 1 hr at 8°C, 2500 ml of water was added at 0–5°C. The organic layer which formed was separated, and the aqueous portion was extracted with six 250-ml portions of chloroform. The organic layer and extracts were combined. The low boiling materials were removed on a rotary evaporator. Distillation of the residue through an 8-in. Vigreux column in the presence of 3 g of 4,4′-methylene-bis-2,6-di-*tert*-butylphenol gave the product in 30–45% yields as a colorless liquid, bp 74°C/0.4 mm, mp 28°C, n_D^{25} 1.4714, with a purity of greater than 99% by gas chromatographic analysis.

ANAL. Calcd for $C_{10}H_{17}NO_2$: N, 7.64%; carbonyl, 15.3%. Found: N, 7.82%; carbonyl, 15.3%.

N-(1,1-Dimethyl-3-hydroxybutyl)methacrylamide

This material was prepared in 70% yield from II by using the sodium borohydride reduction procedure described above for III. IV is a colorless liquid, bp 105°C/0.1 mm, n_D^{25} 1.4724.

ANAL. Calcd for $C_{10}H_{19}NO_2$: N, 7.56%; hydroxyl, 9.18%. Found: N, 7.38%; hydroxyl, 9.32%.

Reduction of Poly(diacetone acrylamide)

Poly-I (500 g) prepared by solution or emulsion polymerization,[1] was dissolved in 10 liters of ethanol. A suspension of 56 g (1.47 mole) of sodium borohydride in 400 ml of ethanol was added over a period of 2 hr. The resulting solution was stirred at room temperature overnight, then 240 g (4.0 mole) of glacial acetic acid was added in small increments (caution: gas evolution and foaming). The polymer was precipitated by pouring the ethanol solution into nine times its volume of well stirred water. The precipitate was separated by filtration and dried to constant weight at 40°C in a vacuum oven. A yield of 429 g (83.4%) of white solid polymer was obtained.

ANAL. Calcd for $C_9H_{17}NO_2$: N, 8.18%; carbonyl, 0%; hydroxyl, 10.0%. Found: N, 7.76%; carbonyl, 0.23%; hydroxyl, 11.8%.

I wish to thank Mr. Paul R. Kaufman and Mr. Philip S. Korosec for technical assistance in this work, Dr. Alan T. Riga for determining the glass transition temperatures, and Mr. Frank Gotto for preparing some of the copolymers.

References

1. L. E. Coleman, J. F. Bork, D. P. Wyman, and D. I. Hoke, *J. Polym. Sci. A*, **3**, 1601 (1965).
2. D. I. Hoke, U.S. Pat. 3,585,125 (to Lubrizol Corp., June 15, 1971).
3. D. I. Hoke, U.S. Pat. 3,525,768 (to Lubrizol Corp., August 25, 1970).
4. M. E. Smith and H. Adkins, *J. Amer. Chem. Soc.*, **60**, 407 (1938).
5. C. L. Ogg, W. L. Porter, and C. O. Wilts, *Ind. Eng. Chem. Anal. Ed.*, **17**, 394 (1945).
6. J. S. Fritz, S. S. Yamamura, and E. C. Bradford, *Anal. Chem.*, **31**, 260 (1959).
7. M. Lora-Tomayo, R. Madronero, G. G. Munoz, and H. Leipprand, *Chem. Ber.*, **97**, 2234 (1964).

Received April 29, 1971
Revised June 10, 1971

JOURNAL OF POLYMER SCIENCE: PART A-1 VOL. 9, 2957–2962 (1971)

Snake-Cage Redox Polyelectrolytes Based on Anion-Exchange Resins

M. A. KESSICK, *W. M. Keck Laboratory of Environmental Health Engineering, California Institute of Technology Pasadena, California 91109*

Synopsis

Redox polyelectrolytes are described where the polyphenols hydroquinone, pyrogallol, and catechol were absorbed as counterions by a strong base anion-exchange resin in the hydroxide form, and then polymerized by refluxing in 1:1 mole ratio with formaldehyde in aqueous solution, thus producing a "snake-cage" configuration. The redox capacities of the resins were determined by oxidation with iodine/iodide solution, and found to approach theoretical at between 5.1 and 5.4 meq/g. The rate of oxidation was found to be controlled by diffusion within the particles. Fe^{3+} was unsatisfactory as an oxidant, owing to the exclusion effect by the fixed positive charges in the resin matrix. At low pH the resin beads were light to reddish brown in the reduced form, black in the oxidized form. The resins, especially that based on catechol, showed much greater stability in 1*N* NaOH solution than simple polyphenol–formaldehyde condensation polymers.

INTRODUCTION

Many methods for the preparation of crosslinked polymers with oxidation-reduction capacity in aqueous solution have been reported in the literature. A detailed review may be found in the recent book by Cassidy and Kun.[1] In brief, however, the resins appear to fall into three main categories; those produced by the addition polymerization of redox-active monomers, such as vinylhydroquinone, those produced by the condensation polymerization of redox active polyphenols, such as hydroquinone, with formaldehyde; and those obtained by the attachment, reversible or irreversible, of redox active materials to preformed polymer matrices.

The synthesis of the addition-type redox polymers has been attended by many difficulties, not least of which is that the monomers themselves often act as inhibitors during the polymerization process.[2,3] The resulting resins tend to be quite hydrophobic and are unsatisfactory for use in aqueous systems unless strongly hydrophilic groups are introduced, for example, by sulfonation. The condensation polymers are more readily formed, but tend also to be intractable and of low porosity unless chemically treated after polymerization, as by sulfonation,[4,5] or unless comonomers such as sodium *o*-benzaldehyde sulfonate are included during the polymerization process.[6] Both addition and condensation redox polymers are subject to

skeletal degradation by certain oxidants and by strong base solution. This seems generally true of polymers where the redox functionality can be considered part of the polymer backbone.

The attachment of redox-active materials to preformed polymer matrices has probably resulted in the most successful resins to date. Duolite S-10, a resin of this type, used commercially for removing dissolved oxygen from solution, depends for its effectiveness on the interconversion between complexed divalent copper and sorbed zero-valent (metallic) copper in an anion-exchange resin matrix.[7] It is unstable below pH 7. Sansoni,[8,9] as well as preparing many systems in cation exchange resin matrices involving absorbed metallic ions capable of redox behavior, such as Fe^{2+}/Fe^{3+}, Sn^{2+}/Sn^{4+}, has also prepared redox anion exchangers by the sorption of hydroquinone type compounds on the hydroxyl forms of Amberlite IRA-400 and Wofatit M. These products, as with Duolite S-10, do not show stability throughout the entire pH range. Redox systems have also been obtained by Friedel-Crafts addition of hydroquinone-type compounds to preformed, chloromethylated, macroreticular styrene–divinylbenzene copolymers.[10] These compounds are hydrophobic and swell little in aqueous solution unless further treated, for instance, by chlorsulfonic acid, or unless some of the chloromethyl groups are reserved for quaternization with tertiary amines.

The present work describes the application of the "snake-cage" polyelectrolyte concept, previously applied only in the production of amphoteric resins,[11] containing polymerized acrylate counterions and used for separations by "ion retardation," to the production of redox polymers. The redox compounds pyrogallol, catechol, and hydroquinone may be absorbed as counterions by a strong base quaternary ammonium anion-exchange resin (in this case Dowex II) in the hydroxyl form, and then polymerized *in situ* by refluxing the resin beads in water containing formaldehyde in equimolar proportion to the absorbed polyphenol. The linear chains of polymerized polyphenol thus formed are trapped in the anion-exchange resin matrix, and the probability of desorption of the redox functionality is thus extremely low, except under conditions which would promote catastrophic degradation of the included polymer chains or the anion-exchange resin matrix itself.

EXPERIMENTAL

Preparation of a Typical Resin

A 50-g portion of Dowex 11 (a strong-base anion-exchange resin of capacity 4.1 ± 0.3 meq/dry gram) was placed in the hydroxyl form by repeated washing with 2% sodium hydroxide solution. After washing away of excess base, the resin beads were stirred in 200 ml of water with an amount of polyphenol (hydroquinone, catechol, or pyrogallol) equivalent to 4.1 mmole per dry gram of resin for 15 min. Formaldehyde in aqueous solution was then added in equivalent molar quantity and the

mixture refluxed for 4 hr. The mixture was cooled, and the beads were then washed several times with 1.0*N* hydrochloric acid by decantation, filtered at the pump, and stored in a moist state. The beads containing the polymerized catechol and pyrogallol were a light brown color in the reduced chloride form whereas those containing polymerized hydroquinone were a deeper, reddish-brown. All were black in the oxidized form. Standing in 1.0*N* sodium hydroxide solution for two days caused moderate discoloration of the solution in the case of the resins based on hydroquinone and pyrogallol and slight discoloration in the case of the resin based on catechol.

Determination of Redox Capacity

A 1-g dry weight sample of resin was placed in the reduced state by stirring for 1 hr with 200 ml of a solution containing sodium hydrosulfite (0.1*M*) and sodium hydroxide (0.2*M*). After washing rapidly with distilled water and 1*N* hydrochloric acid, the resin sample was drained and added to 1 liter of a solution containing potassium iodide (1*N*) and iodine (0.02*N*). This solution had previously been deaerated by flushing with prepurified nitrogen, and the reaction was stirred under nitrogen for the duration of the experiment. Since the pH of the solution remained at 2.5 throughout the determination, this minimized the production of free iodine by air oxidation of iodide. At regular time intervals, aliquots of the iodine/iodide solution were withdrawn and estimated by titration with 0.02*N* sodium thiosulfate solution until no change in iodine concentration was noticed. The decrease in iodine concentration corresponded to the oxidation of the resin, coupled with some absorption of iodine by the resin either as I_3^- counterions or as I_2 molecules. The amount of iodine absorbed in this manner was determined at the end of each oxidation by washing the resin beads several times with distilled water, draining them, and stirring them with a deaerated solution 1*N* in potassium iodide alone. After 1 hr, this solution phase was then estimated for iodine, and the amount determined taken to be that which had been absorbed by the resin, but which had not taken part in the oxidation. From the results obtained the oxidation-reduction capacity of the resin was calculated.

Figure 1 shows the oxidation of the three resins prepared as a function of $t^{1/2}$. The values plotted have each been corrected for the amount of iodine found to be physically absorbed at the end of each determination. The change in volume after each aliquot of solution was withdrawn was also taken into account. Determination of the capacities of the resins by the more usual oxidation with Fe^{3+} and estimation of the ferrous ion produced with standard ceric sulfate solution was found unsatisfactory in this instance. Figure 2 depicts the oxidation of the snake-cage pyrogallol resin as a function of time with both Fe^{3+} and I_3^-. The consequences of the exclusion of the Fe^{3+} ion by the fixed positive charge in the resin are apparent. All determinations were carried out at room temperature.

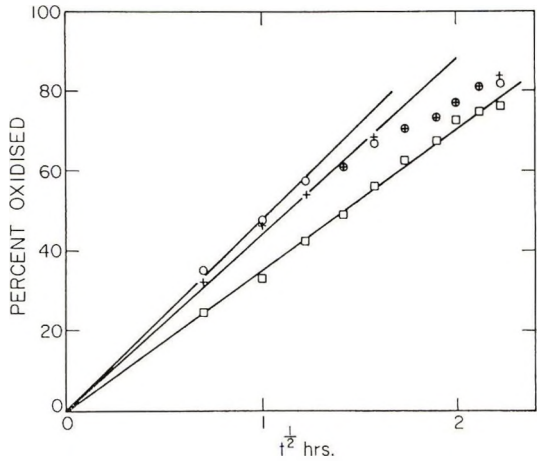

Fig. 1. Oxidation of snake-cage resins based on (○) hydroquinone, (+) catechol and (□) pyrogallol by I_3^-.

Values for redox capacities of 5.3, 5.2, and 5.1 meq/dry gram where determined experimentally for the polymers prepared with pyrogallol, catechol, and hydroquinone respectively, compared with calculated values of 5.20, 5.47, and 5.47 meq/g based on 100% yield. Similarly, values of 1.04, 0.72, and 0.60 meq/g were determined as the absorptive capacities of the resins for iodine.

DISCUSSION

The light coloration of the catechol and pyrogallol resins in their reduced forms, coupled with their stability and near theoretical capacity, indicates that even though polymerization of these polyphenol molecules had been

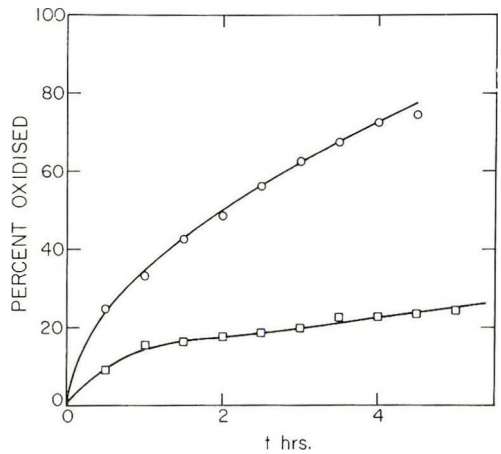

Fig. 2. Oxidation of pyrogallol snake-cage resin by (○) I_3^- and (□) Fe^{3+}.

carried out in their ionized forms at high temperature and in the presence of oxygen, linkage through quinone methide[12] or semi-quinone[13] intermediates was at a minimum. Such linkage is thought to produce the strong coloration, often black, associated with phenoplasts, and it is believed that its lack of formation here may be explained by the positions of the polyphenol molecules in the anion exchange resin matrix during polymerization, with the phenolate ions and adjacent phenol groups being stabilized by orientation towards the fixed positive charges on the anion exchange resin matrix. Compared to the resin prepared with catechol, the resin prepared with hydroquinone showed deeper color in the reduced form and also showed a greater tendency towards degradation by strong base. This is consistent with the fact that both phenolic groups on the hydroquinone molecule cannot be oriented towards fixed positive charges at the same time, one thus being more susceptible to chemical attack, both during the polymerization and during any subsequent reaction. The greater tendency of the pyrogallol based resin to decompose in base, again compared to the catechol resin, may be attributed to increased functionality and thus also less adequate stabilization.

The oxidation of the pyrogallol snake-cage resin by I_3^- as a function of time (Fig. 2) shows a form characteristic of a process controlled by diffusion within the resin beads.[14] This is further confirmed by the straight line dependence on $t^{1/2}$ during the initial stages of oxidation for all three resins (Fig. 1). The straight lines pass through the origin only if the amount of iodine absorbed physically by the resins is subtracted from the outset, indicating that this absorption was a very much more rapid process than that which resulted in oxidation. This may be explained if it is assumed that I_3^- was in fact the predominant oxidative species, and that its diffusion through the resin was appreciably slower than that of the physically absorbed iodine, which did not take part in the oxidation, and which was predominantly in the form of molecular I_2 rather than I_3^- counterions.

The snake-cage redox polyelectrolytes prepared with catechol and pyrogallol suffer few of the drawbacks associated with previously reported redox polymers, as outlined in the introduction. As expected, they show a marked selectivity against cationic species. These two resins also show some capacity for the selective absorption of boron from dilute aqueous solution under reducing conditions. It is intended that this aspect of their chemistry be discussed as part of a future publication.

This work was carried out under Grant No. T 01-ES 00080, National Institute of Environmental Health Sciences, U.S.P.H.S.

References

1. H. G. Cassidy and K. A. Kun, *Oxidation-Reduction Polymers*, Interscience, New York 1965.

2. M. Ezrin and H. G. Cassidy, *Ann. N. Y. Acad. Sci.*, **57**, 79 (1953).

3. M. Ezrin, H. G. Cassidy, and I. H. Updegraff, *J. Amer. Chem. Soc.*, **75**, 1610 (1953).

4. M. Ezrin and H. G. Cassidy, *J. Amer. Chem. Soc.*, **78**, 2525 (1956).
5. L. Luttinger and H. G. Cassidy, *J. Polym. Sci.*, **20**, 417 (1956).
6. H. P. Gregor and M. Beltzer, *J. Polym. Sci.*, **53**, 125 (1961).
7. G. F. Mills and B. N. Dickinson, *Ind. Eng. Chem.*, **41**, 2842 (1949).
8. B. Sansoni, *Naturwiss.*, **39**, 281 (1952).
9. B. Sansoni, *Naturwiss.*, **41**, 212 (1954).
10. K. A. Kun, *J. Polym. Sci. A-1*, **4**, 847 (1966).
11. F. Helfferich, *Ion Exchange*, McGraw-Hill, New York, 1962, p. 59.
12. A. Ravve, *Organic Chemistry of Macromolecules*, Dekker, New York, 1967, pp. 318–321.
13. W. A. Waters, *Mechanisms of Oxidation of Organic Compounds*, Methuen, London, 1964, Chap. 9.
14. F. Helfferich, *Ion Exchange*, McGraw-Hill, New York, 1962, Chap. 6.

Received April 7, 1971
Revised June 30, 1971

JOURNAL OF POLYMER SCIENCE: PART A-1 VOL. 9, 2963–2975 (1971)

Electroinitiated Polymerization of Vinylic Monomers in Polar Systems. III. Polymerization of Acrylates and Methacrylates in Alcohol Solutions

MICHAEL ALBECK and JOSEPH RELIS, *Bar Ilan University, Department of Chemistry, Ramat-Gan, Israel*

Synopsis

Methyl, ethyl, and *n*-butyl acrylates and methacrylates are polymerized by electroinitiation in methanol–, ethanol–, and *n*-propanol–electrolyte mixtures in which the monomers are soluble whereas the polymers obtained are insoluble. The technique of changing the polarity of the electrodes described earlier was used. The relationships between molecular weights and polymer yields as function of current density, initial monomer concentration and dielectric constant of the solvent are described. A kinetic scheme for the initiation, propagation, and termination is given.

Introduction

The electroinitiated polymerization of ethyl methacrylate in methanolic solution in the presence of various lithium salts was described previously.[1] It was shown that with a technique of changing the polarity of the electrodes every 5 min a relatively high yield of polymer of high molecular weight can be obtained. The polymerization was found[1/2] to be initiated and propagated by a free-radical mechanism and takes place in the cathode compartment. It was found that the metal ions which are reduced at the cathode to metal atoms initiate the polymerization whereas hydrogen ions and atoms formed during the electrolysis inhibit the reaction. The relevant literature was referred to in Part II.[1] In this paper the results of the electroinitiated polymerization of methyl, ethyl, and *n*-butyl acrylates and methacrylates in solutions of methanol, ethanol, and *n*-propanol are described. The reaction scheme proposed in Part II[1] is used to account for the behavior of the system at different current densities, and in solvents of different dielectric constant.

Experimental

Acrylates and methacrylates (Fluka, Switzerland, analytical grade) were freed from inhibitor by washing twice with a 5% NaOH solution followed by 5% H_3PO_4 solution and then saturated NaCl solution, dried over Na_2SO_4 or $CaSO_4$ for 24 hr, and finally fractionally distilled under reduced pressure (1 mm Hg). The middle fractions were collected and stored at −30°C.

Methanol, ethanol, and *n*-propanol (Frutarom, Israel, analytical grade) were dried over Mg turnings and fractionally distilled. The middle fractions were collected.

Lithium acetate (Schuchardt, Munich, Germany, analytical grade) was anhydrous and was used without any further treatment.

Molecular weights were determined by the viscosity method. Intrinsic viscosities were measured in Ubbelohde viscometers and the molecular weights determined from the Staudinger equation. The values for K are: 4.5×10^{-5}, 27.7×10^{-5}, 6.85×10^{-5}, 7.24×10^{-5} 2.83×10^{-5} and 4.0×10^{-5} and for α are 0.78, 0.67, 0.75, 0.76, 0.79 and 0.77, for methyl acrylate (MA)[3] (in benzene), ethyl acrylate (EA)[4] (in benzene), *n*-butyl acrylate (BuA)[5] (in acetone), methyl methacrylate (MMA)[6] (in benzene), ethyl methacrylate (EMA)[7] (in 2-butanone), and *n*-butyl methacrylate (BuMA)[8] (in benzene), respectively. Polarographic measurements were performed on an Electroscan 30 polarograph (Beckman Co. U.S.A.). A dropping mercury electrode was employed as indicator electrode and a graphite one (see description of apparatus) as a reference electrode. The distance between the two electrodes was 40 mm. The temperature was 27°C. The voltage was scanned from 0 to 5 V (with reference to graphite electrode). The rate of scanning was 1.2 in./min.

Changing the rate of scanning to 3.0 in./min or to 0.6 in./min affected the results only slightly. Before starting with polarographic measurements, the solution was purged with dry hydrogen until no oxygen reduction wave was observed.

The apparatus and procedure were described in detail elsewhere.[1] Repeated experiments gave results which were reproducible within ±4%. Control experiments showed that under these conditions nonelectroinitiated polymerization did not take place.

Results and Discussion

In polarography of the systems monomer–lithium acetate–solvent two waves develop. The first wave begins at ca. −2 V and the second one at ca. −3 V. Results are given in Table I.

In all cases the first decomposition potential may be assigned to lithium reduction [eq. (1)] and the second one to solvent reduction [eq. (2)] (i.e., the reduction of the proton ot hydrogen atom), since measurements on solutions of methanol saturated with tetramethylammonium bromide and tetramethylammonium acetate (at 25°C) gave the first decomposition potentials at −3.08 and −3.01 V, respectively.

$$Li^+ + e \xrightarrow{k_e} Li\cdot \qquad (1)$$

$$ROH + e \rightarrow RO^- + H\cdot \qquad (2)$$

TABLE I
Decomposition Potentials of Methanolic, Ethanolic, and *n*-Propanolic Solvent Saturated with Lithium Acetate at 25°C and Containing 10% (v/v) of Monomer[a]

	Decomposition potentials, V									
	No monomer		MMA		EMA		MA		EA	
Solvent	1st	2nd	1st	2nd	1st	2nd	1st	2nd	1st	2nd
Methanol	−2.05	−3.30	−1.93	−3.00	−1.90	−2.95	−1.85	−2.85	−1.85	−2.85
Ethanol	−2.13	−3.23	−2.00	−2.98	−1.95	−2.85	−1.85	−2.98	−1.85	−2.75
n-Propanol	−2.15	−2.88	−2.10	−2.63	−2.15	−2.65	−1.80	−2.70	−1.88	−2.70

[a] Measurements made polarographically.

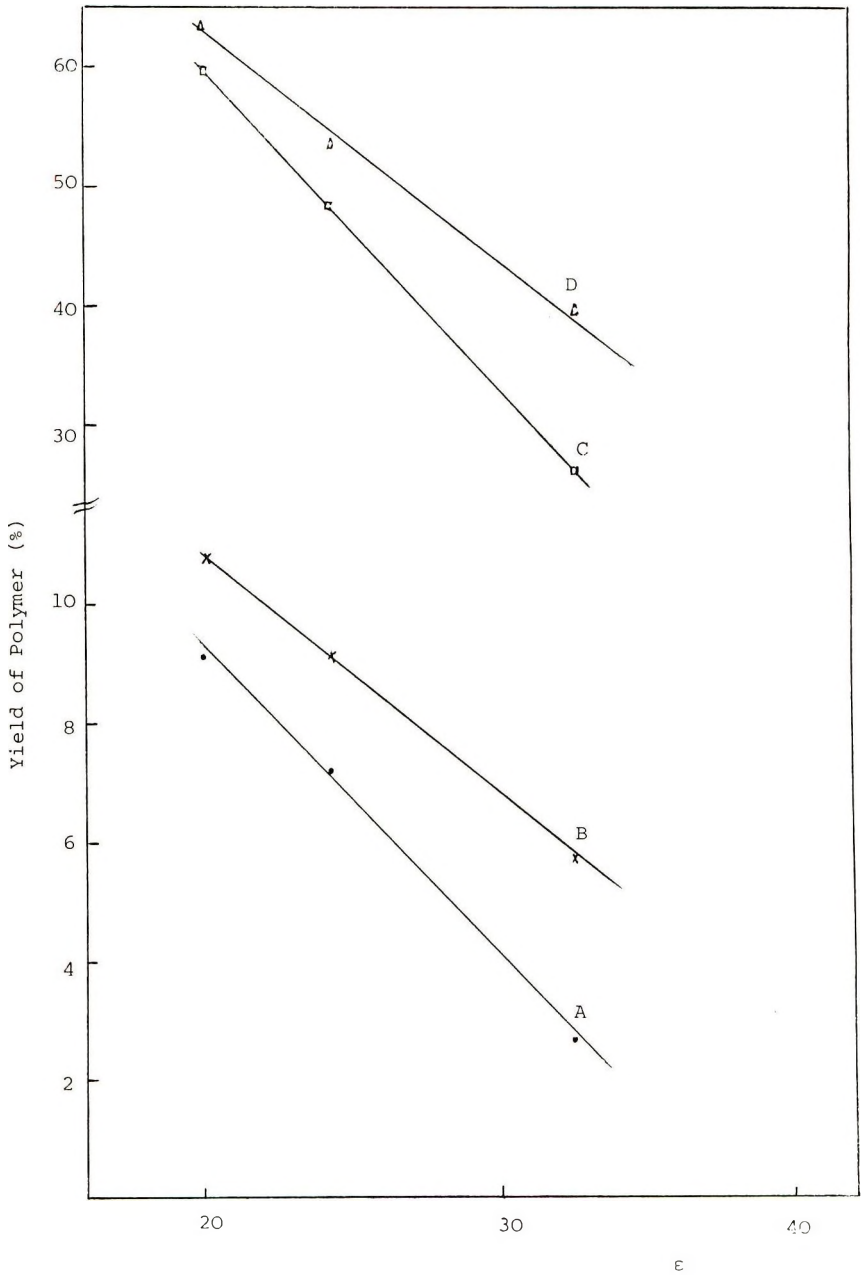

Fig. 1. Yield of polymerization of (*A*) methyl and (*B*) ethyl methacrylates, (*C*) methyl and (*D*) ethyl acrylates as function of the dielectric constants of the solvents methanol, ethanol, and *n*-propanol. Volume ratios of monomer to alcohol 1:1. Polymerization carried out at 50 mA for methacrylates and at 20 mA for acrylates. Reaction time 18 hr at 40°C. Salt concentration 1*M*.

TABLE II
Effect of Solvents on the Yield of Polymer of Methyl and Ethyl Methacrylate and Methyl and Ethyl Acrylate[a]

Solvent	Dielectric constant of the solvent	Yield of polymers, %			
		Methyl methacrylate	Ethyl methacrylate	Methyl acrylate	Ethyl acrylate
Methanol	32.6	2.7	5.7	26.0	39.8
Ethanol	24.3	7.2	9.1	48.5	53.6
n-Propanol	20.1	9.1	10.8	59.7	63.7

[a] Polymerization conducted at 40°C; ratio of monomer to solvent 1:1 (v/v); time of reaction, 18 hr; salt concentration 0.067 g/ml; current 20 mA.

The effect of several polar protic solvents on the yield of the electropolymerization of methyl and ethyl methacrylate and methyl and ethyl acrylates are given in Table II and Figure 1.*

As can be seen from Table II and Figure 1, an inverse linear realtionship exists between the dielectric constant of the solvent and the polymer yield. This linear relationship may be explained as follows. It was found that, in the system under discussion,[1,2] lithium atoms formed at the cathode by reaction (1) are the initiating species of the polymerization.

Lithium atoms are consumed by three main paths: (a) reaction with the monomer to initiate polymerization; (b) reaction with hydrogen ions formed during the electrolysis at the anode according to eq. (3), giving hydrogen atoms and lithium cations according to eq. (4); (c) reaction between lithium atoms and alcohol molecules to give lithium cations and hydrogen atoms according to eq. (5).

$$RCH_2OH \rightarrow RCHO + 2H^+ + 2e \quad (3)$$

$$Li\cdot + H^+ \rightarrow Li^+ + H\cdot \quad (4)$$

$$ROH + Li \rightarrow RO^- + Li^+ + H\cdot \quad (5)$$

Reaction (3) is little affected by the change of the dielectric constant of the solvent (Table I). The reaction between lithium atoms and the solvent molecules (reaction (5)] is, therefore, the main cause of the change in lithium atom concentration in different solvents. The reaction between lithium atoms and the solvent reduces the number of available initiating species and thus a reduction in the yield of the polymerization ensues, which reduction is greater in solvent of higher dielectric constants.

The molecular weights of methyl and ethyl methacrylate and methyl and ethyl acrylate polymerized in methanol, ethanol, and *n*-propanol solutions, are given in Table III. As can be seen, the molecular weights remain practically unchanged, increasing slightly in solvents of lower dielectric constant. The relative constancy of the molecular weights can be explained in the following manner. The decrease in the concentration of the

* Percentage yields are based on initial monomer weight.

initiator which results, generally, in an increase in the molecular weight of the polymer obtained, is compensated by the increase of the concentration of hydrogen atoms terminating the propagation of the polymerization according to eq. (6):

$$M_x\cdot + H\cdot \xrightarrow{k_t} P \tag{6}$$

where $M_x\cdot$ is the growing free radical polymer chain and P the polymer obtained. The increase in hydrogen atom concentration is the result of reaction (5), whose prevalence increases in the order *n*-propanol < ethanol < methanol. [As stated above, reaction (3) is almost unaffected by the change of solvent and therefore the concentration of hydrogen atoms produced according to eqs. (3) and (4) remains practically unchanged.] In other words, the ratio of the rate of propagation R_p to the rate of termination R_t remains unchanged as a result of compensating changes in the two rates in alcoholic solvents of different dielectric constants.

TABLE III
Molecular Weights of Polyacrylates and Polymethacrylates Polymerized in Different Alcoholic Solutions[a]

	Molecular weight × 10^{-4}			
Solvent	Methyl methacrylate	Ethyl methacrylate	Methyl acrylate	Ethyl acrylate
Methanol	69.5	99.6	22.4	2.5
Ethanol	77.9	102.8	23.2	2.6
n-Propanol	88.9	104.4	24.5	2.7

[a] Polymerization conducted at 40°C; ratio of monomer to solvent 1:1 (v/v); time of reaction, 18 hr; salt concentration, 0.067 g/ml; current, 20 mA.

The dependence of yield on current density for polymerization of methyl, ethyl, and *n*-butyl acrylates and for methyl, ethyl, and *n*-butyl methacrylates in methanol solutions are given in Figure 2. In all these polymerizations a maximum in the yield is reached at a certain current value, beyond which an increase in current density causes a decrease in the polymer yield. It has been shown previously[2] that this decrease is due to an increase in hydrogen production by reactions (2)–(4) which becomes significant at higher current densities [see kinetic scheme, eqs. (7)–(11) below]. Furthermore, the reaction between the hydrogen ions and the lithium atoms at higher currents diminishes the initator concentration and as a result reduces the formation of polymer. Lastly, at higher currents, and therefore higher voltages, hydrogen atoms generated according to eq. (2) consume part of the current which would otherwise produce lithium atoms, and thus reduce the extent of the initation.

In general, in the system described, the yields of the acrylates are higher than those of the methacrylates (Fig. 2). Within the methacrylate and acrylate systems the maxima in the yield versus current density are ob-

tained at increasing current values according to the order methyl < ethyl < *n*-butyl esters (Fig. 2) and for each of these groups the yield at the maximum per unit of current increases from methyl to ethyl to *n*-butyl esters. Degree of polymerization (DP) values for the acrylates are generally lower

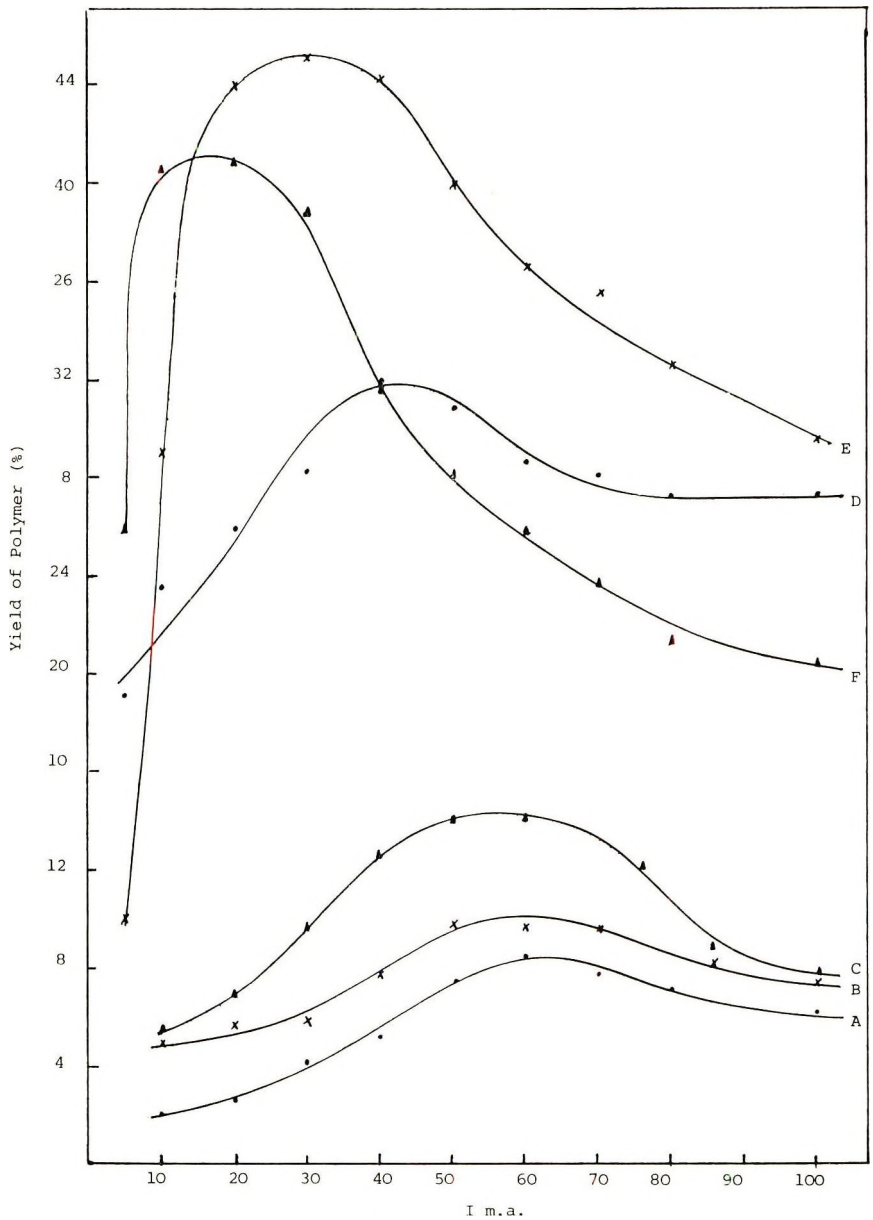

Fig. 2. Yield of polymerization of (*A*) methyl, (*B*) ethyl, and (*C*) *n*-butyl methacrylates and (*D*) methyl, (*E*) ethyl, and (*F*) *n*-butyl acrylates as function of the current. Polymerization carried out in methanol solutions. Volume ratios of monomer to methanol 1:1. Polymerization carried out for 18 hr at 40°C. Salt concentration 1*M*.

TABLE IV
Maximum Yield per Unit Current at the Maximum for Methyl, Ethyl, and *n*-Butyl Acrylates and Methacrylates in Methanol Solutions and the Corresponding DP Values[a]

Ester	Maximum yield per current at the maximum yield, %		DP × 10^{-2}	
	Acrylates	Methacrylates	Acrylates	Methacrylates
Methyl	1.00	0.14	9.3	22.5
Ethyl	1.50	0.20	2.3	41.0
n-Butyl	2.04	0.24	1.3	19.5

[a] DP values taken for polymerization at 60 mA; experiments conducted at 40°C; ratio of monomer to solvent 1:1 (v/v); time of reaction, 18 hr; salt concentration, 0.067 g/ml.

than those for the methacrylates, and an increase in the DP is obtained in the order methyl > ethyl > *n*-butyl esters (with the exception of ethyl methacrylate). The experimental results obtained are given in Table IV.

The amount of soluble material in the methanol solution (oligomers and polymers of lower molecular weights) after the removal of the precipitated polymer, unreacted monomer and salt, were found to be: 15.5 and 2.5% for methyl and ethyl acrylates, respectively, and 106% and 35% for methyl and *n*-butyl methacrylates, respectively (percentages are based on the amount of polymer precipitated in the same run).

A comparison of the rate constants obtained for the free radical initiated polymerization of methyl[9] and *n*-butyl[10] acrylates and for methyl,[11–13] *n*-propyl,[14] and *n*-butyl[15] methacrylates shows that the propagation constant for methyl acrylate is higher than those for methyl, *n*-propyl, and *n*-butyl methacrylate, whereas for *n*-butyl acrylate and within the methacrylate series no consistency was found.[9–15] From the data[16] for heat of polymerization of methyl acrylate[17] and methyl,[17–19] ethyl,[17–19] *n*-propyl,[17] and *n*-butyl[17,18,20] methacrylates, it can be seen that methyl acrylate is more reactive than the methacrylates, whereas within the methacrylate series the reactivity is about the same within the limit of experimental error. The following order of reactivity for methacrylates undergoing radical polymerization (at 30°C) was found by Yokota et al.[21] from rate of polymerization data: phenyl > β-chloroethyl > β-methoxyethyl > β-phenylethyl > γ-phenylethyl > methyl > ethyl. It was found[16,21] that steric substituent constants have no influence on the rate constants for substituted methacrylates.

The results obtained by us (Table IV and Fig. 2) are in accord with the following considerations: (*a*) acrylates are more reactive in initiation and polymerization than the methacrylates, and therefore higher yields are obtained with acrylates compared to methacrylates; (*b*) within the acrylates and the methacrylate series the solubility of the polymers obtained in methanol solution in the order *n*-butyl < ethyl < methyl esters, and therefore the order of increasing yields are polymers of butyl > ethyl > methyl

acrylates and methacrylates (Table IV and Fig. 2); (*c*) acrylates are more reactive than methacrylates in initiation, and therefore, lower DP values are generally obtained for acrylates than for methacryltes; (*d*) as a result of the relative polymer solubilities mentioned above, poly(*n*-butyl acrylate) chains precipitate at lower DP values than poly(ethyl acrylate) chains and the latter at lower DP values than poly(methyl acrylates). The same holds for the relative DP values of the *n*-butyl and methyl methacrylate polymers (Table IV). The behavior of ethyl methacrylate is exceptional and is being further investigated.

A kinetic scheme which accounts for the results obtained in the electroinitiated polymerization system described has the following initiation, propagation, and termination steps:[2]

Initiation:

$$\mathrm{Me}^+ + e \xrightarrow{k_e} \mathrm{Me}\cdot \tag{7}$$

$$\mathrm{Me}\cdot + \mathrm{M} \xrightarrow{k_i} \mathrm{M}\cdot \tag{8}$$

Propagation:

$$\mathrm{M}\cdot + x\mathrm{M} \xrightarrow{k_p} \mathrm{M}\cdot_{x+1} \tag{9}$$

Termination:

$$\mathrm{M}_x\cdot + \mathrm{Me} \xrightarrow{k_t} \mathrm{P} \tag{10}$$

$$\mathrm{M}_x\cdot + \mathrm{H}\cdot \xrightarrow{k_t'} \mathrm{P} \tag{11}$$

where Me^+, $\mathrm{Me}\cdot$, M, $\mathrm{M}\cdot$, $\mathrm{H}\cdot$ and P are lithium cation, lithium atom, monomer, monomer radical, hydrogen atom, and polymer, respectively, and k_e, k_i, k_p, k_t, and k_t' are the rate constants for electrolysis, initiation, propagation, and termination, respectively. In experiments where the polarity of the electrodes was not changed, the polymer formed was deposited as a layer on the cathode surface and eventually stopped the polymerization. This observation is interpeted as indicating that reaction (7) takes place on the cathode surface, whereas reaction (8) may proceed at the outer surface of the polymer formed. This is in accordance with the proposed scheme of Laurin and Parravano[22] for the polymerization of 4-vinylpyridine in liquid ammonia.

The rate of initiation, R_i, is $R_i = fk_e[\mathrm{I}]$, where [I] is the current in Faraday/l. sec and f is the factor representing the fraction of the current which initiate chains according to reaction (7).

The rate of termination, R_t, is $R_t = k_t[\mathrm{M}_x\cdot]\,[\mathrm{Me}\cdot] + k_t'[\mathrm{M}_x\cdot][\mathrm{H}\cdot]$. Under steady-state conditions ($R_i = R_t$), eq. (12) pertains.

$$fk_e[\mathrm{I}] = [\mathrm{M}_x\cdot](k_t[\mathrm{Me}\cdot] + k_t'[\mathrm{H}\cdot)] \tag{12}$$

The rate of propagation R_p is given by $R_p = k_p[\mathrm{M}_x\cdot]\,[\mathrm{M}]$. By letting $[\mathrm{Me}\cdot] = k_c[\mathrm{I}]$ (i.e., the number of lithium atoms formed at the electrode

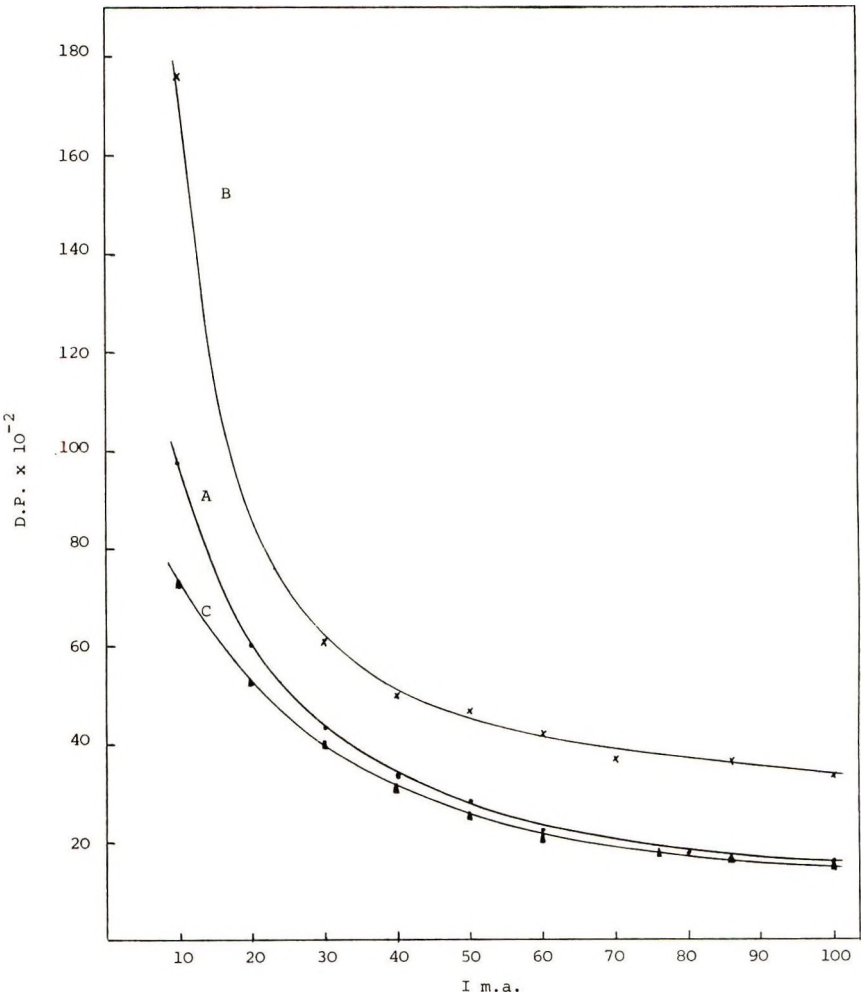

Fig. 3. DP of polymers of (*A*) methyl, (*B*) ethyl, and (*C*) *n*-butyl methacrylates as a function of the current. Polymerization conducted in methanol solutions. Volume ratios of monomer to methanol 1:1. Polymerization carried out at 40°C for 18 hr. Salt concentration 1*M*.

is directly proportional to the current) and by assuming $(k'_t/k_e)[\mathrm{H}\cdot]/[\mathrm{I}] \gg k_t$, the rate of propagation can be written as

$$R_p = (fk_pk_e/k_t')[\mathrm{I}][\mathrm{M}]/[\mathrm{H}\cdot] \tag{13}$$

From eq. (13) it follows that the rate of polymerization is directly proportional to the current supplied and to monomer concentration and inversely proportional to the concentration of hydrogen atoms. The latter is a complicated function of the current [eq. (24) below]. As can be seen from eqs. (13) and (24), at low current values, $[\mathrm{I}]/[\mathrm{H}\cdot] > 1$, and R_p increases with increasing current. Since $[\mathrm{H}\cdot]$ is dependent on a power value of the

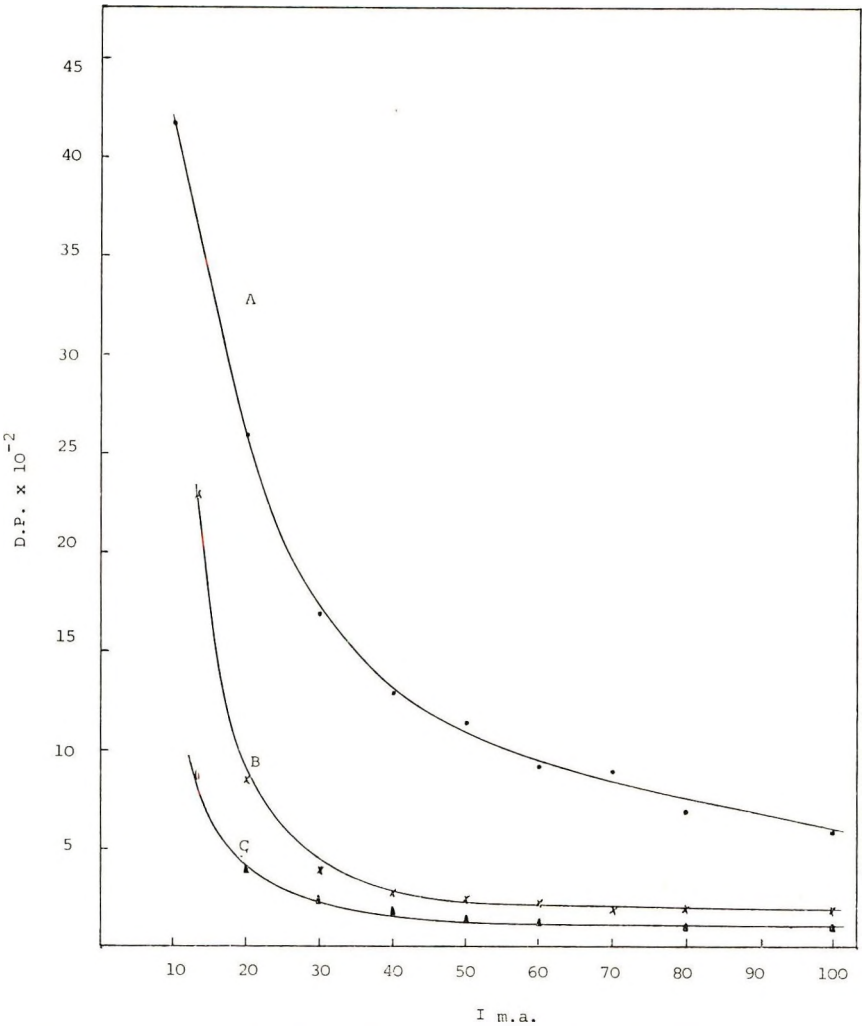

Fig. 4. DP of polymers of (*A*) methyl, (*B*) ethyl, and (*C*) *n*-butyl acrylates as a function of the current. Polymerization conducted in methanol solutions. Volume ratios of monomer to methanol 1:1. Polymerization carried out at 40°C for 18 hr. Salt concentration 1*M*.

current, it reaches a maximum value at $[I]/[H\cdot] = 1$, after which on increasing the current $[H]/[H\cdot] < 1$. The results obtained for the yields of polymers as functions of current density show the expected behavior (Fig. 2).

The kinetic chain length, ν, has the following dependence on the current and monomer concentration

$$\nu = R_p/R_t = k_p/(k_t k_e[I] + k_t'[H\cdot])[H] \quad (14)$$

The terms due to chain transfer and coupling have been omitted since no chain transfer or coupling occurs in the system described.[23]

The kinetic chain length (related to the molecular weight of the polymer since no chain transfer or coupling occurs) increases with monomer concentration and decreases with the current density of the reaction. This behavior is in accord with the results obtained for the polymerization of acrylates and methacrylates at different current densities (Figs. 3 and 4).

The concentration of hydrogen atoms as a function of the variables influencing the reaction can be obtained. Reactions (15)–(21) directly influence the hydrogen atom concentration.

$$\mathrm{Me}\cdot + \mathrm{ROH} \xrightarrow{k_1} \mathrm{Me}^+ + \mathrm{H}\cdot + \mathrm{RO}^- \tag{15}$$

$$\mathrm{Me}\cdot + \mathrm{H}^+ \xrightarrow{k_2} \mathrm{Me}^+ + \mathrm{H}\cdot \tag{16}$$

$$\mathrm{H}^+ + e \xrightarrow{k_3} \mathrm{H}\cdot \tag{17}$$

$$\mathrm{ROH} + e \xrightarrow{k_4} \mathrm{RO}^- + \mathrm{H}\cdot \tag{18}$$

$$2\mathrm{H}\cdot \xrightarrow{k_5} \mathrm{H}_2 \tag{19}$$

$$\mathrm{RO}^- + \mathrm{H}^+ \xrightarrow{k_6} \mathrm{ROH} \tag{20}$$

$$\mathrm{M}_x\cdot + \mathrm{H}\cdot \xrightarrow{k_t'} \mathrm{M}_x\mathrm{H} \tag{21}$$

Under steady-state conditions, were the number of hydrogen atoms produced equal those consumed, the following situation pertains

$$k_1[\mathrm{Me}\cdot][\mathrm{ROH}] + k_2[\mathrm{Me}\cdot][\mathrm{H}^+] + k_3[\mathrm{H}^+] + k_4[\mathrm{ROH}] = k_5[\mathrm{H}\cdot]^2 + k_t'[\mathrm{H}\cdot][\mathrm{M}_x\cdot] \tag{22}$$

From eq. (12) it follows that

$$[\mathrm{H}\cdot] = \frac{fk_e[\mathrm{I}]}{k_t'[\mathrm{M}_x\cdot]} - \frac{k_tk_e[\mathrm{I}]}{k_t'} \tag{23}$$

Introducing this term in eq. (22) gives eq. (24)

$$[\mathrm{H}\cdot] = \frac{[\mathrm{I}](k_1k_e[\mathrm{ROH}] + k_2k_e[\mathrm{I}] + k_3) + k_4[\mathrm{ROH}]}{k_5\{(fk_e[\mathrm{I}]/k_t'[\mathrm{M}_x\cdot]) - (k_tk_e[\mathrm{I}]/k_t')\} + k_t'[\mathrm{M}_x\cdot]} \tag{24}$$

When the concentration of ROH is in excess, $k_3(\mathrm{I})$ can be neglected and $k_4[\mathrm{ROH}] = [\mathrm{I}](1 - k_e)$.

Consequently eq. (24) reduces to eq. (25).

$$[\mathrm{H}\cdot] = \frac{[\mathrm{I}](k_1k_e[\mathrm{ROH}] + k_2k_e[\mathrm{I}] + (1 - k_e)}{k_5\{(fk_e[\mathrm{I}]/k_t'[\mathrm{M}_x\cdot]) - (k_tk_e[\mathrm{I}]/k_t')\} + k_t'[\mathrm{M}_x\cdot]}$$

As was shown above [eq. (2)], the term $k_4[\mathrm{ROH}]$ has to be taken into account in eq. (25) only from a certain value of the potential and up, which value changes from one system to another (i.e., different solvents or monomers). The influence of this complex dependence of hydrogen concentration on the current [eq. (25)] upon polymer yield has already been discussed above.

The results reported herein and in Parts I and II of this series[12] clearly point to the conclusion that the variation of factors such as current density, solvent and monomer concentration in electroinitiated polymerizations with concurrent precipitation of the polymer may be used to control the average molecular weight of the polymers produced. We are currently extending our studies in these techniques to other vinyl monomers, to copolymerizations and to oligomerization reactions.

This work is taken, in part, from the Ph.D. thesis of J. R.

References

1. M. Albeck and J. Relis, *J. Polym. Sci. A-1*, **9**, 1789 (1971) (Part II).
2. M. Albeck, M. Königsbuch, and J. Relis, *J. Polym. Sci. A-1*, **9**, 1375 (1971) (Part I).
3. J. Feisst and H. G. Flias, *Makromol. Chem.*, **82**, 78 (1965).
4. I. B. Eriksson-Quensel and T. Svedberg, *Biol. Bull.*, **71**, 498 (1936).
5. H. K. Schachman, *Protein and Function (Brookhaven Symp. Biol.)*, **13**, 49 (1960).
6. H. C. Beachell and D. W. Carlson, *J. Polym. Sci.*, **40**, 543 (1959).
7. G. B. Rothmann and F. A. Bovey, *J. Polym. Sci.*, **15**, 544 (1955).
8. T. A. Ritscher and H. G. Flias, *Makromol. Chem.*, **30**, 48 (1959).
9. M. S. Matheson, E. E. Auer, E. B. Bevilacqua, and E. J. Hart, *J. Amer. Chem. Soc.*, **73**, 5395 (1951).
10. H. W. Melville and A. F. Bickel, *Trans. Faraday Soc.*, **45**, 1049 (1949).
11. M. S. Matheson, E. E. Auer, E. B. Bevilacqua, and E. J. Hart, *J. Amer. Chem. Soc.*, **71**, 497 (1949).
12. C. H. Bamford and M. J. S. Dewar, *Proc. Roy. Soc.* (London), **197A**, 356 (1949).
13. M. H. Mackay and H. W. Melville, *Trans. Faraday Soc.*, **45**, 323 (1949).
14. G. M. Burnett, M. G. Evans, and H. W. Melville, *Trans. Faraday Soc.*, **49**, 1105 (1953).
15. G. M. Burnett, M. G. Evans, and H. W. Melville, *Trans. Faraday Soc.*, **49**, 1096 (1953).
16. T. Otsu, T. Ito, and M. Imoto, *Macromolecular Chemistry Prague 1965 (J. Polym. Sci. C, 16)*, O. Wichterle and B. Sedlàček, Eds., Interscience, New York, 1967, p. 2121.
17. R. M. Joshi, *Makromol. Chem.*, **66**, 114 (1963).
18. L. K. Tong and W. O. Kenyon, *J. Amer. Chem. Soc.*, **68**, 1355 (1946).
19. F. S. Dainton, K. J. Ivin, and D. A. G. Walmsley, *Trans. Faraday Soc.*, **56**, 1984 (1960).
20. K. G. McCurdy and K. J. Laider, *Can. J. Chem.*, **42**, 818 (1964).
21. K. Yokota, M. Kani, and Y. Ishii, *J. Polym. Sci. A-1*, **6**, 1325 (1968).
22. D. Laurin and G. Parravano, in *Macromolecular Chemistry, Brussels–Louvain 1967 (J. Polym. Sci. C*, **22**), G. Smets, Ed., Interscience, New York, 1978, p. 103.
23. B. L. Funt and K. C. Yu, *J. Polym. Sci.*, **62**, 359(1962).

Received March 29, 1971
Revised May 26, 1971

JOURNAL OF POLYMER SCIENCE: PART A-1 VOL. 9, 2977-2981 (1971)

Initiation of Polymerization of Alkyl 2-Cyanoacrylates in Aqueous Solutions of Glycine and Its Derivatives

R. K. KULKARNI, D. E. BARTAK, and F. LEONARD,
U. S. Army Medical Biomechanical Research Laboratory,
Walter Reed Army Medical Center, Washington, D.C. 20012

Synopsis

The polymerization of methyl 2-cyanoacrylate and heptyl 2-cyanoacrylate was carried out with the use of aqueous solutions of ^{14}C-tagged glycine, methyl glycine, and acetyl glycine as initiators. When glycine and methyl glycine were used, radioactive polymers were formed. When acetyl glycine was used, the polymer formed was not radioactive. The data seem to indicate that free NH_2 groups appear to be necessary for the incorporation of the glycine initiator in the polymer. A possible mechanism for the polymerization is presented.

Introduction

It has been proposed that the initiation of the polymerization of alkyl 2-cyanoacrylates occurs via an anionic mechanism.[1] This mechanism requires that the attacking nucleophile be present as an endgroup in the polymer. That this is the case has been previously reported.[2] For example, when water is used to initiate polymerization, the presence of an OH absorption is observed in the infrared spectrum. Initiation of polymerization in aqueous methanol shows absorption bands due to both the OH group and the OCH_3 group. These data indicate that there is a competition between initiating nucleophiles present for the initiation of polymerization of the 2-cyanoacrylate monomer. Initiation of polymerization of alkyl 2-cyanoacrylates in aqueous solution by use of ^{14}C-glycine indicates that glycine is incorporated into the polymer. The question arises as to whether glycine initiates polymerization through the carboxylate anion or through the amino group. The purpose of this research is to attempt to resolve this question by means of blocking the NH_2 and COOH functions of the glycine molecule before carrying out the polymerization of the alkyl 2-cyanoacrylates. The results of the investigation are presented herein.

Experimental

Aqueous solutions of glycine were prepared containing 2, 4, 8, and 16% (w/v) of glycine. To 100 ml of each of these solutions were added 1.5, 3.0, 6.0, and 12 μl of radioactive glycine solution containing 20 μCi/ml (^{14}C α-carbon). Then 0.1 mole of methyl 2-cyanoacrylate monomer was added

dropwise to the vigorously stirred aqueous solutions of glycine at pH 6.8. The pI for glycine is 5.97. Thus a pH of 6.8 was chosen for this reaction to assure the presence of $NH_2—CH_2—CO_2^-$. Alkaline pH values were not used to avoid high concentrations of OH anions which could minimize initiation by the glycine moiety. After addition of the monomer, the polymer formed was stirred for 2 hr, filtered, and washed with distilled water. The last portions of the wash water had only background count of radioactivity. The polymer was dried at 40°C *in vacuo*, dissolved in acetonitrile, and precipitated from a large quantity of methanol. The polymers were filtered, washed, dried, and subjected to determinations of radioactivity by liquid scintillation counting, using a Packard Tricarb Counter. Number-average molecular weights were determined with a Mechrolab vapor pressure osmometer.

Acetyl glycine[3] (mp 208°C) and methyl ester of glycine hydrochloride[4] (mp 174°C) were prepared from ^{14}C glycine by standard techniques and purified by recrystallization.

The solutions of acetyl glycine and methyl ester of glycine hydrochloride were prepared by using quantities equivalent to the glycine solutions described above. The pH of the solutions was adjusted to 6.8 by using 0.5*N* aqueous NaOH. The polymerization of methyl 2-cyanoacrylate was carried out in these solutions as described, and polymers were isolated, dissolved in acetonitrile, precipitated with methanol, washed with methanol and dried. The radioactivity and number-average molecular weights were determined.

In addition, polymerizations were carried out in ^{14}C-glycine solutions with the use of heptyl 2-cyanoacrylate instead of methyl 2-cyanoacrylate to determine the effect of the chain length of the alcohol residue of the monomer.

The radioactivity of the different compounds used in this investigation was as follows: tagged glycine (α-^{14}C) = 20 μCi/ml; acetyl glycine (α-^{14}C) = 70,200 disintegrations per minute (dpm)/g; glycine methyl ester (α-^{14}C) = 13,000 dpm/g.

Determination of Radioactivity

The polymer sample (0.50 g) was finely powdered and dissolved in 1 ml of hydroxide of Hyamine (10X) (Rohm & Haas) by warming. The solution was transferred to a standard counting vial and diluted to 15 ml by the scintillation fluid. The radioactivity was then measured in a Packard Tricarb Spectrometer, using standard methods. The scintillation fluid contained toluene (1000 ml), dioxane (1000 ml), and methanol (600 ml), 1,4-bis-2-(5-phenyl oxazolyl)benzene (0.26 g), 2,5-diphenyl oxazole (13.00 g), and naphthalene (208.0 g).

Results and Discussion

The radioactivity of the various polymers prepared, the molar ratios of initiator to polymer (calculated from the radioactivity of the polymer) and

TABLE I
Aqueous Anionic Initiation of 2-Cyanoacrylates with Glycine and Derivatives

Initiator concn (aqueous solution), %			Monomer	$\bar{M}_n$ of polymer	Activity, dpm/g polymer	Calculated molar ratio initiator / polymer
Glycine	Methyl ester of glycine	Acetyl Glycine				
2.0	—	—	Me 2-cyano-	2870	108	1/7.7
4.0	—	—	acrylate	2350	236	1/7.3
8.0	—	—		2470	476	1/3.0
16.0	—	—		2790	488	1/2.1
—	4.74	—	Me 2-cyano-	1726	494	1/1.36
—	9.48	—	acrylate	2517	562	1/0.91
—	18.96	—		1650	420	1/1.72
—	—	6.28	Me 2-cyano-	—	33	—
—	—	12.56	acrylate	—	38	—
—	—	25.12		—	72	—
4.0	—	—	Heptyl	3370	444	1/4.3
8.0	—	—	2-cyano-	3940	478	1/3.3
16.0	—	—	acrylate	4970	550	1/1.9

number-average molecular weights are summarized in Table I. In the case of the initiation of the polymerization of methyl 2-cyanoacrylate and heptyl 2-cyanoacrylate with radioactive glycine, the moles of initiator to moles of polymer increased with increasing initiator concentration.

The polymers prepared and isolated from tagged acetyl glycine solutions are very slightly radioactive. The initiating species in this instance in the main may possibly be H_2O molecules and/or OH anions and the initiation of polymerization seems to have taken place with only slight involvement of glycine residues. However, when the methyl ester of glycine is used to initiate polymerization, a relatively large quantity of the glycine moiety appears to be incorporated in the polymer. This behavior of glycine and its derivatives indicates that free NH_2 groups may be essential for the incorporation of glycine residues in the polymer molecules formed.

At the isoelectric point (pH 5.97), the glycine molecule is in the form of a Zwitterion, with equal number of NH_3^+ and COO^- groups, but at 6.8 pH, there is an increase in the $NH_2—CH_2—COO^-$ form. The results indicate that at a concentration of 4% glycine, the poly(methyl 2-cyanoacrylate) formed has on the average one molecule of glycine for 7.3 polymer molecules. At higher concentrations of glycine at the same pH, the availability of NH_2 groups is increased, showing the higher incorporation of glycine molecules in the polymer formed. A similar trend is seen in the polymers formed from heptyl 2-cyanoacrylate. When the methyl ester of glycine is used, the concentration of available free NH_2 groups is maximum because the Zwitterion is unable to form. This could account for the greater incorporation of the glycine moiety in the polymer when the methyl glycine was used as the initiator.

If, as the data seem to indicate, $—NH_2$ groups are essential for polymerization, one mode of initiation of the polymerization reaction may be by the transfer of a lone pair of electrons from the NH_2 group to the electron deficient carbon in the cyanoacrylate molecule. The following mechanism (1) may be written.

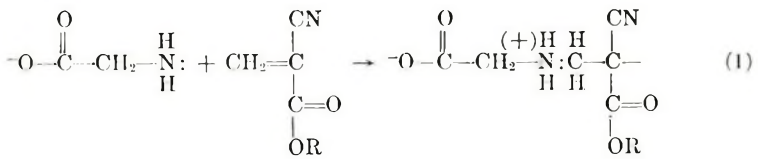

(1)

In the case of the acetyl glycine, a lone pair of electrons may not be readily available on the nitrogen atom under the slightly acidic conditions, possibly because of the predominance of the $R—CO^-=^+NHR$ form, and the overall electronic distribution over the molecule, giving it a neutral character.[5]

The number-average molecular weights obtained in the polymerization reaction do not appear to vary in a systematic manner in the case of the polymerization of methyl 2-cyanoacrylate, whereas in the case of the polymerization of heptyl 2-cyanoacrylate initiated with glycine, the $\bar{M}_n$ seemed

to increase with glycine concentration. These data are not in accord with the known inverse variations in molecular weight with catalyst concentration. The trend of the resulting molecular weights described may be due to the fact that these polymerization reactions are of a heterogeneous nature; other factors, such as rate of stirring and size of the monomer droplet may also affect the average molecular weight of the polymers formed.

References

1. H. W. Coover, F. B. Joyner, N. H. Shearer, Jr., and T. H. Wicker, Jr., *SPE J.*, **15,** 413 (1959).

2. F. Leonard, R. K. Kulkarni, G. Brandes, J. Nelson, and J. L. Cameron, *J. Appl. Polym. Sci.*, **10,** 259 (1966).

3. R. M. Herbst and D. Shemin, *Org. Syn.*, **2,** 11 (1943).

4. J. P. Greenstein and M. Winitz, *Chemistry of the Amino Acids*, Wiley, New York, 1961, Vol. 2, p. 926.

5. R. Q. Brewster and W. E. McEwen, *Organic Chemistry*, Prentice-Hall, 1962, p. 237.

Received May 27, 1971

JOURNAL OF POLYMER SCIENCE: PART A-1 VOL. 9, 2983–2995 (1971)

Synthesis of 1,2-Bis(4-aminocyclohexyl)ethane and Its Polyamides

HIROSHI KOMOTO, FUSAKAZU HAYANO, TOSHIO TAKAMI, and SADAO YAMATO, *Technical Research Laboratory, Asahi Chemical Industry Company Ltd., Tokyo, Japan*

Synopsis

The synthetic route to 1,2-bis(4-aminocyclohexyl)ethane from toluene via *p*-nitrotoluene and *p,p'*-dinitrodibenzyl was established. The distribution of geometric isomers was estimated by NMR and fractional recrystallization. Polyamides were synthesized from 1,2-bis(4-aminocyclohexyl)ethane and dodecanedioic or sebacic acid. Polymer melting temperatures were varied with isomer compositions. A high content of the *trans* conformation causes high melting temperatures. Glass transition temperatures of polyamides were in the range of 105–120°C and were less sensitive to isomer compositions.

INTRODUCTION

Recently polyamides containing cyclohexane rings in the main chain have aroused wide interest because of their remarkably high glass transition temperatures. Fabrics made from the polyamide fibers have excellent properties such as wash-and-wear character.

We were interested in polyamides derived from 1,2-bis(4-amino-cyclohexyl)ethane because of the attractive synthetic route to 1,2-bis(4-amino-cyclohexyl)ethane from toluene [eqs. (1)].

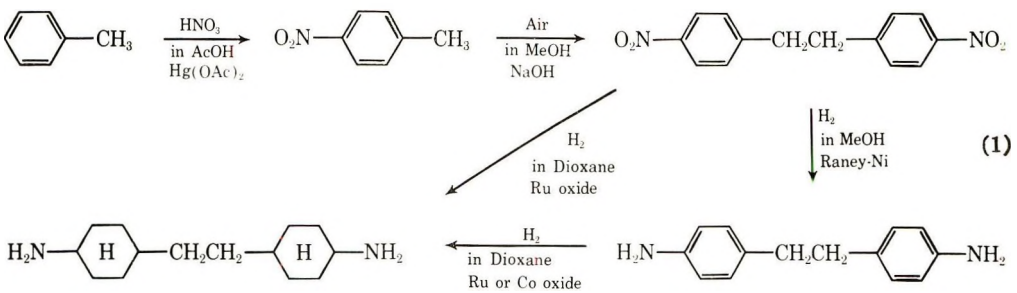

It is well known that the ratio of *o*-, *m*-, and *p*-nitrotoluene is approximately 60:5:35 when toluene was nitrated with a mixture of nitric acid and sulfuric acid. In recent years there has been an increased demand for *p*-nitrotoluene, so it has become very important to nitrate toluene in such a way that an increased yield of *para* isomer is obtained. Attempts have

been made to nitrate toluene with nitric acid in the presence of mercury compounds such as mercuric oxide, whereby the proportion of *p*-nitrotoluene increases. However, the yield of *p*-nitrotoluene itself has remained low.[1–3]

p-Nitrotoluene has been known to undergo oxidative coupling in methanolic potassium hydroxide on introducing air vigorously into the solution, giving dibenzyl and stilbene derivatives.[4–7] Stansbury and Proops also obtained *p,p'*-dinitrodibenzyl together with *p,p'*-dinitrostilbene by oxidative coupling of *p*-nitrotoluene in methanolic sodium hydroxide with ethylenediamine.[8] In these methods, however, it is difficult to obtain a good yield of *p,p'*-dinitrodibenzyl exclusively.

Various catalysts have been described for the hydrogenation of aromatic amines and aromatic nitro compounds to the corresponding alicyclic amines. Among these catalysts, ruthenium dioxide was reported as an excellent catalyst for hydrogenation of *p,p'*-diaminodiphenylmethane to bis(4-aminocyclohexyl)methane.[9] Recently 1,2-bis(4-aminocyclohexyl)-ethane was synthesized from *p,p'*-dinitrodibenzyl by catalytic hydrogenation, using catalysts such as ruthenium on pumice stone and ruthenium dioxide.[10] Takagi and his co-workers reported that ruthenium hydroxide was an effective catalyst for the hydrogenation of aniline to cyclohexylamine at low temperature.[11]

The object of our investigation is to establish the synthetic route to 1,2-bis(4-aminocyclohexyl)ethane from toluene.

Synthesis of polyamide from 1,2-bis(4-aminocyclohexyl)ethane and dodecanedioic acid has been described briefly in the patent literature.[12] It is another object of our investigation to study some properties of the polyamide derived from 1,2-bis-(4-aminocyclohexyl)ethane.

RESULTS AND DISCUSSION

Nitration of Toluene

Mercury-catalyzed nitration of toluene was reinvestigated intensively, and we found that a remarkably high yield of *p*-nitrotoluene was obtained when toluene was nitrated with nitric acid in an acetic acid solution containing dissolved mercuric acetate. Analysis of the products was carried out by gas chromatography. The results are summarized in Tables I–III. The ratio of *p*- to *o*-nitrotoluene produced from this reaction was about 2:1, in contrast with the ratio of the product formed from a reaction in the absence of a mercury catalyst, which was 1:2.

The yield of *p*-nitrotoluene increases with increasing acetic acid and mercuric acetate as shown in Tables I and II. However, selectivity of mononitrotoluene is not so high, presumably because of the formation of byproducts such as dinitrotoluene in this reaction condition, in which 1.5 mole-equivalent nitric acid is used. Diminishing nitric acid to 1.0–1.1 mole-equivalent and raising the reaction temperature to 80°C resulted in

TABLE I
Effect of Acetic Acid Concentration on Nitration of Toluene[a]

Acetic acid, g.	Recovery of toluene, %	Yield of nitrotoluene, %		Ratio *para/ortho*	Selectivity of mononitro-toluene, %[b]
		Para	*Ortho*		
0	46.3	6.1	5.7	1.07	22.0
5	29.8	15.0	8.7	1.73	33.8
10	33.5	25.1	9.7	2.59	52.3
15	30.8	22.6	8.0	2.83	44.2
20	19.5	30.8	11.3	2.73	52.3
25	21.7	31.6	11.6	2.72	55.2
30	22.7	44.6	15.8	2.82	78.1
35	14.0	41.2	16.1	2.56	66.6

[a] Reactions were carried out by using 10 g of toluene, 1.43 g of mercuric acetate, and 1.5 mole-equivalent of nitric acid (specific gravity 1.42) at 50°C for 5 hr.
[b] Yields of *p*- and *o*-nitrotoluene, %/conversion of toluene, %.

TABLE II
Effect of Mercuric Acetate Concentration on Nitration of Toluene[a]

Mercuric acetate, g.	Recovery of toluene, %	Yield of nitrotoluene, %		Ratio *para/ortho*	Selectivity of mononitro-toluene, %[b]
		Para	*Ortho*		
1.43	22.7	44.6	15.8	2.82	78.1
1.0	20.1	34.5	12.1	2.85	58.3
0.5	29.7	32.0	12.8	2.50	63.7

[a] Reactions were carried out by using 10 g of toluene, 30 g of acetic acid, and 1.5 mole-equivalent of nitric acid (specific gravity 1.42) at 50°C for 5 hr.
[b] Yields of *p*- and *o*-nitrotoluene, %/conversion of toluene, %.

TABLE III
Effect of Nitric Acid Concentration on Nitration of Toluene[a]

Nitric acid/ toluene, mole/mole	Temp, °C	Time, hr.	Recovery of tol-uene, %	Yield of nitro-toluene, %		Ratio *para/ ortho*	Selectivity of mono-nitrotol-uene, %[b]
				Para	*Ortho*		
1.0	50	5	51.3	32.7	14.2	2.30	96.3
1.1	50	5	43.1	36.2	17.3	2.09	94.0
1.2	50	5	35.5	36.1	16.3	2.21	81.2
1.5	50	5	29.7	32.0	12.8	2.50	63.7
0.8	80	2	36.6	41.0	20.4	2.01	96.9
0.9	80	2	27.7	45.7	22.3	2.05	94.1
1.0	80	2	23.2	48.5	23.7	2.05	94.0
1.1	80	2	18.3	49.6	24.5	2.02	90.7

[a] Reactions were carried out by using 10 g of toluene, 30 g of acetic acid, and 0.5 g of mercuric acetate.
[b] Yields of *p*- and *o*-nitrotoluene, %/conversion of toluene, %.

an increased yield of *p*-nitrotoluene and higher selectivity of mononitrotoluene, as shown in Table III, even if the amount of mercuric acetate used is comparatively low. A small decrease of *p*- and *o*-nitrotoluene ratio was observed as the reaction temperature was raised. These results imply that the reaction of toluene with nitric acid in the presence of mercuric acetate and acetic acid involves two types of reactions: non-catalytic nitration and mercury-catalyzed reactions. The latter are initiated by the mercuration of toluene, followed by substitution with the nitro group. This scheme favors the *para* isomer because of the *para* orientation of mercuration[13] in contrast with the former, which favors the *ortho* isomer. The fact that the low yield of *para* isomer was obtained in the absence of acetic acid indicates that acetic acid facilitates the nitration via mercurated toluene.

Oxidative Coupling of *p*-Nitrotoluene

Oxidative coupling of *p*-nitrotoluene was carried out in a methanolic sodium hydroxide, bubbling air into the solution. The use of methanolic sodium hydroxide instead of methanolic potassium hydroxide was found to give only *p,p'*-dinitrodibenzyl in excellent yield under appropriate reaction conditions (Table IV). Raising the reaction temperature and prolonging the reaction time causes further oxidation of *p,p'*-dinitrodibenzyl to *p,p'*-dinitrostilbene. Adequate alkali was necessary to complete the reaction without producing any by-products.

TABLE IV
Oxidative Coupling of *p*-Nitrotoluene (*p*-NT)

						Products[a]	
p-NT, g	MeOH, l.	NaOH, g	Temp, °C	Time, hr	Yield, g	DND, %	DNS, %
100	1	200	27	8	58	100	0
100	1	200	35	2	51	100	0
100	1	200	35	4	65	100	0
100	1	200	35	6	86	100	0
100	1	200	35	8	87	97	3
100	1	200	40	4	83	100	0
100	1	200	40	6	85	35	65
100	0.5	100	40	3	69	94	6
100	0.75	150	40	4	69	90	10
100	0.9	175	40	6	87	37	63

[a] DND = *p,p'*-dinitrodibenzyl; DNS = *p,p'*-dinitrostilbene.

Synthesis of 1,2-Bis(4-aminocyclohexyl)ethane

Hydrogenation of *p,p'*-dinitrodibenzyl, *p,p'*-diaminodibenzyl, and *p,p'*-dinitrostilbene was carried out using various catalysts. Ruthenium(III)

oxide trihydrate* was found to be a superior catalyst to other ruthenium compounds, such as ruthenium dioxide and ruthenium on alumina. Hydrogenation of the aromatic nuclei occurred at temperatures as low as 100°C when ruthenium(III) oxide trihydrate was used as a catalyst. Other ruthenium compounds required temperatures of 180–220°C (Table V).

Ruthenium(III) oxide trihydrate was prepared from ruthenium trichloride in dilute hydrochloric acid by neutralization with aqueous sodium hydroxide.[11] No crystalline peak was shown in the x-ray diffraction diagram of ruthenium(III) oxide trihydrate.

1,2-Bis(4-aminocyclohexyl)ethane should exist in three geometrically isomeric forms, namely, *trans-trans*, *trans-cis*, and *cis-cis*. Contents of these isomers in reaction products were estimated by their NMR and fractional recrystallization of formylated isomers.

In NMR spectroscopy it has long been recognized that signals of axial and equatorial protons of the cyclohexane ring appear in different fields.[14,15] As monosubstituted cyclohexane undergoes rapid inversion of each of the two conformers at room temperature, the signal of the α-proton will appear at an average field position rather than at the position appropriate for a purely axial or purely equatorial proton. Dailey and co-workers determined the positions of the signals of purely axial and purely equatorial α-protons of several monosubstituted cyclohexanes by recording the NMR spectra at a temperature low enough to slow down the interconversion of the conformational isomers.[14] Cyclohexylamine, however, shows only a signal of the α-proton at 7.53τ which is assigned to the axial α-proton, even at low temperatures. The signal shifts to 7.50τ at 26°C. They concluded from this that the population of the equatorial α-protons of cyclohexylamine is nearly zero at room temperature.

Eliel and Gianni determined the chemical shifts of axial and equatorial 1-H by measuring the shifts of 4-*tert*-butyl-substituted cyclohexyl compounds.[15] The *cis* isomer gives the signal of equatorial 1-H and the *trans* isomer axial 1-H. However, 4-*tert*-butylcyclohexylamine was not included in their study.

We studied the chemical shifts of a series of cyclohexylamine derivatives in order to evaluate the isomer contents of 1,2-bis(4-aminocyclohexyl) ethane. Results are shown in Table VI. The 4-*tert*-butylcyclohexylamine exhibited broad signals at 7.4 and 6.8τ which were assignable to axial and equatorial 1-H, respectively. As the tertiary butyl group is equatorial, axial 1-H corresponds to the *trans* conformation and equatorial 1-H to the *cis*. Similar signals were found in the spectrum of 4-methylcyclohexylamine. Acetylation of the amino group moved these signals to a lower field as expected. 4-*Tert*-butylcyclohexylamine, 4-methylcyclohexylamine, and *N*-acetyl-4-methylcyclohexylamine were examined

* Otherwise denoted as ruthenium hydroxide; the precise structure of the compound has not been determined.

TABLE V

Synthesis of 1,2-Bis(4-aminocyclohexyl)ethane (Ruthenium Catalyst)

Expt. no.	Starting material		Catalyst		Dioxane, ml	NH_4OH, ml[c]	Temp, °C	Time, hr	Yield, %
	Type[a]	Wt, g	Type[b]	Wt, g					
ACE-1	DND	40	Ru–Ox	0.8	100	—	100	5	77
ACE-2	DND	300	Ru–Ox–C	60	600	30	130	7	61
ACE-3	DND	40	Ru–Ox–C	16	100	5	140	3	81
ACE-4	DND	40	Ru–Ox–C	8	100	5	150	3.5	72
ACE-5	DND	40	Ru–Ox–C	8	100	5	160	3	70
ACE-6	DND	40	Ru–Ox–C	8	100	5	170	2.5	67
ACE-7	DND	40	Ru–Ox	0.8	100	5	200	1	80
ACE-8	DND	40	RuO_2	0.5	100	6.3	200	3	78
ACE-9	DND	40	Ru–A	8	100	5	220	2.5	75
ACE-10	DND	40	K_2RuO_4	2.5	100	6.3	180	2	69
ACE-11	DND	40	K_2RuO_4	2	100	10	200	1	69
ACE-12	DND	40	K_2RuO_4	1.5	100	20(liq.)[d]	200	0.5	75
ACE-13	DAD	52	Ru–Ox	2.5	125	—	100	4	80
ACE-14	DAD	47	Ru–Ox	1	100	20(liq.)[d]	120	5	86
ACE-15	DNS	40	Ru–Ox	0.8	100	5	220	5	45
ACE-16	DNS	40	Pd–C Ru–Ox	4.0	100	5	150	2	45

[a] DND = *p,p'*-dinitrodibenzyl; DAD = *p,p'*-diaminodibenzyl; DNS = *p,p'*-dinitrostilbene.

[b] Ru–Ox = ruthenium(III) oxide trihydrate (or ruthenium hydroxide) prepared from ruthenium trichloride; Ru–Ox–C = ruthenium(III) oxide trihydrate supported on charcoal [Ruthenium(III) oxide trihydrate content was 10 wt-%]; Ru–A = 1% ruthenium on alumina; Pd–C = 5% palladium on charcoal.

[c] Aqueous ammonia (28% concentration).

[d] Liquid ammonia, g.

and found to be a mixture of *trans* and *cis* isomers. *N*-Benzoyl-4-methylcyclohexylamine was separated by fractional recrystallization into trans and cis isomers. Although the *trans* isomer should contain two conformers, where 1-H and 4-H protons are axial-axial or equatorial-equatorial, the fraction of the latter conformer should be very small. Accordingly, the signals of the *trans* isomer at 6.2τ are assignable to axial 1-H. The signal of the *cis* isomer appeared in a different field from that of the *trans* isomer. Its position is considered to be an average field because of an inversion of the 1-H and 4-H position between equatorial-axial and axial-equatorial.

TABLE VI

NMR Spectral Data for 1-H in Cyclohexylamine Derivatives (60 Mc, in $CDCl_3$)

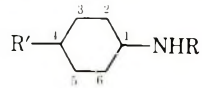

R	R'	Conformation	*Trans*, τ	*Cis*, τ
H	CH_3	Mixture	7.5	7.1
H	$(CH_3)_3C$	Mixture	7.4	6.8
CH_3CO	CH_3	Mixture	6.4	6.0
C_6H_5CO	CH_3	*Trans*[a]	6.2	—
C_6H_5CO	CH_3	*Cis*[b]	—	5.9
H	$H_2NC_6H_{10}C_2H_4$	Mixture	7.4	7.1
H	$H_2NC_6H_{10}C_2H_4$	*Trans*[c]	7.4	—

[a] Mp 175–177°C (from ethyl acetate).

[b] Mp 113–117°C (from acetone).

[c] Obtained by hydrolysis of formylated *trans-trans* isomer.

1,2-Bis(4-aminocyclohexyl)ethane exhibited signals at 7.1 and 7.4τ which were assignable to 1-H of *cis* and *trans* conformers. Therefore, we can estimate the ratio of trans and cis isomers for each cyclohexane ring by integrating the NMR signals at 7.1 and 7.4τ. However, contents of *trans-trans*, *trans-cis*, and *cis-cis* isomers cannot be calculated by NMR data only. In order to evaluate the contents of the three isomers, 1,2-bis-(4-aminocyclohexyl)ethane was formylated and the *trans-trans* isomer was isolated by fractional recrystallization. This formylated *trans-trans* isomer was then hydrolyzed to *trans-trans* 1,2-bis(4-aminocyclohexyl) ethane. Its NMR exhibited only a signal at 7.4τ in the region of 7–8τ. *Trans-cis* and *cis-cis* contents were calculated by combining NMR data with results of fractional recrystallization. The results are summarized in Table VII.

The *trans* content increases in direct proportion to the increase in the reaction temperature. This fact suggests that the isomer composition can be controlled by the hydrogenation temperature.

Cobalt catalysts were also utilized for hydrogenation of *p,p'*-diaminodibenzyl. However, *p,p'*-dinitrodibenzyl was not hydrogenated by these catalysts (Table VIII).

TABLE VII
Isomer Distribution of 1,2-Bis(4-aminocyclohexyl)ethane

Expt. no.[a]	Conformation, %[b]		Isomer distribution, %		
	Trans	*Cis*	*Trans-trans*[c]	*Trans-cis*[d]	*Cis-cis*[d]
ACE-1	39	61	9	54	37
ACE-2	47	53	20	53	27
ACE-3	44	56	19	50	31
ACE-4	50	50	21	58	21
ACE-5	59	41	26	66	8
ACE-6	65	35	30	70	0
ACE-13	36	64	8	56	36

[a] Experiment numbers correspond to those in Table V.
[b] Determined by NMR peaks.
[c] Determined by fractional recrystallization of formylated 1,2-bis(4-aminocyclohexyl) ethane.
[d] Calculated from NMR and fractional recrystallization data.

TABLE VIII
Synthesis of 1,2-Bis(4-aminocyclohexyl)ethane (Cobalt Catalyst)[a]

Starting material		Catalyst		Temp, °C	Time, hr	Yield, %	Isomer distribution, %		
Type	Wt, g	Type	Wt, g				*Trans-trans*	*Trans-cis*	*Cis-cis*
DAD	50	Co_2O_3	5.0	200	7	83	45	55	0
		CaO	7.5						
		Na_2CO_3	3.75						
DAD	50	CoO	5.0	200	16	88	43	57	0
		CaO	7.5						
		Na_2CO_3	3.75						
DAD	50	CoO	5.0	200	10	82	44	56	0
		CaO	7.5						
		Na_2CO_3	3.75						
DND	67	CoO	5.0	200	5	0			
		CaO	7.5						
		Na_2CO_3	3.75						

[a] 100 ml. of tetrahydrofuran was used as solvent.

Hydrogenation of *p,p'*-dinitrodibenzyl to *p,p'*-diaminodibenzyl was successfully carried out by using palladium on alumina or Raney nickel as a catalyst (Table IX).

As hydrogenation of the nitro group is a highly exothermic reaction, control of the reaction temperature is rather difficult in the hydrogenation of *p,p'*-dinitrodibenzyl. *p,p'*-Diaminodibenzyl is preferable for controlling the reaction temperature in order to obtain the desired isomer composition. *p,p'*-Dinitrostilbene gave only a low yield of 1,2-bis(4-aminocyclohexyl) ethane.

TABLE IX
Synthesis of *p,p'*-Diaminodibenzyl

DND, g.	Catalyst		Solvent		Temp, °C	Time, hr.	Yield, %
	Type	Wt, g	Type	Vol, ml			
15	Raney Ni	1.5	MeOH	60	150	4	45.5
15	Raney Ni (W-7)	1.5	MeOH	45	100	2	78
30	Raney Ni (W-7)	3	o-DCB[a]	150	160	2.5	85
80	Pd-Al_2O_3[b]	4	MeOH	350	100	4	82

[a] o-Dichlorobenzene.
[b] 5% Palladium on alumina.

Polyamides

Polyamides were synthesized from mixtures of the geometric isomers of 1,2-bis(4-aminocyclohexyl)ethane and sebacic or dodecanedioic acid by the usual melt condensation method. They exhibited considerable differences in melting temperatures. A high content of the *trans* conformation is inclined to cause high melting temperatures. The results for various compositions are given in Table X.

TABLE X
Polyamides Derived from 1,2-Bis(4-aminocyclohexyl)ethane

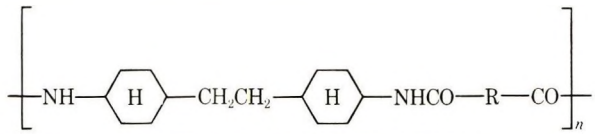

Diamine[a]	R	Mp of nylon salt, °C[b]	Polymerization temp, °C	Polyamide[c]	
				Mp, °C[d]	T_g, °C[d]
ACE-2	—$(CH_2)_{10}$—	188	300	270	105
ACE-3	—$(CH_2)_{10}$—	191	315	277	106
ACE-4	—$(CH_2)_{10}$—	199	330	291	115
ACE-5	—$(CH_2)_{10}$—	210	350	311	109
ACE-6	—$(CH_2)_{10}$—	221	360	316	—
ACE-3	—$(CH_2)_8$—	198	330	—	115
ACE-4	—$(CH_2)_8$—	205	335	305	121
ACE-5	—$(CH_2)_8$—	207	340	329	116
ACE-6	—$(CH_2)_8$—	212	340	333	—

[a] Numbers correspond to those in Table V.
[b] Determined in capillary by the usual method.
[c] Inherent viscosities of the polyamides measured at a concentration of 0.5 g in 100 ml of *m*-cresol at 35°C were in the range of 0.9–1.2.
[d] Determined by differential scanning calorimeter.

Glass transition temperatures of polyamides were in the range of 105–120°C and were less sensitive to isomer compositions.

Fiber spun from the polyamide of dodecanedioic acid showed a melting point at 270°C. Some physical properties of the fiber are listed in Table XI.

TABLE XI
Properties of Fiber from Dodecanedioic Acid and 1,2-Bis(4-aminocyclohexyl)ethane

Sample	Treatment	Tensile strength g/den	Elongation, %	Young's modulus, g/den	Work recovery (3%) Instant, %	Work recovery (3%) Delayed, %
I	Unstretched filament	1.1	250	13		
II	I drawn two times its original length at 120°C	2.3	101	18		
III	I drawn four times its original length at 140°C	2.6	31	34	93	99
IV	III treated in boiling water for 30 min	2.7	44	25	82	94
V	IV heat-set at 160°C for 10 min	2.9	27	29	88	100

EXPERIMENTAL

Nitration of Toluene

A typical procedure is as follows. In a 100-ml four-necked flask equipped with a mechanical stirrer, reflux condenser, thermometer, and dropping funnel, 0.5 g of mercuric acetate was dissolved in 30 g of acetic acid, and 10 g of toluene was added to the solution. The mixture was stirred vigorously, and 5.3 ml. of nitric acid (92 wt-%) was then added dropwise during 10 min at 80°C. After stirring the mixture for 2 hr at 80°C, 100 ml of water was added, and the oily layer was separated and washed twice with 50 ml of water. Yields of the products were determined by gas chromatography (column of 30% SE-30 and 10% KOH at 100°C and 210°C) by using benzene and nitrobenzene as internal standards and methanol as a solvent.

Oxidative Coupling of *p*-Nitrotoluene

Dry air was introduced vigorously into a solution of 200 g. of sodium hydroxide in 1 liter of methanol, and 100 g of finely powdered *p*-nitrotoluene was added to the solution. Vigorous stirring and bubbling of air was continued for 4 hr at 40°C, and the precipitates formed were separated by filtration and washed with hot water and ethanol to give 83 g (83%) of *p,p'*-dinitrodibenzyl. Its purity was found to be more than 99% by gas chromatography (column of 30% SE-30 and 10% KOH at 270°C). It was further purified by recrystallization from benzene, mp 178–180°C.

When the reaction time was prolonged at 40°C, the products became a mixture of *p,p'*-dinitrodibenzyl and *p,p'*-dinitrostilbene. *p,p'*-Dinitrostilbene remained undissolved in benzene and was recrystallized from 1,1,-2,2-tetrachloroethane, mp 280–284°C.

Synthesis of 1,2-Bis(4-aminocyclohexyl)ethane

Ruthenium(III) Oxide Trihydrate on Charcoal. In 2 liters of 0.1*N* aqueous hydrochloric acid was dissolved 50 g of ruthenium trichloride monohydrate, and then 300 g of activated charcoal powder was added. The solution was neutralized by 1*N* aqueous sodium hydroxide, and the mixture was heated at 80°C for 5 min. Charcoal powder containing ruthenium oxide precipitated and was separated by filtration, washed with water until no chloride ion was detected in the filtrate, and dried.

When ruthenium chloride solution was neutralized without adding charcoal powder, precipitates of ruthenium oxide alone were obtained. The x-ray refraction pattern of this ruthenium(III) oxide was amorphous in contrast with that of ruthenium dioxide which showed crystalline peaks.

Potassium Ruthenate on Charcoal. A mixture of 2.053 g of ruthenium trichloride monohydrate, 10 g of potassium hydroxide, and 1 g of potassium nitrate was fused in a nickel crucible and heated for 2 hr. After cooling, it was dissolved in 300 ml of distilled water, and then 17.593 g of active charcoal powder was added to the solution. The mixture was allowed to stand overnight. Active charcoal powder containing potassium ruthenate was separated by filtration and washed with water until no chloride ion was detected in the filtrate. Finally, it was dried at 110°C for 15 hr.

Hydrogenation. A typical procedure is as follows. A mixture of 40 g of *p,p*-dinitrodibenzyl, 100 ml of dioxane, 5 ml of aqueous ammonia (28% concentration), and 16 g of charcoal powder containing 10 wt-% ruthenium(III) oxide trihydrate was charged into a 500-ml autoclave. The autoclave was pressured with hydrogen and purged several times to remove air, after which the autoclave was pressured at 100 kg/cm^2 with hydrogen. The autoclave was heated slowly with vigorous stirring. Hydrogenation of the nitro group proceeded at about 100°C exothermally, temperature rose, and pressure was dropped. Hydrogen was added occasionally to keep the pressure. After the exothermic reaction ceased, the temperature was raised and hydrogenation of aromatic nuclei was carried out at 140°C and 90–105 kg/cm^2 for 3 hr. The reaction mixture was discharged from the autoclave while still warm and the autoclave rinsed with dioxane. The catalyst supported on active charcoal powder was filtered off. The filtrate was evaporated and then distilled under reduced pressure to give 26.5 g (81%) of 1,2-bis(4-aminocyclohexyl)ethane boiling at 164–169°C/5 mm Hg.

Formylation of 1,2-Bis(4-aminocyclohexyl)ethane. To a solution of 9.2 g (0.0410 mole) isomeric mixture of 1,2-bis(4-aminocyclohexyl)ethane in 10 ml of ethanol was added dropwise 15 ml (0.2424 mole) of methyl

formate with stirring over a period of 20 min at room temperature. Stirring was continued an additional hour. After adding 8 ml more of ethanol, the reaction mixture was refluxed 3 hr and then allowed to stand overnight in a refrigerator to give 2.4 g of *trans-trans* isomer as a crystalline product. It was recrystallized from ethanol; mp 238–240°C.

The following experiment confirmed that the amount of diformyl *trans-trans* isomer dissolved in the filtrate by the treatment described above was negligible. To a mixture of 30 ml of ethanol, 5 ml of methyl formate, and 1 ml of methanol was added 3.00 g of diformyl *trans-trans* isomer. The mixture was stirred for 10 min and allowed to stand overnight at room temperature. By this method 2.82 g of diformyl *trans-trans* isomer was recovered.

Polyamides

Preparation of Dodecanedioic Acid Salt of 1,2-Bis(4-aminocyclohexyl)-ethane. To a solution of 56.66 g (0.2525 mole) of 1,2-bis(4-aminocyclohexyl)ethane (mixtures of 20% *trans-trans*, 53% *trans-cis*, and 27% *cis-cis*) in 500 ml of ethanol was added a solution of 57.58 g (0.25 mole) of dodecanedioic acid in 400 ml of ethanol. The salt precipitated immediately as a sticky mass which crystallized by adding 2 liters of acetone to the mixture and storing it in a refrigerator overnight. The microcrystalline salt was collected by suction filtration and dried under reduced pressure at 80°C to give 103.7 g (91%) of nylon salt; mp 185–188°C.

Preparation of Polyamides. Into a glass tube were added 10 g of salt and 0.1 ml of water. The tube was evacuated and filled with oxygen-free nitrogen four times at atmospheric pressure, and then evacuated and sealed. The sealed tube was heated at 200°C for 2 hr. The tube was then cooled and opened and contents were heated with stirring under nitrogen atmosphere and then reduced pressure at 300°C for 30 min.

Inherent viscosities of the polyamide measured at a concentration of 0.5 g in 100 ml of *m*-cresol at 35°C was 1.03. Polymer melting temperatures and glass transition temperatures determined by differential scanning calorimeter were 270 and 105°C, respectively.

Fiber Spinning

Filament was prepared from a polymer showing a melting point at 270°C by extruding molten polymer at 285°C through a spinneret.

References

1. T. L. Davis, D. E. Worrall, N. L. Drake, R. W. Helmkamp, and A. M. Young, *J. Amer. Chem. Soc.*, **43**, 594 (1921).

2. S. Tsutsumi and E. Iwata, *Nippon Kagaku Zasshi*, **72**, 141 (1951).

3. T. Yoshida, T. Ozawa, M. Tamura, and K. Namba, *Kogyo Kagaku Zasshi*, **70**, 1367 (1967).

4. O. Fischer and E. Hepp, *Ber.*, **26**, 2231 (1893).

5. A. G. Green, A. H. Davies, and R. S. Horsfall, *J. Chem. Soc.*, **91**, 2076 (1907).

6. R. C. Fuson and H. O. House, *J. Amer. Chem. Soc.*, **75**, 1325 (1953).

7. T. Tsuruta, T. Fueno, and J. Furukawa, *J. Amer. Chem. Soc.*, **77**, 3265 (1955).
8. H. A. Stansbury, Jr., and W. R. Proops, *J. Org. Chem.*, **26**, 4162 (1961).
9. A. E. Barkdoll, D. C. England, H. W. Gray, W. Kirk, Jr., and G. M. Whitman, *J. Amer. Chem. Soc.*, **75**, 1156 (1953).
10. Imperial Chemical Ind. Ltd., French Pat. 1,554,775 (Jan. 24, 1969).
11. S. Nishimura, T. Shu, T. Hara, and Y. Takagi, *Bull. Chem. Soc. Japan*, **39**, 329 (1966).
12. E. I. du Pont de Nemours and Company, Japan. Pat. 9676 (May 6, 1969).
13. H. C. Brown and K. L. Nelson, *J. Amer. Chem. Soc.*, **75**, 6292 (1953).
14. B. P. Dailey, A. Gawer, and W. C. Neikam, *Discussions Faraday Soc.*, **34**, 18 (1962).
15. E. L. Eliel and M. H. Gianni, *Tetrahedron Letters*, **1962**, No. 3, 97.

Received April 26, 1971
Revised June 15, 1971

JOURNAL OF POLYMER SCIENCE: PART A-1 VOL. 9, 2997–3008 (1971)

Hydrodimerization in Liquid Ammonia

H. ROSEN and M. LEVY, *Plastics Research Department, Weizmann Institute of Science, Rehovot, Israel*

Synopsis

The hydrodimerization of acrylonitrile (M_1), ethyl acrylate (M_2), and α-methyl acrylonitrile (M_3) in liquid ammonia by Na amalgam was studied. It was found that the concentration of phenol, as protonating agent, affects the rate of electron transfer from the amalgam to the monomer. This was explained by assuming the active species to be the protonated monomer complex MH^-. Cross hydrodimerization rate constants were measured for the three monomers. The values of the ratios obtained were: $k_{11}/k_{12} = 0.89$, $k_{22}/k_{21} = 0.39$, $k_{11}/k_{13} = 5.8$, $k_{33}/k_{31} = 0.12$, $k_{22}/k_{23} = 1.7$, $k_{33}/k_{32} = 0.36$.

INTRODUCTION

Na amalgam reacts readily with some acrylic monomers to yield the monomer radical anion $M^{\cdot-}$. This can then participate in three parallel reactions:

Hydrogenation:

$$M^{\cdot-} + H^+ \rightarrow \cdot MH \xrightarrow[+H^+]{+Na} MH_2 \tag{1}$$

Hydrodimerization:

$$M^{\cdot-} + M \rightarrow \cdot MM^- \xrightarrow[+2H^+]{+Na} HMMH \tag{2}$$

Polymerization:

$$M^{\cdot-} + nM \rightarrow \sim\sim M^- \tag{3}$$

The outcome of the reaction depends on the solvent medium used and on the proton donor. Suitable aprotic polar solvents, such as dimethyl sulfoxide (DMSO) and liquid ammonia, favor the hydrodimerization and they were used for a kinetic study of the reaction.[1,2] Furthermore, on adding two monomers simultaneously, cross hydrodimers were obtained and relative rate constants for homo and cross hydrodimerization were estimated.[3]

However, on further study it was found that in liquid ammonia some anomalies are encountered; e.g., on addition of α-methylacrylonitrile to acrylonitrile, the amount of adiponitrile formed increases instead of decreasing. This presented a problem that could not be explained by the

simple mechanism proposed previously, and it was therefore necessary to carry out a more detailed study of the liquid ammonia system.

EXPERIMENTAL

As discussed previously,[1,3] in order to derive any kinetic data from a heterogeneous system, it is very important to be able to control the degree of dispersion of the two phases. Therefore, the physical characteristics of the reactor, the rate of stirring, and the volumes of the two phases have to be kept constant. The reactor used consisted of a round-bottomed flask equipped with a stirrer connected to an rpm counter and an electric stop watch. It contained also a cold finger to return the evaporating ammonia and an exit tube at the bottom for collecting the amalgam and products. The flask was maintained in a bath at (−40°C) and the reaction was carried out for 10 sec. at 280 rpm. DMSO experiments, carried out for comparison, were run at 0°C and at 400 rpm. The monomers, acrylonitrile, AN (M_1), ethyl acrylate, EA (M_2) and α-methylacrylonitrile, MeAN (M_3) were distilled before use. Liquid ammonia, pure grade, was distilled from Na metal and stored in a Dewar flask. Phenol was analytical grade. The products were determined by gas chomatography. They consisted of (1) hydrogenation products: propionitrile (PN), ethyl propionate (EP), and isobutyronitrile (IBN); (2) hydrodimers: adiponitrile (ADN), ethyl adipate (EAD), and 2,5-dimethyladiponitrile (diMeADN); (3) cross hydrodimers: ethyl-δ-cyanovalerate (ECV), 2-methyladiponitrile (MeADN), and ethyl-2-methyl-5-cyanovalerate (EMeCV).

The experimental procedure was the following: 45 cc amalgam were introduced into the reaction flask and allowed to cool for 10 min. The stirrer was operated for 10 sec to avoid any heterogeneity of the amalgam. The reaction mixture (cooled to −40°C) was then added. The stirrer and stop watch were operated (by the same switch), and after 10 sec stirring, the amalgam was separated, the solution was collected in a flask, NH_3 evaporated, 25 cc diglyme added, and the products analyzed by G. C. The internal standards used were butyronitrile for the low-boiling fractions and *p*-tolunitrile for the higher-boiling fractions (5% of the weight of monomers). The standards were added from the beginning with the reactants. Control experiments showed that they had no effect on the outcome of the reaction. The experiments presented in Figures 1 and 2 were run for longer periods to high degrees of conversion.

RESULTS AND DISCUSSION

Effect of Proton Donor

Three proton donors were studied: H_2O, NH_4Cl, and phenol.

H_2O. The effect of water as proton donor in the reaction of AN and Na amalgam is shown in Figure 1. The molar ratio of PN/ADN is plotted as a function of the initial molar ratio of H_2O/NH_3. It can be seen that

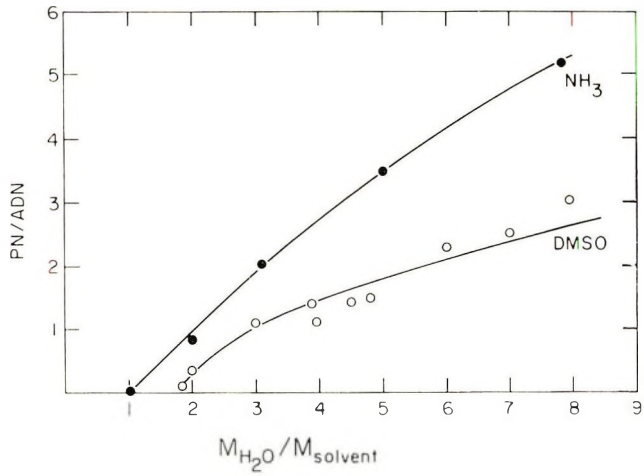

Fig. 1. Comparison of effect of water concentrations on the ratio of PN/ADN in liquid ammonia and in DMSO. 5% AN concentration. Reaction carried out to almost complete conversion.

when the latter ratio is equal to unity no PN is detected and the major product is ADN. This indicates that when most of the water is bound as NH_4OH it is extremely ineffective in the hydrogenation reaction, while it is still effective enough as a terminator for the hydrodimerization and also as inhibitor of the polymerization. This behavior is parallel to that shown by DMSO (Fig. 1). DMSO can bind two molecules of water, and consequently at a molar ratio of H_2O/DMSO = 1.8, the PN/ADN ratio goes to zero. However, the reactivity of water under these conditions is low and at least a tenfold excess of water to monomer is necessary for effectively inhibiting the polymerization reaction. Other proton donors tested were more effective.

NH_4Cl. Ammonium chloride in liquid ammonia is a very strong acid. Its effect on the reaction of AN, EA, and MeAN was studied, and the results are presented in Figure 2. Here the ratio of the hydrogenated monomer to its hydrodimer, MH_2/M_2H_2, is plotted versus the molar ratio of NH_4Cl/monomer. The striking result is that both AN and EA yield no hydrogenated products when equimolar amounts of NH_4Cl and monomer are present. When excess of NH_4Cl is added, however, the PN/ADN increases sharply, while EP/EAD increases also but to a lesser extent. For MeAN the results are quite different: even at very low NH_4Cl/MeAN the IBN/diMeADN is considerable, and it is impossible to obtain only diMeADN with NH_4Cl as proton donor.

To account for the behavior of NH_4Cl we assume that NH_4^+ is associated with the monomer to give a protonated species MH^+ at the amalgam interface, and this is the reactive species. The equilibrium

$$M + NH_4^+ \rightleftarrows MH^+ + NH_3$$

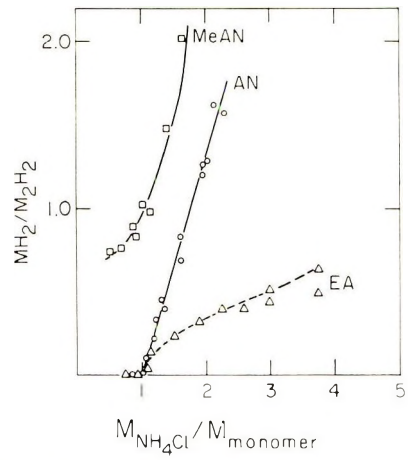

Fig. 2. Effect of the molar ratio of NH_4Cl/monomer on the molar ratio of hydrogenated monomer to hydrodimer in liquid ammonia. Monomer concentration 5%. Reaction carried out to almost complete conversion.

at the interface will affect the rate of the reaction. If we assume that the equilibrium constants for AN and EA are high, we can expect a high yield of the respective hydrodimers when the NH_4Cl/monomer ratios are unity. Increasing the NH_4Cl concentration beyond this ratio will result in the presence of free NH_4^+ at the double layer and this will cause hydrogenation of the monomers. In the case of MeAN, however, the equilibrium constant for $MeANH^+$ formation is apparently low, and the hydrogenation rate is high, and this is the reason why the major product is the hydrogenated monomer IBN.

Phenol. The results of the experiments carried out with phenol as proton donor are presented in Figure 3. In this case all three monomers yield mainly the hydrodimers when the ratio phenol/monomer = 1. This is due to the fact that phenol is a much weaker proton donor than NH_4Cl. One can see that the rate of hydrogenation increases considerably in the order AN, EA, MeAN. We have also added in Figure 3 the results obtained in diglyme–DMSO under comparable conditions. In this case the ratios of MH_2/M_2H_2 are much higher. This is an indication that phenol is a more powerful hydrogenating agent in DMSO. It should be noticed that in both solvents MH_2/M_2H_2 for EA is higher than for AN, in contrast with the results obtained with NH_4Cl.

Further information can be obtained from kinetic measurements. It became evident that phenol affects the rate of the electron transfer process which is assumed to be the rate determining step in the reaction. The rates of hydrodimerization measured as % hydrodimer formed in 10 sec as well as the rates of the overall reaction, namely % ($MH_2 + M_2H_2$) formed in 10 sec are presented in Figure 4 for liquid ammonia. It can be seen that at constant AN concentration, increasing the phenol/AN ratio from 1 to 2 increases the rate of ADN formation from 17.5% to 26.5%. Further in-

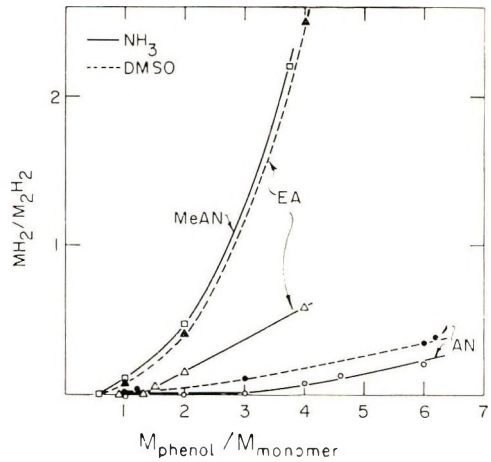

Fig. 3. Effect of the molar ratio of phenol/monomer on the molar ratio of hydrogenated monomer to hydrodimer in liquid ammonia and in diglyme–DMSO. In liquid ammonia: monomers, 0.2 M; Na, 2.0M, 280 rpm; t, 10 sec; in diglyme–DMSO: EA, 0.15M; 400 rpm; AN, 0.15M; 650 rpm, Na, 0.7M; DMSO, 6.1M; t, 10 sec.

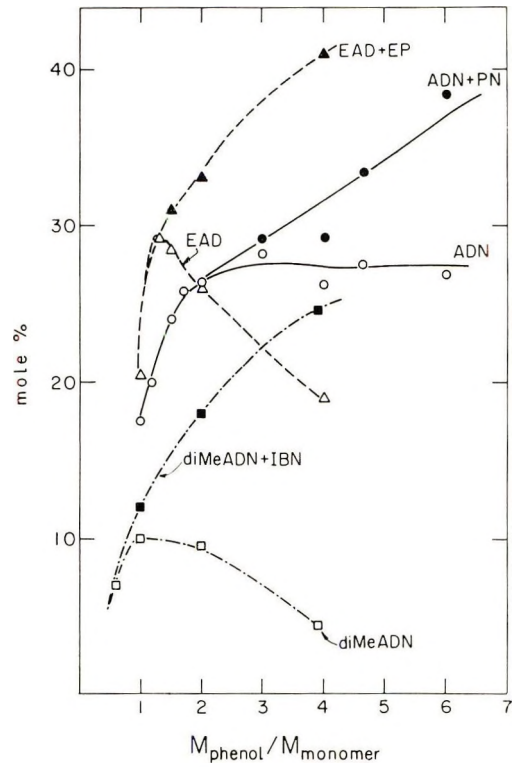

Fig. 4. Effect of the molar ratio phenol/monomer on the rate of hydrodimerization (mole-% M_2H_2/10 sec) and the overall rate of reaction [mole-% (M_2H_2 + MH_2)/10 sec] in liquid ammonia. Monomer, 0.2 M; Na, 2.0M; 280 rpm; t, 10 sec.

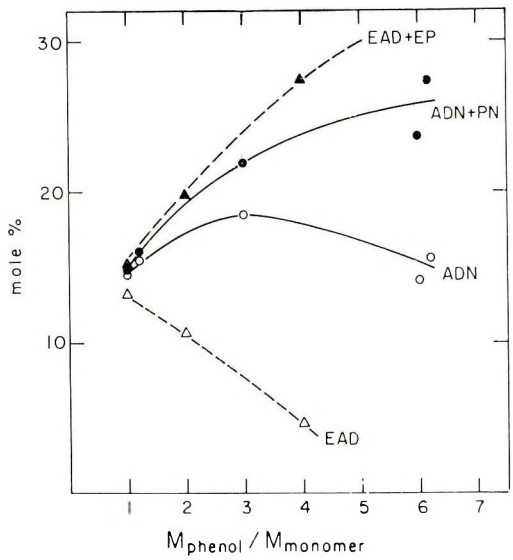

Fig. 5. Effect of the molar ratio of phenol/monomer on the rate of hydrodimerization (mole-% M_2H_2/10 sec) and the overall rate of reaction [mole-% (M_2H_2 + MH_2)/10 sec] in diglyme–DMSO. Monomer, 0.15*M*; Na, 0.7*M*; DMSO, 6.1*M*; 400 rpm; *t*, 10 sec.

crease results in little change in the rate of ADN formation, but the overall rate of reaction continues to increase considerably. A somewhat similar situation is found for EA. The EAD rate of formation increases to a maximum at a ratio of 1.2 and then decreases sharply while the overall rate continues to increase. Here the hydrogenation is so fast that it competes with the hydrodimerization. MeAN has a flat maximum for hydrodimerization at a ratio of phenol/monomer of between 1 and 2 while the overall rate of reaction continues to increase sharply. A more or less similar behavior is observed in DMSO, as can be seen from Figure 5. MeAN was not studied in DMSO because the overall rate of reaction of MeAN is slower by a factor of 120 in comparison with AN and it could not be measured in the time scale used in these series of experiments. It should be realized that in liquid ammonia the reaction of MeAN is only twice as slow as that of AN.

As in the case of NH_4Cl, we assume that phenol interacts with the monomers to give the protonated species MH^+ at the amalgam interface. The concentration of the reactive species MH^+ is determined by the equilibrium

$$M + HA \rightleftharpoons MH^+ + A^-$$

and this depends on the concentration of phenol. Therefore the overall rate of the reaction will increase with the phenol concentration in spite of the fact that the monomer concentration is kept constant.

Support for this interpretation comes from the study of the effect of the monomer concentration at a fixed ratio of phenol/monomer = 1. One can see (Table I) that the reaction is first-order in respect to monomer and

the per cent conversion remains constant over a 25-fold change in concentration, for the three monomers studied. As the phenol/monomer ratio was maintained constant, it means that the phenol concentration was also changed by a factor of 25, without affecting the rate, and this is due to the fact that the equilibrium remained unchanged, in line with the above interpretation.

TABLE I
Effect of Monomer Concentration on the Rate of Reaction[a]

Monomer	[Monomer] × 10^2, M	Dimer, % (w/w)
AN	5	33.8
	10	27.0
	20	34.3
	40	32.0
	80	26.6
	120	24.0
EA	5	31.4
	10.5	37.4
	20	34.8
	40	35.0
	80	37.5
	120	36.1
MeAN	5.5	18.6
	10	19.4
	20	20.0
	40	18.9
	80	16.8
	120	12.7

[a] [Na] = $2.0M$; $\frac{M_{\text{phenol}}}{M_{\text{monomer}}} = 1$; $t = 10$ sec; 280 rpm.

Effect of Na Concentration

The Na concentration in the amalgam is an important factor in amalgam reactions. It was shown previously that, in solvents such as diglyme, diglyme–DMSO, and liquid ammonia, the rate of AN reaction was directly proportional to the concentration of Na in the amalgam over a limited range of concentrations. On further study it was found that this was not always the case. The results presented in Figure 6 are representative of a large number of experiments at different monomer concentrations. They show that while the rate of reaction of MeAN increases linearly with the Na concentration, AN is very slightly affected by the Na content. EA on the other hand, reacts faster at lower Na concentrations. To interpret these findings we have to remember that amalgam reactions are basically indirect electrolytic reactions and as such they depend strongly on the potential surface at the amalgam. An increase in Na concentration from 0.3 to $2M$ corresponds to an increase in potential of 0.05 V. For MeAN, whose reduction potential is high (−2.05 V), this increase is important, and it leads to a corresponding increase in rate. AN has a reduction potential of (−1.91 V)

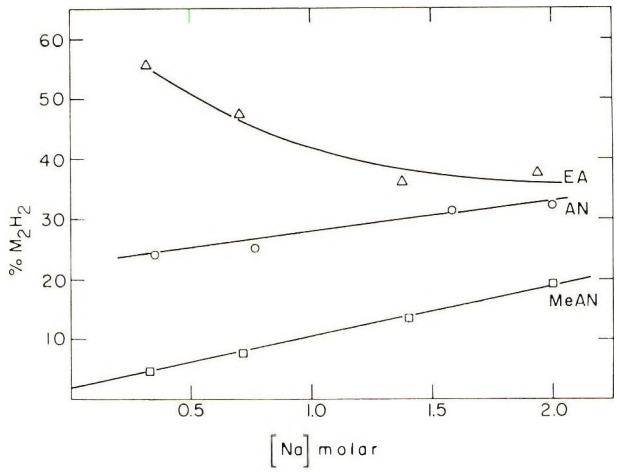

Fig. 6. Effect of the Na concentration in the amalgam on the rate of reaction, expressed as % hydrodimer formation in 10 sec, in liquid ammonia. Monomer, 0.2*M*; 280 rpm; *t*, 10 sec.

which is about the potential of the amalgam (−1.96 to −2.01 V). This, therefore, is in the range of the reaction and has only a moderate effect. EA on the other hand, is below this region (−1.85 V), and it may be that the decrease in rate is due to a lowering of the adsorption of the monomer as a result of getting away from the electrocapillary maximum, because of the increase of negative charge on the amalgam. Similar cases were reported by Petrovich et al.,[4] where an increase in potential led to a decrease in product formation. These relative potential values are probably very much dependent on the solvent medium, and this may account for the different behavior in liquid ammonia and DMSO.

Cross Hydrodimerization

In view of the results described above, it seems that the optimal Na concentration in the amalgam for cross hydrodimerization studies in liquid ammonia would be 2*M*. At this range the rates of EA and AN reactions are similar and MeAN has a high enough rate so that considerable formation of

TABLE II
Cross Hydrodimerization of AN + EA in Liquid Ammonia

AN/EA, mmole	ADN, mmole	EAD, mmole	ECV, mmole	k_{11}/k_{12}	k_{22}/k_{21}
2/8	0.05	1.16	0.76	0.69	0.61
2/4	0.1	0.40	0.64	0.85	0.49
2/2	0.16	0.09	0.44	1.05	0.31
4/4	0.30	0.20	0.94	0.85	0.34
4/2	0.44	0.03	0.48	1.40	0.19
			Average	0.89	0.39

TABLE III
Cross Hydrodimerization of AN + MeAN in Liquid Ammonia

AN/MeAN mmole	ADN, mmole	diMeADN, mmole	MeADN, mmole	k_1/k_3	k_{11}/k_{13}	k_{33}/k_{31}
$^2/_8$	0.28	0.20	0.52	3.8	9.1	0.11
$^2/_4$	0.35	0.05	0.32	5.8	5.7	0.12
$^2/_2$	0.39	0	0.15	—	3.2	—
$^4/_4$	0.75	0	0.21	—	4.5	—
$^4/_2$	0.83	0	0.11	—	4.8	—
$^8/_2$	1.42	0	0.07	—	6.2	—
				Average	5.8	0.12

TABLE IV
Cross Hydrodimerization of EA + MeAN in Liquid Ammonia

EA/MeAN mmole	EAD, mmole	diMeADN, mmole	MeECV, mmole	k_2/k_3	k_{22}/k_{23}	k_{33}/k_{32}
$^2/_8$	0.14	0.38	0.56	3.4	1.8	0.35
$^2/_4$	0.22	0.15	0.45	3.3	1.8	0.33
$^2/_2$	0.33	0.06	0.38	3.8	1.5	0.40
$^4/_4$	0.61	0.08	0.62	3.7	1.8	0.36
$^4/_2$	0.81	0.03	0.42	4.6	1.7	0.40
				Average	1.7	0.36

$MeAN^{\cdot-}$ can be expected. The optimal ratio of phenol/monomers is unity, because under these conditions very little hydrogenation products or polymers are formed.

The results obtained under these conditions for AN, EA, and MeAN cross hydrodimerization are summarized in Tables II–IV. Each number represents an average of at least 2–3 runs.

Reactions (1)–(6) have to be considered in cross hydrodimerization.

$$M_1 + Na \xrightarrow{k_1} M_1^{\cdot-} + H^+ \quad (1)$$

$$M_2 + Na \xrightarrow{k_2} M_2^{\cdot-} + Na^+ \quad (2)$$

$$M_1^{\cdot-} + M_1 \xrightarrow{k_{11}} (M_1H)_2 \quad (3)$$

$$M_1^{\cdot-} + M_2 \xrightarrow{k_{12}} (HM_1M_2H)_{M_1}^{\cdot-} \quad (4)$$

$$M_2^{\cdot-} + M_2 \xrightarrow{k_{22}} (M_2H)_2 \quad (5)$$

$$M_2^{\cdot-} + M_1 \xrightarrow{k_{21}} (HM_1M_2H)_{M_2}^{\cdot-} \quad (6)$$

where $(HM_1M_2H)_{M_1}^{\cdot-}$ and $(HM_1M_2H)_{M_2}^{\cdot-}$ designate the cross hydrodimers formed from the radical ions $M_1^{\cdot-}$ and $M_2^{\cdot-}$, respectively.

We assume steady state conditions for $M_1^{\cdot-}$ and $M_2^{\cdot-}$ and use the fact that the experimental value for the cross hydrodimer must equal the fractions formed from $M_1^{\cdot-}$ and $M_2^{\cdot-}$, which cannot be evaluated separately, namely

$$HM_1M_2H = (HM_1M_2H)_{M_1^{\cdot-}} + (HM_1M_2H)_{M_2^{\cdot-}} \tag{7}$$

On solving the equations derived from the above scheme, one gets the expression (8):

$$\frac{k_{22}}{k_{21}} = \frac{([M_1]/[M_2])[M_2H]_2\{1 + (k_1[M_1]/k_2[M_2])\}}{[M_1H]_2 + [HM_1M_2H] - (k_1[M_1]/k_2[M_2])[M_2H]_2} \tag{8}$$

As we cannot calculate the ratio k_1/k_2 from the cross-hydrodimerization experiments, we have to assume that the rates of electron transfer to each monomer is independent of the presence of the other one, and therefore the results of the homodimerization experiments, under identical conditions, can be used for the calculation of k_1/k_2. (A check for this assumption was obtained by comparing the experimental sum of hydrodimers in the cross-hydrodimerization experiments with the sum obtained in the homodimerization experiments under identical conditions.) The data obtained from homodimerization experiments given in Table I were used to obtain k_1/k_2, and this value was used for the calculation of k_{11}/k_{12} and k_{22}/k_{21} for AN and EA (Table II).

The values are not very constant, and they differ by a factor of 3. However, considering the fact that the experimental results of ADN/EAD change by a factor of 340 this can be considered reasonable, especially in view of the large experimental error involved in determining very small concentrations of products. On the other hand, the trends in the magnitude of the constants are probably meaningful. These could be rationalized on the basis of small differences in the equilibrium constants for MH^+ formation between the monomers leading to phenol/monomer ratios different from unity for each one. As seen from Figure 4, the rates of electron transfer as a function of phenol/monomer ratio differs in AN and EA, and this can bring about changes in k_1/k_2 for the extreme cases of the monomer ratios.

In the cross hydrodimerization of AN and MeAN it was found that in high MeAN/AN ratios the amount of ADN obtained was higher than in the corresponding homodimerization experiments. In the low MeAN/AN experiments no diMeADN could be detected. It seems obvious that we cannot use the values of k_1/k_3 calculated from homodimerization. Nor can we use the expression used above for the low MeAN/AN experiments, because no diMeADN is formed.

The increase in the ADN formation can be readily explained by considering the data of Figure 4. The rate of ADN formation increases when the phenol/AN ratio increases. Therefore, we can conclude that when the reaction mixture contains phenol in equimolar quantities to the sum of AN and MeAN a higher fraction of the phenol is bound to AN than to MeAN, namely the equilibrium constant for the protonation of AN is larger. As

we do not have, at this stage, any measure of the equilibrium constants, we shall assume that the difference is large enough so that the maximal value for ADN formation will be reached before any interaction of phenol with MeAN can be considered. In other words, whenever phenol/AN ≤ 2 all the phenol will be bound to AN and therefore no diMeADN will be found (see Table III). For these experiments the simple equation

$$k_{11}/k_{13} = [\text{ADN}][\text{MeAN}]/[\text{MeADN}]\,[\text{AN}]$$

can be used, and obviously k_{33}/k_{31} cannot be evaluated as $\text{MeAN}^{\cdot-}$ was not formed.

When phenol/An > 2, the excess phenol will be bound to MeAN and the value of k_1/k_3 can be calculated from Figure 4 and used for the evaluation of k_{11}/k_{13} and k_{33}/k_{31}. The calculated rate constants are given in Table III. It can be seen that although k_{11}/k_{13} was calculated from two different equations, the results are reasonably close.

Similar arguments were used for EA and MeAN. Here the maximal value for EA is at phenol/EA = 1.2 (Fig. 4). The results of the calculated rate constants are given in Table IV.

CONCLUSIONS

All the cross-hydrodimerization constants in both liquid ammonia and DMSO are summarized in Table V. In general terms, it can be concluded that AN and EA are quite similar, but in both cases crossing is favored as is very often the case in copolymerization reactions. MeAN is always less reactive than the other two monomers. The results in both solvents are similar, in spite of the considerable effect of liquid ammonia on the rate of electron transfer to MeAN.

TABLE V
Rate Constant Ratios for Cross Hydrodimerization of AN, EA, and MeAN

Monomers	DMSO – Diglyme	Liquid NH_3
AN + EA	$k_{11}/k_{12} = 0.65$; $k_{22}/k_{21} = 0.25$	$k_{11}/k_{12} = 0.89$; $k_{22}/k_{21} = 0.39$
AN + MeAN	$k_{11}/k_{13} = 4.0$	$k_{11}/k_{13} = 5.8$; $k_{33}/k_{31} = 0.12$
EA + MeAN	$k_{22}/k_{23} = 1.2$	$k_{22}/k_{23} = 1.7$; $k_{33}/k_{32} = 0.36$

In view of our assumption that the active species is the protonated monomer

$$M_1 + HA \underset{}{\overset{K_1}{\rightleftharpoons}} M_1H^+ + A^- \tag{9}$$

we should write the cross-hydrodimerization reactions

$$M_1H^+ + Na \xrightarrow{k_1'} {}^{\cdot}M_1H + Na^+ \xrightarrow[\text{fast}]{+Na} {}^{-}M_1H + 2Na^+ \tag{10}$$

and

$${}^{-}M_1H + M_1H^+ \xrightarrow{k_{11}'} (M_1H)_2 \text{ etc.} \tag{11}$$

This will not change the whole kinetic scheme developed above, it will only mean that the rate constants calculated will actually include the equilibrium constants namely, $k_{11} = k_{11}'K_1$, $k_{12} = k_{12}'K_2$, etc. As we do not have any definite proof for the existence of such equilibrium, we prefer at this stage to present the experimental results as such. We hope that additional work will help in the final elucidation of the problem.

References

1. Y. Arad, M. Levy, H. Rosen, and D. Vofsi, *J. Polym. Sci. A-1*, **7**, 2159 (1969).
2. Y. Arad, M. Levy, H. Rosen, and D. Vofsi, *J. Polym. Sci. B*, **7**, 197 (1969).
3. H. Rosen, Y. Arad, M. Levy, and D. Vofsi, *J. Amer. Chem. Soc.*, **91**, 1425 (1969).
4. J. P. Petrovich, J. D. Anderson, and M. M. Baizer, *J. Org. Chem.*, **31**, 3897 (1966).

Received April 9, 1971

JOURNAL OF POLYMER SCIENCE: PART A-1 VOL. 9, 3009–3025 (1971)

Effects of Temperature on Styrene–Methacrylonitrile Copolymerization

A. RUDIN and R. G. YULE, *Department of Chemistry, University of Waterloo, Waterloo, Ontario, Canada*

Synopsis

The free-radical copolymerization of styrene and methacrylonitrile was studied in toluene solution at 60, 90, and 120°C. Copolymer composition was estimated from gas-chromatographic measurement of unreacted monomer concentrations. Reactions were carried to about 20% conversion to minimize analytical errors. Reactivity ratios were calculated by using an integrated form of the Mayo-Lewis simple copolymerization equation. Reactivity ratios were not sensitive to reaction temperature. The values at 90°C are $r_1 = 0.41$ (methacrylonitrile) and $r_2 = 0.37$ (styrene). The r_1 values are higher than those reported by other workers, presumably because of advantages in the present analytical technique and calculation method. The negligible temperature dependence of reactivity ratios is in accord with theory. If monomer pairs exhibit pronounced dependence of reactivity ratios on polymerization temperature, this may indicate a change in mode of placement of units in the polymer chain.

Introduction

Copolymerization reactivity ratios have been studied by a large number of workers.[1] Agreement between different laboratories is, however, not always as close as could be desired. A recent review[2] cites several reasons for this, including inaccuracy in estimation procedures and polymer analyses. The use of linear forms of the differential copolymer equation can result in uncertainties in reactivity ratios because of abnormal weighting of some observations in the calculations. This error, and that due to changes in relative monomer concentration during reaction, can be avoided by applying an integrated form of a suitable copolymer equation.[3,4] This procedure, which has become practical only with the availability of digital computers, is used in the study reported here.

Reactivity ratios of monomers containing the nitrile group seem to be subject to peculiar analytical uncertainties. Carbon, nitrogen, or chlorine assays were not consistent in a study of vinylidene chloride–acrylonitrile,[5] and Kjeldahl nitrogen estimates of acrylonitrile content of styrene copolymers were lower than nuclear magnetic resonance values.[6] These and other examples cited below suggest that a reexamination of the free radical copolymerization of styrene and methacrylonitrile could be worthwhile.

The analytical method used in this study is based on gas–liquid chromatographic measurements of unreacted monomer. This method does not

require isolation and cleaning of the polymer before analysis and avoids potential errors due to loss of low molecular weight polymer and products of side reactions. The gas-chromatographic method is easily calibrated with pure monomers as primary standards. It has been used to measure reactivity ratios with other monomer pairs.[7–9] An effort was made in this study to extend the gas-chromatographic analysis to copolymerizations with high monomer conversion, using a computer solution of an integrated form of the simple copolymer equation.

Polymer composition is inferred from measurements of unreacted monomer concentrations. The absolute error in a single assay of residual monomer is independent of degree of conversion, but the relative uncertainty in the measurement of the amount of monomer consumed is inversely proportional to conversion. The errors inherent in the analytical method are thus reduced by working at higher conversions, which require calculations based on integrated rather than instantaneous copolymer compositions.

The temperature dependence of reactivity ratios has not received much attention and is usually considered to be negligible. This assumption seems to be based more on convenience than bulk of evidence, as most reactivity ratios are reported for free-radical copolymerizations at 60°C and the vast majority of large-scale copolymerizations are conducted at other temperatures. Two studies of temperature effects were reported in 1948 with rather contradictory results. Lewis and co-workers[10] reported copolymerizations of styrene in which activation energies of reactivity ratios were slight and there was essentially no difference in the activation entropies of the competing propagation reactions. Goldfinger and Steidlitz[11] studied the copolymerizations of styrene and acrylonitrile with 2,5-dichlorostyrene and found a preponderance of negative activation energies, especially with low reactivity ratios. The activation entropy differences were very large and apparently inexplicable. The conclusion of Lewis et al. is generally considered to be definitive, but recent work by Johnston and Rudin[12] gave results similar to those of Goldfinger and Steidlitz, again with a system (styrene–α-methylstyrene) with rather low reactivity ratios.

In analysis of possible effects of temperature on reactivity ratios,[13] the assumption is usually made that activation entropies are essentially the same for the two propagation reactions postulated in the Mayo-Lewis simple copolymer scheme.[14] Steric effects are therefore excluded. It must also be assumed that attack of a given monomer on a radical leads to a single transition state and that several transition states, with comparable energies, do not exist. It is not surprising then that this simple model fails, particularly when styrene is copolymerized with monomers like dichlorostyrene and α-methylstyrene, nor that entropy of activation differences calculated in these cases are not easily explained.

It was of interest to extend the studies cited by measuring temperature effects in the copolymerization of styrene and methacrylonitrile, which has some of the characteristics of the comonomers mentioned above. Gold-

finger and Steidlitz[11] reported that the temperature dependence of the copolymerization of styrene and acrylonitrile is small in the range 41–86°C. Methacrylonitrile is a more hindered monomer than acrylonitrile. Its copolymers are generally more soluble than those of acrylonitrile and are less likely to form heterogeneous polymerization systems.

Experimental

The copolymerization of methacrylonitrile with styrene was carried out in toluene at 60, 90, and 120°C. The solvent and monomers were purified by distillation at atmosphere pressure (toluene) or reduced pressure. Only the middle half of the distillate was used in each case. Distilled monomers were stored cold until polymerization, within 2 days of distillation. The refractive indices of the purified monomers at 20°C were: styrene, 1.5453; methacrylonitrile, 1.3998. Both monomers gave single peaks in the gas-chromatographic separation described below.

The reaction mixtures were always made up of 7 ml of toluene and 10 ml of monomers. The major part of the mixture was prepared in bulk by adding 100 ml of monomers to 50 ml of toluene. (A slightly different procedure was used for 120°C; see below.) This mixture was degassed by alternate freezing and thawing at least twice under vacuum. Nine 15-ml aliquots were then pipetted into small reaction bottles. These were flushed out with nitrogen and were then tightly capped with rubber stoppers containing septums. Seven of the aliquots were designated as samples and placed in a constant temperature oil bath where polymerization was initiated immediately.

The initiating solution was azobisisobutyronitrile (AZBN), at about 7 mg/ml in toluene; 2 ml of this solution was injected into a sample through the septum. The volume of toluene in the reaction mixture was then the aforementioned total of 7 ml, and the total volume was 17 ml. After injection, a syringe was used to bleed gas out of the reaction bottles and reduce the pressure inside to slightly less than atmospheric.

At 120°C the reaction proceeded spontaneously without addition of initiator. Thermal initiation of styrene is well known at these temperatures, and this behavior was expected. The procedure therefore was modified: 70 ml of toluene was used in the bulk made-up and 17-ml aliquots were taken. These were sealed as usual, and the seven sample aliquots were placed in the 120°C bath and left until ready for termination. New septum stoppers were used, and these were not punctured to bleed off the internal pressure. Despite the low boiling points of the components the polymerization mixtures refluxed, but did not boil out.

At selected times the samples were removed from the bath and the reaction was terminated. The reaction times were evenly spaced to a maximum estimated to give 20–30% conversion. Termination was accomplished by addition of 10 ml of a saturated solution of hydroquinone in toluene. After termination, the samples were stored in the cold until analysis later the same day.

The remaining two (of the original nine) aliquots were used as standards for the analysis. For comparison with 60 and 90°C polymerizations, 2 ml of terminating solution was injected in place of the initiator solution. Then 10 ml of the hydroquinone mixture was added from a pipet to all standards. These were stored in the cold until analysis, and were of course, never placed in the temperature baths.

Six different feeds were used at each temperature. The volumes (totalling 10 ml) of the monomers for these runs (expressed as volume methacrylonitrile:volume styrene) were: run 1, 5:5; run 2, 3:7; run 3, 7:3; run 4, 1.5:8.5; run 5, 8.5:1.5; run 6, 2:8.

Analysis

The analyses were made by gas chromatography on a Carle Model 9000 gas chromatograph with hydrogen flame detector. The column packing was 8% dinonyl phthalate on Anakron ABS. The flow rate of helium carrier gas was 15–18 ml/min, and the column temperature was 118 ± 3°C. The column contained a 1-in. glass wool plug in the inlet, to trap the polymer and terminator in the reacted sample. This plug was changed after every run because polymer buildup caused severe tailing of the peaks and ruined the analysis. Samples were analyzed in numerical order from the least polymerized to the most reacted so as to keep the column free of polymer as long as possible. Analysis of the seventh sample was sometimes unreliable or omitted because of the polymer buildup from previous samples and high polymer content in these samples.

One of the two standard solutions was analyzed first and the other was assayed after the third or fourth sample solution. In this way a check was obtained on the sensitivity and accuracy of the analysis. Any large difference between the two standards showed an error in make-up, or more likely, a change in detector sensitivity. This rarely happened, but when it did, the polymerization was repeated. At least three replicate analyses were obtained for every sample.

Calculations

Many of the terms used in this report are computer-oriented, as they have been taken directly from the associated programs. Monomers A and B are methacrylonitrile and styrene, respectively. The calculations described are somewhat more convenient than those reported recently in relation to a gas chromatographic measurement of reactivity ratios.[9]

The mole per cent of monomer A (A_0) and the mole ratio of A to B in the feed (FM) are calculated from the make-up volumes (V_A, V_B), densities (ρ_A, ρ_B), and molecular weights of the monomers (MW_A, MW_B).

$$M_A = V_A \rho_A / MW_A$$
$$M_B = V_B \rho_B / MW_B \tag{1}$$

$$A_0 = [M_A/(M_A + M_B)]\ 100\% \tag{2}$$
$$(FM) = M_A/M_B$$

An arbitrary solvent peak area (SPKS) is used in the calculations. This area is chosen to be close to the average solvent peak area measured, but is rounded off for easy comparison with other runs. If the peak areas for one injection are P_S, P_A, and P_B, for the solvent and two monomers, respectively, the monomer peak areas are normalized on SPKS by:

$$(CP_A) = P_A \text{ SPKS}/P_S$$

or (3)

$$(CP_B) = P_B \text{ SPKS}/P_S$$

where (CP_A) and (CP_B) are the normalized monomer peak areas.

The monomer peak areas are also normalized for the two standard aliquots, mentioned above. The standard areas, S_A and S_B, are found for the monomers by the equations:

$$\begin{aligned} S_A &= (\overline{CP}_A) \\ S_B &= (\overline{CP}_B) \end{aligned} \tag{4}$$

where $(\overline{CP}_A)$ and $(\overline{CP}_B)$ are the average values of the normalized peak areas.

The unreacted mole fractions of the monomers, U_A and U_B, are calculated by:

$$\begin{aligned} U_A &= (CP_A)/S_A \\ U_B &= (CP_B)/S_B \end{aligned} \tag{5}$$

From the unreacted mole fractions of A and B, the mole per cent of monomer A in the copolymer (AP), and the mole ratio of A to B in the copolymer (FP) may be calculated:

$$(MP_A) = M_A - (M_A U_A) \tag{6a}$$

$$(MP_B) = M_B - (M_B U_B) \tag{6b}$$

where (MP_A) and (MP_B) are the moles of monomer converted to polymer.

$$(\text{AP}) = \{(MP_A)/[(MP_A) + (MP_B)]\}\ 100\% \tag{7}$$

$$(\text{FP}) = (MP_A)/(MP_B) \tag{8}$$

The weight per cent conversion (WC) is:

$$(WC) = \{[(MP_A)(MW_A) + (MP_B)(MW_B)]/[(M_A)(MW_A) + M_B(MW_B)]\}\ 100\% \tag{9}$$

These quantities are calculated for each injection, and the average and standard deviation are found for each parameter.

Finally, linear least squares fits are obtained for plots of U_A and U_B (unreacted mole fractions of monomers) against (WC) requiring that these plots pass through (1,0) (i.e., no monomer is reacted at zero conversion). From these plots, best fit values for U_A, U_B, (FP), and (AP), may be calculated for various values of (WC) between 5% and 30%.

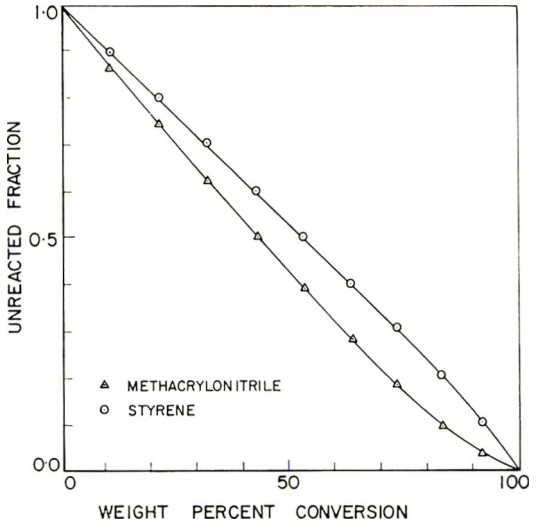

Fig. 1. Predicted plot of unreacted fractions of monomer vs. weight per cent conversion.

The linear least squares fit of U_A or U_B against (WC) is a contradiction of theory which predicts these plots to be curved. The theoretical curves are shown in Figure 1. (The method used to obtain these curves is described below.) It is seen that the curvature is very slight. Since the experimental data extend only to 30% conversion the curvature may be taken to be negligible. The linear least-squares results from the calculations described are therefore used to calculate reactivity ratios.

A value for the per cent conversion (WC) had to be selected for calculations using the integrated form of the simple copolymer equation. Although this choice could be subjective, an effort was made to chose (WC) near the point where the curves (as in Fig. 1) and the least-squares straight line coincided. This was usually near 20% conversion. Calculations for different values of (WC) had little effect on reactivity ratios.

Reactivity ratios were also calculated by using three common procedures which employ the differential form of the Mayo-Lewis simple copolymer equation:[14]

$$dM_A/dM_B = m_A/m_B = M_A(r_1M_A + M_B)/M_B(M_A + r_2M_B) \quad (10)$$

where m_A/m_B is the instantaneous monomer mole ratio in the copolymer and r_1, r_2 are reactivity ratios. Two such widely used calculation methods were suggested by Fineman and Ross.[15] Substituting

$$f = m_1/m_2 \text{ and } F = M_1/M_2$$

into eq. (10) and rearranging yields:

$$(F/f)(f - 1) = -r_2 + r_1(F^2/f) \quad (11)$$

and

$$(f - 1)/F = r_1 - r_2(f/F^2) \quad (12)$$

Both eqs. (11) (Fineman-Ross = FR) and (12) (reciprocal Fineman-Ross = RFR) are in linear form, so that the slopes and intercepts yield estimates of r_1 and r_2. Note that f and F are equivalent to (FP) and (FM), respectively (Table I). Least-squares straight lines are found for the plots. Standard deviations may be calculated for the slopes and intercepts, but these estimates may be misleading because the observed polymer composition is contained in both the "independent" and "dependent" variables in the linear equations.[2]

Equation (10) may also be arranged to give

$$r_2 = F[(1/f) - 1] + r_1(F^2/f) \tag{13}$$

Thus for each F, f pair, a straight line on a plot of r_1 versus r_2 may be obtained, and the intersections of a number of these lines will give estimates of r_1 and r_2. Joshi and Kapur[16] modified this method to take into account the intersections of all lines and to weight them in proportion to the tangent of the angle of intersection. Computer calculations of reactivity ratios were also made using this procedure. Reactivity ratios were calculated at 5 wt-% conversion, with the three linear forms of the differential copolymer equation.

The preferred method for calculating reactivity ratios involves the integrated form of the simple copolymer equation[14]:

$$\ln \frac{M_2'}{M_2} = \frac{r_2}{1 - r_2} \ln \frac{M_2}{M_1} \frac{M_1'}{M_2'} - \frac{1 - r_1 r_2}{(1 - r_1)(1 - r_2)} \times \ln \left[\frac{(r_1 - 1)(M_1'/M_2') - r_2 + 1}{(r_1 - 1)(M_1/M_2) - r_2 + 1} \right] \tag{14}$$

where M_1' and M_2' are the final monomer concentrations.

The computer program, to calculate reactivity ratios from this equation, is an adaptation of that described by Harwood.[17] The program first calculates A_i, B_i, A_f, B_f, the number of moles of monomer A and B initially and finally in per gram of sample. It is seen that $A_i/B_i = M_1/M_2$ and so on. Thus eq. (14) becomes

$$\ln \frac{B_f}{B_i} = \frac{r_2}{1 - r_2} \ln \frac{B_i A_f}{B_f A_i} - \frac{1 - r_1 r_2}{(1 - r_1)(1 - r_2)} \times \ln \left[\frac{(r_1 - 1)(A_f/B_f) - r_2 + 1}{(r_1 - 1)(A_i/B_i) - r_2 + 1} \right] \tag{15}$$

With the definition:

$$P \equiv \frac{(1 - r_1)}{(1 - r_2)}$$

the contents of the bracket in the second term on the right-hand side of eq. (15) may be rearranged to:

$$\frac{(r_1 - 1)(A_f/B_f) - r_2 + 1}{(r_1 - 1)(A_i/B_i) - r_2 + 1} = \frac{1 - P(A_f/B_f)}{1 - P(A_i/B_i)} \tag{16}$$

This is defined as the function (ARG) so that:

$$\ln \frac{B_f}{B_i} = \frac{r_2}{1 - r_2} \ln \frac{B_i A_f}{B_f A_i} - \frac{1 - r_1 r_2}{(1 - r_1)(1 - r_2)} \ln (AGR) \tag{17}$$

which may be rearranged to:

$$r_2 = \frac{\ln (B_i/B_f - (1/P) \ln (ARG)}{\ln (A_i/A_f) + \ln (ARG)} \tag{18}$$

If an initial value of P is given, eq. (18) will generate a value of r_2, and r_1 may then be obtained from eq. (16). Thus the program input requires estimates of r_1 and r_2. The standard deviations σ of the reactivity ratios are also required, to put limits on P according to:

$$\begin{aligned} P_{\text{high}} &= \frac{1 - r_1 + \sigma_1}{1 - r_2 - \sigma_2} \\ P_{\text{low}} &= \frac{1 - r_1 - \sigma_1}{1 - r_2 - \sigma_2} \end{aligned} \tag{19}$$

The difference between these limits is divided into nine increments, and ten values for r_1 and r_2 are calculated for values of P between P_{low} and P_{high}. A linear least-squares fit is then found for the r_1 and r_2 values plotted against each other. This is repeated for all A_0, (AP), and (WC) data sets calculated.

The intersections of the least-squares lines give estimates of the values of r_1 and r_2. The values for all intersections are calculated but when the angle of intersection is less than 15°, the values are ignored. The average and standard deviation are calculated, and then the values are scanned. Any intersection giving a value of r_1 or r_2 more than two standard deviations from the mean is rejected. The average r_1 and r_2 are then calculated from the remaining points.

The integrated approach is better than differential equation methods for systems that have a high conversion or a rapidly changing feed,[3] and the results from this method were considered to be definitive in this study.

The curves shown in Figure 1 were calculated from eq. (14) by substituting

$$\begin{aligned} M_1/M_2 &= (FM) \\ M_2'/M_2 &= U_B \\ M_1'/M_1 &= U_A \\ Q &= r_2/(1 - r_2) \\ R &= (1 - r_1 r_2)/[(1 - r_1)(1 - r_2)] \end{aligned}$$

to obtain

$$\ln U_B = Q \ln \frac{U_A}{U_B} - R \ln \left[\frac{(r_1 - 1)(U_A/U_B)(FM) - r_2 + 1}{(r_1 - 1)(FM) - r_2 + 1} \right]$$

which was rearranged to

$$U_A = \exp\left\{\frac{(1+Q)\ln U_B - R\ln(r_1-1)(FM) - r_2 + 1}{Q}\right\} \times [(r_1-1)(U_A/U_B)(FM) - r_2 + 1]^{R/Q} \quad (20)$$

For any feed (FM) and any reactivity ratio values, a value for U_A can be found for any value of U_B if an initial estimate for U_A is substituted into eq. (15), and this procedure is repeated until the new value for U_A found is constant. A program was written to do these calculations, as well as to find (WC). The results which are shown in Figure 1 agree well with experiment.

The (AP) and (FP) (polymer composition) values calculated seemed to be least reliable at low conversions. The polymer composition is found by subtracting the value found for the unreacted fraction of monomer in a test sample from 1.00. Thus an error of 1% in the analysis of the sample leads to a 20% error in the calculation of polymer composition at 5% conversion (e.g. if the unreacted fraction of monomer is found to be 0.95 ± 0.01, then the fraction converted to polymer is calculated to be 0.05 ± 0.01). The standard deviation in monomer analysis was usually less than two percent, but was seldom very close to zero. Therefore, the values for (FP) and (AP) found for each sample were not used. Instead, the (FP) and (AP) values calculated from the best fit U_A and U_B versus (WC) plots were taken. Plots of the unreacted fractions of the monomers against the weight per

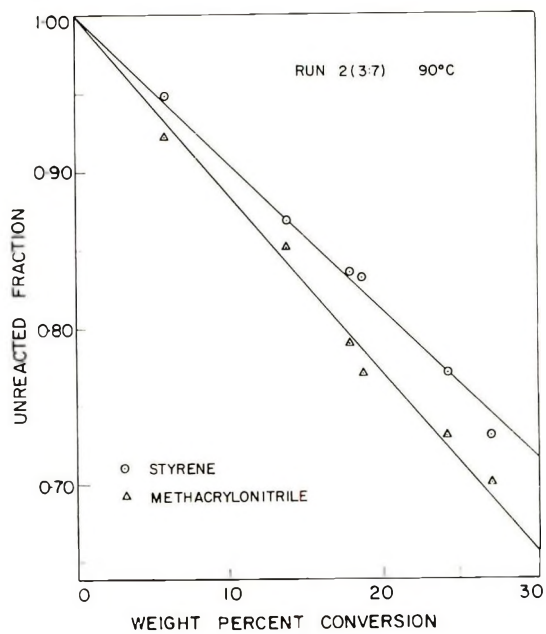

Fig. 2. Unreacted fraction of monomer vs. weight per cent conversion.

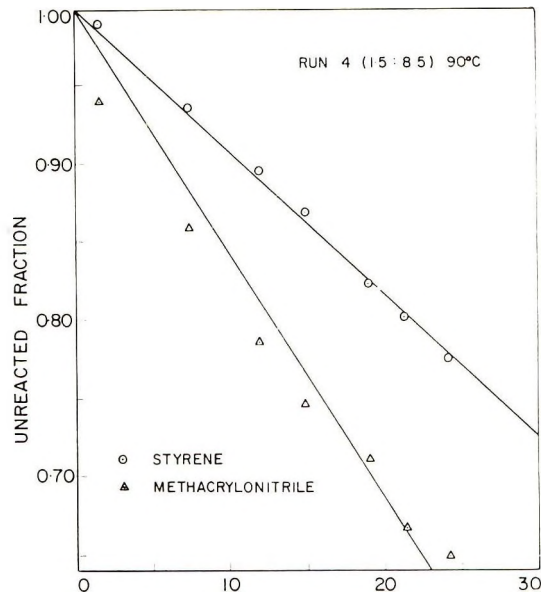

Fig. 3. Unreacted fraction of monomer vs. weight per cent conversion at high styrene feed.

cent conversion were made for every run, and the best fit straight line was drawn. As was expected, the experimental points coincided well with the straight line despite the theoretical curvature in such plots. In the runs with monomer value ratios (1.5:8.5) and (8.5:1.5), the curvature was slightly more pronounced. The 90°C plots of unreacted fractions against weight per cent conversion are shown for run 2 (3:7), mentioned above (Fig. 2) and run 4 (1.5:8.5) (Fig. 3).

Results

The advantages of working near 20% conversion are evident in these figures. Plots of mole fraction of methacrylonitrile in the feed ($A_0/100$) against the mole fraction of methacrylonitrile in the polymer [$(AP)/100$] are shown for each experimental temperature (Fig. 4). These plots are almost identical, indicating little change with temperature.

Figures 5 and 6 are the Fineman-Ross (FR) and reciprocal Fineman-Ross (RFR) plots for 90°C. Note that the points are unevenly spaced in both plots. In the FR plot, the point for run 5 (high methacrylonitrile content in the feed) has a very large influence on the slope and intercept of the best fit line, thus partially negating the averaging value usually obtained by doing a least squares fit. Run 4 (high styrene feed) has the same overwhelming influence in the RFR case. For this reason these two methods of Fineman and Ross are considered for comparison only. The Joshi-Kapur (JK) method seemed to be the best of the three differential copolymer equation methods. The results from this method were fairly close to the values

found from use of the integrated copolymer equation, which were taken as definitive.

The uncertainties in the Fineman-Ross techniques can be reduced by using a nonlinear least-squares fit to the data.[4] This improvement was not pursued in the present work because the analyses are most reliable at high conversions, which require an integrated copolymer equation.

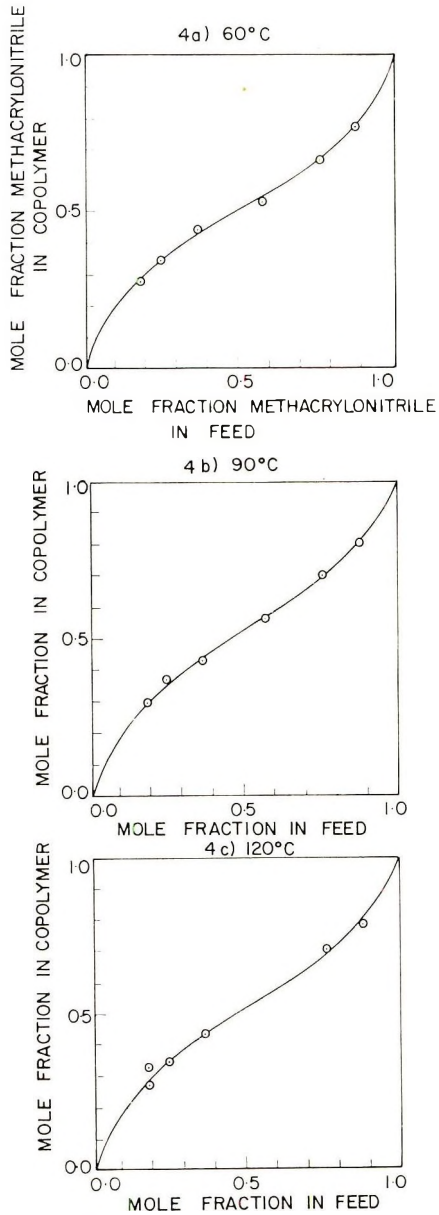

Fig. 4. Feed-composition diagram for methacrylonitrile: (*a*) 60°C reaction; (*b*) 90°C reaction; (*c*) 120°C reaction.

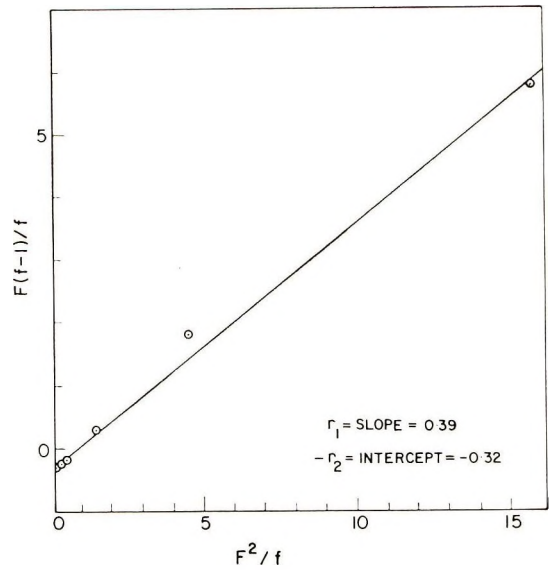

Fig. 5. Fineman-Ross plot (90°C).

Table I lists the reactivity ratios calculated. Standard deviations of reactivity ratios are also included for convention, but these are subject to reservations for the reasons given above.

TABLE I
Experimental Reactivity Ratios for
Methacrylonitrile (M_1)–Styrene (M_2)

Temperature, °C	Basis of estimate	Reactivity ratios			
		r_1	σ	r_2	σ
60	Integrated equation	0.32	0.05	0.39	0.07
	Differential equation				
	FR	0.32	0.01	0.35	0.06
	RFR	0.43	0.01	0.44	0.02
	JK	0.36	—	0.41	—
90	Integrated equation	0.41	0.05	0.37	0.06
	Differential equation				
	FR	0.39	0.01	0.32	0.08
	RFR	0.43	0.06	0.39	0.02
	JK	0.42	—	0.39	—
120	Integrated equation	0.42	0.15	0.38	0.08
	Differential equation				
	FR	0.37	0.02	0.29	0.14
	RFR	0.33	0.28	0.36	0.16
	JK	0.42	—	0.39	—

Figure 7 is a plot of the mole fraction of methacrylonitrile in the feed against the mole fraction of methacrylonitrile in the polymer made at 90°C.

This plot was obtained when the values for r_1 and r_2 found in this work were substituted into the simple copolymer equation in the form

$$f = \frac{r_1F^2 + F(1 - F)}{r_1(F^2) + 2F(1 - F) + r_2(1 - F)^2} \tag{21}$$

Values for f were found for values of F between 0 and 1.0 at 0.1 intervals and then plotted.

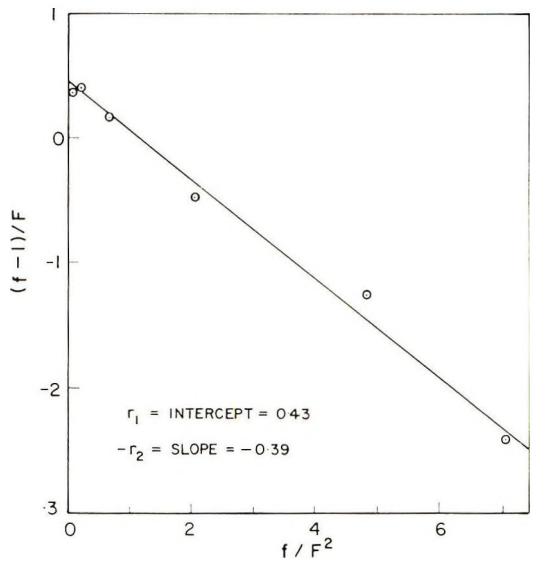

Fig. 6. Reciprocal Fineman-Ross plot (90°C).

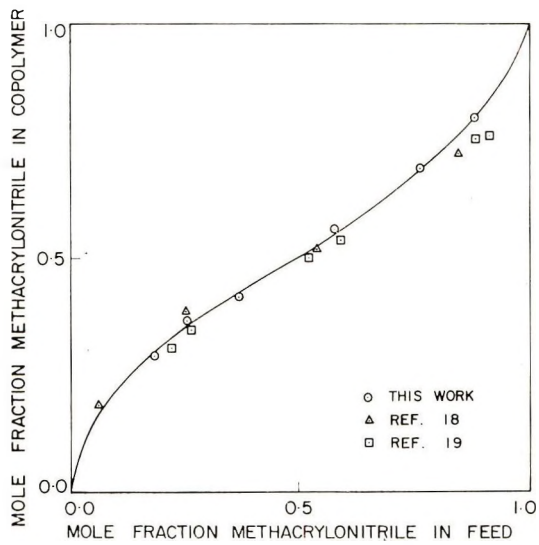

Fig. 7. Mole fraction methacrylonitrile in feed vs. mole fraction in copolymer (90°C).

Also shown in Figure 7 are the 80°C data of Fordyce et al.[18] and Cameron et al.[19] All sets of predictions agree fairly well except in the region of the feed where methacrylonitrile predominates ($0.6 < F < 1.0$). This discrepancy is the major difference between reactivity ratios found in this work and those reported previously.

Table II lists published reactivity ratios for the methacrylonitrile–styrene system and the current results. The present r_1 values fall within the range of published results, but the r_2 values found here are significantly higher. That is to say, copolymers are assayed at higher methacrylonitrile contents in this work than in the other studies cited. This may perhaps be connected with difficulties in analysis for nitrogen content of copolymers. All the previous work relied completely on nitrogen analysis for estimation of copolymer composition.

TABLE II
Reactivity Ratios for Methacrylonitrile (M_1)–Styrene (M_2)

Source	Temperature, °C	Reactivity ratios			
		r_1	σ	r_2	σ
This work	60	0.32	0.05	0.39	0.07
	90	0.41	0.05	0.37	0.06
	120	0.42	0.15	0.38	0.08
Lewis et al.[21]	60	0.16	0.06	0.30	0.10
Fordyce et al.[18]	80	0.25	0.02	0.25	0.02
Cameron et al.[19]	80	0.26	0.05	0.38	0.05
Rocke and Carey[20]	80	0.28	—	0.43	—

Fordyce and co-workers[18] used a micro-Dumas method for nitrogen analysis. Examination of polyacrylonitrile and polymethacrylonitrile yielded nitrogen contents lower than expected, and an empirical correction was made in the copolymer data to take this deficiency into account. Cameron and co-workers[19] employed Kjeldahl analysis. Tests on polymethacrylonitrile samples gave low nitrogen values and results for the copolymers were also adjusted empirically. The analytical method used by Lewis et al.[21] is referred to as "standard" and that of Rocke and Carey[20] is not given.

Since the samples used in this work were sealed except for brief periods, it seems very unlikely that the higher r_1 values reported here could be due to losses of unreacted methacrylonitrile monomer from the system. The boiling point of this monomer is not much lower than those of styrene and toluene and both the latter components would be expected to permeate faster through rubber septums.

Since a reactivity ratio is the ratio of two rate constants, it may be expressed[10] as:

$$r_i = \exp\left\{\frac{\Delta S_{ii} - \Delta S_{ij}}{R} - \frac{\Delta H_{ii} - \Delta H_{ij}}{RT}\right\}_{i \neq j} \tag{22}$$

where ΔS_{ii}, ΔH_{ii}, ΔS_{ij}, ΔH_{ij} are, respectively, the entropies and heats of activation for reaction of a radical ending in monomer i with monomers i and j. A plot of $\ln r_i$ against $1/T$ affords a measure of the differences in entropies and enthalpies of activation. The data points at the three temperatures studied in this work did not produce good straight lines in such plots. Estimates of the entropy differences are:

$$\Delta S_{11} - \Delta S_{12} = 0$$

and

$$\Delta S_{22} - \Delta S_{21} = 2 \text{ eu/mole}$$

(Recall that methacrylonitrile and styrene are referred to by subscripts 1 and 2, respectively.) Estimates of activation energy differences are $\Delta H_{11} - \Delta H_{12} = 120$ cal/mole and $\Delta H_{22} - \Delta H_{21} = 0$. These are the same orders of magnitude as the values reported by Lewis et al.[10] for styrene copolymerization with methyl methacrylate, at two temperatures.

Discussion

The present work differs from previous studies of styrene-methacrylonitrile copolymerizations in both the analytical method and the handling of experimental data. Systematic errors in analyses of nitrile-containing polymers discussed above should be absent from the gas-chromatographic method in which methacrylonitrile monomer forms one of the primary standards. The analytical method itself is, however, probably no more precise than chemical analyses.

The advantages in use of an integrated copolymer equation have also been discussed above. Wiley and co-workers[22] have found different values for reactivity ratios, using integrated and differential equations, with data on copolymerizations of styrene with divinyl benzene and para-isopropylstyrene. The differences in analyses and calculations may account for the systematic discrepancy between the present work and the preceding reports cited above.

The temperature effects observed in this study are consistent with those reported by Lewis and co-workers.[10] O'Driscoll[13] has pointed out that the assumption of equal entropies of activition for the two competing propagation reactions assumed in the definition of a reactivity ratio leads to the expectation that the only reactivity ratios which will exhibit significant temperature dependence will be those which are very large or very small.

It seems reasonable to assume that the entropies of activation are at least approximately equal in normal head-to-tail copolymerization. Joshi[23] notes that the transition state for monomer addition to a polymer radical will not differ much from the final state, in view of observations that preexponential factors in propagation rate constants vary only by about

two orders of magnitude. The entropy of activation thus differs little from the entropy of polymerization and observed values of this parameter are generally in the narrow range between 25 and 30 cal/deg-mole.

The small entropy of activation differences observed in this work and by Lewis and co-workers[10] are consistent with this reasoning, particularly since they are accompanied by low activation energy differences.

Johnston and Rudin[9] studied styrene copolymerization with α-methylstyrene at two temperatures. Activation entropy differences were -8 eu/mole (styryl radical) and -18 eu/mole (α-methylstyryl radical). These observations may indicate that head-to-tail placement does not predominate at all temperatures. This is consistent with the production of oligomers, rather than high polymer, in this system, and could result from the combinative termination of unreactive α-methylstyryl radicals. Similar considerations may apply to the report of Goldfinger and Steidlitz on copolymerizations of dichlorostyrene with styrene and with acrylonitrile.[11] This rationalization is conjectural, of course, but it is consistent with the data available and might be at least a useful rule-of-thumb approach to untested copolymer systems.

The authors thank the Defence Research Board of Canada for financial assistance and H. K. Johnston for advice and help.

References

1. L. J. Young, *J. Polym. Sci.*, **54**, 411 (1961).
2. P. W. Tidwell and G. A. Mortimer, *J. Macromol. Sci. Revs.*, **C4**, 281 (1970).
3. D. W. Behnken, *J. Polym. Sci. A*, **2**, 645 (1964).
4. P. W. Tidwell and G. A. Mortimer, *J. Polym. Sci. A*, **3**, 369 (1965).
5. F. M. Lewis, F. R. Mayo, and W. F. Hulse, *J. Amer. Chem. Soc.*, **67**, 1701 (1948).
6. W. M. Ritchey and L. E. Ball, *J. Polym. Sci. B* **4**, 557 (1966).
7. H. J. Harwood, H. Baikowitz and H. F. Trommer, paper presented at American Chemical Society Meeting, 1963; *Polym. Preprints*, **4**, 133 (1963).
8. A. Guyot and J. Guillot, *J. Macromol. Sci.*, **A1**, 793 (1967).
9. H. K. Johnston and A. Rudin, *J. Paint Technol.*, **42**, 429 (1970).
10. F. M. Lewis, C. Walling, W. Cummings, E. R. Briggs, and F. R. Mayo, *J. Amer. Chem. Soc.*, **70**, 1519 (1948).
11. G. Goldfinger and M. Steidlitz, *J. Polym. Sci.*, **3**, 786 (1948).
12. H. K. Johnston and A. Rudin, *J. Paint Technol.*, **42**, 435 (1970).
13. K. F. O'Driscoll, *J. Macromol. Sci.*, **A3**, 307 (1969).
14. F. R. Mayo and F. M. Lewis, *J. Amer. Chem. Soc.*, **66**, 1594 (1944).
15. M. Fineman and J. D. Ross, *J. Polym. Sci.*, **5**, 269 (1950).
16. R. M. Joshi and S. L. Kapur, *J. Polym. Sci.*, **14**, 508 (1954).
17. H. J. Harwood, N. W. Johnston, in *The Computer in Polymer Science* (*J. Polym. Sci. C*, **25**), J. B. Kinsinger, Ed., Interscience, New York, 1968, p. 23.
18. R. G. Fordyce, E. C. Chapin, and G. E. Ham, *J. Amer. Chem. Soc.*, **70**, 2489 (1948).
19. G. G. Cameron, D. H. Grant, N. Grassie, J. E. Lamb, and I. C. McNeil, *J. Polym. Sci.*, **36**, 173 (1959).
20. A. Rocke and G. Carey, unpublished data; through ref. 1.

21. F. M. Lewis, C. Walling, W. Cummings, E. R. Briggs, and W. J. Wenisch, *J. Amer. Chem. Soc.*, **70,** 1527 (1948).

22. R. H. Wiley, S. P. Rao, J.-I. Jin, and K. S. Kim, *J. Macromol. Sci. Chem.*, **A4,** 1453 (1970).

23. R. M. Joshi, in *Vinyl Polymerization*, G. E. Ham, Ed., Vol. 1, Part 1, Dekker, New York, 1967.

Received May 21, 1971
Revised July 12, 1971

JOURNAL OF POLYMER SCIENCE: PART A-1 VOL. 9, 3027–3038 (1971)

Inorganic Coordination Polymers. XI. A New Family of Chromium(III) Bis(phosphinate) Polymers, $[Cr(OH)(OPRR'O)_2]_x$*

PIERO NANNELLI, H. D. GILLMAN, AND B. P. BLOCK,
Technological Center, Pennwalt Corporation, King of Prussia, Pennsylvania 19406

Synopsis

Heating hydroxyaquochromium(III) bis(phosphinates) at temperatures up to 200°C under vacuum yields the corresponding anhydrous polymers $[Cr(OH)(OPRR'O)_2]_x$. The infrared and visible spectra and solution properties lead to the following conclusions. When R and R′ are phenyl groups, the hydroxyl groups appear to bridge between adjacent chromium atoms in the chain together with the phosphinate ligands to yield a linear, triple-bridged polymer. When at least one substituent on the phosphorus is an alkyl group, some of the hydroxyl groups crosslink between chains to yield less soluble polymers. Comparison of the properties of these new polymers with the parent polymers suggests that the latter should be formulated $[Cr(H_2O)_n(OH)(OPRR'O)_2]_x \cdot pH_2O$ and that they contain more than one kind of monomer unit. The parent polymers can be readily prepared by a new method which involves reaction of a soluble chromium(III) salt with alkali metal phosphinates or of chromium(III) hydroxide with phosphinic acids in a water–tetrahydrofuran mixture.

INTRODUCTION

Many poly(metal phosphinates) have been prepared and studied in this laboratory.[2] An important part of this effort has been devoted to the synthesis and characterization of a family of chromium(III) bis(phosphinates) which were suggested to be linear coordination polymers with the general formula $[Cr(H_2O)(OH)(OPRR'O)_2]_x$, where R and R′ are inert alkyl or aryl groups.[1,3,4] We now wish to present a study of coordination polymers with the general formula $[Cr(OH)(OPRR'O)_2]_x$ obtained by dehydration of the hydroxyaquo polymers. Structures are proposed for these new polymers, the structures proposed earlier for the parent hydroxyaquo polymers are modified, and a convenient method of preparing these coordination polymers is reported.

EXPERIMENTAL

Materials

The phosphinic acids, which were supplied by Hynes Chemical Research (Durham, North Carolina, 27704), were purified by recrystallization from

* For Part X of this series, see Maguire and Block.[1]

ethanol. Chromium pellets (99.999% pure) were purchased from United Mineral and Chemical Corp. (New York, N.Y., 10013). Other chemicals and solvents were reagent grade and were used without further purification.

$[Cr(H_2O)(OH)(OPRR'O)_2]_x$

Samples used in these studies were first prepared by a method which involves synthesis of a chromium(III) bis(phosphinate) from chromium metal followed by oxidation in the presence of water.[1] Subsequently, an improved method, which appears to yield identical compounds quantitatively in considerably less time, was developed. In the new procedure the starting compound is either a soluble chromium(III) salt or chromium(III) hydroxide as exemplified by the following preparations.

The diphenyl polymer $\{Cr(H_2O)(OH)[OP(C_6H_5)_2O]_2\}_x$ was prepared by adding a solution of $NaOP(C_6H_5)_2O$ (4.80 g, 0.0200 mole) and K_2CO_3 (0.69 g, 0.0050 mole) in 50 ml of water with stirring to a solution of $CrCl_3.6H_2O$ (2.66 g, 0.100 mole) in 50 ml of THF (tetrahydrofuran). The reaction mixture was brought to boiling and the THF allowed to evaporate. An oily product separated and solidified upon evaporation of the THF. After most of the THF had been removed, additional water (about 50 ml) was added, and the suspension was kept boiling until the precipitate could be easily ground with a spatula. The powdered solid was then collected on a filter, thoroughly washed with water, loosely covered with aluminum foil, and allowed to dry in the air. After three days the weight was 5.2 g, corresponding to a 99.8% yield of $Cr(H_2O)(OH)[OP(C_6H_5)_2O]_2$. Exposure to air for longer periods of time was found to result in additional loss of water, especially when the relative humidity was low. Fresh chloroform solutions of the compounds had intrinsic viscosities of about 0.04 dl/g which increased to about 0.4 dl/g on standing at 55°C for a few days.

ANAL. Calcd for $C_{24}H_{23}CrO_6P_2$: C, 55.29%; H, 4.45%; Cr, 9.97%; P, 11.88%. Found: C, 55.01%; H, 4.53%; Cr, 9.74%; P, 11.67%.

The methylphenyl polymer $\{Cr(H_2O)(OH)[OP(CH_3)(C_6H_5)O]_2\}_x$ was prepared in similar fashion by adding a solution of $(CH_3)(C_6H_5)P(O)OH$ (3.12 g, 0.0200 mole) and K_2CO_3 (2.07 g, 0.0150 mole) in 50 ml of water with stirring to a solution of $CrCl_3 \cdot 6H_2O$ (2.66 g, 0.0100 mole) in 50 ml of THF. An analogous work-up gave 3.85 g of the methylphenyl polymer corresponding to a 97% yield. Chloroform solutions of this product had intrinsic viscosites of about 0.4 dl/g which did not change appreciably on standing at 55°C for a few days.

ANAL. Calcd for $C_{14}H_{19}CrO_6P_2$: C, 42.33%; H, 4.82%; Cr, 13.09%; P, 15.59%. Found: C, 42.38%; H, 4.81%; Cr, 12.90%; P, 15.36%.

The dioctyl polymer $\{Cr(H_2O)(OH)[OP(C_8H_{17})_2O]_2\}_x$ was made by adding a solution of $(C_8H_{17})_2P(O)OH$ (5.81 g, 0.020 mole) and Na_2CO_3 (1.60 g, 0.015 mole) in 60 ml of water and 60 ml of THF with stirring to a solution of $Cr(NO_3)_3 \cdot 9H_2O$ (4.00 g, 0.010 mole) in a mixture of 50 ml of water and

50 ml of THF. A work-up analogous to that of the previous experiments, except that the product was dried under vacuum at room temperature for one day, gave 6.39 g of the polymer corresponding to a 96% yield. The intrinsic viscosity of the product in chloroform was about 0.30 dl/g and did not change appreciably on standing.

ANAL. Calcd for $C_{32}H_{71}CrO_6P_2$: C, 57.72%; H, 10.75%; Cr, 7.81%; P, 9.30%. Found: C, 57.78%; H, 10.57%; Cr, 7.94%; P, 9.52%.

An alternate approach to the dioctyl polymer is via chromium(III) hydroxide. A solution of $CrCl_3 \cdot 6H_2O$ (2.66 g, 0.010 mole) in 100 ml of water was treated with 35 ml of 1*M* NH_3 with stirring. The resulting $Cr(OH)_3 \cdot xH_2O$ was separated by gravity filtration and washed with water until the washings were neutral. The filter paper containing the $Cr(OH)_3 \cdot xH_2O$ was then added to a solution of $(C_8H_{17})_2P(O)OH$ (5.81 g, 0.020 mole) in 120 ml of THF and 25 ml of water. The $Cr(OH)_3 \cdot xH_2O$ slowly dissolved while the mixture was stirred at 50°C. After it had all dissolved, the filter paper was removed by filtration. The solution was then boiled to remove the THF, and water was occasionally added to keep the volume approximately constant. After the THF was completely removed, the precipitated polymer was collected on a filter, washed with water, and dried under a vacuum for one day at room temperature. The yield of $\{Cr(H_2O)(OH)[OP(C_8H_{17})_2O]_2\}_x$ was quantitative. Its intrinsic viscosity in chloroform was about 0.67 dl/g.

ANAL. Calcd for $C_{32}H_{71}CrO_6P_2$: C, 57.72%; H, 10.75%; Cr, 7.81%; P, 9.30%. Found: C, 57.96%; H, 10.80%; Cr, 7.92%; P, 9.60%.

$[Cr(OH)(OPRR'O)_2]_x$

When the hydroxyaquo bis(phosphinate) polymers were heated under vacuum at temperatures up to 200°C, water was removed and $[Cr(OH)(OPRR'O)_2]$ was formed. Most of the water was removed during the first 4 hr of heating, and constant weight was reached by heating under vacuum for up to 10 hr. In the case of the dioctyl derivative the heating temperature was kept under 160°C since higher temperature could cause decomposition of the polymer. The following are typical sets of analytical data for the anhydrous hydroxy bis(phosphinates) prepared.

ANAL. Calcd for $\{Cr(OH)[OP(C_6H_5)_2O]_2\}_x$: C, 57.27%; H, 4.21%; Cr, 10.33%; P, 12.31%. Found: C, 57.25%; H, 4.32%; Cr, 10.20%; P, 12.50%.

Calcd for $\{Cr(OH)[OP(CH_3)(C_6H_5)O]_2\}_x$: C, 44.34%; H, 4.52%; Cr, 13.71%; P, 16.34%. Found: C, 44.13%; H, 4.77%; Cr, 13.30%; P, 16.56%.

Calcd for $\{Cr(OH)[OP(C_8H_{17})_2O]_2\}_x$: C, 59.33%; H, 10.74%; Cr, 8.03%; P, 9.56%. Found: C, 58.98%; H, 10.68%; Cr, 7.78%; P, 9.62%.

The carbon content is the most reliable analytical value for distinguishing between the hydrated and anhydrous polymers. A series of different samples of $\{Cr(OH)[OP(C_6H_5)_2O]_2\}_x$ gave the following values for C: 57.09%, 57.26%, 57.30%, 57.38%, 57.38%, and 57.49%. The calculated value for the hydrated polymer is 55.29%, for the anhydrous polymer 57.27%.

The methylphenyl and dioctyl polymers are virtually insoluble in chloroform or benzene; however, upon addition of small amounts of alcohol the polymers can be slowly dissolved. The diphenyl derivative is soluble in both solvents. Its fresh chloroform solutions have an intrinsic viscosity of about 0.12 dl/g, which increases to about 1.0 dl/g on standing at 55°C for a few days.

Deuteration of the polymers was accomplished by addition of excess D_2O to a benzene solution of $[Cr(H_2O)(OH)(OPRR'O)_2]_x$. After the solution was shaken for about 10 hr in a stoppered flask, it was evaporated under nitrogen. The anhydrous deuterated polymers were obtained by heating the residue under vacuum, as described earlier.

Intrinsic Viscosities and Spectra

Intrinsic viscosities were determined in chloroform at 30 ± 0.1°C with a Cannon-Ubbelohde dilution viscometer by a procedure described previously.[4] Infrared spectra were recorded with a Perkin-Elmer 337 grating spectrophotometer on either Nujol or hexachlorobutadiene mulls between KBr disks. Visible spectra were recorded in chloroform solutions (1.5%) with a Perkin-Elmer 450 spectrophotometer.

DISCUSSION

General

The procedure reported here for the preparation of the parent chromium(III) hydroxyaquo bis(phosphinates) is a significant improvement over the methods used earlier.[1,3,4] It is based on the reaction of a soluble chromium(III) salt such as $CrCl_3 \cdot 6H_2O$ or $Cr(NO_3)_3 \cdot 9H_2O$ with two equivalents of alkali metal phosphinate and one equivalent of alkali metal hydroxide or carbonate in water–tetrahydrofuran medium. The overall stoichiometry is summarized by eq. (1):

$$2CrCl_3 \cdot 6H_2O + 4NaOPRR'O + K_2CO_3 \rightarrow 2Cr(H_2O)(OH)(OPRR'O)_2 + 4NaCl + 2KCl + CO_2 + 9H_2O \quad (1)$$

Alternatively, the polymers can be prepared by the reaction of chromium(III) hydroxide with two equivalents of phosphinic acids in the same solvent mixture. This approach avoids the time-consuming preparation and handling of air-sensitive chromium(II) intermediates and permits the polymers to be prepared on a laboratory scale in about $^1/_2$ hr in quantitative yield.

Removal of the water from the polymers which analyze as $Cr(H_2O)(OH)(OPRR'O)_2$ produces polymers with the composition $Cr(OH)(OPRR'O)_2$. Infrared spectra, which are discussed in some detail later, and carbon analyses indicate quite unambiguously that the water has been essentially completely removed and that new species have indeed been prepared. The dehydration can be achieved either by heating under vacuum to constant weight at a temperature appropriate to the thermal stability of the

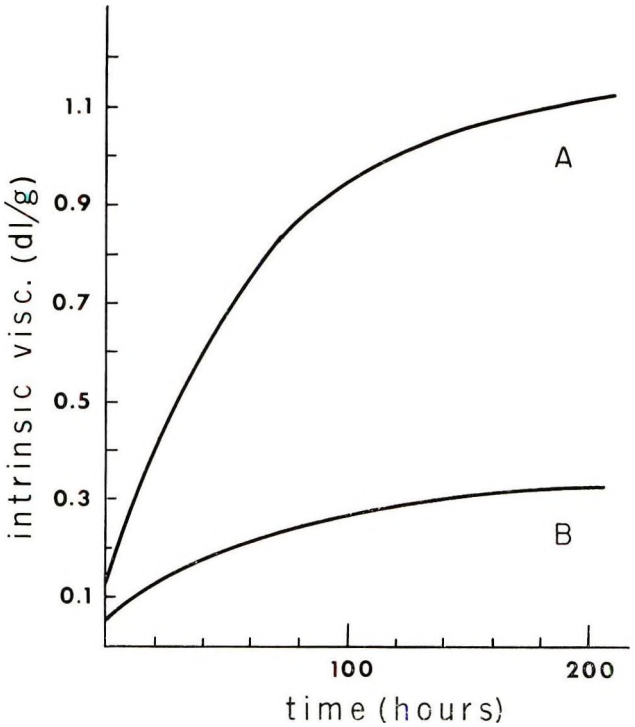

Fig. 1. Change in intrinsic viscosity with time at 55°C for chloroform solutions of: (*A*) $\{Cr(OH)[OP(C_6H_5)_2O]_2\}_x$; (*B*) $\{Cr(H_2O)(OH)[OP(C_6H_5)_2O]_2\}_x$.

species involved or by azeotropic distillation. Prolonged exposure of the anhydrous polymers to an atmosphere saturated with water causes recapture of only a fraction of the water originally present in the parent hydroxyaquo polymer.

The physical properties of the anhydrous polymers depend on the nature of the side groups on the phosphorus. Like its parent hydroxyaquo polymer, the anhydrous $\{Cr(OH)[OP(C_6H_5)_2O]_2\}_x$ is soluble in inert organic solvents such as chloroform and benzene. The intrinsic viscosities of fresh chloroform solutions, which range from 0.08 to 0.28 dl/g, are somewhat higher than those of similar solutions of the parent polymer. The higher values in the range, which are observed for samples prepared by azeotropic distillation, are probably attained because the dehydration is carried out in a homogeneous system during distillation, whereas dehydration by heating the solid polymer is heterogeneous. There is an increase in intrinsic viscosity when solutions of $\{Cr(OH)[OP(C_6H_5)_2O]_2\}_x$ are aged. Figure 1 compares typical intrinsic viscosity–time plots for chloroform solutions of the parent polymer and the anhydrous polymer held at 55°C. The most likely explanation for the increase in molecular size is growth via end-group interaction.[1] The difference in rate between the two kinds of polymers is not surprising, particularly because the parent polymer contains water

which could hinder interchain condensation by competing with phosphinate groups for coordination sites on the terminal chromium atoms.

Although freshly prepared $\{Cr(H_2O)(OH)[OP(CH_3)(C_6H_5)O]_2\}_x$ and $\{Cr(H_2O)(OH)[OP(C_8H_{17})_2O]_2\}_x$ are soluble in organic solvents, their anhydrous derivatives are virtually insoluble, in contrast to the similarity just discussed for the diphenyl analogs. This observation suggests that removal of the water molecules is accompanied by some degree of crosslinking. It is interesting to note that, even in a sealed container, samples of the parent methylphenyl and dioctyl polymers become less soluble as they stand and within a few months are completely insoluble. However, addition of a few drops of alcohol to a suspension of the stored samples (or the anhydrous polymers) in chloroform or benzene causes the solubility to be slowly restored. Other anhydrous dialkyl derivatives, such as the dibutyl polymer, appear to be similar to the methylphenyl and dioctyl polymers, not to the diphenyl polymer.

Structures of $[Cr(OH)(OPRR'O)_2]_x$

All of the samples of the anhydrous polymers investigated are amorphous to x-rays, as are their parent hydroxyaquo polymers. It is therefore necessary to turn to other evidence for structure assignment. The solubilities and intrinsic viscosities of the solutions of the three parent hydroxyaquo polymers and the anhydrous diphenyl polymer indicate that they are all basically linear polymers. The insolubility of the anhydrous methylphenyl and dioctyl polymers, on the other hand, suggest that they are crosslinked to a reasonable extent. Since the anhydrous polymers contain fewer groups, it is appropriate to consider their structures first.

It is reasonable to assume that these polymers are based on chromium(III) centers with a coordination number of six held together by phosphi-

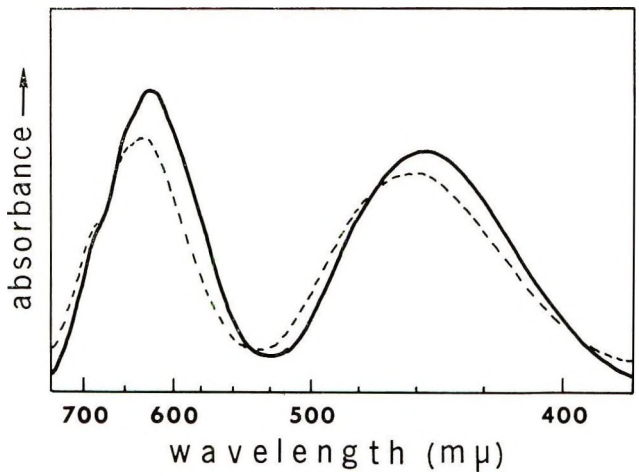

Fig. 2. Visible-light spectra of (——) $\{Cr(H_2O)(OH)[OP(C_6H_5)_2O]_2\}_x$ and (- - - -) $\{Cr(OH)[OP(C_6H_5)_2O]_2\}_x$ in chloroform solution.

nate and/or hydroxy bridges. The bridging groups are, of course, capable of functioning as crosslinks where appropriate. It is also possible for the phosphinate group to function as a chelating ligand, but there is evidence that the bridging function is favored.[5] Thus the repeat units I–X are the most likely possibilities.

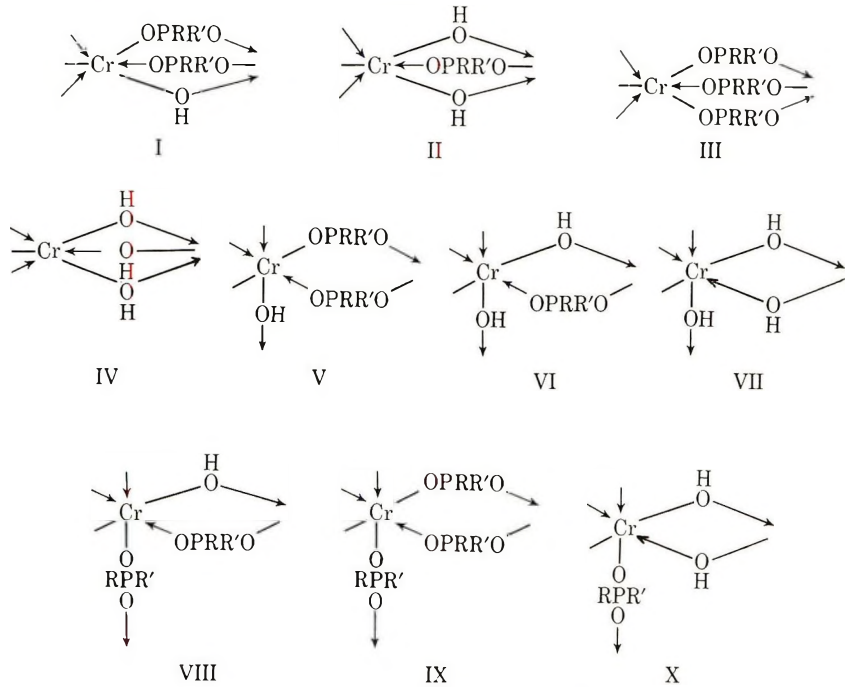

There is some evidence bearing on each of the major features in these repeat units.

The visible spectrum of $\{Cr(OH)[OP(C_6H_5)_2O]_2\}_x$, shown as the dashed line in Figure 2, contains the usual bands at about 450 and 620 mμ of approximately equal intensity attributable to the *d-d* transitions of octahedrally coordinated chromium(III). The green color of the insoluble species indicates that they too contain octahedrally coordinated chromium(III).

In the 400–1300 cm^{-1} region of the infrared, all the anhydrous polymers give very similar spectra which are almost identical to the spectra for the respective parent polymers. The spectra for $\{Cr(OH)[OP(CH_3)(C_6H_5)O]_2\}_x$ and $\{Cr(H_2O)(OH)[OP(CH_3)(C_6H_5)O]_2\}_x$ shown in Figure 3 are typical. The strong bands at about 1045 and 1130 cm^{-1} are associated with the symmetric and asymmetric PO_2 stretchings, respectively.[6] They are quite sharp except for the splitting on the low-frequency side of the 1045 band which is probably caused by the phenyl group and is not present in the spectra of the dialkyl species. The other bands in the 800–1300 cm^{-1} region can be accounted for as due to methyl groups (870, 1300 cm^{-1}) or hydroxyl (940 cm^{-1}), except for the small band at 1220 cm^{-1} which could also be due to PO but probably does not represent a major contribution to

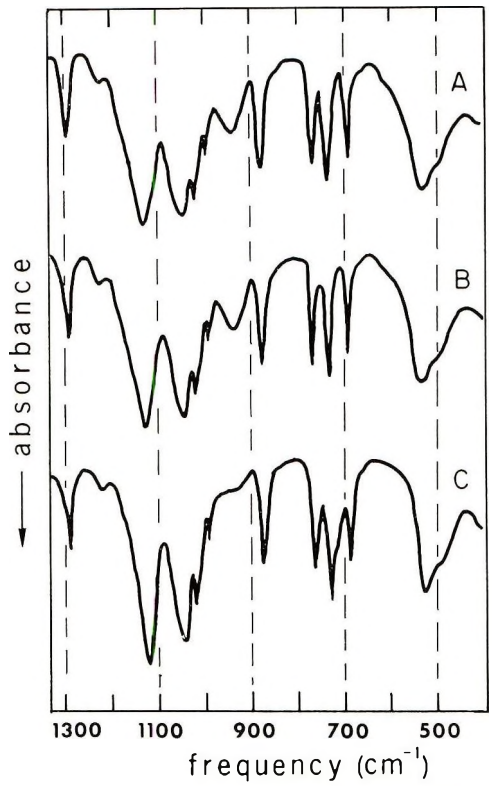

Fig. 3. Infrared spectra in Nujol mull of: (*A*) $\{Cr(OH)[OP(CH_3)(C_6H_5)O]_2\}_x$; (*B*) $\{Cr(H_2O)(OH)[OP(CH_3)(C_6H_5)O]_2\}_x$; (*C*) $\{Cr(OD)[OP(CH_3)(C_6H_5)O]_2\}_x$.

the structure. Consequently it appears that most of the phosphinate groups are basically equivalent and that they are bridging groups, because their PO_2 stretchings are virtually identical in shape and frequency to those for the corresponding chromium(III) tris(phosphinates) in which it is most likely that the phosphinates are bridging groups in order to explain the polymeric nature of the tris(phosphinates).[7] We plan to publish infrared spectra for this type of phosphinate shortly.

None of the anhydrous polymers absorb in the 1600–1630 cm^{-1} range (HOH bending mode), confirming the absence of water. The 2300–4000 cm^{-1} range of the spectra of $\{Cr(OH)[OP(C_6H_5)_2O]_2\}_x$, $\{Cr(OH)[OP(CH_3)(C_6H_5)O]_2\}_x$, and $\{Cr(OH)[OP(C_8H_{17})_2O]_2\}_x$ and their parent polymers is given in Figure 4. In addition to the CH stretching of the phenyl group in the 3000–3100 cm^{-1} range, the anhydrous diphenyl polymer (curve *A*) shows a single, strong, sharp band at about 3620 cm^{-1} which can only be assigned to the OH stretching. The other two anhydrous polymers (curves *C* and *E*) have, in addition to absorption in the CH region, the strong, sharp band at 3620 cm^{-1} and a somewhat broader band at about 3500 cm^{-1} which is probably also due to OH. Deuteration shifts both bands as expected.

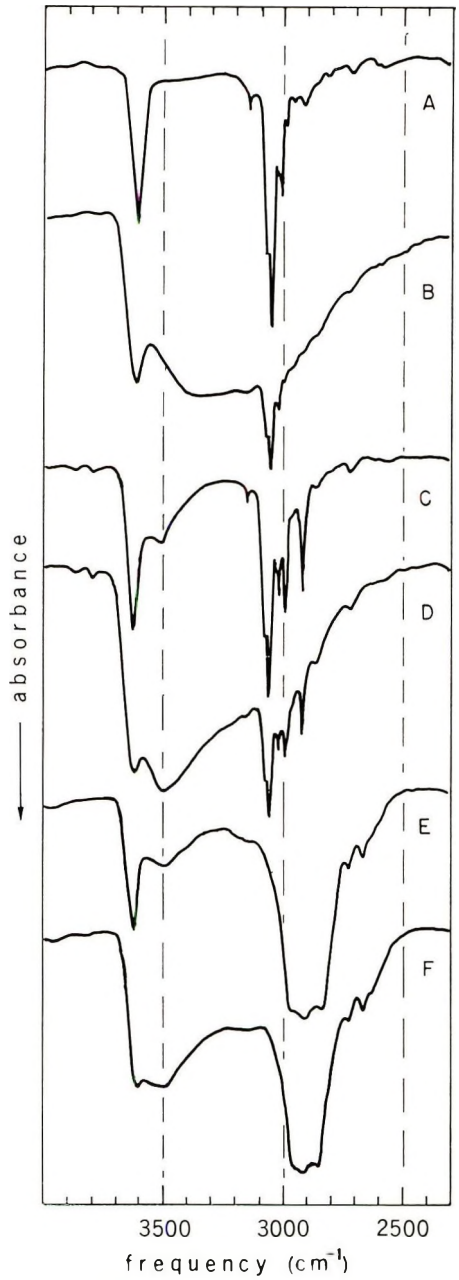

Fig. 4. Spectra of (*A*) $\{Cr(OH)[OP(C_6H_5)_2O]_2\}_x$; (*B*) $\{Cr(H_2O)(OH)[OP(C_6H_5)_2O]_2\}_x$; (*C*) $\{Cr(OH)[OP(CH_3)(C_6H_5)O]_2\}_x$; (*D*) $\{Cr(H_2O)(OH)[OP(CH_3)(C_6H_5)O]_2\}_x$; (*E*) $\{Cr(OH)[OP(C_8H_{17})_2O]_2\}_x$; (*F*) $\{Cr(H_2O)(OH)[OP(C_8H_{17})_2O]_2\}_x$.

There thus appears to be one kind of OH in the diphenyl species, but more than one in the other two polymers.

The band at 940 cm^{-1} in all the polymers, parent and anhydrous, is also affected by deuteration and consequently involves OH groups. It is apparently shifted underneath the peak at about 730 cm^{-1} in accordance with the expected isotopic shift and probably represents a Cr-OH deformation.[8a]

Since no significant changes are observed in this band in the spectra of the various phosphinates, it is impossible to establish whether the OH groups involved in this deformation are exclusively of one type or are of all the types apparently present in these polymers. This is probably due to the facts that this absorption is relatively weak and that nearby there are absorptions due to other groups.

On the basis of the foregoing data it is reasonable to conclude that the soluble $\{Cr(OH)[OP(C_6H_5)_2O]_2\}_x$ is a linear polymer in which repeat unit I predominates on a statistical basis but that II, III, and perhaps IV can contribute as well. It is, however, unlikely that units V–X are present to any extent, both because of solubility and because the infrared spectrum indicates that only one kind of phosphinate and one kind of hydroxyl are present. The insoluble $\{Cr(OH)[OP(CH_3)(C_6H_5)O]_2\}_x$ and $\{Cr(OH)[OP(C_8H_{17})_2O]_2\}_x$, on the other hand, appear to contain repeat units V, VI, and VII as well as I–IV to explain their insolubility and the different kinds of hydroxyl absorptions in their spectra. There is no evidence for a significant contribution to their structures by units VIII–X. The peak at 3620 cm^{-1} present in all the anhydrous polymers apparently is due to the OH groups bonding between chromium(III) centers in the same chain, since only this OH stretching is observed in the spectrum of the anhydrous diphenyl polymer, whereas the broader peak at 3500 cm^{-1} apparently arises from the OH groups bonding between chromium(III) centers in different chains.

The absence of crosslinking in the anhydrous diphenyl polymer is most likely a steric phenomenon. Models suggest that the phenyl groups are sufficiently bulky and rigid that interchain bonding via the OH groups is greatly inhibited when the bridging group is diphenyl phosphinate, whereas the small methyl group and the flexible alkyl chains do not hinder crosslinking.

Structures of $[Cr(H_2O)(OH)(OPRR'O)_2]_x$

The results of this study suggest that the earlier speculation[1,3,4] that the hydrated parent polymers have structures consisting predominantly of repeat units of the type XI

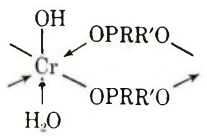

XI

should be modified. The sharp infrared band at 3620 cm^{-1} originally assigned to the unidentate OH in XI now appears more likely to be due to intrachain OH bridging than to unidentate OH groups because the same band appears in the spectra for all the anhydrous polymers as well as for the parent polymers.

A strong broad band due to water and perhaps to unidentate OH covers most of the 2500–3700 cm^{-1} range in the spectra of the parent polymers. Because it overlaps with the OH absorptions already mentioned, it is difficult to determine the exact intensity of the latter. This raises the question as to whether or not the water is actually coordinated to the chromium. The infrared spectra are not definitive in these systems because the rocking and wagging modes expected in the 658–880 cm^{-1} region for coordinated water[8b] do not give rise to very intense bands and could well be covered by other bands for these polymers in this region. There are two pieces of evidence that suggest that these polymers do contain coordinated water. The slight shift in the visible spectrum in going from $\{Cr(H_2O)(OH)[OP(C_6H_5)_2O]_2\}_x$ to $\{Cr(OH)[OP(C_6H_5)_2O]_2\}_x$ (see Fig. 2) suggests that the water is sufficiently strongly bonded to affect the ligand field around the chromium. The possibility that the shift shown in Figure 2 could be due to other factors is unlikely. The most likely alternative, that changes in endgroups might be responsible, is ruled out by the observation thast amples of the parent polymer with different molecular weights all gave the same spectrum and that samples of the anhydrous polymer with different molecular weights all gave the same shifted spectrum. If variation in endgroups has an observable effect, differences should be observed as molecular weight is varied. The marked difference in solubility between the hydroxyaquo and hydroxy methylphenyl- and dioctylphosphinates suggests that the water is an integral part of those parent polymers also.

There is no significant difference in the PO bands for any of the parent polymers compared to their anhydrous derivatives, so it appears that the phosphinate groups are bonded in the same way in both types of polymers.

The evidence now in hand leads to the conclusion that the so-called hydroxyaquo polymers contain the originally proposed monomer units XI and in addition contain the triply bridged monomer units I–IV with some contribution from the crosslinking monomer units V–VII in the methylphenyl and dioctyl polymers. The overlap in the OH region makes it difficult to decide about relative amounts of the various units. Perhaps at present it is best to formulate these polymers as $[Cr(H_2O)_n(OH)(OPRR'O)_2]_x \cdot pH_2O$ where $n < 1$ and to consider them to have a multiplicity of repeat units, the presence of some of which depends on the side groups on the phosphorus.

This investigation was supported in part by the Office of Naval Research. H. D. McLaughlin assisted in some of the experimental work, and our analytical department performed the elemental analyses.

References

1. K. D. Maguire and B. P. Block, *J. Polym. Sci. A-1*, **6**, 1397 (1968) (Part X).
2. B. P. Block, *Inorg. Macromol. Rev.*, **1**, 115 (1970) and references therein.
3. A. J. Saraceno and B. P. Block, *J. Am. Chem. Soc.*, **85**, 2018 (1963).
4. A. J. Saraceno and B. P. Block, *Inorg. Chem.*, **3**, 1699 (1964).
5. B. P. Block, E. S. Roth, C. W. Schaumann, and L. R. Ocone, *Inorg. Chem.*, **1**, 860 (1962).
6. R. A. Nyquist, *J. Mol. Structure*, **2**, 111 (1968).
7. A. J. Saraceno, J. P. King, and B. P. Block, *J. Polymer Sci. B*, **6**, 15 (1968).
8. K. Nakamoto, *Infrared Spectra of Inorganic and Coordination Compounds*, 2nd ed., Wiley, New York, 1970, (a) p. 169; (b) p. 167.

Received June 11, 1971
Revised July 15, 1971

JOURNAL OF POLYMER SCIENCE: PART A-1 VOL. 9, 3039–3053 (1971)

1,4 Polymerization of Isoprene by Titanate Catalyst Systems*

SAMUEL E. HORNE, JR. and CHARLES J. CARMAN, *B. F. Goodrich Research Center, Brecksville, Ohio 44141*

Synopsis

Titanates are versatile in the 1,4 polymerization of isoprene. The $(R'O)_4Ti/RAlCl_2$ catalyst gives either *cis*- or *trans*-1,4-polyisoprene, depending on the nature of both the titanate and the solvent. Primary titanates give *cis*-1,4-polyisoprene in both aliphatic and aromatic solvents. Secondary titanates give *cis*-polyisoprene in aliphatic solvents, and trans-1,4-polyisoprene in aromatic solvents. Tertiary titanates give *trans*-polyisoprene in both aliphatic and aromatic solvents. A mechanism is postulated which takes into consideration the role of the solvent. ESR studies of the various titanate–$RAlCl_2$ catalysts were made; the paramagnetic structures are related to polymerization mechanisms.

INTRODUCTION

The polymerization of dienes by alkyl titanates and trialkylaluminums is well known.[1] Butadiene[2–4] polymerizes to 1,2-polybutadiene and both isoprene[5,6] and 2-n-propylbutadiene[7] polymerize to the 3,4-polymer structures with these catalysts. Interestingly, pentadiene-1,3 is converted to isotactic *cis*-1,4 polymer by this catalyst system;[8] this is the only reported example of 1,4 polymerization by $R_3Al/Ti(OR')_4$.

The use of the $RAlCl_2$–$Ti(OR')_4$ system was reported in the copolymerization of α-olefins with vinyl chloride.[9,10] The catalytic activity in these systems is apparently related to uncharacterized soluble complexes.

Recently, Cucinella et al. reported the use of $RAlCl_2$–$Ti(OR')_4$ to prepare *cis*-1,4-polyisoprene and crystalline *trans*-1,4-polybutadiene.[11] These workers report on only a single set of catalyst components, $C_2H_5AlCl_2$ and $(n\text{-}C_4H_9O)_4Ti$, in an aliphatic solvent, heptane. Our results for isoprene are in agreement under this single set of conditions; but we will show that by changing the titanate and the solvent, either *cis*- or *trans*-1,4-polyisoprene can be prepared by the $RAlCl_2$–$Ti(OR')_4$ catalyst.

The reduction of tetravalent titanium to trivalent titanium in a Ziegler catalyst system produces titanium structures which have an unpaired electron ($3d^1$ configuration). Consequently, many electron spin resonance (ESR) studies[12–23] have been made on a number of Ziegler-Natta catalyst

* Paper presented at the 1st Akron Chemists' Symposium, Akron, Ohio, May 20, 1971.

systems. We have used ESR to show that the paramagnetic titanium species present in the $RAlCl_2$–$Ti(OR')_4$ system is a function of titanate and solvent. The ESR results are interpreted in light of the ESR data which has been reported for $TiCl_4$–R_3Al, $TiCl_4$–$RAlCl_2$, and $TiCl_4$–R_2AlCl systems.

EXPERIMENTAL

All handling, distillation, storage, transfer, and polymerization operations were carried out under an oxygen-free dry nitrogen atmosphere.

Materials

Isoprene was dried over calcium hydride, distilled from sodium, and stored under nitrogen pressure at −22°C. Solvents were dried and purified by accepted methods. Tertiary amines were dried over calcium hydride and distilled from sodium. Isobutylaluminum dichloride (Texas Alkyls Corp.) was used as received. Commercially available titanium alkoxides (tetramethyl, tetra-*n*-butyl, tetraisopropyl, and tetra-2-ethylhexyl titanates) were purified by either vacuum distillation or vacuum sublimation. Tetra-*tert*-butyl titanate was prepared by the method of Bradley.[24] Tetraneopentyl titanate was prepared by the exchange reaction between excess neopentyl alcohol and tetraisopropyl titanate followed by vacuum distillation.[25]

Polymerization

The polymerizations were carried out in crown cap beverage bottles, by using the technique previously described.[26] Charging order was: solvent, organoaluminum compound, titanate, amine, and isoprene. The bottles were capped with puncture-type, self-sealing, crown caps. The capped bottles were tumbled at 30°C in a constant-temperature bath. After the desired time of polymerization, the bottles were shortstopped by injecting an alcohol–benzene–antioxidant–tertiary amine mixture, and the polymer was precipitated by pouring into a large volume of alcohol containing antioxidant. The polymers were thoroughly washed with alcohol (containing additional antioxidant) to remove catalyst residues and then vacuum-dried at 50°C for at least 18 hr.

Polymer Characterization

Infrared determinations were carried out on films cast from either benzene or toluene solutions. In a few cases, pressed films were used.

Insoluble polymer (gel) and swelling index determinations were carried out by the well-known sol-gel method.[27]

Polymer molecular weight was estimated by using a single-point viscosity determination. Dilute solution viscosity, (DSV) is defined by the equation:

$$DSV = 2.3 \log \eta_r / C$$

η_r being the viscosity of the polymer solution relative to that of the solvent (toluene) at 25°C, where C is the polymer concentration (about 0.2 g/100 ml toluene).

Electron Spin Resonance

Electron spin resonance spectra were obtained with a Varian E-3 spectrometer operating at 9.52 GHz and 100 KHz modulation. The catalyst samples were contained in quartz tubes of 4 mm od which had been carefully cleaned, dried, and purged with nitrogen. The catalyst samples were transferred with a syringe while maintaining a sweep of dry nitrogen through the tube. The samples were then sealed under nitrogen. The ESR spectra were obtained at room temperature or, where noted, at various low temperatures by using the Varian variable-temperature controller and dewared cavity insert.

RESULTS AND DISCUSSION

The structure of the polyisoprene produced in the polymerization of isoprene by i-$BuAlCl_2$–$(i\text{-}C_3H_7O)_4Ti$ depends on the nature of the hydrocarbon solvent. When the benzene is used as the polymerization solvent, isoprene polymerizes to *trans*-1,4-polyisoprene (α-balata configuration), but with pentane as the solvent, *cis*-1,4-polyisoprene results. Table I shows a typical recipe along with characteristic polymer properties. The catalyst system is high in Lewis acid character, and a tertiary amine is added to counteract this acid nature.

TABLE I
Typical Recipe for $i\text{-}C_4H_9AlCl_2$–$(i\text{-}C_3H_7O)_4Ti$-$(n\text{-}C_4H_9)_3N$–Isoprene[a]

Solvent	Time, hr	Gel, %	DSV	Polyisoprene structure
Benzene	24	0	~1, 9	*trans*-1,4 (α-balata)
Pentane	48	8–10	2.4–3.0	*cis*-1,4

[a] Conditions: solvent, 500 ml; $i\text{-}C_4H_9AlCl_2$, 3.60 mmole; $(i\text{-}C_3H_7O)_4Ti$, 0.672 mmole; $(n\text{-}C_4H_9)_3N$, 0.378 mmole; isoprene, 45 g; Ti/Al, 0.187; N/Ti, 0.562; temperature, 30°C; conversion, >90%.

The recipes of Table I are based on a titanate from a secondary alcohol. If a titanate from a primary alcohol, $(n\text{-}C_4H_9O)_4$ Ti, is employed, isoprene polymerizes to the *cis*-1,4 structure in both pentane and in benzene. However, the use of a tertiary titanate $(t\text{-}C_4H_9O)_4Ti$, leads to the formation of *trans*-1,4-polyisoprene in both the aliphatic and the aromatic solvent systems. These data are illustrated in Table II.

A small change in polymer structure with a family change in the titanium ligand is well established. The best known example of this is in the polymerization of butadiene by R_3Al–TiX_4.[1] As the halogen is changed from

TABLE II
Influence of Titanate Type[a]

$(RO)_4Ti$	Solvent	Ti/Al	N/Ti	Conversion, %	DSV	Polyisoprene structure
$(n\text{-}C_4H_9O)_4Ti$	Benzene	0.187	0.416	66	2.3	*cis*-1,4
$(n\text{-}C_4H_9O)_4Ti$	Hexane	0.187	—	44	3.1	*cis*-1,4
$(i\text{-}C_3H_7O)_4Ti$	Benzene	0.187	0.625	89	1.7	*trans*-1,4
$(i\text{-}C_3H_7O)_4Ti$	Pentane	0.187	0.625	83	2.6	*cis*-1,4
$(t\text{-}C_4H_9O)_4Ti$	Benzene	0.187	0.625	94	—	*trans*-1,4
$(t\text{-}C_4H_9O)_4Ti$	Pentane	0.167	0.813	33	1.0	*trans*-1,4

[a] Conditions: $i\text{-}C_4H_9AlCl_2$, 2.16 mmoles; amine, $(n\text{-}C_4H_9)_3N$; temperature, 30°C; isoprene, 18 g.; solvent, 200 ml.

TABLE III
Influence of Primary Titanate Structure[a]

Titanate	Solvent	Ti/Al	N/Ti	Conversion, %	Gel, %	DSV	Polyisoprene structure
$(n\text{-}C_4H_9O)_4Ti$	Benzene	0.187	0.416	66	8	2.3	*cis*-1,4
"	Hexane	0.187	—	61	22	2.8	*cis*-1,4
(Neopentyl-O)$_4$Ti	Benzene	0.178	—	67	25	2.2	*cis*-1,4
"	Hexane	0.178	—	100	39	3.6	*cis*-1,4
(2-Ethylhexyl-O)$_4$	Benzene	0.22	—	78	0	1.7	*cis*-1,4
$(CH_3O)_4Ti$	Benzene	0.187	—	50	40	2.7	*cis*-1,4
$(CH_3O)_4Ti$	Benzene	0.187	0.625	50	25	3.0	*cis*-1,4

[a] Conditions: solvent, 200 ml; $i\text{-}C_4H_9AlCl_2$, 2.16 mmole; temperature, 30°C; amine, $(n\text{-}C_4H_9)_3N$; isoprene, 18 g.

Cl to Br to I, the *cis*-1,4 content of the polybutadiene increases from about 60% to about 95%. However, examples of a total change in polymer structure by a family change in the titanium ligand or by a change in the type of hydrocarbon solvent are unknown. The $RAlCl_2$–$Ti(OR_4')$ catalyst system is very intriguing from the standpoint of these effects. This is particularly true in view of the reports that $RAlCl_2$ is not a stereospecific catalyst for the polymerization of isoprene with either $TiCl_4$ or β-$TiCl_3$.[28–30]

In order to determine the importance of the structure of the titanate, a number of simple and complex primary titanates were used with *i*-$BuAlCl_2$ to initiate the polymerization of isoprene. These primary titanates included the crystalline, insoluble tetramethyl titanate and the branched and structurally hindered tetra-2-ethylhexyl and tetraneopentyl titanates. All of the primary titanates showed the same results, *cis*-1,4-polyisoprene formed in both pentane and in benzene. Some typical results are shown in Table III. Thus it is the primary nature of the titanate, and not the complexity, that directs the course of the isoprene polymerization.

Further effects of the titanate structure were studied by using mixtures of $(i\text{-}C_3H_7O)_4Ti$ and $(n\text{-}C_4H_9O)_4Ti$ with $i\text{-}C_4H_9AlCl_2$–$(n\text{-}C_4H_9)_3N$. The results are those of Table IV. The data clearly shows the primary titanate influence to predominate for with the equimolar mixture, only the *cis*-1,4-polyisoprene structure was found.

TABLE IV
Polymerization of Isoprene with Mixed Titanates–$i\text{-}C_4H_9AlCl_2$–$(n\text{-}C_4H_9)_3N$[a]

Titanate			
$(i\text{-}C_3H_7O)_4Ti$, mole-%	$(n\text{-}C_4H_9O)_4Ti$, mole-%	Conversion, %	Polyisoprene structure
100	0	89	*trans*-1,4
80	20	94	*cis*–*trans* mixed
50	50	50	*cis*-1,4
33	67	61	*cis*-1,4
20	80	56	*cis*-1,4

[a] Conditions: benzene, 200 ml; isoprene, 18 g; $i\text{-}C_4H_9AlCl_2$, 2.16 mmole; temperature, 30°C; Ti/Al = 0.187; N/Ti = 0.625.

The unusual solvent effect of the $(i\text{-}C_3H_7O)_4Ti$–$i\text{-}C_4H_9AlCl_2$–$(n\text{-}C_4H_9)_3N$ catalyst was investigated in detail.. The use of benzene, toluene, or ethylbenzene as the polymerization solvent resulted in *trans*-1,4-polyisoprene. Similarly, the use of pentane, hexane, heptane, or cyclohexane as solvent for the polymerization of isoprene resulted in *cis*-1,4-polyisoprene. Thus it is the aliphatic or aromatic nature of the hydrocarbon solvent that determines the role $(i\text{-}C_3H_7O)_4Ti$ plays in the polymerization. Polymerization in mixed aliphatic–aromatic solvents showed the data of Table V.

In a further study of the effects of solvent, concentrated $(i\text{-}C_3H_7O)_4Ti$–$i\text{-}C_4H_9/AlCl_2$—$(n\text{-}C_4H_9)_3N$ catalysts were prepared in benzene and in hexane. Aliquots of these concentrated catalysts were used to initiate isoprene

TABLE V
Polymerization in Mixed Solvents[a]

Solvent				
Benzene, vol-%	Cyclohexane, vol-%	Gel, %	DSV	Polyisoprene structure
100	0	0	1.70	*trans* 1,4
50	50	0	1.08	~50/50 *cis*/*trans*-1,4
12.5	87.5	0	0.53	*cis*-1,4
0	100	0	0.96	*cis*-1,4

[a] Conditions: i-$C_4H_9AlCl_2$, 2.16 mmole; $(i\text{-}C_3H_7O)_4Ti$, 0.403 mmole; $(n\text{-}C_4H_9)_3N$, 0.252 mmole; temperature, 30°C; solvent, 200 ml; isoprene, 18 g; Ti/Al = 0.187; N/Ti = 0.625.

polymeriztion at 30°C in benzene and in hexane. For catalyst prepared in benzene: (a) aliquot to benzene–isoprene gave *trans*-1,4-polyisoprene; (b) aliquot to hexane–isoprene gave *cis*-1,4-polyisoprene. For the catalyst prepared in hexane: (a) aliquot to benzene–isoprene gave *trans*-1,4-polyisoprene; (b) aliquot to hexane–isoprene gave *cis*-1,4-polyisoprene. These results show that the solvent does not become bound or tied to the active species. Instead, the solvent present in the largest amount determines which 1,4-polyisoprene structure is formed with the secondary titanate catalyst system. This is also in agreement with the mixed solvent results of Table V.

As would be expected, the Ti/Al ratio in the catalyst was found to influence the polyisoprene properties. Some typical data are shown in Table VI.

The primary titanate catalysis shows an influence of Ti/Al ratio on rate, polymer structure, and polymer molecular weight. At the lowest two Ti/Al ratios the polymer structure is mostly *cis*-1,4 but some *trans*-1,4 structure can be detected. This *trans* content may be due to the high cationic character of the catalyst at these lower ratios.

The Ti/Al ratio of catalysts containing the secondary titanate shows an effect on gel content and polymer structure. At the lower Ti/Al ratios, *trans*-1,4-polymer of high gel content is obtained; very high levels of $(n\text{-}C_4H_9)_3N$ do not prevent this gelation from occurring. At a Ti/Al ratio of 0.218 only a chalky polymer is formed; this has been repeated, checked, and found to be true.

The catalyst contains a high level of a Lewis acid, i-$C_4H_9AlCl_2$. A Lewis base is a necessary catalyst component with secondary and tertiary titanates to suppress gel formation. The effect of $(n\text{-}C_4H_9)_3N$ is shown in Table VII. The noticeable effects on the $(i\text{-}C_3H_7O)_4Ti$ catalyst system are: (1) a decrease in gel formation, (2) a decrease in the gel crosslink density as manifested in the swelling index, (3) a decrease in the rate of polymerization. There is no effect on the *cis-trans* structure of the polymer. It is also shown that the base is not necessary for the primary titanate. While data are not shown, the $(t\text{-}C_4H_9O)_4Ti$ catalyst requires the

TABLE VI
Effect of Ti/Al Ratio[a]

$(RO)_4Ti$	Ti/Al	N/Ti	Time, hr	Conversion, %	Gel, %	Swelling index	DSV	Polyisoprene structure
$(n\text{-}C_4H_9O)_4Ti$	0.108	—	29	22	12	—	0.5	*cis–trans* mixed
"	0.133	—	"	22	9	—	0.7	*cis–trans* mixed
"	0.162	—	"	39	9	—	1.6	*cis*-1,4
"	0.189	—	"	56	6	—	2.1	*cis*-1,4
"	0.217	—	"	67	4	—	2.2	*cis*-1,4
$(i\text{-}C_3H_7O)_4Ti$	0.124	0.47	2	78	87	22	0.6	*trans*-1,4
"	0.124	2.2	22	89	62	58	1.1	*trans*-1,4
"	0.156	0.47	4	89	60	57	1.2	*trans*-1,4
"	0.187	0.47	22	89	0	—	1.3	*trans*-1,4
"	0.187	0.625	30	89	0	—	1.2	*trans*-1,4
"	0.218	0.47	13 days	39	—	—	—	Chalky powder

[a] Conditions: benzene, 200 ml; isoprene, 18 g; $i\text{-}C_4H_9AlCl_2$, 2.16 mmole; temperature, 30°C; DSV (25°C), in toluene, ~0.2 g/100 ml.

TABLE VII
Effect of $(n\text{-}C_4H_9)_3N$ Level on Gel Formation[a]

Titanate	N/Ti	Conversion, %	Gel, %	Swelling index	DSV	Polyisoprene structure
$(n\text{-}C_4H_9O)_4Ti$	—	61	6	—	1.80	*cis*-1,4
$(i\text{-}C_3H_7O)_4Ti$	—	89	84	36	0.29	*trans*-1,4
"	0.16	95	61	62	0.43	"
"	0.31	72	9	182	1.30	"
"	0.62	50	4	61	2.85	"
"	0.73	100	1	64	1.50	"
"	1.1	Trace	—	—	—	—
"	2.2	Trace	—	—	—	—

[a] Conditions: benzene: 200 ml; $(i\text{-}C_4H_9)AlCl_2$, 2.16 mmole; isoprene, 18 g; temperature; 30°C; Ti/Al = 0.187.

base and shows the same effects as the $(i\text{-}C_3H_7O)_4Ti$ catalyst systems. Other tertiary amines may be substituted for the $(n\text{-}C_4H_9)_3N$.

It is theoretically feasible to write a equilibrium equation between the catalyst components. The preferred Ti/Al ratio of 0.187 means a molar ratio of 1/5.35. The equation becomes:

$$5.35\ RAlCl_2 + (R'O)_4Ti \underset{\leftarrow}{\overset{(n\text{-}Bu)_3N}{\rightarrow}} 4RAl\begin{matrix}Cl\\ \diagup\\ \\ \diagdown\\ OR'\end{matrix} + TiCl_4 + 1.35\ RAlCl_2 \qquad (1)$$

This equation predicts that one could start from the right-hand side of the equation and prepare catalysts that show the same—OR′ effects as shown by $Ti(OR')_4$ in the polymerization of isoprene. This was found to be a valid assumption (Table VIII).

TABLE VIII

Catalyst Prepared From $RAl\begin{matrix}Cl\\ \diagup\\ \diagdown\\ OR'\end{matrix}$ –$TiCl_4$–$(n\text{-}Bu)_3N$–$RAlCl_2$[a]

	Polyisoprene formed	
—OR′	In benzene	In hexane
$n\text{-}C_4H_9O$—	*cis*-1,4	*cis*-1,4-
$i\text{-}C_3H_7O$	*trans*-1,4	*cis*-1,4-
$s\text{-}C_4H_9O$	*trans*-1,4	*cis*-1,4-
$t\text{-}C_4H_9O$	*trans*-1,4	*trans*-1,4

[a] Conditions: solvent, 200 ml: temperature, 30°C; isoprene, 18 g; RAlClOR′/$TiCl_4$ = 4; total Al/Ti = 5.35; N/Ti = 0.625.

It is quite clear that both the titanate and solvent system govern the stereoregularity of the polyisoprene formed. We used ESR to establish the common active titanium species for *cis*-polymer formation in those titanate systems which produced *cis* polymer and the common active titanium species for *trans* formation in the titanate systems which produced *trans* polymer.

As was seen in Table II, the tertiary titanate–$RAlCl_2$–$(n\text{-}C_4H_9)N$ system produced *trans*-1,4-polyisoprene in both benzene and pentane. We chose to examine this catalyst system by looking at the ESR signals produced in benzene or heptane containing just the titanate and $(i\text{-}C_4H_9)AlCl_2$ as well as this cocatalyst plus amine, and cocatalyst plus amine and isoprene.

In the system containing just the tertiary titanate and the alkyl aluminum dichloride in benzene, there are at least four ESR signals evident soon after mixing the components. The most prominent species evident immediately is at $g = 1.968$. This ESR resonance has been assigned by Ono and Keii[13] to a trivalent titanium compound having absorbed aluminum alkyl on the surface. Within 20 min after mixing, resonances with $g =$

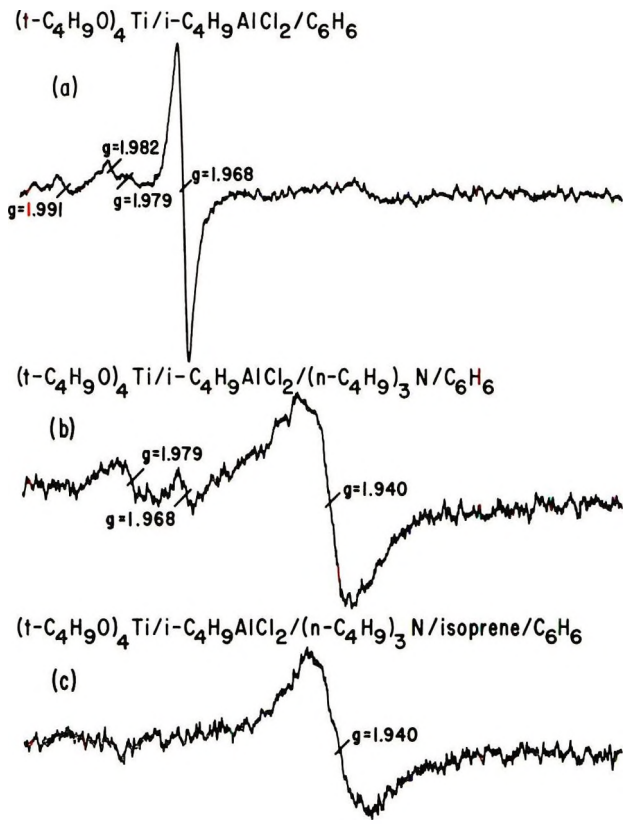

Fig. 1. Electron spin resonance signals produced in the tertiary titanate catalyst system in benzene.

1.980 and $g = 1.991$ are evident. (The peak at 1.980 breaks into two with $g = 1.979$ and 1.982 after 100 min.) All of these signals increase in intensity with time. The addition of isoprene to this system immediately produced a new signal with $g = 1.940 \pm 0.003$. In the presence of isoprene the signal continued to grow while the signals at 1.980 ± 0.002, 1.990 ± 0.002, and 1.968 decreased. These data are shown in Figures 1*a* and 1*b*.

Starting with $(t\text{-}C_4H_9O)_4Ti$, $i\text{-}C_4H_9AlCl_2$, and $(n\text{-}C_4H_9)_3N$ in benzene produced with $g = 1.940$ initially, as well as the three signals with $g = 1.986$, 1.980 and 1.991. In this system, $g = 1.940$ increased more rapidly than the other signals. When isoprene was present from time zero, the only signal seen was the one with $g = 1.940$ (Fig. 1*c*). The relative increase in the signal is shown in Figure 2. It is interesting to note that polymerization was evident both in the ESR tube and the polymerization bottles 59 min after mixing.

As was expected, heptane greatly affected the ESR signals observed. To begin with, none of the peaks with $g = 1.968$, 1.980, or 1.991 were detected either in the absence or presence of the amine and isoprene with the tertiary titanate–$RAlCl_2$ system. For $(t\text{-}C_4H_9O)_4Ti$ and $i\text{-}C_4H_9AlCl_2$ in heptane, a

peak with $g = 1.933 \pm 0.003$ is the only peak present up to 90 min aging time. After this time a very weak peak with $g = 1.940$ is barely detectable. When the catalyst containing amine is examined, the $g = 1.933$ peak is still the only peak initially produced. But $g = 1.940$ is evident after 155 min and obviously grows with time. When the catalyst system includes both amine and isoprene from the time of initial mixing, the peak with $g = 1.933$ is present initially, but the peak with g = 1.940 is now present after 23 min. The peak at 1.940 grows in the system while the peak with $g = 1.933$ decreases. These data are shown in Figure 3. Polymerization is present after 23 min and seems to be related with the presence of the $g = 1.940$ resonance peak.

If the paramagnetic Ti^{3+} species having g value of 1.940 is related to the formation of *trans*-1,4-polyisoprene, it will be present in the secondary titanate catalyst system in benzene but not in the secondary titanate system in heptane. This proved to be the case.

In the absence of amine and isoprene, the secondary titanate and i-C_4H_9-$AlCl_2$ in benzene produced Ti^{3+} species with $g = 1.943$, 1.969, and 1.972. The Ti^{3+} species with $g = 1.943$ has the strongest signal. All signals increase in intensity with time with $g = 1.972$ eventually becoming the most intense peak (after 21 hr). When amine is present or when amine and isoprene is present, the only peak present is the one with $g = 1.940 \pm 0.003$. This is shown in Figure 4*a*. The Ti^{3+} species with the larger g values are never formed when amine and isoprene is present.

Similar to the tertiary titanate system, the secondary titanate catalyst system in heptane produced an initial signal with a g value of 1.933 ± 0.003 (Fig. 4*b*). No signals with larger g values were ever present. The signal increased with time to a maximum, then decreased to a point of being barely detectable. No new signals were produced. The effect of amine or amine and isoprene was to increase the rate at which the Ti^{3+} species, with $g = 1.933$, disappeared. At the point where polymerization was evident no paramagnetic Ti^{3+} was detected (Fig. 4*c*). Consequently the formation of *cis*-1,4-polyisoprene, with the secondary titanate in heptane, seems to be associated with the lack of a paramagnetic Ti^{3+} species.

This interpretation was strengthened by the ESR studies of the primary titanate catalyst system in both benzene and heptane. There were no ESR signals detected in the primary titanate systems in either solvent, neither in the absence or presence of amine, nor amine and isoprene. The fact that a paramagnetic Ti^{3+} ($g = 1.933$) precursor to the apparent active species was seen for the secondary titanate in heptane, led us to speculate that the absence of a signal for the primary titanate may be due to kinetics. The ESR experiments which have been described were performed at room temperature (since this approximates the polymerization temperature). Consequently, we prepared the primary titanate catalyst at $-80°C$ in heptane and obtained ESR spectra at $-80°C$. Within 20 min a very strong signal with $g = 1.936$ was evident. Above $-60°C$ the signal grows weaker until it disappears, when the temperature is raised above 0 to $+10°C$. An im-

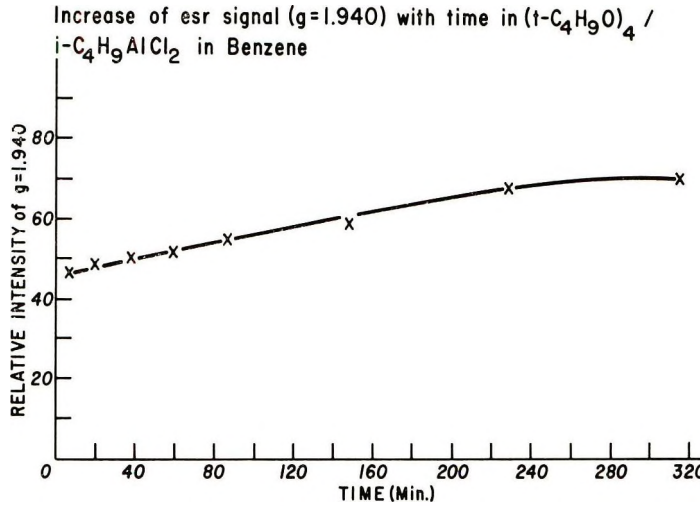

Fig. 2. Increase of ESR signal (g = 1.940) with time in (t-$C_4H_9O)_4$–i-$C_4H_9AlCl_2$ in benzene.

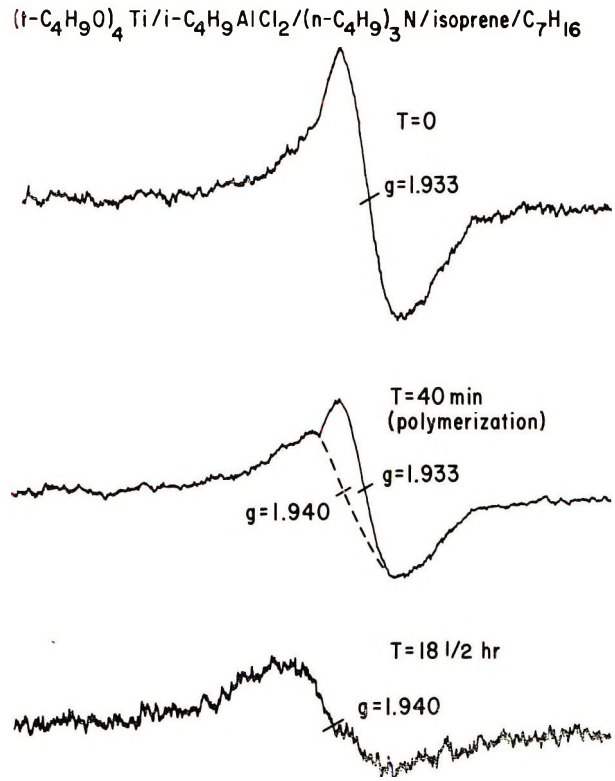

Fig. 3. Electron spin resonance signals produced in the tertiary catalyst system in the heptane.

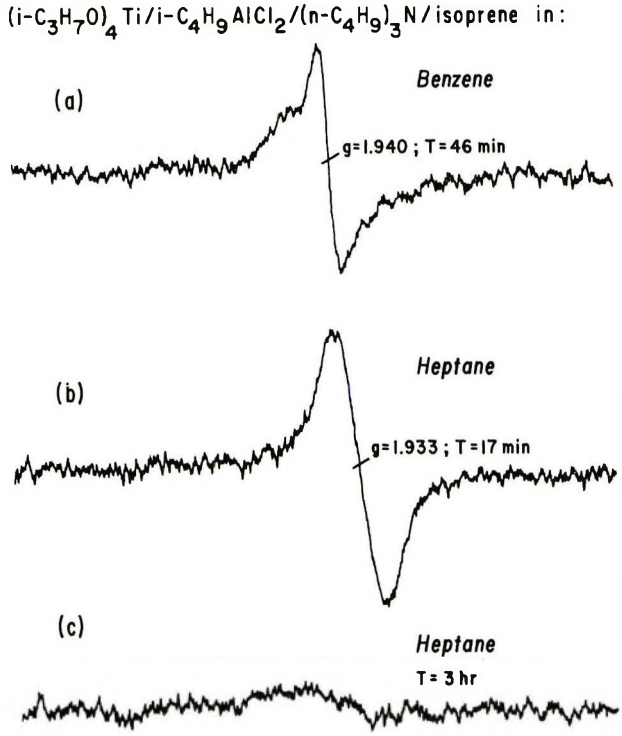

Fig. 4. Electron spin resonance signals produced with the secondary catalyst system in benzene and heptane.

portant observation is that the signal does not reappear when the system is recooled to −80°C. Consequently, an equilibrium is not present. The paramagnetic Ti^{3+} species which is transformed into a diamagnetic species, for the *cis*-polyisoprene-producing catalyst, is less stable for a primary titanate at room temperature than for a secondary titanate at room temperature.

A summary of our interpretation of the esr data and catalyst activity is in Table IX. These data can be interpreted in terms of the formation of α or β crystalline modifications of $TiCl_3$. It has been shown in ESR studies of many Ziegler catalyst systems that the $3d^1$ electron in β-$TiCl_3$ is spin-paired with other β-$TiCl_3$ molecules thus, prohibiting an ESR signal.[11,12,14–16] Adema[14] has reported a g value of 1.933 for a Ti^{3+} signal in the $TiCl_4$-$C_2H_5AlCl_2$ system. He assigned a structure consisting of a complex between $TiCl_3$ and a dimer of the aluminum alkyl chloride. Furthermore, he postulates that this complex is formed as shown by the equation:

$$TiCl_3 + (AlC_2H_5)Cl_2)_2 \rightleftharpoons TiCl_3 \cdot [Al(C_2H_5)Cl_2]_2 \qquad (2)$$

It seems reasonable that this complex could then disproportionate to β-$TiCl_3$ which would have no ESR signal. Cucinella et al.[11] analyzed the $(n\text{-}C_4H_9O)_4Ti$–$C_2H_5AlCl_2$ catalyst system in heptane. They also related

the activity of isoprene polymerization to the formation of β-$TiCl_3$ and verified the presence of β-$TiCl_3$ by x-ray diffraction. It is interesting to note that Cucinella observed the same ESR signal as Ono and Keii[13] (g = 1.959) for alkyl aluminum absorbed on $TiCl_3$. The fact that we did not see this signal may be because we were using i-$C_4H_9AlCl_2$ and the other workers were using $(C_2H_5)_3Al$,[13] $(C_2H_5)_2AlCl$,[13] and $C_2H_5AlCl_2$.[11]

TABLE IX
Solvent Dependence of ESR Signals

Titanate type	ESR signal g			
	Benzene		Heptane	
	Initial	Final[b]	Initial	Final[b]
Primary	No signal	No signal	No signal[a]	No signal
Secondary	1.940	1.940	1.933	No signal
Tertiary	1.940	1.940	1.933	1.940

[a] Below + 10°C, g = 1.936 is present.
[b] Present at onset of polymerization.

On the other hand, the signal with g = 1.940 (Table IX) is consistent with a complex of α-$TiCl_3$, where the complex involves an alkoxy group in the complex. It has been shown[12-23] that the g value of Ti^{3+} species depends on the extent of alkylation. The g values which have been reported are in the range 1.91–2.00, with the small g values associated with the more chlorinated Ti^{3+} structures. Tkac[12] has reported that oxygen in the $TiCl_4$–(i-$C_4H_9)_3Al$ system produced a signal to g = 1.937 at the expense of a signal at g = 1.92, which he had shown to be related to α-$TiCl_3$. The signal (g = 1.940) we detected is due to α-$TiCl_3$ which is complexed with an OR′ group. Possibly the complex is formed as shown in eq. (3) by reacting with the alkyl aluminum chloride proposed by eq. (1).

$$TiCl_3 + R(OR')AlCl \rightleftharpoons TiCl_3 \cdot R(OR')AlCl \quad (3)$$

Consequently, the $TiCl_3$ in the complex is the α-modification. We have found that the addition of α-$TiCl_3$ to the secondary titanate catalyst system in benzene does not alter the peaks in the ESR spectrum, whereas the addition of β-$TiCl_3$ produces a different spectrum which changes in time to that found in the α-$TiCl_3$ experiments.

The Ti–Ti bond distances in the α and β modified $TiCl_3$ are consistent with the α form producing *trans*-polyisoprene and the β form producing *cis*-polyisoprene. Bradley[25] has studied the structure of titanates both in the pure state and in solution. He reports these structures to be as summarized in Table X.

It is reasonable to assume the titanate structure to be the same in an aliphatic solvent—which should not participate in coordination—as in the pure state. A polymeric titanate would have a shorter Ti–Ti distance than a monomeric titanate. If these polymeric or monomeric structures are

TABLE X

OR in $Ti(OR)_4$	Structure	
	Pure	In benzene solution
Methoxy	Polymeric	Polymeric
n-Butoxy	Polymeric	Polymeric
Neopentoxy	Polymeric	Polymeric
Isopropoxy	Polymeric	Monomeric
tert-Butoxy	Monomeric	Monomeric

preserved in the reaction of $Ti(OR)_4$ with $RAlCl_2$, the resulting catalysts would have Ti–Ti distances similar to the distances in α and β $TiCl_3$. The reported Ti–Ti distances in α- and β-$TiCl_3$ are 3.54 and 2.91 Å, respectively.[28] The C_1–C_4 distance in the *trans* form of isoprene is 3.7 Å; the corresponding distance in the *cis* conformation is not known, but should be on the order of 3.0 Å from comparison with the distance in the *cis* form of butadiene. Saltman[28] has reported that α-$TiCl_3$–R_3Al polymerizes isoprene to the *trans*-1,4 structure, while β-$TiCl_3$–R_3Al gives *cis*-1,4-polyisoprene. Thus we postulate that the dramatic titanate solvent effect is to form α and β $TiCl_3$ type active catalysts, and thus to orient and effect the polymerization of the isoprene in the conformation corresponding to the Ti–Ti distance.

SUMMARY

The course of the 1,4-polymerization of isoprene by the i-$C_4H_9AlCl_2$–$(RO)_4Ti$ catalyst system is dependent on the structure of the titanate and on the solvent of polymerization. ESR studies show the titanate to be a precursor for the formation of α and β $TiCl_3$ type complex. Primary titanates in either alipatic or aromatic solvents give β-$TiCl_3$ type while secondary titanates give the β-$TiCl_3$ type only in aliphatic solvents. Tertiary titanates give the α-$TiCl_3$ type in both aliphatic and aromatic solvents, but secondary titanates give the α-$TiCl_3$ type in aromatic solvents. Conditions leading to the α-$TiCl_3$ type give *trans*-1,4-polyisoprene, and conditions leading to the β-$TiCl_3$ type give *cis*-1,4-polyisoprene. All experimental observations are consistant with this mechanism. The α-$TiCl_3$ type catalyst species has an ESR signal with a g value of 1.940 $\pm$0.003. The β-$TiCl_3$ type catalyst species does not have an ESR signal, due to spin pairing. However, the precursor to β-$TiCl_3$ type species is paramagnetic and has a g value of 1.930 $\pm$ 0.003.

References

1. W. Cooper and T. Vaughan, in *Progress in Polymer Science*, Vol. I, A. D. Jenkins, Ed., Pergamon Press, London, 1967, p. 128.
2. G. Natta, *J. Polym. Sci.*, **48**, 219 (1960).
3. G. Natta, L. Porri, and A. Carbonaro, *Makromol. Chem.*, **77**, 126 (1964).
4. D. H. Dawes and C. A. Winkler, *J. Polym. Sci. A*, **2**, 3029 (1964).
5. G. Wilke, *Angew. Chem.*, **68**, 306 (1956).

6. G. Natta, L. Porri, A. Carbonaro, and G. Stoppa, *Makromol. Chem.*, **77**, 114 (1964).

7. W. Marconi, A. Mazzer, S. Cucinella, M. Cesari, and E. Pauliezzi, *J. Polym. Sci. A*, **3**, 123 (1965).

8. G. Natta, L. Porri, and S. Valenti, *Makromol. Chem.*, **67**, 225 (1963).

9. S. Mesono, Y. Uchida, and K. Yamada, *J. Polym. Sci.* **5B**, 401 (1967).

10. N. Yamazaki, K. Sasaki, T. Nishimura, and S. Kambara, paper presented at American Chemical Society Meeting, 1964; *Polym. Preprints*, **5**, 667 (1964).

11. S. Cucinella, A. Mazzer, W. Marconi, and C. Busetto, *J. Macromol. Sci.-Chem.*, **A4**, 1549 (1970).

12. A. Tkac, *Coll. Czech. Chem. Commun.*, **33**, 1629 (1968).

13. Y. Ono and T. Keii, *J. Polym. Sci. A-1*, **4**, 2441 (1966).

14. E. H. Adema, in *Macromolecular Chemistry, Prague* **1965** (*J. Polym. Sci. C*, **16**), O. Wichterle and B. Sedláček, Eds., Interscience, New York, 1968, p. 3643.

15. E. H. Adema, H. J. M. Bartelink, and J. Smidt, *Rec. Trav. Chem.*, **81**, 73 (1962).

16. E. H. Adema, H. J. M. Bartelink, and J. Smidt, *Rec. Trav. Chem.*, **80**, 173 (1961).

17. G. Henrici-Olive and S. Olive, in *Macromolecular Chemistry, Brussels-Louvain 1967* (*J. Polym. Sci. C*, **22**), G. Smets, Ed., Interscience, New York, 1969, p. 965.

18. G. Henrici-Olive and S. Olive, *Adv. Polym. Sci.*, **6**, 421 (1969).

19. H. Hirai, K. Hiraki, J. Noguchi, and S. Makrishima; *J. Polym. Sci. A-1*, **8**, 147 (1970).

20. H. Hirai, K. Hiraki, J. Noguchi, T. Inoue, and S. Makrishima, *J. Polym. Sci. A-1*, **8**, 2393 (1970).

21. K. Hiraki, T. Inoue, and H. Hirai, *J. Polym. Sci., A-1*, **8**, 2543 (1970).

22. H. L. Krauss, H. Huttmann, and V. Deffner, *Z. Anorg. and Allgem. Chem.*, **341**, 164 (1965).

23. J. Peyroche, Y. Girad, R. Laputte, and A. Guyot, *Makromol. Chem.*, **129**, 215 (1969).

24. D. C. Bradley, R. C. Mehrotra, and W. Wardlaw, *J. Chem. Soc.*, 4204 (52).

25. D. C. Bradley, in *Progress In Inorganic Chemistry*, Vol. II, F. A. Cotton, Ed., Interscience, New York, 1960.

26. S. E. Horne, Jr., C. F. Gibbs, J. H. Macey, and H. Tucker, *Kautschuk & Gummi*, **13**, WT336 (1960).

27. J. A. Yanko, *J. Polym. Sci.*, **13**, 576 (1958).

28. W. M. Saltman, *J. Polym. Sci. A*, **1**, 373 (63).

29. G. J. Van Amerongen, in *Advances in Chemistry*, Vol. 52, American Chemical Society, Washington, D.C. 1966, p. 136.

30. N. G. Gaylord, I. Kössler, B. Matyska, and K. Mach, *J. Polym. Sci. A-1*, **6**, 125 (1968).

Received July 2, 1971
Revised August 11, 1971

NOTES

Isolation and Identification of Oligomers Formed During Cationic Polymerization of Propylene Sulfide

Cationic polymerization of propylene sulfide (PS) under the influence of triethyl oxonium tetrafluoroborate (TEFB) or boron trifluoride etherate in methylene chloride produces polymer together with low molecular weight substances.

Isolation and Purification of Oligomers

As shown in Figure 1, gel-permeation chromatography (GPC) of a polymerizing mixture, permitted separation of polymer (PPS), oligomers (O_1 and O_2), monomer (PS), and solvent (CH_2Cl_2). The changes in concentration of the oligomers in function of time were determined with biphenyl (BP) as an internal standard. Figure 1 shows chromatograms obtained 2 hr and 8 days after initiation. From the areas of the peaks of oligomers O_1 and O_2 and of BP (ratios determined with a Du Pont curve resolver), the results shown in Figure 2 were obtained. The concentration of oligomer O_2 continues to increase for 5 days (at 20°C) and then reaches a constant value.

The polymerization of PS was complete after about 12 hr. This proves that the oligomers are not formed directly from the monomer but by degradation of the polymer. After 5 days the reaction mixture consisted of 30% oligomer and 70% polymer (initial monomer concentration 2.0 mole/l.; TEFB concentration, 0.05 mole/l). Analogous results were obtained when the polymerization was initiated with boron trifluoride etherate.

Structure of the Oligomers

The oligomers could be separated completely by gas chromatography (Fig. 3). By coupling of the gas chromatograph to an MS-9 mass spectrometer,[1] the mass spectra of the two substances were obtained. From the m/e values of the parent ions it follows that the major product (peak A in Fig. 3) has the formula $C_{12}H_{24}S_4$ and the other product (peak B in Fig. 3) is $C_{15}H_{30}S_5$. The oligomers thus are tetramers and pentamers of PS.

Small amounts of pure oligomers were obtained by preparative-scale gas chromatography. Samples of the thus obtained products were analyzed by GPC. This showed that peak A in the gas chromatogram (tetramer) corresponds to oligomer O_2 and peak B (pentamer) to oligomer O_1.

Figure 4 shows the NMR spectra of the tetramer and the pentamer. These NMR spectra are consistent with cyclic structures. The tetramer is a crystalline substance with m.p. 135°C; the pentamer is a viscous oil.

The sharp melting point and the uncomplicated signal of the methyl protons in the NMR spectrum of the tetramer indicate that it is a single substance. This is rather surprising, because theoretically many isomeric forms of the tetramer are possible. If all four PS units are linked to each other head-to-tail, four different geometrical isomers are possible: $\overbrace{\text{RRRR}}$ (all-*cis*), $\overbrace{\text{RSSS}}$ (*trans-cis-cis-trans*), $\overbrace{\text{RSRS}}$ (all-*trans*) and $\overbrace{\text{RRSS}}$ (*cis-trans-cis-trans*). If also head-to-head linkages are possible, 23 different geometrical isomers of $(PS)_4$ are possible.[2] More details about the structure could not be obtained at this moment because of the complexity of the NMR spectrum in the $\delta = 2$–3 region.

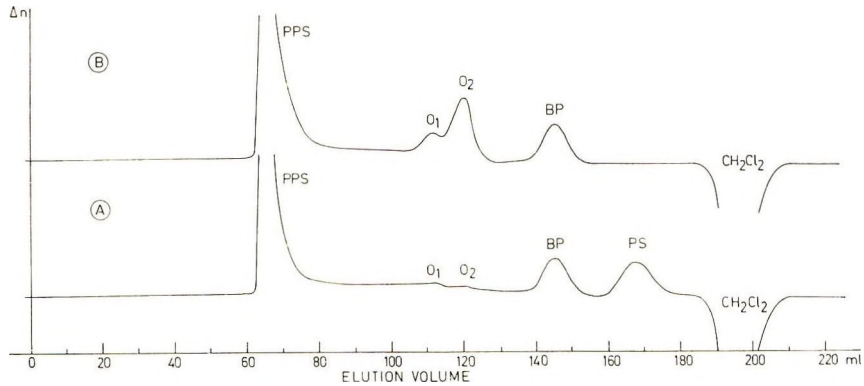

Fig. 1. GPC analysis of polymerizing mixtures of PS in CH_2Cl_2 under the influence of TEFB (*A*) 2 hr and (*B*) 8 days after initiation, on a Sephadex LH-20 column of 58 cm length, diameter 2.4 cm; chloroform as eluent, 1.2 ml/min; detector: Waters Associates differential refractometer, Model 403.

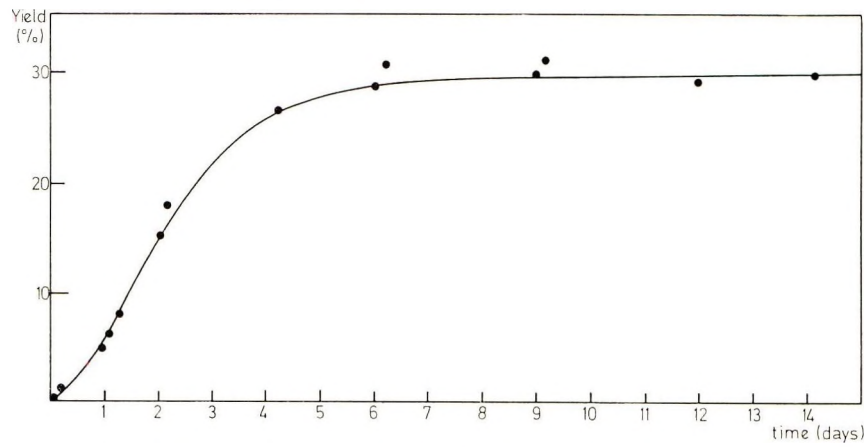

Fig. 2. Concentration of oligomer O_2 (tetramer) in the reaction mixture as a function of time at 20°C.

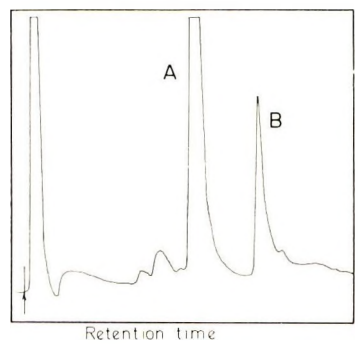

Fig. 3. Separation of tetramer (peak A) and pentamer (peak B) by gas chromatography on a 1.5 m column; stationary phase 0.2% SE.30 on Chromosorb P 90–100; temperature programmed from 60 to 200°C at 6°C/min.

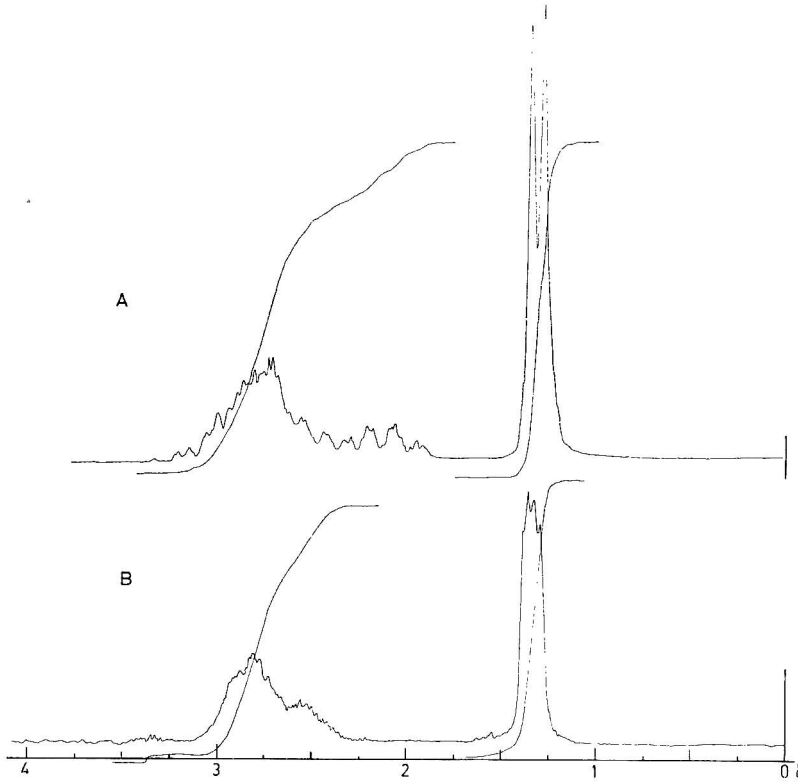

Fig. 4. NMR spectra of tetramer (A) and of pentamer (B) in carbon tetrachloride (Varian HA 100-Mcps apparatus).

The formation of twelve-membered rings during the cationic polymerization of three-membered ring heterocyclic compounds has already been mentioned in the cases of propylene oxide[2] and of 1-benzyl-2-ethyl aziridine.[3] However, in many other cases the formation of cyclic dimers has been reported.[4–7] In the case of PS the dimer would be 2,5- or 2,6-dimethyl-1,3-dithiane. In order to be certain that no dimers are formed in this polymerization, a mixture of these substances has been synthesized from 1,2-dibromopropane and propane-1,2-dithiol. Comparison of the GPC chromatogram of the dimers with that of the polymerization mixture proved that no dimers are formed during or after polymerization of PS.

Mechanism of Formation of the Oligomers

It is believed that cationic polymerization of PS occurs via cyclic sulfonium ions [eq. (1)].

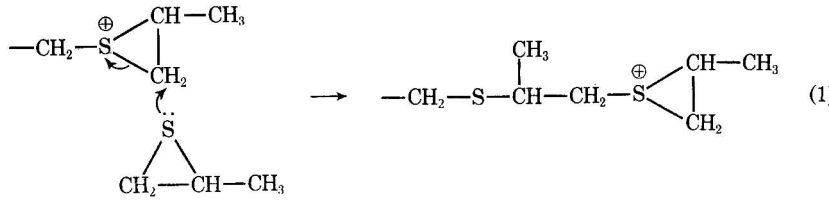

(1)

Most probably branched tertiary sulfonium ions are formed by attack of a sulfur atom of poly-PS on a growing chain as in the case of poly(3,3-dimethyl)thietane.[8] Formation of a macrocyclic sulfonium ion occurs when a sulfonium ion (three-membered ring or branched) is attacked by a sulfur atom of its own chain [eq. (2)].

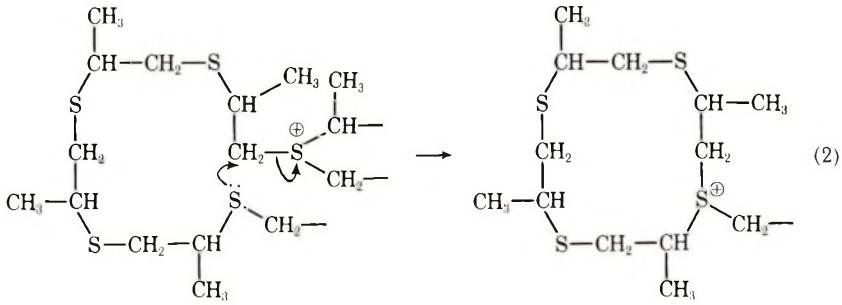

(2)

Attack of any other sulfur atom on the exocyclic carbon atom of this sulfonium ion results in the formation of cyclic oligomer and another sulfonium ion. This process can be repeated several times for each sulfonium ion present in solution even when all monomer has polymerized.

References

1. K. Van Cauwenberghe, M. Vandewalle, and M. Verzele, *J. Gaschromatog.*, **6**, 72 (1968).

2. R. J. Katnik and J. Schaefer, *J. Org. Chem.*, **33**, 384 (1968).

3. S. Tsuboyama, K. Tsuboyama, I. Higashi, and M. Yanagita, *Tetrahedron Letters*, **16**, 1367 (1970).

4. D. J. Worsfold and A. M. Eastham, *J. Amer. Chem. Soc.*, **79**, 900 (1957).

5. A. Noshay and C. C. Price, *J. Polym. Sci.*, **54**, 533 (1961).

6. R. O. Colclough, G. Gee, W. C. E. Higginson, J. B. Jackson, and M. Litt; *J. Polym. Sci.*, **34**, 171 (1959).

7. W. M. Pasica, *J. Polym. Sci., A*, **3**, 4287 (1965).

8. E. J. Goethals and W. Drijvers, *Makromol. Chem.*, **136**, 73 (1970).

J. L. Lambert
D. van Ooteghem
E. J. Goethals

Laboratory of Organic Chemistry
University of Ghent
Ghent, Belgium

Received April 22, 1971
Revised May 24, 1971

Acidity and Stability of Sulfonyl Carbamates and Ureas

Previously we reported that *p*-toluenesulfonyl isocyanate (p-TSI) readily reacts with polymeric alcohols to produce polymers containing the sulfonyl carbamate linkage. We also reported that the sulfonyl carbamate group possessed an acidity comparable to acetic acid and that the anion was stable to excess alkali for months; thus the chemistry of this group would seem to be quite analogous to that of a carboxyl group.[1,2] Recently some other workers have reported some very interesting results on derivatizing cellulose with p-TSI to high degrees of substitution, thereby creating ion-exchange resins of high capacity.[3] We have also done some further work with p-TSI and would like to comment on some statements in the above paper and amplify them with some of our more recent, unpublished results.

In our original work we reported the pK_a of *O*-ethyl-*N*-*p*-tosyl carbamate (I) to be 3.7. We became curious as to whether the corresponding ureas would also be relatively strong acids and prepared several model compounds. Because many of the compounds prepared did not dissolve in water, we chose a mixed solvent (1:1 water–ethanol) system and measured the acidities by titration with alkali. The compounds were the reaction products from p-TSI with ethanol, phenol, isobutylamine and aniline. For internal references benzoic acid and phenol were also measured in the same mixed solvent system since the addition of ethanol to water depresses the acidity of most compounds (a higher apparent pK_a). It will be seen from Table I that the carbamates are stronger acids than the ureas and that the aromatic ring has an effect in increasing the acidity in either the carbamate or urea series.

In our original work we found the anions of the carbamates to be stable. In the more recent work,[3] we are led to believe that the carbamate linkages are stable to acids. During the preparation of our model compounds, however, we noticed that when water was used to recrystallize the ethanol derivative of p-TSI, the recovered product was *p*-toluenesulfonamide. We found that when the carbamate is dissolved in hot water, carbon dioxide is quantitatively evolved leaving the sulfonamide fragment in solution. The other compounds including the ureas also behaved in a similar manner. Although sulfonyl ureas are frequently purified by recrystallization from ethanol–water,[4] we find that a hydrolytic decomposition does occur only at a much slower rate. Because of low water solubility, the isobutylamine derivative took several days to decompose in hot water, whereas the ethanol derivative will rapidly decompose in several hours. Recently it has been reported that tertiary alcohol derivatives of p-TSI are thermally unstable and decompose smoothly at relatively low temperatures to give *p*-toluenesulfonamide, carbon dioxide, and olefin.[5] It has also been reported that this thermal instability should not be a disadvantage with most polymeric substrates where primary or secondary alcohols predominate.[6] We feel that we must add a further caution. Although the compounds are novel acids with stable anions, they are unstable in water over periods of time, hydrolyzing to sulfonamides. Although ordinary carbamate linkages are stable to acidic conditions, these acidic sulfonyl carbamates and ureas are capable of catalyzing their own hydrolyses. Although in the case of a polymer which may not be soluble in water, the rate of hydrolysis may be slow, we feel we must point out that hydrolysis is a definite possibility for any polymeric application where stability towards any type of high humidity or weathering are considerations.

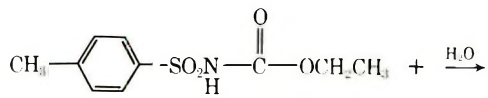

I

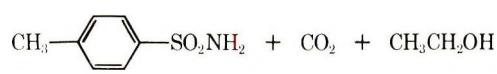

TABLE I

Compound	pK_a (1:1 water–ethanol)	Analysis								Melting point, °C	IR (C = O), cm^{-1}
		Calcd				Found					
		C, %	H, %	N, %	S, %	C, %	H, %	N, %	S, %		
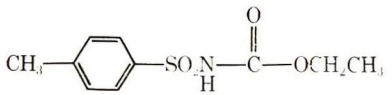	5.6	49.4	5.4	5.8	13.2	49.2	5.4	5.8	12.9	80–81	1750
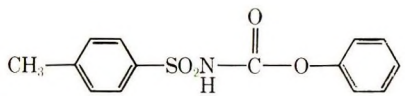	4.5	57.8	4.5	4.8	11.0	57.6	4.7	5.0	11.3	112–117	1765
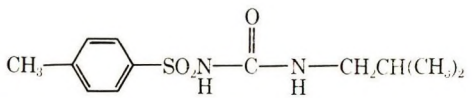	7.2	53.3	6.7	10.4	11.9	53.2	6.8	10.4	12.1	172–176	1660
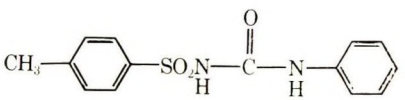	5.9	57.9	4.8	9.7	11.0	57.8	5.0	9.5	10.8	170–171	1655
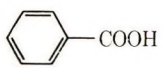	5.6				—					—	—
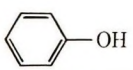	11.1				—					—	—

Experimental

The model compounds were prepared by allowing 0.13 mole of either alcohol or amine to react with 0.10 mole of p-TSI in 25 ml. of dry benzene. After 1 hr hexane was added, and the product precipitated. The material was collected and recrystallized from benzene-hexane. The pertinent analytical data appears in Table I.

The pK_a determinations were done by dissolving a weighed amount of the model compounds in 50% ethanol at room temperature. A few drops of 1.*N* acid or base were added and the mixture was quickly titrated potentiometrically with either standardized acid or base using a combination glass electrode. The pK_a was calculated from:

$$pK_a = \log (\text{concn}) + 2\ pH$$

The model compounds were heated in water on a steam cone. In all cases bubbles of gas were observed to form from the solid or in the case of a water soluble derivative such as the ethanol one, the solution formed bubbles. When the solutions were allowed to cool, a new compound was observed to crystallize with a loss of carbonyl absorption, mp 139°C, in all cases. The compound was shown to be *p*-toluenesulfonamide on the basis of identical infrared and NMR spectra with an authentic sample. In the case of the sulfonyl urea derived from isobutyl amine, again gas evolution was noted and *p*-toluenesulfonamide was recovered. Recently a report has appeared which discusses the instability of "tolbutamide" in organic solvents.[7] The above compound is the *n*-butylamine derivative of p-TSI and it was theorized that this compound undergoes thermal dissociation to p-TSI and *n*-butylamine. We feel that in the case of the hydrolysis reaction of sulfonyl ureas it is not necessary to postulate this mechanism. For example, our isobutylamine derivative has been characterized by thermogravimetric and differential thermal analyses (TGA, DTA). The DTA curve of the sample indicates a crystalline melt at 177°C, followed by decomposition beginning at 183°C. TGA shows no significant weight loss prior to decomposition. For DTA, a sample was heated in water in a sealed aluminum cell. Hydrolysis of the sample begins at 60°C. Thus it is not necessary to postulate thermal dissociation followed by hydrolysis of p-TSI, but it is also likely that a direct hydrolysis of the ureas can occur. More detailed work must be done to settle this point.

References

1. L. D. Taylor, M. Pluhar, and L. E. Rubin, *J. Polym. Sci. B*, **5**, 77 (1967).
2. L. D. Taylor, U. S. Pat. 3,422,075 (1969).
3. R. W. Rousseau, C. D. Callihan, and W. H. Daly, *Macromolecules*, **2**, 502 (1969).
4. F. J. Marshall and M. V. Sigal, *J. Org. Chem.*, **23**, 927 (1958).
5. L. C. Roach and W. H. Daly, *Chem. Commun.*, **1970**, 606.
6. W. H. Daly, paper presented at American Chemical Society Meeting, Los Angeles, 1971, *Polym. Preprints*, **12**, 28 (1971).
7. F. Bottari, M. Mannelli, and M. F. Saettone, *J. Pharm. Soc.*, **59**, 1663 (1970).

Lloyd D. Taylor
Russell J. MacDonald
Leon E. Rubin

Research Laboratories
Polaroid Corporation
Cambridge, Massachusetts 02139

Received April 7, 1971
Revised June 4, 1971

Effect of Oxygen on Radical Formation in Polyethylene by Ultraviolet Irradiation

Electron spin resonance studies of polyethylene irradiated with ultraviolet light have been reported by several authors.[1-7] The spectrum observed at −196°C immediately after irradiation was believed to be mainly a six-line spectrum and was attributed to alkyl radicals, $-CH_2-\dot{C}H-CH_2-$.[1-4] Recently we reported that the observed spectrum had an eight-line component[5] and that radical formation in polyethylene by ultraviolet irradiation at −196°C was initiated by the Norrish type I reaction of carbonyl groups contained in the polymer.[8] For polypropylene we also reported the finding that the radical yield after photolysis ($\lambda > \sim 200$ mμ) in the oxygen atmosphere was larger than that in the nitrogen atmosphere and tentatively attributed to participation of the charge transfer complexes of polypropylene with oxygen molecules in absorption of ultraviolet light.[9] In this connection we want to report here an analogous finding in the photolysis ($\lambda > \sim 200$ mμ) of polyethylene. As for the effect of oxygen on radical formation in polymers, Milinchuk reported alkyl radical formation in the photolysis of O_2/hydrogen-containing polymers at $\lambda > 300$ mμ and participation of an active form of oxygen was suggested.[10]

Experimental

High-density polyethylene (Sumitomo Chemical Co., Ltd.) was purified by dissolving it in boiling xylene, precipitating in cold methanol, and washing with *n*-hexane. The purified sample was pressed at 150°C between stainless-steel frames to give rod-shaped specimens, 2 mm², which were immersed in *n*-hexane for over 2 days. The samples were evacuated to 10^{-6} mm Hg in the ESR sample tube, and subsequently nitrogen or oxygen gas was introduced at 1 atm. Thin films for optical measurements were made similarly by pressing polyethylene between aluminum foils and immersed in *n*-hexane. The films were evacuated to 10^{-6} mm Hg in a 1 cm² optical cell, and then nitrogen or oxygen gas was introduced at 1 atm.

The procedures of ultraviolet irradiation have been described elsewhere,[5] and a series of color glass filters was applied to control the wavelength of the incident light. ESR spectra were recorded at −196°C with an X-band spectrometer with 100 kc field modulation (Japan Electron Optics Lab. Co., model JES, 3BS-X). Ultraviolet absorption spectra were recorded at room temperature with a Perkin-Elmer 450 spectrophotometer with nitrogen replacement.

Result and Discussion

Polyethylene is known to show an ESR spectrum as shown in Figure 1 after ultraviolet irradiation at −196°C both in nitrogen and in oxygen atmospheres.[5] This spectrum can be attributed to free radicals $-CH_2-CH_2\cdot$ and $-CH_2-\dot{C}H-CH_2-$,[8] although $-CH_2-\dot{C}(CH_3)-CH_2-$ radical was supposed initially instead of the former radical.[5] The primary photochemical process for radical formation is the Norrish type 1 reaction of carbonyl groups in the polymer, and these radicals are produced by the reactions (1) and (2):[8]

$$-CH_2\underset{\underset{O}{\|}}{C}CH_2- \xrightarrow{h\nu} -CH_2\cdot + -CH_2\underset{\underset{O}{\|}}{C}\cdot \xrightarrow{h\nu} -CH_2\cdot + CO \qquad (1)$$

$$-CH_2\cdot + -CH_2CH_2CH_2- \rightarrow -CH_3 + -CH_2\dot{C}HCH_2- \qquad (2)$$

A noticeable point is a difference in radical yields for photolysis in the nitrogen and in the oxygen atmospheres. As shown in Figure 2, radical yield in an oxygen atmosphere was larger than that in a nitrogen atmosphere at all the wavelengths studied here. The following mechanisms could be supposed for the explanation of this higher radical

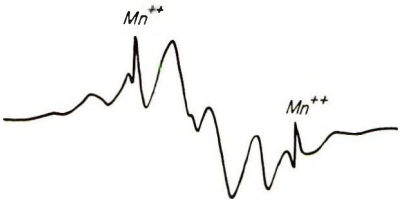

Fig. 1. ESR spectrum of high-density polyethylene irradiated by ultraviolet light at −196°C in nitrogen or in oxygen atmospheres. The separation between two Mn^{++} peaks is 86.7 gauss.

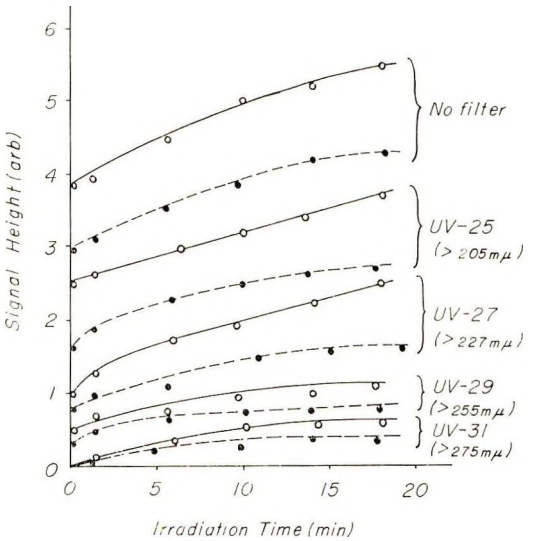

Fig. 2. Dependence of signal intensity of free radicals in polyethylene on irradiation time: Signal intensities obtained after irradiation at −196°C (——) in oxygen and (- -) in nitrogen atmospheres. The irradiations were carried out successively from with the light of longer wavelength to with the light of shorter wavelength by using color glass filters.

yield in the oxygen atmosphere: (1) chain reactions of oxidation;[11] (2) participation of excited oxygen molecules in radical formation;[10,12,13] (3) participation of charge transfer complexes of polyethylene with oxygen molecules in absorption of light.

In the case of irradiation at −196°C, however, the first two possibilities could easily be excluded, since the identical spectral shape was observed after photolysis of polyethylene at −196°C both in the nitrogen and in the oxygen atmospheres.

In order to examine the third possibility, the formation of the charge transfer complexes of polyethylene with oxygen molecules should be recognized. Therefore the ultraviolet absorption spectra of a polyethylene film (0.20 mm) were measured both in nitrogen and in oxygen atmospheres. The obtained spectra are shown in Figure 3.

The increase of absorbance with decreasing wavelength was observed in nitrogen, which could be attributed to surface or Rayleigh scattering of the sample.[14] Broad absorption was observed between 400 and 230 mμ which could not be removed by *n*-hexane immersion. This absorption might be attributed to some carbonyl groups[14] contained in the polymer as irregular bonds which were detected also by infrared spec-

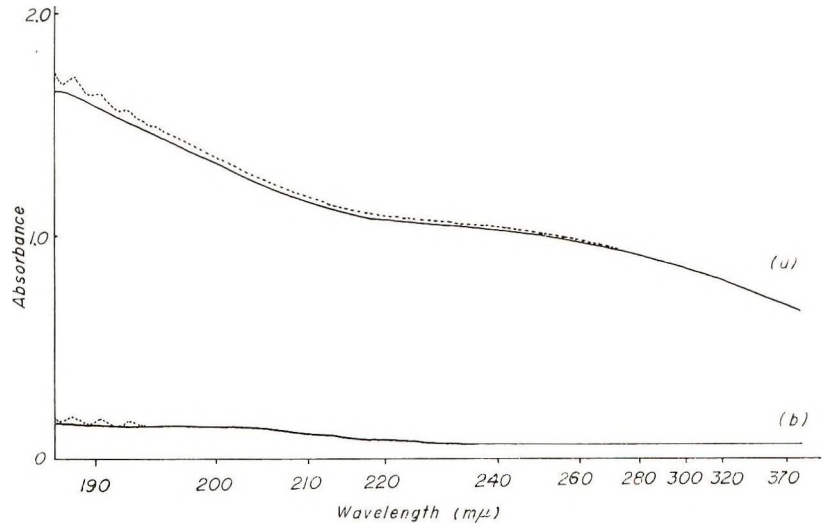

Fig. 3. Ultraviolet absorption spectra of polyethylene film (0.20 mm): (*a*) polyethylene film in the 1 cm² optical cell; (*b*) only the optical cell (control experiment). Absorption spectra shown were observed when (——) nitrogen or (- -) oxygen gas was introduced in the cell. Vibrational structures observed near 190 mμ seem to be due to a part of Schumann-Runge bands of gaseous oxygen molecules in the cell.

troscopy. It is clear that the absorbance in the oxygen atmosphere is greater than that in the nitrogen atmosphere apparently at the wavelengths shorter than about 270 mμ. Such a large difference can not be expected from the difference in extent of surface or Rayleigh scattering of the sample in the nitrogen and oxygen atmospheres, if any. Oxygen molecules themselves have no such a large absorption in the near ultraviolet region as is obvious from the control experiment, although the Herzberg forbidden continuum has a very low absorption coefficient in this region.[15] The oxygen-perturbed $S \rightarrow T$ transition is unlikely to contribute so much to the ultraviolet absorption of the alkane–oxygen systems.[16] Therefore, this extra absorption can be ascribed mainly to the charge transfer complexes of polyethylene with oxygen. The complex formation of paraffinic parts of polyethylene with oxygen molecules is expected, and similar absorption spectra have been reported for *n*-hexane–oxygen and *n*-heptane–oxygen systems.[17] Some complex formation with unsaturating parts in polyethylene is also expected,[18] but not with carbonyl groups, since no ketones make the charge transfer complexes with oxygen molecules.[19]

From these considerations, the increased radical formation observed for photolysis in the oxygen atmosphere must be attributed to extra absorption of the energy of light by the charge transfer complexes.

The possible mechanisms for participation of the charge transfer complexes in radical formation are as follows: (1) the complexes absorb the energy of light and transfer to other part of the polymer to produce free radicals; (2) the complexes themselves make free radicals through the excited states by ultraviolet irradiation.

The second possibility has been postulated for some kinds of radical formation reactions[20,21] and may not be excluded, but in the present case no definite evidence was obtained for radical formation from the charge-transfer complexes themselves. The identity of the ESR spectra at −196°C in the nitrogen and oxygen atmospheres rather supports the first possibility. It is plausible that the energy of light absorbed by the charge transfer complexes is transferred presumably through the polymer chain[22] to

carbonyl groups which are supposed to initiate photo-degradation reactions.[8] Very recently radical formation in the photolysis of O_2/3 methylpentane glasses at $\lambda > 190$ mμ was reported[23] and suggested is the possibility of energy transfer from the excited ^3CT state to a dissociative level of an alkane triplet state with the O_2 returning to its triplet ground state. This mechanism might be operative somewhat in the present system.

The authors wish to express their gratitude to Drs. S. Kodama, T. Nishikida, and A. Segawa for their kind guidance and encouragement, and to Dr. Y. Kubota for his continued interest and helpful discussions. Thanks are also due to Dr. T. Takeshita for his helpful discussions.

References

1. A. Charlesby and R. H. Partridge, *Proc. Roy. Soc.* (London), **A283,** 320 (1965).
2. B. Rånby and H. Yoshida, in *Perspectives in Polymer Science* (*J. Polym. Sci. C*, **12**), E. S. Proskauer, E. H. Immergut, and C. G. Overberger, Eds., Interscience, New York, 1966, p. 263.
3. H. L. Browning, Jr., H. D. Ackermann, and H. W. Patton, *J. Polym. Sci., A-1,* **4,** 1433 (1966).
4. B. Rånby and P. Carstensen, *Advan. Chem. Ser.*, **66,** 256 (1967).
5. K. Tsuji and T. Seiki, *J. Polym. Sci. B,* **7,** 839 (1969).
6. Y. Hama, Y. Furui, K. Hosono, and K. Shinohara, *Repts. Progr. Polym. Phys. Japan,* **12,** 481 (1969).
7. K. Tsuji and T. Seiki, *Repts. Progr. Polym. Phys. Japan,* **13,** 507 (1970).
8. K. Tsuji and T. Seiki, *Polym. J.*, **2,** in press.
9. K. Tsuji and T. Seiki, *J. Polym. Sci. B,* **8,** 817 (1970).
10. V. K. Milinchuk, *Vysokomol. Soedin.*, **7,** 1293 (1965).
11. T. Kawashima, M. Nakamura, S. Shimada, H. Kashiwabara, and J. Sohma, *Repts. Progr. Polym. Phys. Japan,* **12,** 469 (1969).
12. A. M. Trozzolo and F. H. Winslow, *Macromolecules,* **1,** 98 (1968).
13. D. R. Kearns and A. U. Khan, *Photochem. Photobiol.*, **10,** 193 (1969).
14. R. H. Partridge, *J. Chem. Phys.*, **45,** 1679 (1966).
15. R. M. Langer, *Phys. Rev.*, **85,** 740 (1952).
16. J. C. W. Chien, *J. Phys. Chem.*, **69,** 4317 (1965).
17. A. U. Munk and J. F. Scott, *Nature,* **177,** 587 (1956).
18. H. Tsubomura and R. S. Mulliken, *J. Amer. Chem. Soc.*, **82,** 5966 (1960).
19. H. Tsubomura and M. Hori, *J. Syn. Org. Chem. Japan,* **26,** 929 (1968).
20. R. L. Ward, *J. Chem. Phys.*, **38,** 2588 (1963).
21. G. B. Sergeev and Chén Yu-Kún, *Dokl. Akad. Nauk SSSR,* **169,** 1354 (1966).
22. R. B. Fox and R. F. Cozzens, *Macromolecules,* **2,** 181 (1969).
23. J. K. Roy and P. K. Ludwig, *J. Chem. Phys.*, **53,** 843 (1970).

Kozo Tsuji
Toshifumi Seiki

Central Research Laboratory
Sumitomo Chemical Co., Ltd.
Takatsuki, Osaka, Japan

Received May 3, 1971
Revised July 6, 1971

Preparation and Reactions of Lithiated Poly(2,6-diphenyl-1,4-phenylene ether)

INTRODUCTION

The direct metallation of poly(2,6-dimethyl-1,4-phenylene ether)[1] (II) and the use of the metallated polymer for the controlled synthesis of graft copolymers has recently been disclosed.[2,3] This paper gives details of corresponding reactions with poly(2,6-diphenyl-1,4-phenylene ether) (I).

EXPERIMENTAL

Materials

Poly(2,6-diphenyl-1,4-phenylene ether) was obtained from General Electric Chemical Development Operation, Pittsfield, Mass. It was prepared by the oxidative coupling of 2,6-diphenylphenol[4] and had $[\eta]^{30}_{CHCl_3} = 0.62$ dl/g. Other materials have been previously described.[1-3]

Reactions

Procedures previously described for polymer metallation[1] and graft copolymer synthesis were employed.[2,3] To prevent the formation of vinyl homopolymers, after addition of butyllithium to a solution of II in THF, the lithiated polymer was either left 20 hr at room temperature or refluxed for 30 min before addition of vinyl monomer.

RESULTS AND DISCUSSION

Polymer Metallation

Addition of butyllithium to a 2% solution of I in THF resulted in the immediate formation of a pale brown color which slowly deepened and became progressively more blue until after one hour the solution was light purple. No precipitation of metallated polymer occurred as it had with II.[1] After varying times, the reaction was terminated with trimethylchlorosilane and precipitated into methanol containing a trace of pyridine or a mixture of 75% acetone/25% water.

The NMR spectrum of I shows two well separated aromatic absorptions at 2.8 and 3.7 τ corresponding to substituent phenyl (A) and backbone phenyl (B), respectively, where the ratio of areas B/A has the expected value 0.2. Trimethylsilyl substitution results in a single additional absorption at 10.4 τ and slightly lower values for B/A. From the area of the 10.4 τ peak the fraction of substituted polymer units was calculated and used to obtain a value of B/A assuming solely backbone substitution. These values agreed reasonably well with the ratios of B/A found (Table I). The assumption that metallation occurs solely on the polymer backbone is supported by the single trimethylsilyl absorption and its high value, attributed to shielding by σ-phenyl.

The amount of metallation found was significantly lower than was the case for II and the values were not improved by the removal of traces of quinone from I by various methods of purification. The low yields of lithium found on the polymer were attributed instead to the lower reactivity of I compared with II, causing a greater loss of butyllithium by reaction with tetrahydrofuran. A study of the rate of the latter reaction was consistent with this conclusion.

Gel-permeation chromatography showed little chain scission in the recovered polymers. For times of metallation up to 60 min, the molecular weight remained unchanged at 150,000. After 7 hr the value was 130,000 and after 48 hr 100,000.

TABLE I
Metallation of 2% I in THF with Butyllithium 25°C[a]

Expt. no.	Reaction time, min	Li on Polymer, %[b]	Ratio B/A[c]	
			Found	Theory[d]
1	0.25	0	0.20	0.20
2	1	3.1	0.20	0.20
3	2	6.6	0.21	0.19
4	4	11	0.21	0.19
5	20	15	0.17	0.18
6	60	16	0.17	0.18
7	180	17	0.16	0.18
8	420	18	0.17	0.18
9	960	17	0.14	0.18
10	2880	16	0.17	0.18
11	60	15.3	0.18	0.17
12	60	9.5	0.17	0.15

[a] BuLi/(I) [moles BuLi per oxygen of I] = 1 for experiments 1–10, BuLi/(I) = 2 for experiment II, and 5 for experiment 12.

[b] From NMR.

[c] Ratio of the areas of the NMR absorptions due to aromatic protons (B due to backbone, A, due to subsituent phenyls).

[d] Calculated assuming solely backbone metallation.

Reactions of the Metallated Polymer

Reaction of lithiated I with chlorosilanes was found to be considerably slower than with lithiated II. In the latter case reaction with trimethylchlorosilane or triethylchlorosilane was practically instantaneous. In the former case, however, reaction with trimethylchlorosilane took a few minutes and with triethylchlorosilane over an hour at room temperature. It seems reasonable to ascribe this difference to the greater steric hindrance of metallated I compared with metallated II.

The lower reactivity of metallated (I) compared with metallated II was also apparent in its reactions with vinyl monomers. Addition of styrene gave a noticeable exotherm, but the purple color of the metallated polymer was not completely replaced by the reddish color of the styryl anion unless a considerable excess of styrene was added a little at a time. The rate of initiation is apparently much slower than the rate of propagation. In experiment 13, the styrene was added rapidly, and there was little change in the purple color of the solution, even after several hours. In experiment 14, the styrene was added slowly (over 4 hr) and gave a much more significant change in color, suggesting reaction with a greater fraction of the lithiated sites on I. This was confirmed by examination of the NMR spectra of polymers from experiments 13 and 14 after terminating the reaction with trimethylchlorosilane. In the former case the $SiMe_3$ absorption occurred predominantly at 10.4 τ corresponding to silicon on (I) while the latter gave an absorption largely at 10.1–10.3 τ corresponding to $SiMe_3$ on polystyrene.[2] 1,1-Diphenylethylene reacted extremely slowly with the lithiated polymer. Both this and the reaction of styrene were greatly increased in rate by the addition of hexamethylphosphoramide. However this reagent appeared to affect the rate of polymerization as much, or more, than the rate of initiation since it did not help in increasing the fraction of lithiated sites on I which reacted with styrene. It also gave rise to some crosslinking. Methyl methacrylate reacted rapidly with lithiated I in THF even at −70°C, completely discharging the purple color. Crosslinking was not a problem as it was for the reaction of

methyl methacrylate with lithiated II. Thus use of 1,1-diphenylethylene was unnecessary.[2]

Gel-permeation chromatography showed the expected increase in molecular weight for the graft copolymers over that for the original I (Table II). Homopolymerization of the vinyl monomers could lead to molecular weight fractions lower than that for I, but none were found. Extraction of the polystyrene–I graft with cyclohexane gave no styrene homopolymer. Extraction of the poly(methyl methacrylate)–I graft with acetone gave no poly(methyl methacrylate), but there was some fractionation. Thus after 50% extraction, the fraction of poly(methyl methacrylate) had increased from 78 to 82% in the extracted material. These results are similar to those found for II.[3]

TABLE II
Styrene and Methyl Methacrylate Graft Polymerizations on Lithiated I in THF

Expt. no.	Monomer	Ratio monomer/I[a] Added	Ratio monomer/I[a] Found	Yield of graft, %	Molecular weight[b]
13	Styrene	4.8	4.2[c]	60	$\sim 10^6$
14	Styrene	6.4	7.4[c] 7.5[d]	90	$\sim 10^6$
15	Methyl methacrylate	4.5	3.3[c]	80	3×10^5
16	Methyl methacrylate[e]	4.5	3.5[c]	90	2×10^5

[a] Moles/244 g I.

[b] Value corresponds to maximum of gel permeation chromatogram (to be compared with a value of 1.5×10^6 for I relative to polystyrene standards). Apparatus by Waters Associates, columns 10^6, 10^5, 10^4, 10^3, 10^2; solvent benzene at 55°C.

[c] By NMR.

[d] By infrared (polystyrene absorption 700 cm^{-1}, absorption of I at 1200 cm^{-1}).

[e] Reacted at −70°C.

Hexamethylcyclotrisiloxane, however, gave only homopolymer when reacted with lithiated I in THF. Presumably the lithium alkoxides formed by the reaction of butyllithium with THF are considerably more reactive than lithiated I for cyclic siloxane polymerization.

References

1. A. J. Chalk and A. S. Hay, *J. Polym. Sci. A-1*, **7**, 691 (1969).
2. A. J. Chalk and T. J. Hoogeboom, *J. Polym. Sci. A-1*, **7**, 1359 (1969).
3. A. J. Chalk and T. J. Hoogeboom, *J. Polym. Sci. A-1*, **7**, 2537 (1969).
4. D. M. White and H. J. Klopfer, *J. Polym. Sci. A-1*, **8**, 1427 (1970).

A. J. Chalk
T. J. Hoogeboom

General Electric Research and Development Center
Schenectady, New York 12301

Received June 29, 1971
Revised August 12, 1971

Polyimides: Poly[(2,5-dioxo-1,3-pyrrolidinediyl)dimethylene]

Recently, we reported on the synthesis and polymerization of 4-carboxy-2-piperidone.[1] On the basis of earlier studies on β-carboxymethyl caprolactam,[2] we concluded that the corresponding polymer was poly[(2,5-dioxo-1,3-pyrrolidinediyl) dimethylene] being characterized by a repeat unit of the structure I.

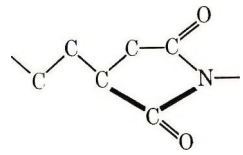

I

In this paper we shall present additional evidence for the proposed structure and report results on the characterization of this polymer.

Spectral Analyses

The infrared spectrum of a thin polymer film that had been cast from a trifluoroethanol solution resembled very much the one of the poly[(2,6-dioxo-1,4-piperidinediyl) trimethylene].[2] There were strong absorptions at 1705 and 1790 cm^{-1} which have been attributed respectively to asymmetrical and symmetrical carbonyl vibrations. Additional imide group related absorptions occurred at 1390 and 1150 cm^{-2}; they have been assigned to C-N-C antisymmetrical stretching and imide group vibrations, respectively. An absorption stemming from bending in the ring methylene group occurred at 1445 cm^{-1}, whereas absorption at 1495 and 2940 cm^{-1} are related to bending and vibrations of the methylene groups of the methylene moiety. A 15% solution of the polymer in formic acid was used for the NMR analysis. The spectrum showed a broad complex multiplet in the range 1.17–2.13 ppm, the area of which corresponded to two protons. This multiplet was assigned to the protons of the methylene group adjacent to the ring. Multiplets at 2.49 and 3.26 ppm have been assigned to the protons of the ring methylene group and the one adjacemt to the nitrogen atom, respectively. The peak related to the methine proton was obscured by these two broad multiplets, the total area of which corresponded to five protons.

Thermogravimetric and Differential Thermal Analyses

The thermal stability of the polymer was studied by determining the weight loss in both a nitrogen and air atmosphere employing a programmed heating rate of 10°C/min. The results are shown in Figure 1.

There is no apparent reason why the main decomposition of the higher molecular weight polymer should occur at slightly lower temperatures than that of the lower molecular weight material. It is possible that the particular higher molecular weight polymer sample had some structural imperfections. There appears, however, to be a definite effect of the molecular weight on the glass transition temperature as determined

TABLE I
Differential Thermal Analysis Data

	Glass transition, °C		Main decomposition temperature,
η_{sp}/c	a	b	°C
0.41	102	120	400
1.50	127	135	400

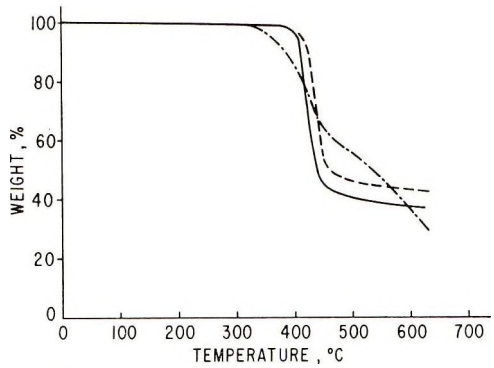

Figure 1. Thermal stability as a function of molecular weight and environment: (——) η_{sp}/c = 1.50, N_2; (·—·) η_{sp}/c = 1.50, air; (- -) η_{sp}/c = 0.41, N_2.

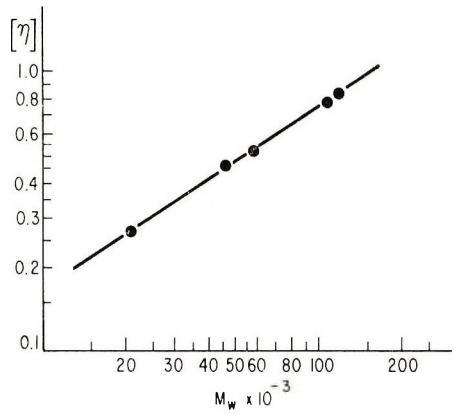

Fig. 2. Relationship between $[\eta]$ and M_w.

by DTA. The corresponding data are shown in Table I for both a low and a high molecular weight polymer. The T_g values in column a pertains to the original sample, whereas those in column b were obtained on a sample that had been heated to 250°C and then quenched before determining the transition temperature.

Viscosity–Molecular Weight Relations

Solutions of 0.52 g of polymer in 100 ml of either *m*-cresol or trifluoroethanol were used for determining the reduced viscosities. Identical values were obtained for both solvents. Intrinsic viscosities were determined on *m*-cresol solutions and evaluated by using the Huggins equation, $\eta_{sp}/c = [\eta] + k'[\eta]^2 c$. A value of 0.41 was determined for k'. Figure 2 shows a plot of $[\eta]$ versus the weight-average molecular weight $\bar{M}_w$ (obtained from light-scattering measurements).

The straight line in Figure 2 corresponds to the equation:

$$[\eta] = 4.3 \times 10^{-4} \bar{M}_w^{0.647}$$

Mechanical Properties

Tensile properties were determined according to ASTM D1708 on films obtained by compression molding. Polymer samples comprising the $\bar{M}_w$ range of 28000 to 210000

were tested at relative humidities (RH) of 0% and 50%. There was no significant effect on the humidity on tensile strength, elongation, and modulus (2% secant). Depending on the molecular weight, tensile strengths of 9000 to 16000 lb/in^2 at elongations of 3 to 10%, and moduli of 320000 to 520000 were obtained. Tear strengths (Graves, ASTM D1004) were at 1000 to 1500 lb/in.

The equilibrium moisture regain was not affected by the molecular weight of the sample; it was 3.6 at 50% and 11.3 at 100% RH. Permeabilities for oxygen and carbon dioxide were measured according to ASTM D1434; the respective values were 1.6×10^{-12} and 8.8×10^{-13}. Water vapor transmission was determined according to ASTM E-96; a value of 2.5 g/m^2-d was found.

References

1. H. K. Reimschuessel, K. P. Klein, and G. J. Schmitt, *Macromolecules*, **2**, 567 (1969).

2. H. K. Reimschuessel, L. G. Roldan, and J. P. Sibilia, *J. Polym. Sci. A-2*, **6**, 559 (1968).

H. K. Reimschuessel
K. P. Klein

Corporate Research Laboratory
Allied Chemical Corporation
Morristown, New Jersey 07960

Received July 7, 1971

Ziegler Polymerization of Olefins. X. Transition Metal Salts Having Four and More d-Electrons

Introduction

In the course of our investigations of Ziegler-type catalysts we examined a variety of transition metal salts as one of the components of this catalyst. This paper collects and describes our findings which were obtained when transition metal salts having four and more *d*-electrons were used, e.g., $CrCl_2$, $MnCl_2$, $Mn(AcAc)_2$, $FeCl_2$, $FeBr_2$, and $Fe(AcAc)_2$. These Cr(II), Mn(II), and Fe(II) salts contain four, five, and six *d*-electrons, respectively. $AlEt_3$ or $AlEt_2Cl$ was used as the metal alkyl component, and while some of these catalysts were used to polymerize propylene, most of the work was done with ethylene. Very little work has been reported on catalysts of this type.[1-5] Most of the studies of Ziegler catalysts were done with transition metal salts which had zero to three *d*-electrons, e.g., $ScCl_3$, $TiCl_3$, VCl_3, and $CrCl_3$.

Experimental Results and Discussion

The polymerization results are given in Tables I–IV, while Table V shows the emission and x-ray fluorescence analysis of $CrCl_2$ and $MnCl_2$.

Table I shows that catalysts based on $MnCl_2$ or Mn(acetylacetonate)$_2$ in combination with $AlEt_2Cl$ or a mixture of $AlEt_2Cl$ and $AlEt_3$ are active for polymerizing ethylene or propylene but only very sluggishly. To produce even these catalyst activities it was first necessary to either heat the $MnCl_2$ sample at about 250°C and 10^{-5} mm Hg or to ball-mill it for 15 hr. Even in a 120-hr run at ambient temperatures (expt. 1) only 1 g polyethylene was formed per gram $MnCl_2$, corresponding to an average rate of about 0.0003 g polymer per gram $MnCl_2$ per hour per atmosphere ethylene ($N = 0.0003$).

In comparison, $CrCl_2$ was considerably more active (Tables II and III). It is interesting that under our experimental conditions $CrCl_2$ was less active than $CrCl_3$ for polymerizing ethylene when combined with $AlEt_3$ (expts. 1 and 2, Table 2), but when combined with $AlEt_2Cl$ it was slightly more active (expts. 3 and 4, Table II). Propylene was also polymerized to isotactic polymer with the $CrCl_2$–$AlEt_2Cl$ system (expts. 5 and 6, Table II).

Table 4 demonstrates that $FeCl_2$, $FeBr_2$, and Fe(acetylacetonate)$_2$ ($FeAc_2$) can be made active for the polymerization of ethylene. However, the conversions at ambient temperatures were low, viz., only 13.7 g polyethylene was formed in a 68-hr polymerization in which 3.0 g $FeAc_2$ was used in combination with 40 mmole $AlEt_2Cl$ and at an initial ethylene pressure of 500 psig. It is interesting that all of the FeX_2-based catalysts were more active for the polymerization of ethylene than $MnCl_2$-based catalyst.

Table III demonstrates the improvements in activity of $CrCl_2$ which result from ball-milling. The "as-received" sample (expt. 1) produced a yield of 0.9 g polyethylene, while the ball-milled sample (expt. 2) resulted in a yield of 10.7 g polymer. If this ball-milled $CrCl_2$ sample was heated at 300°C for 20 hours in presence of hydrogen and subsequently ball-milled again (expt. 3) it became more active for polymerizing ethylene (17 g polymer was produced).

Also, higher conversions are obtained when the polymerizations are done in presence of 1/4-in. stainless steel balls and thus ensuring constant exposure of new catalyst surfaces (expts. 3 and 3a, Table II). In this experiment the 1/4-in. stainless steel balls became encapsulated in the polymer.

We propose that the higher activities resulting from ball-milling were due to an increase in the polymer of active centers. In our view the ball-milling (a) exposed fresh surfaces which were more easily alkylated by the metal alkyl to form active centers and (b) exposed an overall larger surface area of the transition metal salt, thereby allowing a higher concentration of active centers to be present during the initial stage of the

TABLE I
MnX_2 as Cocatalyst (X = Cl, acetylacetonate = Ac)[a]

Expt. no.	MnX_2 (2.0 g)	Pretreatment[b]	Metal alkyl: Amt, mmol	Metal alkyl: Type	Monomer: Type	Monomer: (Wt, g)	Polymerization: Reaction method	Polymerization: Duration, hr	Polymer yield, g
1	$MnCl_2$[c]	Heat for 15 hr at 250°C at 10^{-5} mm Hg	4.5	$AlEt_2Cl$	Ethylene	30 (600 psig)	B[d]	120	2.0
2	$MnCl_2$[c]	Heat for 15 hr at 250°C at 10^{-5} mm Hg	4.5	$AlEt_2Cl$	Propylene	28	A[d]	72	0.4
3	$MnCl_2$[c]	Ball-mill 15 hr in presence of 500 psig H_2	15	$AlEt_2Cl$	Ethylene	30 (600 psig)	B	24	0.1
4	$MnAc_2$[c]	Pulverize in mortar manually	60	$AlEt_2Cl$	Ethylene	30 (600 psig)	B	108	0.7
5	$MnAc_2$[c]	Pulverize in mortar manually	40 10	$AlEt_2Cl$ $AlEt_3$	Ethylene	30 (600 psig)	B	108	0.6
6	$MnAc_2$[c]	Pulverize in mortar manually	60	$AlEt_2Cl$	Ethylene	30 (600 psig)	B[d]	24	0.3

[a] The polymerizations were done in 100 ml heptane at ambient temperatures; see polymerization procedure for descriptions of methods A and B.
[b] The transfer of salts to the reactor was carried out in a dry box under a blanket of nitrogen.
[c] The $MnCl_2$ and $MnAc_2$ were purchased from A. D. Mackay and Chemical Procurement Laboratories, respectively.
[d] In these polymerizations 1/4-in. stainless steel balls were also placed in the reactor. The intent was to form fresh surfaces by ball-milling of the catalyst particles during the polymerization.

TABLE II
$CrCl_2$- and $CrCl_3$-Based Catalysts[a]

Expt. no.	Chromium salt[b]	Weight used, g	Pretreatment of Cr Salt Before Use	Polymerization Data: Alkyl	Monomer: Type	Monomer: Wt, g	Reaction method	Time, hr	Temp, °C	Polymer yield, g
1	$CrCl_2$	0.15	Ball-mill at ambient temperature for 20 hr under 1 atm N_2	$AlEt_3$	C_2H_4	32	B	2	30	4.2
2	$CrCl_3$	0.15	Ball-mill at ambient temperature for 20 hr under 1 atm N_2	$AlEt_3$	C_2H_4	32	B	2	c	>28
3	$CrCl_2$	0.15	Ball-mill at ambient temperature for 20 hr under 1 atm N_2	$AlEt_2Cl$	C_2H_4	32	B	4	30	2.6
3a	$CrCl_2$	0.15	Ball-mill at ambient temperature for 20 hr under 1 atm N_2	$AlEt_2Cl$	C_2H_4	32	B[d]	4	30	15.0
4	$CrCl_3$	0.15	Ball-mill at ambient temperature for 20 hr under 1 atm N_2	$AlEt_2Cl$	C_2H_4	32	B	4	30	1.2
5	$CrCl_2$	2.0	Ball-mill 20 hr in presence of 500 psig H_2 at ambient temperature	$AlEt_2Cl$	C_3H_6	29	A	16	50	0.8
6	$CrCl_2$	2.0	Used as received	$AlEt_2Cl$	C_3H_6	35	A[d]	64	30	1.8

[a] 150 ml Heptane was used as solvent.
[b] These were purchased from A. D. Mackay.
[c] The polymerization caused an exotherm to develop and the temperature rose to about 100°C.
[d] Stainless steel balls, 1/4 in., were also present, thus causing ball-milling of the catalyst during the polymerization.

polymerization. Table III shows that the increases in surface area of $CrCl_2$ from 0.85 to 7.65 to 10.7 m^2/g (due to treatments described) resulted in yields of 0.9 to 10.7 to 17 g polyethylene, respectively.

Admittedly, site counting findings would have been more definitive, but this was not done.

We have also considered the possibility that the observed activity of $CrCl_2$ was due to higher valence state transition metal compounds present as impurities. Our experimental evidence argues against this view. Table III shows that the activity of $CrCl_2$ was not due to the presence of small amount of $CrCl_3$ impurity. It is seen from experiments 2 and 3 that polyethylene yield increased from 10.7 to 17 g even though the $CrCl_3$ content was decreased from 0.83 to 0.36%w by heating the $CrCl_2$ sample in the presence of hydrogen. The ball-milling step itself (compare expts. 1 and 2) caused only a 0.01% increase in $CrCl_3$ (within experimental error), while the polyethylene yield was increased from 0.9 to 10.7 g. Also, Table II shows that $CrCl_2$ in combination with $AlEt_2Cl$ is slightly more active than $CrCl_3$ (expts. 3 and 4); this could hardly be possible if the activity of $CrCl_2$ was entirely due to presence of $CrCl_3$ impurity.

The possibility that other impurity transition metal compounds are responsible for the observed catalyst activity in $CrCl_2$ or $MnCl_2$ does not seem probable in the light of Table V. For example, if the activity of $CrCl_2$ was due to the Mo salt impurity (0.03 wt-%) and if 1 out of 100 Mo atoms can be assumed to be active, then the formation of 4.2 g (exp. 1, Table II) would correspond to 10^7 g polyethylene per gram Mo, a value too high by a factor of about 10^4 or more than previously found for molybdenum compounds.

Discussion

Very little has been published on the activity of transition metal salts which have four or more *d*-electrons[1-5] and lanthanide salts[6,7]* as components of Ziegler-type catalysts for the polymerization of olefins. This is regrettable because any detailed mechanistic proposals which intend to describe the various features of the Ziegler-type catalysts have to stand the test of polymerization data involving a wide range of salts of known composition, site number, valence and crystal structure before they can be finally accepted.

The few patent examples that have been published indicated that the above transition metal and lanthanide metal salts lead to catalysts which had very low activities. For example, Ziegler found that only 0.013 g polyethylene was formed per hour per atmosphere ethylene per gram $MnCl_2$ at 100°C when $AlEt_2Cl$ was chosen as cocatalyst.[1] We found at ambient temperature an activity value of 0.0003 g polymer per hour per atmosphere ethylene per gram $MnCl_2$ for the same catalyst.

More active catalysts were reported when iron salts were used. For example, activity values in the range 0.02–0.75 g polymer per hour per atmosphere ethylene per g $FeCl_3$ were reported when the polymerizations were done at 70–100°C[1-3] and about 0.01 g polymer per hour per atmosphere ethylene per g $FeCl_2$ when the polymerizations were done at 110°C. The $FeCl_3$ and $CrCl_2$ were also reported to be active in Ziegler-type

* These two patents disclosed that high-density polyethylene was formed with catalysts consisting of $AlEt_3$ and $SmCl_2$, $SmCl_3$, $YbCl_2$ and $YbCl_3$[6] and that 83.5% isotactic polypropylene was formed in presence of $AlEt_3$ and $SmCl_3$.[7] To the best of our knowledge there exists only one other report that isotactic polypropylene was formed with nontransition metal based catalysts. Earlier, Hoeg reported that isotactic polypropylene was made with AlF_3 alone or when combined with a metal alkyl.[8] Interestingly, the activity of the $AlEt_3$–$SmCl_3$ catalyst for the isotactic polymerization of propylene was comparable to that found for the iron and chromium salts, e.g., about 0.16 g polymer was formed per hour per gram $SmCl_3$ per atmosphere propylene. The presence of transition metal salts as impurities in some of these catalysts may, however, account for the observed activities.

TABLE III
Relationship between Activity, Surface Area, and $CrCl_3$ in the $CrCl_2$-Based Catalysts[a]

Expt. no.	Treatment of $CrCl_2$	Surface area, m^2/g[b]	$CrCl_3$ impurity, wt-%[c]	Polymer formed per 0.3 g $CrCl_2$, g
1	None; used as received[d]	0.45	0.73	0.9
2	Sample above was ball-milled under a blanket of nitrogen in presence of 1/4 in. stainless steel balls during 20 hr at 30°C	7.65	0.83	10.7
3	Sample 2 was heated at 300°C for 20 hr while percolating hydrogen gas through it; it was again ball-milled at 30°C for 20 hr	10.7	0.36	17.0

[a] The polymerizations were done by method B, 150 ml heptane, 0.3 g $CrCl_2$, 7.5 mmole $AlEt_2Cl$ and 30 g ethylene were placed in the reactor. Polymerization occurred during 5 hours at 50°C.

[b] Determined by N_2 adsorption.

[c] These values were determined polarographically by Dr. D. Olsen of this laboratory.

[d] Purchased from A. D. Mackay.

catalysts by Natta and co-workers, but no detailed data were given.[4] We confirmed these findings in our laboratory with $FeCl_2$, $FeBr_2$, and Fe(acetylacetonate)$_2$ salts. We found approximate activities of about 0.0002 to 0.003 g polymer per hour per atmosphere ethylene per gram iron salt with these salts ($AlEt_2Cl$ cocatalyst) at ambient temperatures.

We found no examples of Ziegler-type catalysts based on $CrCl_2$. However, Grace workers have demonstrated that ball-milled $CrCl_2$ was active even in the absence of a metal alkyl when the polymerization of ethylene (30 atmospheres) was carried out at 140°C. Understandably, the activity value (N = 0.004) was low compared to that found by us at ambient temperatures when $AlEt_2Cl$ was also present (N = 0.56).

Our findings indicate the following order of activity when these salts are combined with $AlEt_2Cl$: $CrCl_2 > FeX_2$ (X = Cl, Br or Ac) > MnX_2 (X = Cl or Ac). However, the levels of activities achieved were still considerably lower than usually reported for titanium- and vanadium-based Ziegler-type catalysts, e.g., about 10^3 to 10^5 times less active. Unfortunately, we did not measure the concentration of active centers in these catalysts and thus the catalyst activities cannot be related to the fundamental properties of the atoms which form the active centers.

Polymerization Procedure

Two polymerization procedures were used. When method A was used, the polymerizations were done in 8-oz glass bottles by a procedure already described.[9] In method B the polymerizations were carried out in 220-cc stainless steel vessels. These were first baked in an oven at 120°C for 20 hr, then cooled and placed in a dry box containing nitrogen (oxygen content was less than several ppm as demonstrated by lack of fuming of a 25 wt-% $ZnEt_2$ heptane solution). Weighed amounts of the solid salts were added and the vessel was sealed. The other components (solvent and metal alkyl) were added through a serum cap, which was finally removed and the vessel was connected to cylinder containing the olefin. The desired amount of the olefin was added under pressure. The vessel was inserted into two cork rings and rotated on a rolling mill at ambient temperatures. At the completion of the polymerization the unreacted olefin

TABLE IV
Ferrous Salts as Cocatalysts (FeX_2 when X = Cl, Br or acetylacetonate = Ac)

Expt. no.	FeX_2 (3.0 g)	Pretreatment of FeX_2	Heptane, ml	$AlEt_2Cl$, mmole	Ethylene, g	Polymerization: Reaction method[b]	Polymerization: Time, (25°C), hr	Polymer yield, g
1	$FeCl_2$[a]	None	75	45	18.5	B	144	2.1
2	$FeBr_2$[a]	None	75	45	19.4	B	141	7.1
3	$FeAc_2$	Ball-mill 68 hr in presence of 500 psig H_2	88	40	23.4	B	68	13.7

[a] The ferrous salts were purchased from A. D. Mackay.
[b] A stainless steel vessel was used as described in text.

TABLE V
Transition Metal Impurities in $CrCl_2$ and $MnCl_2$ as Determined by Emission and X-Ray Fluorescence Analysis[a]

Metal salt	Impurity transition metal[b]	Impurity, wt-%	
		By emission[c]	By x-ray fluorescence[d]
$CrCl_2$	Fe	1.1[e]	1.0[e]
	Ni	<0.006	Not detected
	Mo	0.03	Not detected
	Mn	0.014	0.01
$MnCl_2$	Fe	0.013	0.001
	Mo	<0.01	<0.001
	V	<0.01	Not detected
	Ti	<0.1	0.002
	Ni	<0.01	0.002
	Co	0.03	0.001
	Cr	<0.01	Not detected
	Hf	<0.03	Not detected
	Ta	<0.03	Not detected
	Zr	<0.03	Not detected
	W	<0.1	Not detected
	Nb	<0.1	Not detected
	Sc	Not detected	Not detected

[a] These analyses were carried out by Mr. E. Sandborn and Dr. T. C. Yao of this laboratory.

[b] Non-transition metal impurities were present but these are not reported here.

[c] Results are usually correct within a factor of two.

[d] Limit of detection usually about 0.01 wt-%.

[e] A ball-milled $CrCl_2$ sample was analyzed. The high Fe value originated from the ball-milling operation is a stainless-steel autoclave.

was vented off and the contents were added to a beaker containing an acidified mixture of methanol and isopropyl alcohol. It was then worked up in the usual way.[9]

References

1. U. K. Pat. 826,638 (to Ziegler) (January 13, 1960).
2. U. S. Pat. 3,221,002 (to Cabot) (November 30, 1965).
3. U. S. Pat. 3,205,178 (to Cabot) (September 7, 1965).
4. G. Natta, A. Zambelli, I. Pasquon, and J. Giongo, *Chim. Ind.* (Milan), **48**, 1307 (1966).
5. U. K. Pat. 879,309 (to Grace) (October 11, 1961).
6. U. S. Pat. 3,111,511 (to Grace) (November 19, 1963).
7. U. K. Pat. 935,984 (to Grace) (September 4, 1963).
8. D. Hoeg, U. S. Pat. 3,138,578 (to Grace) (June 23, 1964).
9. J. Boor, Jr., in *First Biannual American Chemical Society Polymer Symposium J. Polym. Sci., C*, **1**), H. W. Starkweather, Jr., Ed., Interscience, New York, 1963, p. 237.

J. Boor, Jr.

Shell Development Company
Emeryville, California 94608

Received May 18, 1971

Contents (continued)

The *Journal of Polymer Science* publishes results of fundamental research in all areas of high polymer chemistry and physics. The *Journal* is selective in accepting contributions on the basis of merit and originality. It is not intended as a repository for unevaluated data. Preference is given to contributions that offer new or more comprehensive concepts, interpretations, experimental approaches, and results. Part A-1 *Polymer Chemistry* is devoted to studies in general polymer chemistry and physical organic chemistry. Contributions in physics and physical chemistry appear in Part A-2 *Polymer Physics*. Contributions may be submitted as full-length papers or as "Notes." Notes are ordinarily to be considered as complete publications of limited scope.

Three copies of every manuscript are required. They may be submitted directly to the editor: For Part A-1, to C. G. Overberger, Department of Chemistry, University of Michigan, Ann Arbor, Michigan 48104; and for Part A-2, to T. G Fox, Mellon Institute, Pittsburgh, Pennsylvania 15213. Three copies of a short but comprehensive synopsis are required with every paper; no synopsis is needed for notes. Books for review may also be sent to the appropriate editor. Alternatively, manuscripts may be submitted through the Editorial Office, c/o H. Mark, Polytechnic Institute of Brooklyn, 333 Jay Street, Brooklyn, New York 11201. All other correspondence is to be addressed to Periodicals Division, Interscience Publishers, a Division of John Wiley & Sons, Inc., 605 Third Avenue, New York, New York 10016.

Detailed instructions in preparation of manuscripts are given frequently in Parts A-1 and A-2 and may also be obtained from the publisher.